การทดสอบจุดกดแบบปรับเปลี่ยนของหินผนังบ่อ ที่เหมืองแร่ทองคำชาตรี

นายชาติชาย อินทรประสิทธิ์

วิทยานิพนธ์นี้เป็นส่วนหนึ่งของการศึกษาตามหลักสูตรปริญญาวิศวกรรมศาสตรมหาบัณฑิต

สาขาวิชาเทคโนโลยีธรณี

มหาวิทยาลัยเทคโนโลยีสุรนารี

ปีการศึกษา 2552

MODIFIED POINT LOAD TESTS OF PIT WALL ROCK AT CHATREE GOLD MINE

Chatchai Intaraprasit

A Thesis Submitted in Partial Fulfillment of the Requirements for the

Degree of Master of Engineering in Geotechnology

Suranaree University of Technology

Academic Year 2009

MODIFIED POINT LOAD TESTS OF PIT WALL ROCK AT CHATREE GOLD MINE

Suranaree University of Technology has approved this thesis submitted in partial fulfillment of the requirements for a Master's Degree.

Thesis Examining Committee

_____

(Asst. Prof. Thara Lekuthai)

Chairperson

_____

(Assoc. Prof. Dr. Kittitep Fuenkajorn)

Member (Thesis Advisor)

_____

(Dr. Prachya Tepnarong)

Member

_____

(Prof. Dr. Pairote Sattayatham)

Acting Vice Rector for Academic Affairs

_____

(Assoc. Prof. Dr. Vorapot Khompis)

Dean of Institute of Engineering

ชาติชาย อินทรประสิทธิ์ : การทดสอบจุดกดแบบปรับเปลี่ยนของหินผนังบ่อที่เหมืองแร่ทองคำชาตรี (MODIFIED POINT LOAD TESTS OF PIT WALL ROCK AT CHATREE GOLD MINE) อาจารย์ที่ปรึกษา : รองศาสตราจารย์ ดร. กิตติเทพ เฟื่องขจร, 191 หน้า

การทดสอบจุดกดแบบปรับเปลี่ยนได้ถูกนำมาใช้ในการหาค่าความเค้นกด แรงดึง และค่าความยืดหยุ่นของหินตัวอย่างในห้องปฏิบัติการทดสอบ มาเป็นเวลาเกือบสิบปีแล้ว วิธีการทดสอบนี้ได้ถูกประดิษฐ์ และจดทะเบียนลิขสิทธิ์โดยมหาวิทยาลัยเทคโนโลยีสุรนารี เครื่องมือ และวิธีการทดสอบถูกออกแบบให้มีราคาถูกและง่าย เมื่อเปรียบเทียบกับวิธีการทดสอบเพื่อหาคุณสมบัติเชิงกลของหินแบบดั้งเดิม เช่น วิธีการทดสอบตามมาตรฐาน ISRM และ ASTM ในอดีตการทดสอบจุดกดแบบปรับเปลี่ยนส่วนใหญ่มักทดสอบในแท่งตัวอย่างหินที่เป็นรูปวงกลม และรูปสี่เหลี่ยมมุมฉาก ในขณะที่มีการอ้างว่าการทดสอบแบบจุดกดแบบปรับเปลี่ยนนี้สามารถใช้ได้กับหินทุกรูปร่าง แต่ผลทดสอบวิธีนี้กับหินที่มีรูปร่างไม่เป็นทรงเรขาคณิตยังมีน้อยมาก เนื่องจากเหตุนี้จึงยังไม่มีการยืนยันอย่างเพียงพอว่า วิธีการทดสอบจุดกดแบบปรับเปลี่ยนสามารถใช้ได้จริงและมีความสม่ำเสมอเพียงพอในการตรวจหาคุณสมบัติทางกลศาสตร์พื้นฐานของหินในภาคสนามซึ่งไม่สามารถจัดหาเครื่องเจาะและเครื่องตัดหินได้

วัตถุประสงค์ของงานวิจัยนี้คือ เพื่อประเมินศักยภาพของการทดสอบของวิธีการทดสอบแบบจุดกดแบบปรับเปลี่ยนในหินตัวอย่างที่มีรูปร่างไม่เป็นทรงเรขาคณิต ตัวอย่างหินสามชนิดจำนวน 150 ตัวอย่างเป็นอย่างน้อย ได้แก่ porphyritic andesite, silicified-tuffaceous sandstone และ tuffaceous sandstone ซึ่งเก็บรวบรวมมาจากผนังบ่อทางด้านทิศเหนือของเขาหม้อที่เหมืองแร่ทองคำชาตรี จะถูกนำมาใช้ในการทดสอบนี้ อัตราส่วนระหว่างความหนาของหินตัวอย่างต่อเส้นผ่าศูนย์กลางของหัวกด แปรผันระหว่าง 2 ถึง3 และ อัตราส่วนระหว่างเส้นผ่าศูนย์กลางของตัวอย่างหินกับเส้นผ่าศูนย์กลางของหัวกดแปรผันระหว่าง 5 ถึง 10 การสูญเสียรูปร่างและการแตกหักของหินจะถูกนำมาใช้ในการคำนวณหาค่าความยืดหยุ่นและความแข็งแรงของหิน และจะมีการทดสอบแรงกดในแกนเดียวและแรงกดในสามแกน การทดสอบแรงดึง และการทดสอบจุดกดแบบดั้งเดิมในหินทั้งสามชนิดด้วยเช่นกันเพื่อนำผลการทดสอบที่ได้มาใช้ในการเปรียบเทียบกับผลที่ได้จากการทดสอบจุดกดแบบปรับเปลี่ยน แบบจำลองโดยใช้โปรแกรมคอมพิวเตอร์จะถูกนำมาใช้ในการศึกษาการกระจายตัวของแรงเค้นในก้อนตัวอย่างหินของการทดสอบจุดกดแบบปรับเปลี่ยนภายใต้อัตราส่วนระหว่างความหนาของหินตัวอย่างต่อเส้นผ่าศูนย์กลางของหัวกดที่ต่างๆกัน และจะมีการประเมินเชิงปริมาณของผลกระทบของความมีรูปร่างที่ไม่เป็นรูปทรงทางเรขาคณิตของหินตัวอย่าง ความเหมือนและความแตกต่างของผล

การทดสอบจุดกดแบบปรับเปลี่ยนและการทดสอบจุดกดแบบดั้งเดิมจะถูกนำมาพิจารณา อาจมีการประยุกต์การคำนวณที่เป็นแบบแผนของการทดสอบจุดกดแบบปรับเปลี่ยน เพื่อเพิ่มความสามารถในการคาดคะเนคุณสมบัติทางกลศาสตร์ของหินตัวอย่างที่มีรูปร่างไม่เป็นรูปทรงทางเรขาคณิตได้ดียิ่งขึ้น

สาขาวิชา เทคโนโลยีธรณี ลายมือชื่อนักศึกษา _____

ปีการศึกษา 2552 ลายมือชื่ออาจารย์ที่ปรึกษา _____

CHATCHAI INTARAPRASIT: MODIFIED POINT LOAD TESTS OF PIT WALL ROCK AT CHATREE GOLD MINE. THESIS ADVISOR: ASSOC. PROF. KITTITEP FUENKAJORN, Ph. D., PE 191 PP.

TRIAXIAL COMPRESSIVE STRENGTH/UNIAXIAL COMPRESSIVE STRENGTH/ ELASIC MODULUS/ POINT LOAD/TENSILE STRENGTH

For nearly a decade, modified point load (MPL) testing has been used to estimate the compressive and tensile strengths and elastic modulus of intact rock specimens in the laboratory. This method was invented and patented by Suranaree University of Technology. The test apparatus and procedure are intended to be inexpensive and easy, compared to the relevant conventional methods of determining the mechanical properties of intact rock, e.g. those given by the International Society for Rock Mechanics (ISRM) and the American Society for Testing and materials (ASTM). In the past much of the MPL testing practices have been concentrated on circular and rectangular disk specimens. While it has been claimed that MPL method is applicable to all rock shapes, the test results from irregular lumps of rock have been rare, and hence are not sufficient to confirm that the MPL testing technique is truly valid or even adequate to determine the basic rock mechanical properties in the field where rock drilling and cutting devices are not available.

The objective of this research is to experimentally assess the performance of the modified point load testing on rock samples with irregular shapes. Three rock types obtained from the north pit-wall of Khao Moh at Chatree gold mine will be used as rock samples. A minimum of 150 samples of porphyritic andesite, silicified-tuffaceous sandstone, and tuffaceous sandstone will be collected from the site. The

sample thickness-to-loading diameter ratio (t/d) is varied from 2 to 3, and the sample diameter-to-loading diameter ratio (D/d) from 5 to 10. The sample deformation and failure will be used to calculate the elastic modulus and strengths of the rocks. Uniaxial and triaxial compression tests, Brazilian tension test and conventional point load test will also be conducted on the three rock types to obtain data basis for comparing with those from the MPL testing. Finite difference analysis will be performed to obtain stress distribution within the MPL samples under different t/d and D/d ratios. The effects of the sample irregularity will be quantitatively assessed. Similarity and discrepancy of the test results from the MPL method and from the conventional methods will be examined. Modification of the MPL calculation scheme may be made to enhance its predictive capability for the mechanical properties of irregular shaped specimens.

School of Geotechnology Student's Signature_____

Academic Year 2009 Advisor's Signature_____

ACKNOWLEDGMENTS

I wish to acknowledge the funding support of Suranaree University of Technology (SUT) and Akara Mining Company Limited.

I would like to express my sincere thanks to Assoc. Prof. Dr. Kittitep Fuenkajorn, thesis advisor, who gave a critical review and constant encouragement throughout the course of this research. Further appreciation is extended to Asst. Prof. Thara Lekuthai, chairman, school of Geotechnology and Dr. Prachya Tepnarong Suranaree University of Technology who are member of my examination committee. Grateful thanks are given to all staffs of Geomechanics Research Unit, Institute of Engineering who supported my work.

Chatchai Intaraprasit

TABLE OF CONTENTS

Page

TABLE OF CONTENTS (Continued)

Page

TABLE OF CONTENTS (Continued)

Page

TABLE OF CONTENTS (Continued)

Page

LIST OF TABLES

Table **Page**

LIST OF TABLE (Continued)

Table **Page**

LIST OF TABLE (Continued)

Table **Page**

LIST OF TABLE (Continued)

Table **Page**

LIST OF FIGURES

Figure **Page**

LIST OF FIGURES (Continued)

Figure **Page**

LIST OF FIGURES (Continued)

Figure **Page**

LIST OF FIGURES (Continued)

Figure **Page**

LIST OF SYMBOLS AND ABBREVIATIONS

A	=	Original cross-section Area
c	=	cohesive strength
CP	=	Conventional Point Load
D	=	Diameter of Rock Specimen
D	=	Diameter of Loading Point
D_e	=	Equivalent Diameter
E	=	Young's Modulus
E_{mpl}	=	Elastic Modulus by MPL Test
E_t	=	Tangent Elastic Modulus
I_S	=	Point Load Strength Index
L	=	Original Specimen Length
L/D	=	Length-to-Diameter Ratio
MPL	=	Modified Point Load
P_f	=	Failure Load
P_{mpl}	=	Modified Point Load Strength
t	=	Specimen Thickness
α	=	Coefficient of Stress
α_E	=	Displacement Function
β	=	Coefficient of the Shape
ΔL	=	Axial Deformation

LIST OF SYMBOLS AND ABBREVIATIONS (Continued)

ΔP	=	Change in Applied Stress
$\Delta \delta$	=	Change in Vertical of Point Load Platens
ε_{axial}	=	Axial Strain
ν	=	Poisson's Ratio
ρ	=	Rock Density
σ	=	Normal Stress
σ_1	=	Maximum Principal Stress (Vertical Stress)
σ_3	=	Minimum Principal Stress (Horizontal Stress)
σ_B	=	Brazilian Tensile Stress
σ_c	=	Uniaxial Compressive Strength (UCS)
σ_m	=	Mean Stress
τ	=	Shear Stress
τ_{oct}	=	Octahedral Shear Stress
ϕ_i	=	angle of Internal friction

CHAPTER I

INTRODUCTION

1.1 Background and rationale

In geological exploration, mechanical rock properties are one of the most important parameters that will be used in the analysis and design of engineering structures in rock mass. To obtain these properties, the rock from the site is extracted normally by mean of core drilling, and then transported the cores to the laboratory where the mechanical testing can be conducted. Laboratory testing machine is normally huge and can not be transported to the site. On site testing of the rocks may be carried out by some techniques, but only on a very limited scale. This method is called for point load strength Index testing. However, this test provides unreliable results, and lacks theoretical supports. Its results may imply to other important properties (e.g., compressive and tensile strength), but only based on an empirical formula, which usually poses a high degree of uncertainty.

For nearly a decade, modified point load (MPL) testing has been used to estimate the compressive and tensile strength and elastic modulus of intact rock specimens in the laboratory (Tepnarong, 2001). This method was invented and patented by Suranaree University of Technology. The test apparatus and procedure are intended to be in expensive and easy, compared to the relevant conventional methods of determining the mechanical properties of intact rock, e.g., those given by the International Society for Rock Mechanics (ISRM) and the American Society for

Testing and Materials (ASTM). In the past much of the MPL testing practices has been concentrated on circular and disk specimens. While it has been claimed that MPL method is applicable to all rock shapes, the test results from irregular lumps of rock have been rare, and hence are not sufficient to confirm that the MPL testing technique is truly valid or even adequate to determine the basic rock mechanical properties in the field where rock drilling and cutting devices are not available.

1.2 Research objectives

The objective of this research is to experimentally assess the performance of the modified point load testing on rock samples with irregular shapes. Three rock types obtained from the north pit-wall of Khao Moh at Chatree gold mine are used as rock samples. A minimum of 150 rock samples of porphyritic andesite, silicified-tuffaceous sandstone and tuffaceous sandstone are collected from the site. The sample thickness-to-loading diameter ratio (t/d) is varied from 2 to 3 and the sample diameter-to-loading diameter ratio (D/d) from 5 to 10. The sample deformation and failure are used to calculate the elastic modulus and strengths of rocks. Uniaxial and triaxial compression tests, Brazilian tension test and conventional point load test are conducted on the three rock types to obtain data basis for comparing with those from MPL testing. Finite difference analysis is performed to obtain stress distribution within the MPL samples under different t/d and D/d ratios. The effect of the irregularity is quantitatively assessed. Similarity and discrepancy of the test results from the MPL method and from the conventional method are examined. Modification of the MPL calculation scheme may be made to enhance its predictive capability for the mechanical properties of irregular shaped specimens.

1.3 Research concept

A modified point load (MPL) testing technique was proposed by Fuenkajorn and Tepnarong (2001) and Fuenkajorn (2002). The objectives of this testing are to determine the elastic modulus, uniaxial compressive strength and tensile strength of intact rocks. The application of testing apparatus is modified from the loading platens of the conventional point load (CPL) testing to the cylindrical shapes that have the circular cross-section while they are half-spherical shapes in CPL.

The modes of failure for the MPL specimens are governed by the ratio of specimen diameter to loading platen diameter (D/d) and the ratio of specimen thickness to loading platen diameter (t/d). This research involves using the MPL results to estimate the triaxial compressive strength of specimens which various D/d and t/d ratios and compare to the conventional compressive strength test.

1.4 Research methodology

This research consists of six main tasks; literature review, sample collection and preparation, laboratory testing, finite difference analysis, comparison, discussions and conclusions. The work plan is illustrated in the Figure 1.1

1.4.1 Literature review

Literature review is carried out to study the state-of-the-art of CPL and MPL techniques, including theories, test procedure, results, analysis and applications. The sources of information are from journals, technical reports and conference papers. A summary of literature review is given in this thesis. Discussions have been also been made on the advantages and disadvantages of the testing, the validity of the test results

Preparation

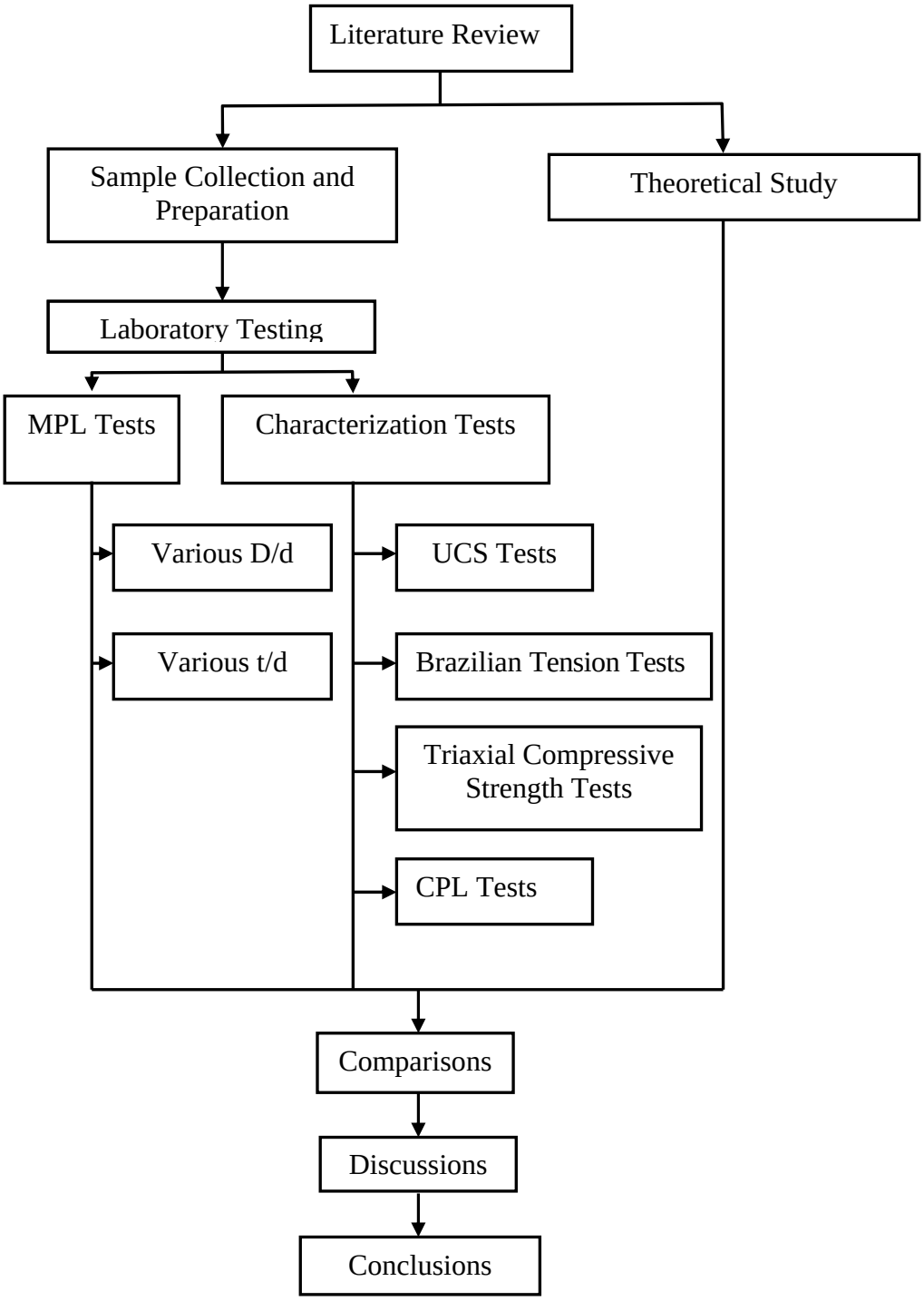

Figure 1.1 Research methodology.

when correlating with the uniaxial compressive strength of rocks, and on the failure mechanism the specimens.

1.4.2 Sample collection and preparation

Rock samples are collected from the north pit-wall of Khao Moh at Chatree gold mine. Three rock types are tested with a minimum of 50 samples for each rock type. The selection criteria are that the rock should be homogeneous as much as possible, and that sample collection should be convenient and repeatable. Sample preparation is carried out in the laboratory at Suranaree University of Technology.

1.4.3 Theoretical study of the rock failure mechanism

The theoretical work primarily involves numerical analyses on the MPL specimens under various shapes. Failure mechanism of the modified point load test specimens is analyzed in terms of stress distributions along loaded axis. The finite difference code FLAC is used in the simulation. The mathematical solutions are derived to correlate the MPL strengths of irregular-shaped samples with the uniaxial and traiaxial compressive strengths, tensile strength and elastic modulus of rock specimens

1.4.4 Laboratory testing

Three prepared rock type samples are tested in laboratory which are divided into two main groups as follows.

1.4.4.1 Characterization tests

The characterization tests include uniaxial compressive strength tests (ASTM D7012-07), Brazilian tensile strength tests (ASTM D3967, 1981), triaxial compressive strength tests (ASTM D7012-07), and conventional point

load index tests (ASTM D5731, 1995). The characterization testing results are used in verifications of the proposed MPL concept.

1.4.4.2 Modified point load tests

Three rock types of rock from the north pit-wall of Khao Moh at Chatree gold mine are used as rock samples. A minimum of 150 rock samples of porphyritic andesite, silicified-tuffaceous sandstone and tuffaceous sandstone are used in the MPL testing. The sample thickness-to-loading diameter ratio (t/d) is varied from 2 to 3 and the sample diameter-to-loading diameter ratio (D/d) from 5 to 10. The sample deformation and failure are used to calculate the elastic modulus and strengths of rocks. The MPL testing results are compared with the standard tests and correlated the relations in terms of mathematic formulas.

1.4.5 Analysis

Finite difference analysis is performed to obtain stress distribution within the MPL samples under various shapes with different t/d and D/d ratios. The effect of the irregularity is quantitatively assessed. Similarity and discrepancy of the test results from the MPL method and from the conventional method are examined. Modification of the MPL calculation scheme may be made to enhance its predictive capability for the mechanical properties of irregular shaped specimens.

1.4.6 Thesis writing and presentation

All aspects of the theoretical and experimental studies mentioned are documented and incorporated into the thesis. The thesis discusses the validity and potential applications of the results.

1.5 Scope and limitations

The scope and limitations of the research include as follows.

1 Three rock types of rock from the pit wall of Chatree gold mine are selected as a prime candidate for use in the experiment.

2 The analytical and experimental work assumes linearly elastic, homogeneous and isotropic conditions.

3 The effects of loading rate and temperature are not considered. All tests are conducted at room temperature.

4 MPL tests are conducted on a minimum of 50 samples.

5 The investigation of failure mode is on macroscopic scale. Macroscopic phenomena during failure are not considered.

6 The finite difference analysis is made in axis symmetric and assumed elastic, homogeneous and isotropic conditions.

7 Comparison of the results from MPL tests and conventional method is made.

1.6 Thesis contents

The first chapter includes six sections. It introduces the thesis by briefly describing the background and rationale, and identifying the research objectives that are describes in the first and second section. The third section describes the proposed concept of the new testing technique. The fourth section describes the research methodology. The fifth section identifies the scope and limitation of the research and the description of the overview of contents in this thesis are in the sixth section.

CHAPTER II

LITERATURE REVIEW

2.1 Introduction

This chapter summarizes the results of literature review carried out to improve an understanding of the applications of modified point load testing to predict the strengths and elastic modulus of the intact rock. The topics reviewed here include conventional point load test, modified point load test, characterization tests, and size effects.

2.2 Conventional point load tests

Conventional point load (CPL) testing is intended as an index test for the strength classification of rock material. It has long been practiced to obtain an indicator of the uniaxial compressive strength (UCS) of intact rocks. The testing equipment (Figure 2.1) is essentially a loading system comprising a loading flame, hydraulic oil pump, ram and loading platens. The geometry of the loading platen is standardized (Figure 2.2) having 60 degrees angle of the cone with 5 mm radius of curvature at the cone tip. It is made of hardened steel. The CPL test method has been widely employed because the test procedure and sample preparation are simple, quick and inexpensive, as compared with conventional tests as the unconfined compressive strength test. Starting with a simple method to obtain a rock properties index, the International Society for Rock Mechanics (ISRM) commissions on testing methods have issued a recommended procedure for the point load testing (ISRM, 1985) the test has also been established as a standard test method by the American Society for Testing and Materials in 1995 (ASTM, 1995).

Although the point load test has been studied extensively (e.g. Broch and Franklin, 1972; Bieniawski, 1974 and 1975; Wijk, 1980; Brook, 1985), the theoretical solutions for the test result remain rare. Several attempts have been made to truly understand the failure mechanism and the impact of the specimen size on the point load strength results. It is commonly agreed that tensile failure is induced along the axis between loading points (Evans, 1961; Hiramutsu, 1976; Wijk, 1978, 1980). The most commonly accepted formula relating the CPL index and the UCS is proposed by Broch and Franklin (1972). The UCS (or σ_c) can be estimated as about 24 times of the point load strength index (I_s) of rock specimens with the diameter-to-length ratio of 0.5. The I_S value should also be corrected to a value equivalent to the specimen diameter of 50 mm. The factor of 24 can sometimes load to an error in the prediction of the UCS. Most previous studied have been done experimentally, but rare theoretical attempt has been made to study the validity of Broch and Franklin formula.

The CPL testing has been performed using a variety of sizes and shapes of rock specimen (Wijk, 1980; Foster, 1983; Panek and Fannon, 1992; Chau and Wong, 1996; Butenuth, 1997). This is to determine the most suitable specimen sizes. These investigations have proposed empirical relations between the I_S and σ_c to be universally applicable to various rock types. However, some uncertainly of these relations remains.

Panek and Fannon (1992) show the results of the CPL tests, UCS tests and Brazilian tension tests that are performed on three hard rocks (iron-formation, metadiabase, and ophitic basalt). The CPL strength is analyzed in terms of the

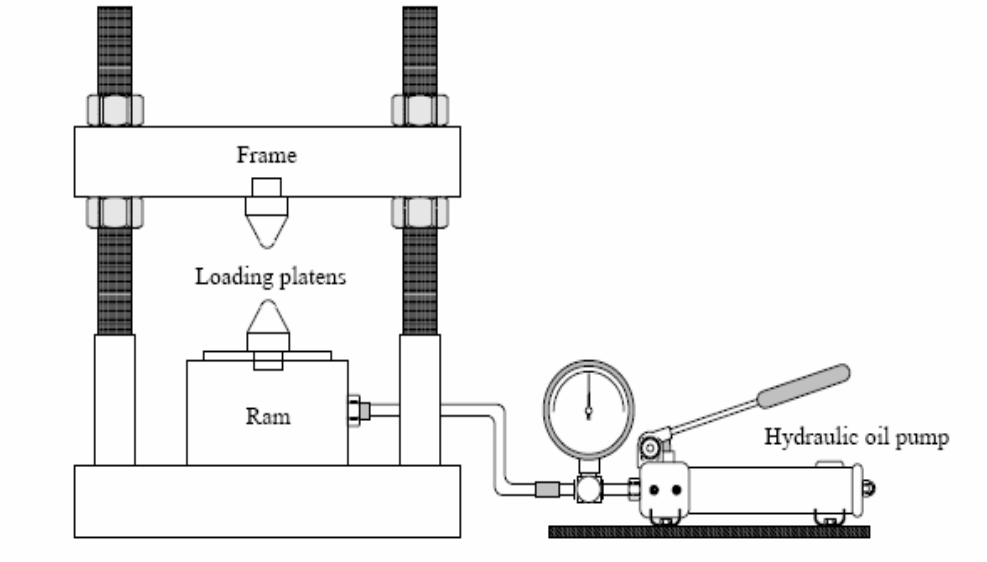

Figure 2.1 Loading system of the conventional point load (CPL) (Tepnarong, 2001)

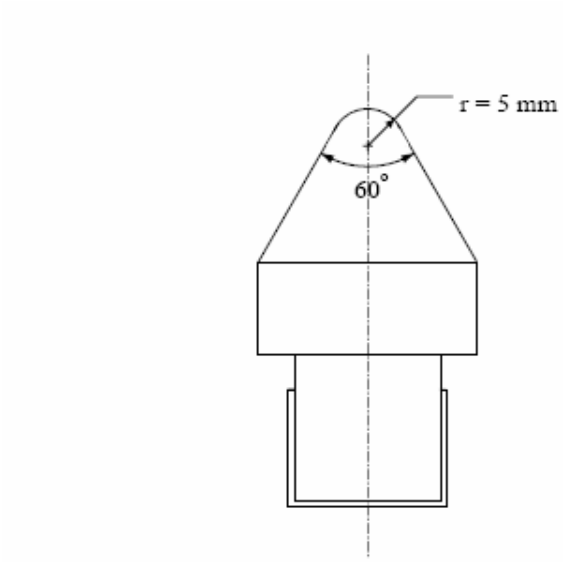

Figure 2.2 Standard loading platen shape for the conventional point load testing (ISRM suggested method and ASTM D5731-95)

size and shape effects. More than 500 an irregular lumps were tested in the field. The shape effect exponents for compression have been found to be varied with rock types. The shape effect exponents in CPL tests are constant for the three rocks. Panek and Fannon (1992) recommended that the monitoring of the compressive and tensile strengths should have various sizes and shapes of specimen to obtain the certain properties.

Chau and Wong (1996) study analytically the conversion factor relating between σ_c and I_S. A wide range of the ratios of the uniaxial compressive strength to the point load index has been observed among various rock types. It has been found that the uniaxial compressive strength of rocks can vary from 6.2 (Nevada test site tuff) to 105 (Flaming Gorge shale) times the I_S, depending on rock type. The conversion factor relating σ_c to be I_s depends on compressive and tensile strengths, the Poisson's ratio, and the length and diameter of specimen. The conversion factor of 24 (Broch and Franklin, 1972) falls within this range but it is no by meaning universal.

2.3 Modified point load tests

Tepnarong (2001) proposed a modified point load testing method to correlate the results with the uniaxial compressive strength (UCS) and tensile strength of intact rocks. The primary objective of the research is to develop the inexpensive and reliable rock testing method for use in field and laboratory. The test apparatus is similar to the conventional point load (CPL), except that the loading points are cut flat to have a circular cross-section area instead of using a half-spherical shape. To derive a new solution, finite element analyses and laboratory experiments were

carried out. The simulation results suggested that the applied stress required failing the MPL specimen increased logarithmically as the specimen thickness or diameter increased. The MPL tests, CPL tests, UCS tests and Brazilian tension tests were performed on Saraburi marble under a variety of sizes and shapes. The UCS test results indicated that the strengths decreased with increased the length-to-diameter ratio. The test results can be postulated that the MPL strength can be correlated with the compressive strength when the MPL specimens are relatively thin, and should be an indicator of the tensile strength when the specimens are significantly larger than the diameter of the loading points. Predictive capability of the MPL and CPL techniques were assessed. Extrapolation of the test results suggested that the MPL results predicted the UCS of the rock specimens better than the CPL testing. The tensile strength predicted by the MPL also agreed reasonably well with the Brazilian tensile strength of the rock.

Tepnarong (2006) proposed the modified point load testing technique to determine the elastic modulus and triaxial compressive strength of intact rocks. The loading platens are made of harden steel and have diameter (d) varying from 5, 10, 15, 20, 25, to 30 mm. The rock specimens tested were marble, basalt, sandstone, granite and rock salt. Basic characterization tests were first performed to obtain elastic and strength properties of the rock specimen under standard testing methods (ASTM). The MPL specimens were prepared to have nominal diameters (D) ranging from 38 mm to 100 mm, with thickness varying from 18 mm to 63 mm. Testing on these circular disk specimens was a precursory step to the application on irregular-shaped specimens. The load was applied along the specimen axis while monitoring the increased of the load and vertical displacement until failure. Finite element

analyses were performed to determine the stress and deformation of the MPL specimens under various D/d and t/d ratios. The numerical results were also used to develop the relationship between the load increases (ΔP) and the rock deformation ($\Delta\delta$) between the loading platens. The MPL testing predicts the intact rock elastic modulus (E_{mpl}) by using an equation: $E_{mpl} = (t/\alpha_E) \cdot (\Delta P/\Delta\delta)$, where t represents the specimen thickness and α_E is the displacement function derived from numerical simulation. The elastic modulus predicted by MPL testing agrees reasonably well with those obtained from the standard uniaxial compressive tests. The predicted E_{mpl} values show significantly high standard deviation caused by high intrinsic variability of the rock fabric. This effect is enhanced by the small size of the loading area of the MPL specimens, as compared to the specimen size used in standard test methods.

The results of the numerical simulation were used to determine the minimum principal stress (σ_3) at failure corresponding to the maximum applied principal stress (σ_1). A simple relation can therefore be developed between σ_1/σ_3 ratio, Poisson's ratio (ν) and diameter ratio (D/d) to estimate the triaxial compressive strengths of the rock specimens: $\sigma_1/\sigma_3 = 2[(\nu/(1-\nu))(1-(d/D)^2)]^{-1}$. The MPL test results from specimens with various D/d ratios can provide σ_1 and σ_3 at failure by assuming that $\nu = 0.25$ and that failure mode follows Coulomb criterion. The MPL predicted triaxial strengths agree very well with the triaxial strength obtained from the standard triaxial testing (ASTM). The discrepancy is about 2-3% which may be due to the assumed Poisson's ratio of 2.5, and due to the assumption used in the determination of σ_3 at failure. In summary, even through slight discrepancies remain in the application of MPL results to determine the elastic modulus and triaxial compressive strength of intact rocks, this approach of

predicting the rock properties shows a good potential and seems promising considering the low cost of testing technique and ease of sample preparation.

2.4 Characterization tests

2.4.1 Uniaxial compressive strength tests

The uniaxial compressive strength test is the most common laboratory test undertaken for rock mechanics studies. In 1972 the International Society of Rock Mechanics (ISRM) published a suggested method for performing UCS tests (Brown, 1981). Bieniawski and Bernede (1979) proposed the procedures in American Society for Testing and Materials (ASTM) designation D2938.

The tests are also the most used tests for estimating the elastic modulus of rock (ASTM D7012). The axial strain can be measured with strain gages mounted on the specimen or with the Linear Variable Differential Tranformers (LVDTs) attached parallel to the length of the specimen. The lateral strain can be measured using strain gages around the circumference, or using the LVDTs across the specimen diameter.

The UCS (σ_c) is expressed as the ratio of the peak load (P) to the initial cross-section area (A):

$$\sigma_c = P/A \tag{2.1}$$

And the Young's modulus (E) can be calculated by:

$$E = \Delta\sigma/\Delta\varepsilon \tag{2.2}$$

Where $\Delta\sigma$ is the change in stress and $\Delta\varepsilon$ is the change in strain

The ratio of lateral strain and axial strain magnitudes ($\varepsilon_{lat}/\varepsilon_{ax}$) determines the value of Poisson' ratio (ν):

$$\nu = - (\varepsilon_{lat}/\varepsilon_{ax}) \quad (2.3)$$

2.4.2 Triaxial compressive strength tests

Hoek and Brown (1980b) and Elliott and Brown (1986) used the triaxaial compressive strength tests to gain an understanding of rock behavior under a three-dimensions state of stress and to verify, and even validate, mathematical expressions that have been derived to represent rock behavior in analytical and numerical models.

The common procedures are described in ASTM designation D7012 to determine the triaxial strengths and D7012 to determine the elastic moduli, and in ISRM suggested methods (Brown, 1981).

The axial strain can be measured with strain gages mounted on the specimen or with the LVTDs attached parallel to the length of the specimen. The lateral strain can be measured using strain gages around the circumstance within the jacket rubber.

At the peak load, the stress conditions are $\sigma_1 = P/A$, $\sigma_3=p$, where P is the maximum load parallel to the cylinder axis, A is the initial cross-section area, and p is the pressure in the confining medium.

The Young's modulus (E) and Poisson's ratio (ν) can be calculated by:

$$E = \Delta(\sigma_1-\sigma_3)/\Delta \varepsilon_{ax} \quad (2.4)$$

and

$$\nu = (\text{slope of axial curve}) / (\text{slope of lateral curve}) \quad (2.5)$$

where $\Delta(\sigma_1-\sigma_3)$ is the change in differential stress and $\Delta\,\varepsilon_{ax}$ is the change in axial strain.

2.4.3 Brazilian tensile strength tests

Caneiro (1974) and Akazawa (1953) proposed the Brazilian tensile strength test of intact rocks. Specifications of Brazilian tensile strength test have been established by ASTM D3967 and suggested approach is provided by ISRM (Brown, 1981)

Jaeger and Cook (1979) proposed the equation for calculate the Brazilian tensile strength as:

$$\sigma_B = (2P) / (\pi Dt) \quad (2.6)$$

where P is the failure load, D is the disk diameter, and t is the disk thickness.

2.5 Size effects on compressive strength

The uniaxial compressive strength normally tested on cylindrical-shaped specimens. The length-to-diameter (L/D) ratio of the specimen influences the measured strength. Typically, the strength decreases with increasing the L/D ratio, but it tends to become constant or ratios in the order of 2:1 to 3:1 (Hudson et al, 1971; Obert and Duvall, 1967). For higher ratios the specimen, strength may be influenced by bulking.

The size of specimen may influence the strength of rock. Weibull (1951) proposed that a large specimen contains more flaws than a small one. The large specimen therefore also has flaws with critical orientation relative to the applied shear stresses than the small specimen. A large specimen with a given shape is

therefore likely to fail and exhibit lower strength than a small specimen with the same shape (Bieniawski, 1968; Jaeker and Cook, 1979; Kaczynski, 1986).

Tepnarong (2001) investigated the results of uniaxial compressive strength test on Saraburi marble and found that the strengths decrease with increase the length-to-diameter (L/D) ratio. And this relationship can be described by the power law. The size effects on uniaxial compressive strength are obscured by the intrinsic variability of the marble. The Brazilian tensile strengths also decreased as the specimen diameter increased.

CHAPTER III

SAMPLE COLLECTION AND PREAPATION

This chapter describes the sample collection and sample preparation procedure to be used in the characterization and modified point load testing. The rock types to be used including porphyritic andesite, silicified-tuffaceous sandstone and tuffaceous sandstone. Locations of sample collection, rock description are described.

3.1 Sample collection

Three rock types include porphyritic andesite, silicified-tuffaceous sandstone and tuffaceous sandstone collected from Chatree Gold Mine, Akara Mining Company Limited, Phichit, Thailand are used in this research. The rock samples are collected from the north pit-wall of Khao Moh. Three rock types are tested with a minimum of 50 samples for each rock type. The selection criteria are that the rock should be homogeneous as much as possible, and that sample collection should be convenient and repeatable. The collected location is shown in Figure 3.1.

3.2 Rock descriptions

Three rock types are used in this research; there are porphyritic andesite, silicified tuffaceous sandstone and tuffaceous sandstone. Tuffaceous sandstone is medium brownish grey, the clasts are andesite, rhyolite, andesitic tuff, and quartz fragments, and sub-rounded to sub-angular, matrix: sand andesitic tuff, rock fragment

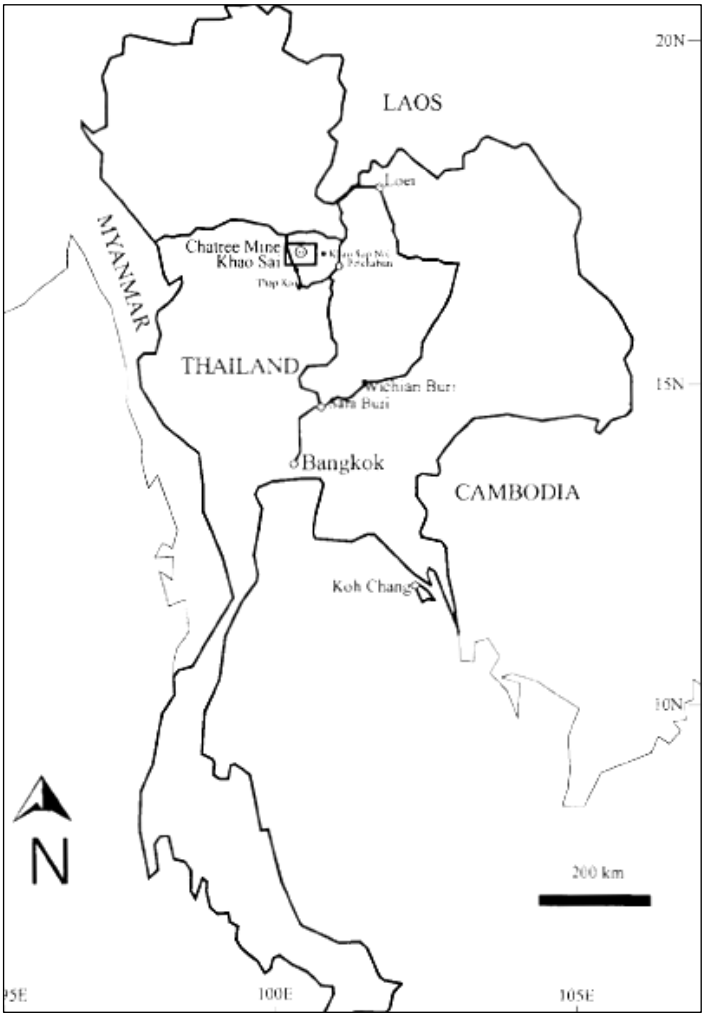

Figure 3.1 The location of rock samples collected area.

< 10% quartz, 3% pyrite, and litho-facies: massive, ungraded, clast supported, moderately sorted. Silicified tuffaceous sandstone is medium brown; clasts are fine to medium sand and silt, sub-rounded shape, quartz rich with siliceous matrix, massive, non-graded, well sorted, moderately Silicified. Porphyritic andesite is grayish green, medium-coarse, euhedral, evenly distributed phenocrysts are abundant, most conspicuous are hornblende phenocrysts, fine-grained groundmass. Those samples are collected from Chatree Gold Mine, Akara mining Co., Ltd. Phichit, Thailand.

3.3 Sample preparation

Sample preparation has been carried out to obtain different sizes and shapes for testing. It is conducted in the laboratory facility at Suranaree University of Technology. For characterization testing, the process includes coring and grinding. Preparation of rock samples for characterization test follows the ASTM standard (ASTM D4543-85). The nominal sizes of specimen that following the ASTM standard practices for the characterization tests are shown in table 3.1. And grinding surface at the top and bottom of specimens at the position of loading platens for unsure that the loading platens are attach to the specimen surfaces and perpendicular each others as shown in Figure 3.2. The shapes of specimens are irregularity-shaped. The ratio of specimen thickness to platen diameter (t/d) is around 2.0-3.0 and the specimen diameter to platen diameter (D/d) varies from 5 to 10.

Table 3.1 The nominal sizes of specimens following the ASTM standard practices for the characterization tests.

Testing Methods	L/D Ratio	Nominal Diameter (mm)	Nominal Length (mm)	Number of Specimens
1.UniaxialCompressive Strength Test and Elastic Modulus Measurement (ASTM D7012)	2.5	54	135	10
2. Triaxial Compressive Strength Test (ASTM D7012)	2.0	54	108	10
3. Brazilian Tensile Strength Test (ASTM D3967)	0.5	54	27	10
4. Point Load Strength Index Test (ASTM D 5731)	1.0	54	54	10

Figure 3.2 Some prepared rock specimens of porphyritic andesite for MPL Tests.

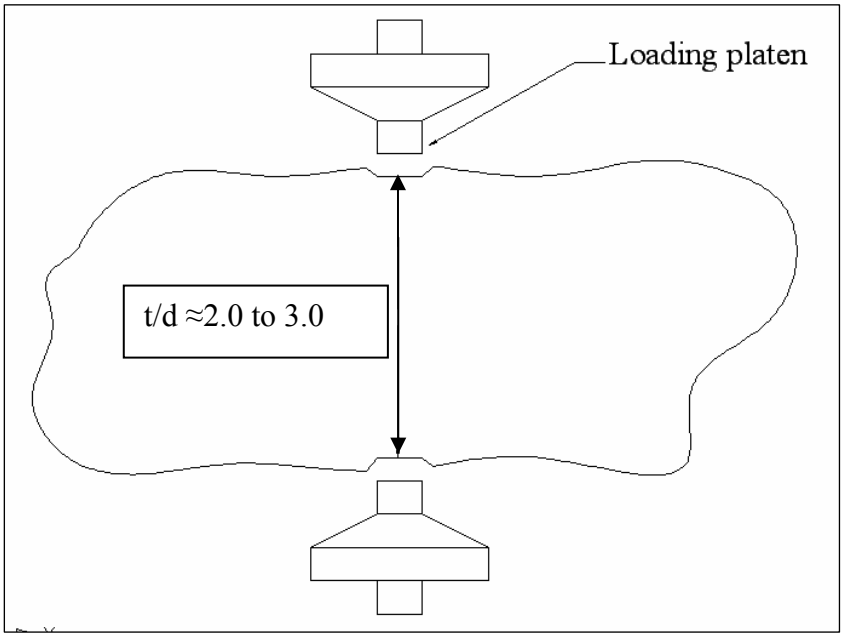

Figure 3.3 The concept of specimen preparation for MPL testing.

CHAPTER IV

LABORATORY TESTS

Laboratory testing is divided into two main tasks including the characterization tests and the modified point load tests. Three rock types: porphyritic andesite, silicified-tuffaceous sandstone, and tuffaceous sandstone are used in this research.

4.1 Literature reviews

4.1.1 Displacement function

Tepnarong (2006) proposed a method to compute the vertical displacement of the loading point as affected by the specimen diameter and thickness (D/d and t/d ratios) by used the series of finite element analyses. To accomplish this, a displacement function (α_E) is introduced as $(\Delta P/\Delta\delta)\cdot(t/E)$, where ΔP is the change in applied stress, $\Delta\delta$ is the change in vertical displacement of point load platens, t is the specimen thickness, and E is elastic modulus of rock specimen. The displacement function is plotted as a function of D/d.. And found that the α_E is dimensionless and independent of rock elastic modulus. α_E trend to be independent of D/d when D/d is beyond 15. The α_E is sensitive to ν particularly when υ is between 0.25 and 0.5. This agrees with the assumption that as the Poisson's ratio increases, the α_E value will increase because under higher ν the $\Delta\delta$ will be reduced. This is due to the large confinement resulting from the higher Poisson's ratio. Nevertheless, most rocks have Poisson's ratio within a range between 0.20 and 0.30, particularly for moderate to

hard rocks. As a result, the Poisson's ratio of 0.25 will provide a reasonable prediction of the value of α_E values.

Figure 5.1 plots α_E or $(\Delta P/\Delta\delta)\cdot(t/E)$, as a function of t/d for the ratios of $D/d \geq 10$. The displacement function increase as the t/d increases, which can be expressed by a power equation,

$$\alpha_E = (\Delta P/\Delta\delta)\cdot(t/E) = 1.50\ (t/d)^{0.64} \tag{5.1}$$

by using the least square fitting. The curve fit gives good correlation (R^2=0.998). These curves can be used to estimate the elastic modulus of rock from MPL results. By measuring the MPL specimen thickness, t and the increment of applied stress (ΔP) and displacement ($\Delta\delta$).

4.2 Basic characterization tests

The objectives of the basic characterization tests are to determine the mechanical properties of each rock type to compare their results with those from the modified point load tests (MPL). The basic characterization tests include uniaxial compressive strength (UCS) tests with elastic modulus measurements, triaxial compressive strength tests, Brazilian tensile strength tests and conventional point load strength index tests.

4.2.1 Uniaxial compressive strength tests and elastic modulus measurements

The uniaxial compressive strength tests are conducted on the three rock types. Sample preparation and test procedure are followed the ASTM standards (ASTM D7012) and the ISRM suggested methods (Brown, 1981). The core size is

54 mm in diameter (NX size) and the ratio of the length to diameter is 2.5. A total of 10 specimens are tested for each rock type.

A constant loading rate of 0.5 to 1.0 MPa/s is applied to the specimens until failure occurs. Tangent elastic modulus is measured at stress level equal to 50% of the uniaxial compressive strength. Post-failure characteristics are observed.

The uniaxial compressive strength (σ_c) is calculated by dividing the maximum load by the original cross-section area of loading platen:

$$\sigma_c = p_f / A \tag{4.1}$$

where p_f is the maximum failure load and A is the original cross-section area of loading platen. The tangent elastic modulus (E_t) is calculated by the following equation:

$$E_t = (\Delta\sigma_{axial}) / (\Delta\varepsilon_{axial}) \tag{4.2}$$

And the axial strain can be calculated from:

$$\varepsilon_{axial} = \Delta L / L \tag{4.3}$$

where the ΔL is the axial deformation and L is the original length of specimen.

The average uniaxial compressive strength and tangent elastic modulus of each rock types are shown in Tables 4.1 through 4.4

Figure 4.1 Pre-test samples of porphyritic andesite for UCS test

Figure 4.2 Pre-test samples of tuffaceous sandstone for UCS test

Figure 4.3 Pre-test samples of silicified tuffaceous sandstone for UCS test

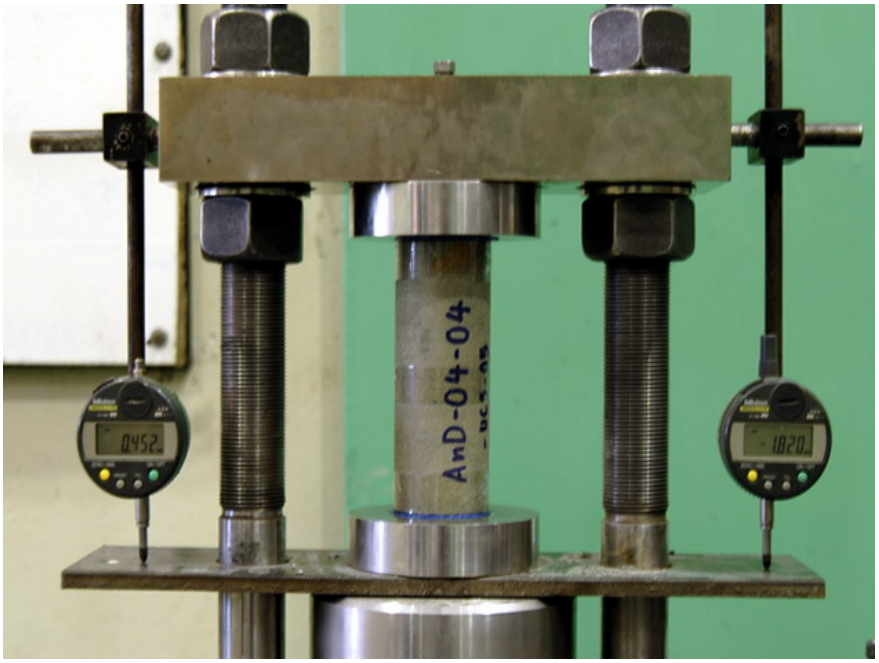

Figure 4.4 Preparation of testing apparatus for UCS test

Figure 4.5 Post-test rock samples of porphyritic andesite from UCS test

Figure 4.6 Post-test rock samples of tuffaceous sandstone from UCS test

Figure 4.7 Post-test rock samples of silicified-tuffaceous sandstone from UCS

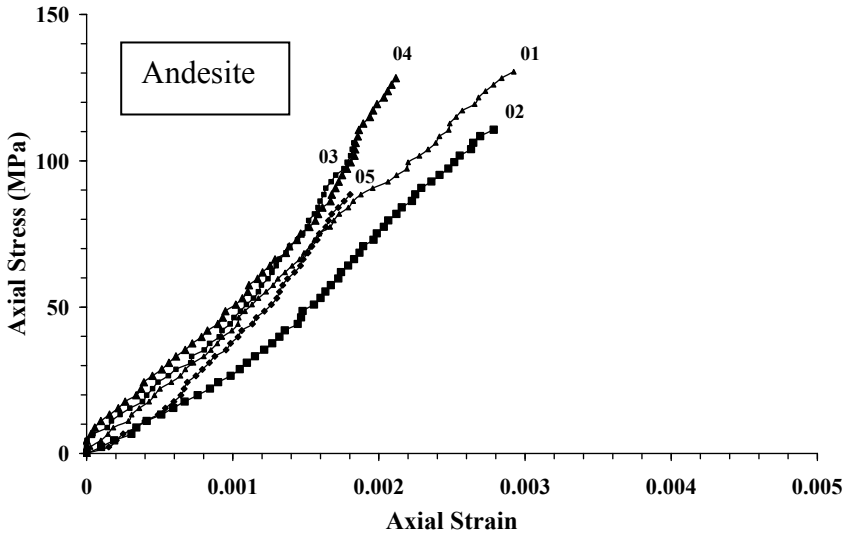

Figure 4.8 Results of uniaxial compressive strength test and elastic modulus measurements of porphyritic andesite. The axial stresses are plotted as a function of axial strain.

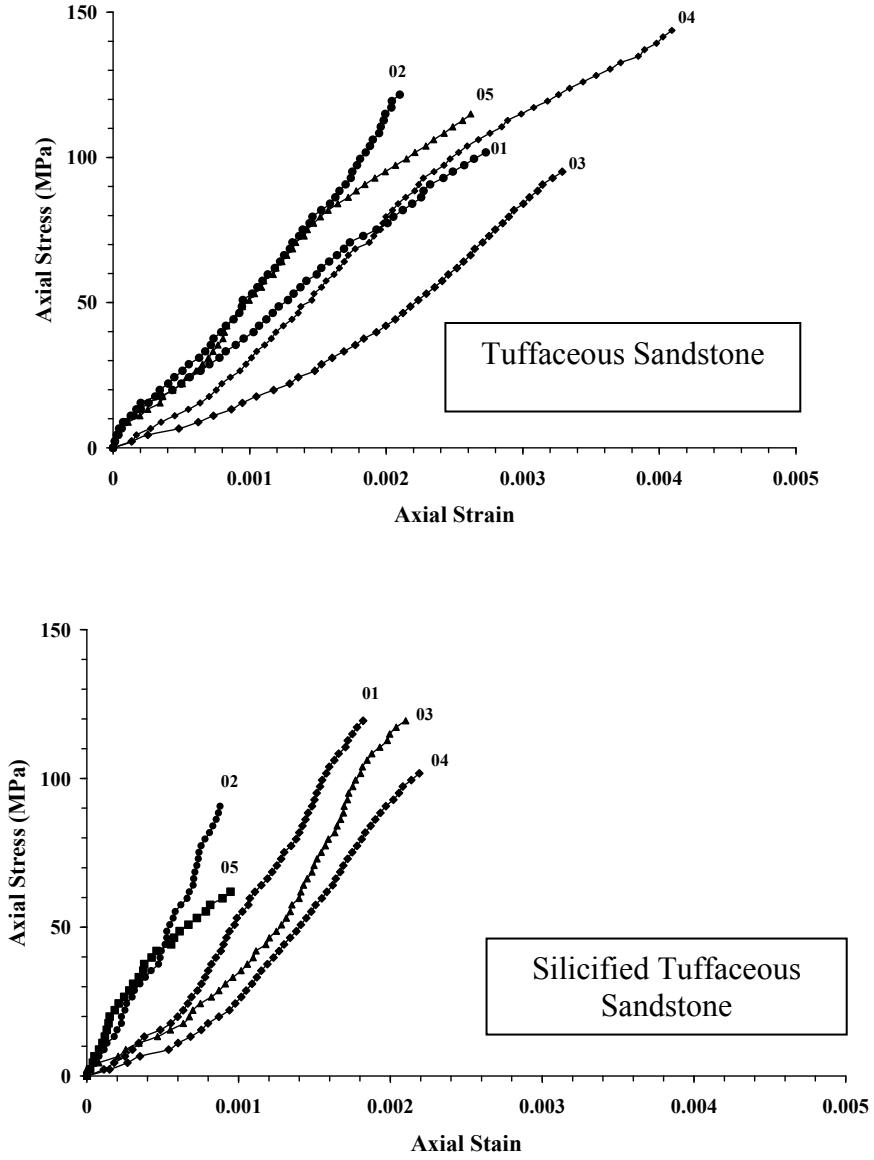

Figure 4.9 Results of uniaxial compressive strength test and elastic modulus measurements of tuffaceous sandstone (top) and silicified tuffaceous sandstone (bottom). The axial stresses are plotted as a function of axial strain.

Table 4.1 Testing results of porphyritic andesite

Sample No.	Diameter (mm)	Length (mm)	Density (g/cc)	σ_c (MPa)	E (GPa)
And-02-02-UCS-01	53.66	134.86	2.82	132.7	45.1
And-06-03-UCS-02	53.66	134.94	2.83	110.6	39.7
And-02-01-UCS-03	53.66	134.85	2.80	106.1	47.0
And-08-03-UCS-04	53.66	134.17	2.84	128.2	39.2
And-04-04-UCS-05	53.66	135.64	2.85	97.3	43.8
Average				**115.0 ± 15.0**	**43.0 ± 3.4**

Table 4.2 Testing results of tuffaceous sandstone

Sample No.	Diameter (mm)	Length (mm)	Density (g/cc)	σ_c (MPa)	E (GPa)
TST-08-02-UCS-01	53.66	138.10	2.66	101.7	53.8
TST-01-02-UCS-02	53.66	132.36	2.68	123.8	54.5
TST-02-04-UCS-03	53.66	135.58	2.64	97.3	44.1
TST-06-09-UCS-04	53.66	135.15	2.67	145.9	47.5
TST-02-02-UCS-05	53.66	137.45	2.63	88.4	56.6
Average				**111.4 ± 23.3**	**51.3 ± 5.3**

Table 4.3 Testing results of silicified tuffaceous sandstone

Sample No.	Diameter (mm)	Length (mm)	Density (g/cc)	σ_c (MPa)	E (GPa)
SST-02-01-UCS-01	53.66	133.09	2.71	119.4	65.6
SST-07-01-UCS-02	53.66	135.47	2.67	93.0	63.2
SST-07-03-UCS-03	53.66	130.95	2.68	119.4	50.3
SST-02-06-UCS-04	53.66	134.75	2.69	161.4	66.1
SST-06-02-UCS-05	53.66	135.77	2.70	110.6	71.3
Average				**120.7 ± 25.2**	**63.3 ± 8.0**

Table 4.4 Uniaxial compressive strength and tangent elastic modulus measurement results of three rock types.

Rock Type	Number of Test Samples	Uniaxial Compressive Strength, σ_c (MPa)	Tangential Elastic Modulus, E_t (GPa)
Porphyritic andesite	50	115.0±15.0	43.0±3.4
Silicified-tuffaceous sandstone	50	120.7±25.2	63.3±8.0
Tuffaceous sandstone	50	111.4±23.3	51.3±5.3

4.2.2 Triaxial compressive strength tests

The objective of the triaxial compressive strength test is to determine the compressive strength of rock specimens under various confining pressures. The sample preparation and test procedure are followed the ASTM standard (ASTM D7012-07) and the ISRM suggested method (Brown, 1981). A total of 16 rock specimens are tested under various confining pressures: 6 specimens of porphyritic andesite, 5 specimens of silicified-tuffaceous sandstone, and 5 specimens of tuffaceous sandstone. The applied load onto the specimens is at constant rate until failure occurred within 5 to 10 minutes of loading under each confining pressure. The constant confining pressures used in this experiment are ranged from 0.345, 0.67, 1.38, 2.76, and 4.14 MPa (50, 100, 200, 400, and 600 psi) in andesite, 0.345, 0.69, 2.76, 4.14 and 5.52 MPa (50, 100, 400, 600, and 800 psi) in silicified-tuffaceous sandstone, and 0.345, 0.69, 1.38, 2.07, and 2.76 MPa (50, 100, 200, 300 and 400 psi) in pebbly tuffaceous sandstone. Post-failure characteristics are observed.

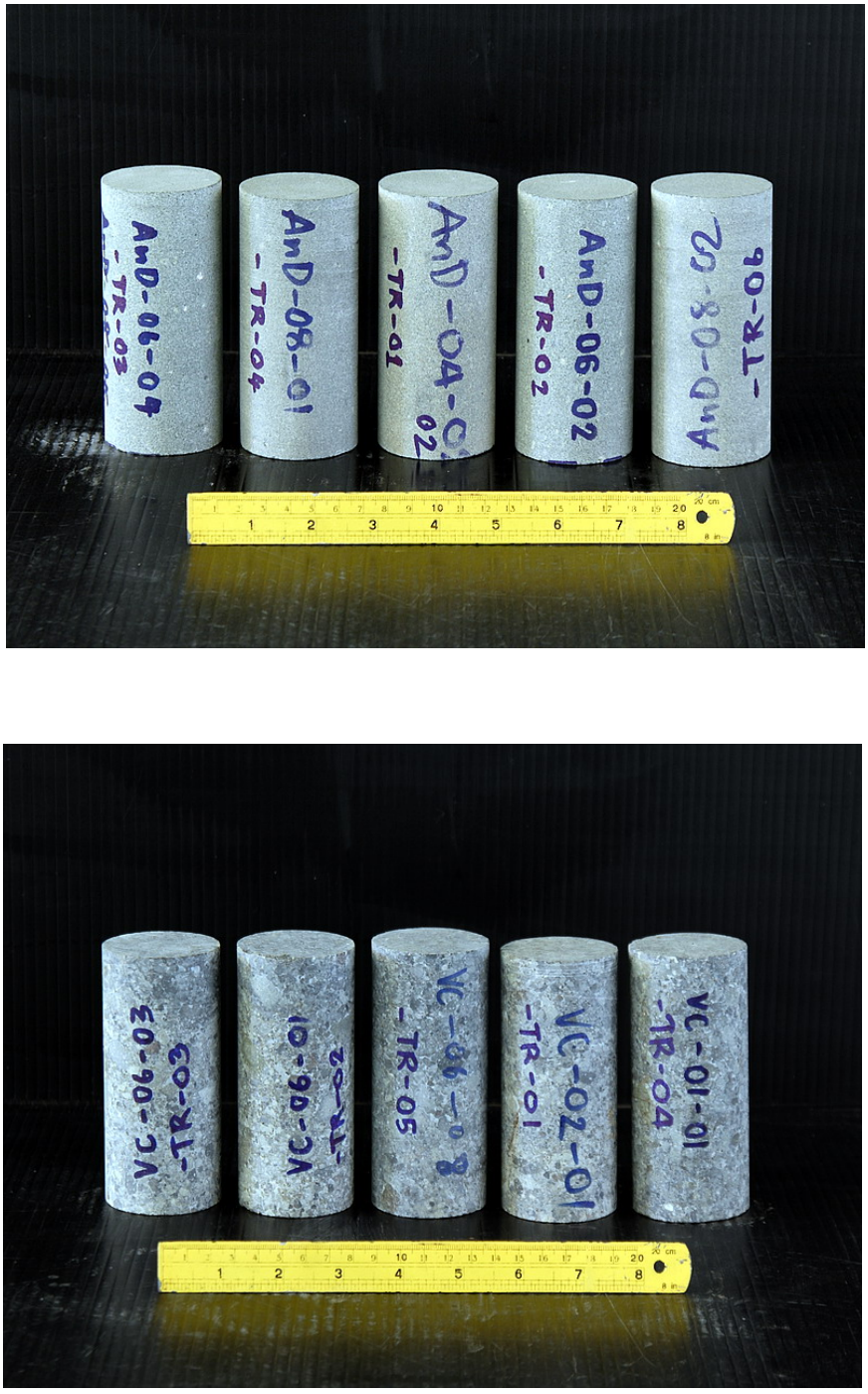

Figure 4.10 Pre-test samples for triaxial compressive strength test, the top is porphyritic andesite and the bottom is tuffaceous sandstone.

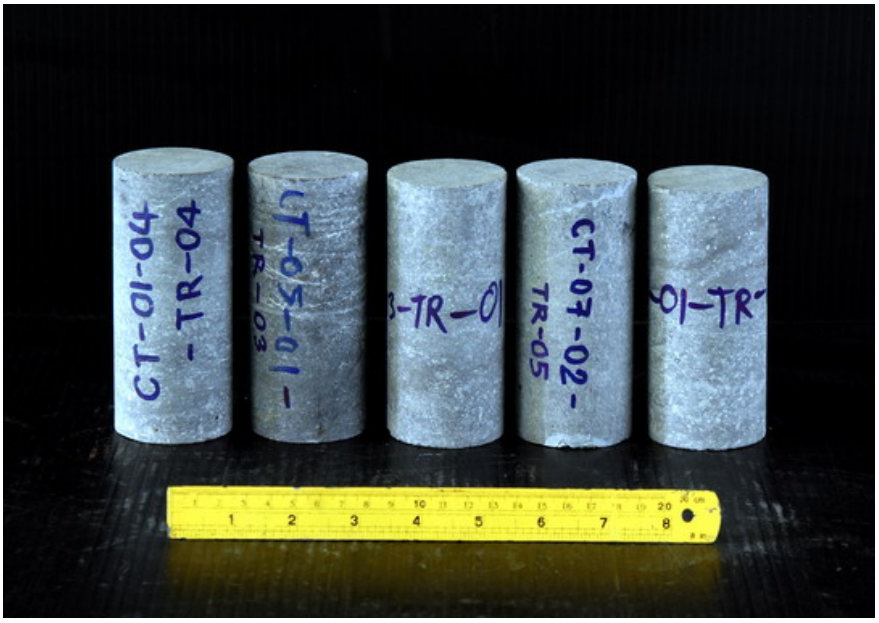

Figure 4.11 Pre-test samples of silicified tuffaceous sandstone for triaxial compressive strength test

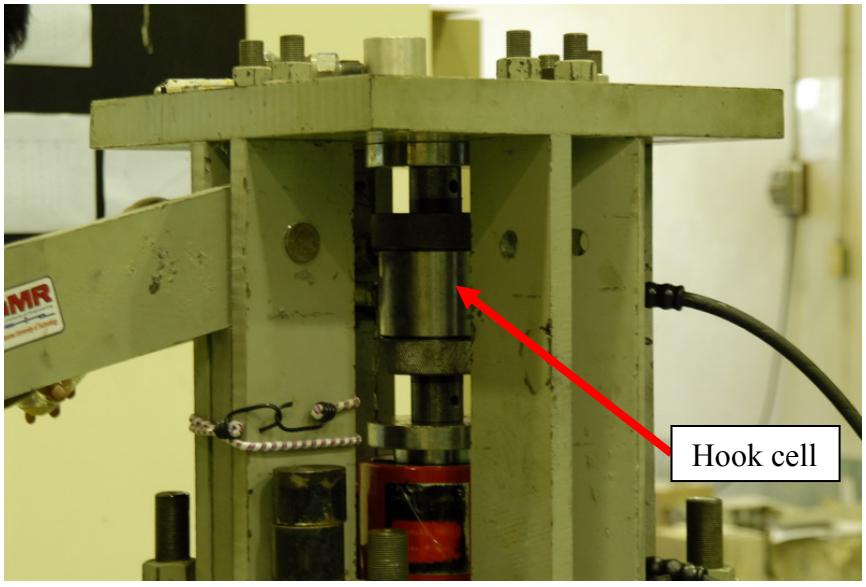

Figure 4.12 Triaxial testing apparatus

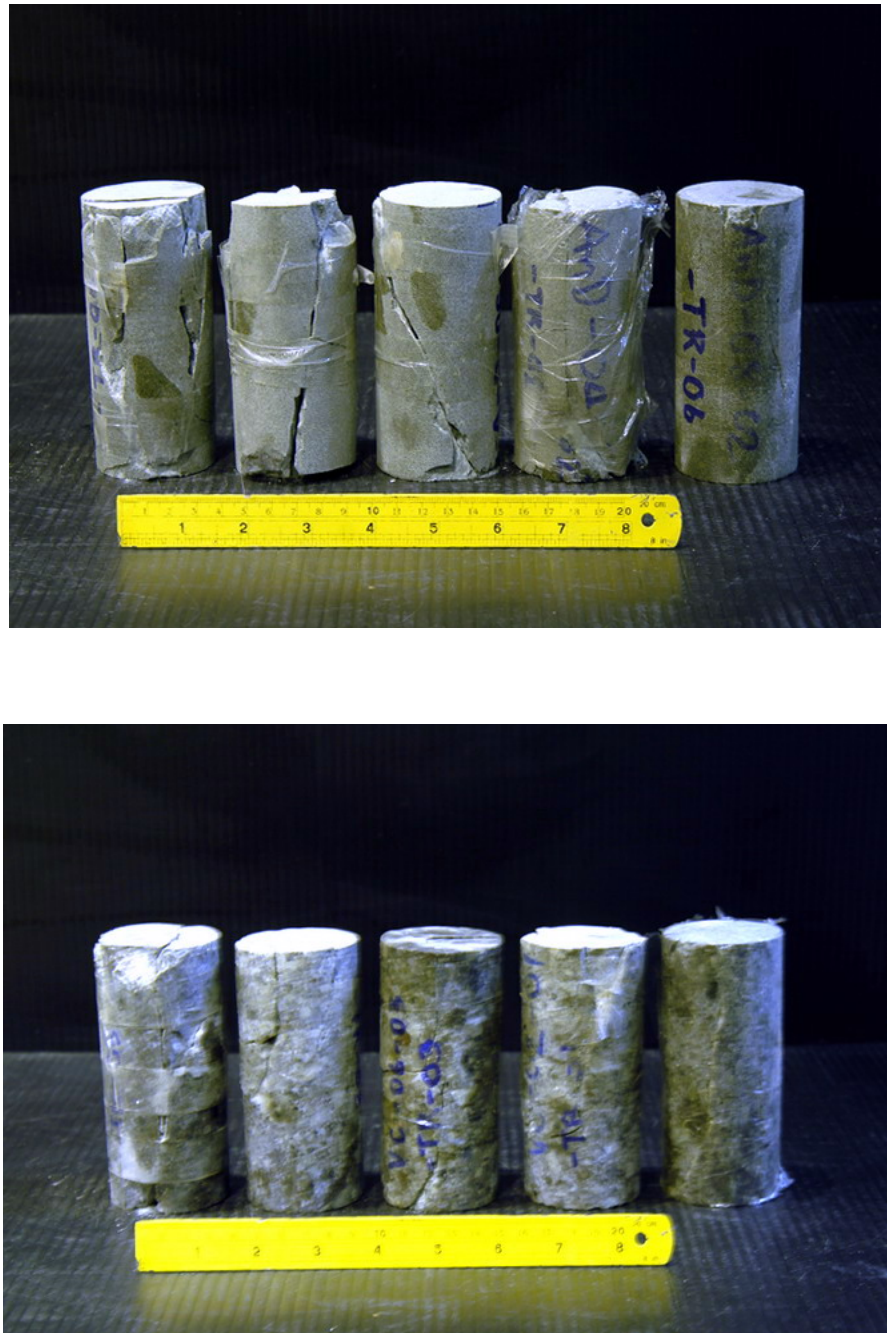

Figure 4.13 Post-test rock samples from triaxial compressive strength tests. The top is porphyritic andesite and the bottom is tuffaceous sandstone

Figure 4.14 Post-test rock samples of silicified tuffaceous sandstone from triaxial compressive strength test

Table 4.5 Triaxial compressive strength testing results of porphyritic andesite

Sample No.	Length (mm)	Diameter (mm)	Density (g/cc)	σ_3 (MPa)	σ_1 (MPa)
And-04-02-TR-01	108.03	53.66	2.85	0.4	145.9
And-06-04-TR-03	108.06	53.66	2.84	0.7	152.6
And-06-02-TR-02	108.06	53.66	2.83	1.4	163.6
And-08-01-TR-04	106.65	53.66	2.84	2.8	203.4
And-08-02-TR-05	109.48	53.66	2.83	4.1	252.0

Table 4.6 Triaxial compressive strength testing results of tuffaceous sandstone

Sample No.	Length (mm)	Diameter (mm)	Density (g/cc)	σ_3 (MPa)	σ_1 (MPa)
TST-01-01-TR-04	109.89	53.66	2.66	0.4	106.1
TST 02-01-TR-01	108.52	53.66	2.62	0.7	123.8
TST-06-01-TR-02	108.89	53.66	2.64	1.38	141.5
TST-06-03-TR-03	107.55	53.66	2.64	2.01	181.3
TST-06-08-TR-05	110.25	53.66	2.67	2.8	205.6

Table 4.7 Triaxial compressive strength testing results of silicified tuffaceous sandstone

Sample No.	Length (mm)	Diameter (mm)	Density (g/cc)	σ_3 (MPa)	σ_1 (MPa)
SST-05-01-TR-01	108.75	53.66	2.66	0.4	130.5
SST-07-02-TR-02	107.90	53.66	2.66	1.4	137.1
SST-01-04-TR-03	110.22	53.66	2.67	2.8	159.2
SST-01-03-TR-04	107.13	53.66	2.67	4.1	190.1
SST-01-01-TR-05	105.30	53.66	2.65	5.5	225.5

The results of triaxial tests are shown in Table 4.2. Figures 4.13 and 4.14 show the shear failure by triaxial loading at various confining pressures (σ_3) for the three rock types. The relationship between σ_1 and σ_3 can be represented by the Coulomb criterion (Hoek, 1990):

$$\tau = c + \sigma \tan \phi_i \tag{4.4}$$

where τ is the shear stress, c is the cohesion, σ is the normal stress, and ϕ_i is the internal friction angle. The parameters c and ϕ_i are determined by Mohr-Coulomb diagram as shown in Figures 4.15 through 4.17

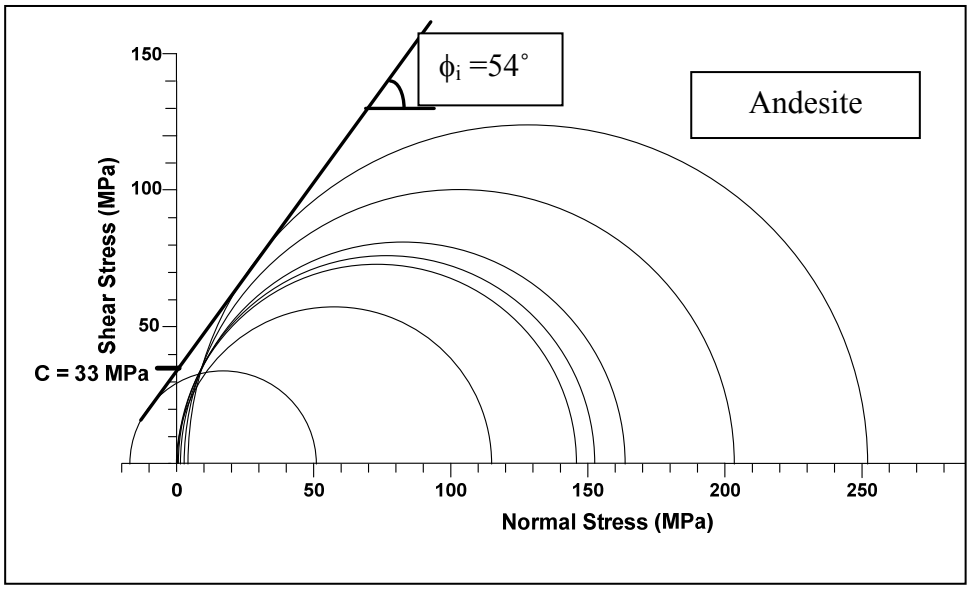

Figure 4.15 Mohr-Coulomb diagram for andesite

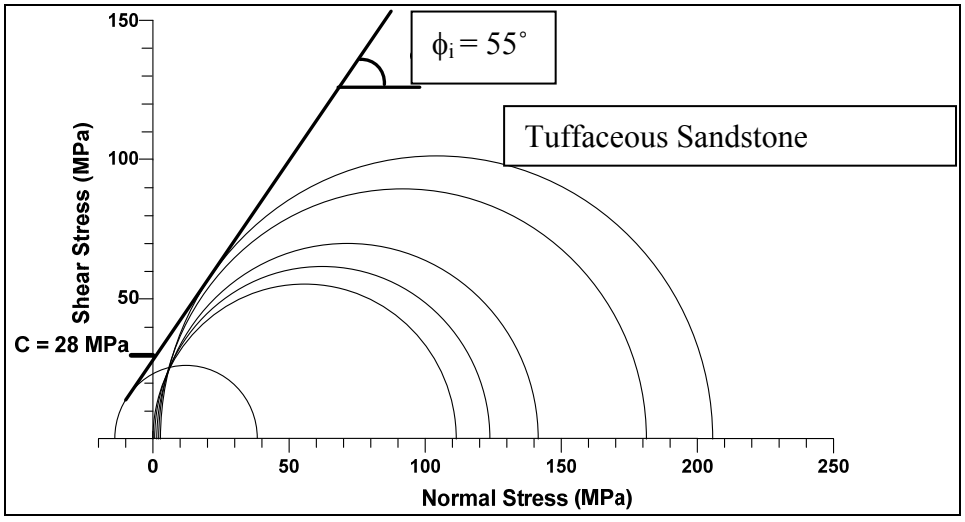

Figure 4.16 Mohr-Coulomb diagram for pebbly tuffaceous sandstone

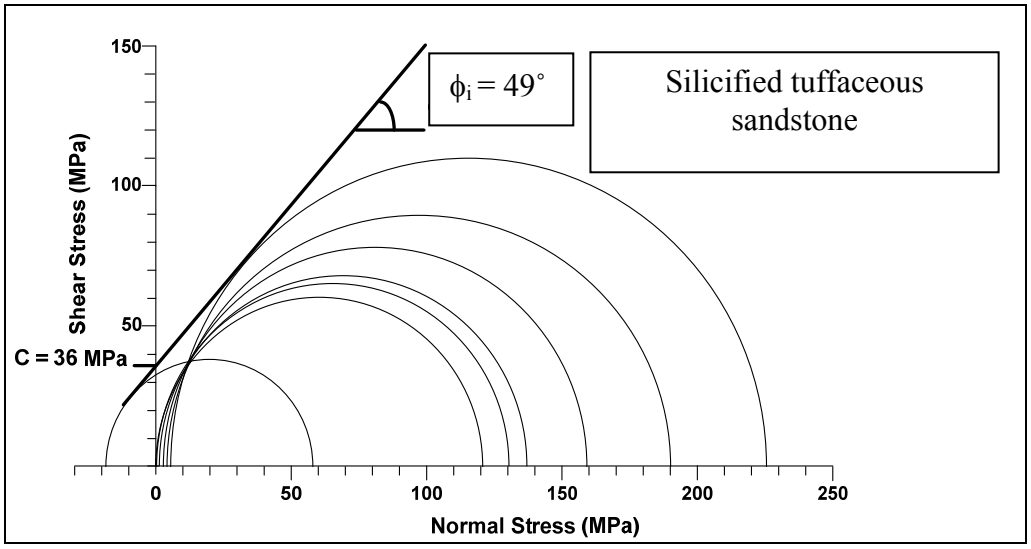

Figure 4.17 Mohr-Coulomb diagram for silicified tuffaceous sandstone

Table 4.8 Results of triaxial compressive strength tests on three rock types.

Rock Type	Number of Samples	Average Density (g/cc)	Cohesion, c (MPa)	Internal Friction Angle, ϕ_i (degrees)
Porphyritic Andesite	5	2.83	33	54
Tuffaceous Sandstone	5	2.65	28	55
Silicified Tuffaceous Sandstone	5	2.67	36	49

4.2.3 Brazilian Tensile Strength Tests

The objectives of the Brazilian tensile strength test are to determine the tensile strength of rock. The Brazilian tensile strength tests are performed on all rock types. Sample preparation and test procedure are followed the ASTM standard (ASTM D3967-81) and the

ISRM suggested method (Brown, 1981). Ten specimens for each rock type have been tested. The specimens have the diameter of 55 mm with 25 mm thick.

The Brazilian tensile strength of rock can be calculated by the following equation (Jaeger and Cook, 1979):

$$\sigma_B = (2p_f)/ (\pi Dt) \quad (4.5)$$

where σ_B is the Brazilian tensile strength, p_f is the failure load, D is the diameter of disk specimen, and t is the thickness of disk specimen. All of specimens failed along the loading diameter (Figure 4.20). The results of Brazilian tensile strengths are shown in Table 4.9. The tensile strength trends to decrease as the specimen size (diameter) increase, and can be expressed by a power equation (Evans, 1961):

$$\sigma_B = A\ (D)^{-B} \quad (4.6)$$

where A and B are constants depending upon the nature of rock.

4.2.4 Conventional point load index (CPL) tests

The objectives of CPL tests are to determine the point load strength index for use in the estimation of the compressive strength of the rocks. The sample preparation, test procedure, and calculation are followed the standard practices (ASTM D 5731-02) and the ISRM suggested method (Brown, 1981). Twenty specimens of each rock types are tested. The length-to-diameter (L/D) ratio of the specimen is constant at 1.0. The specimen diameter and thickness are maintained constant at 54 mm (Figure 4.21). The core specimen is loaded along its axis, as shown in Figure 4.22. Each specimen is loaded to failure at a constant rate such that

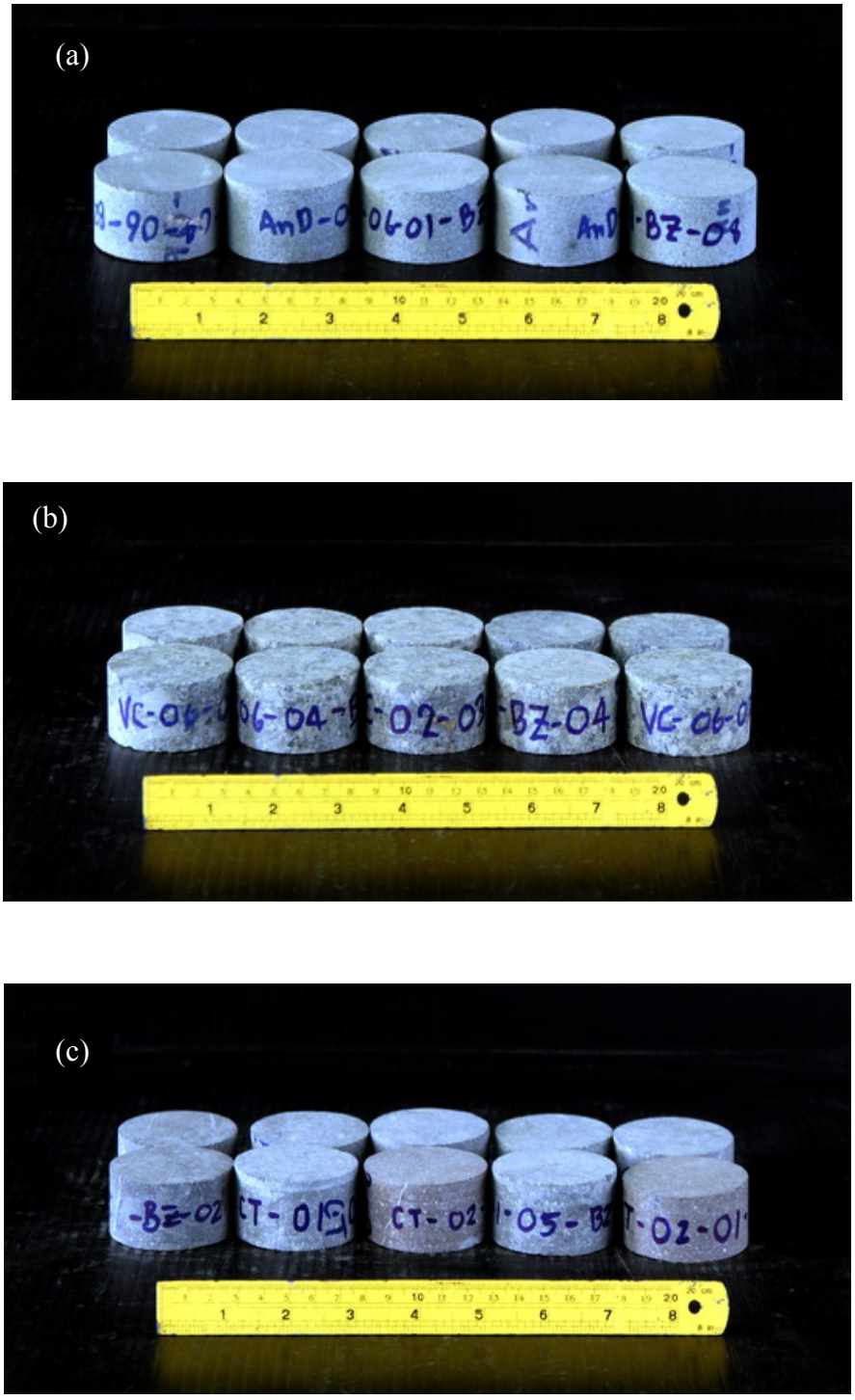

Figure 4.18 Pre-test samples for Brazilian tensile strength test, (a) porphyritic andesite, (b) tuffaceous sandstone, and (c) silicified tuffaceous sandstone

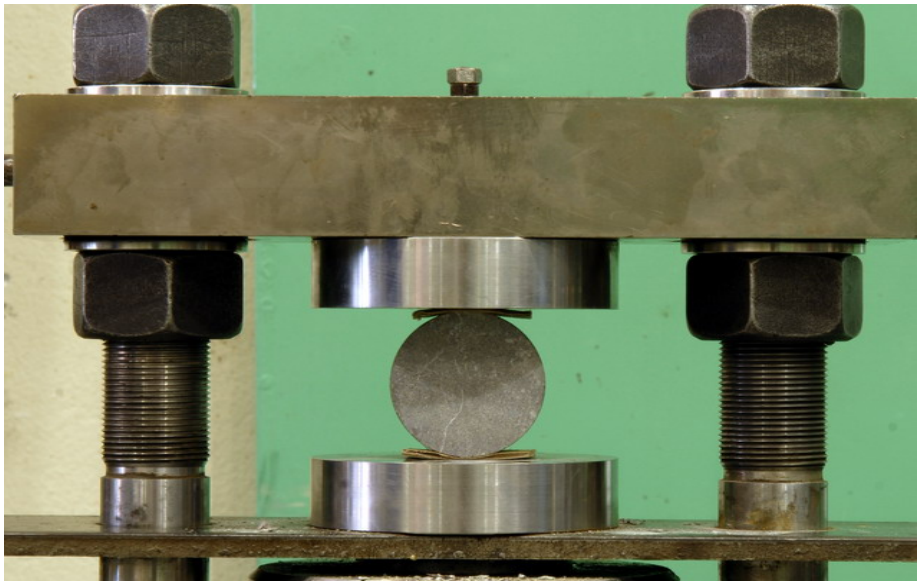

Figure 4.19 Brazilian tensile strength test arrangement.

Table 4.9 Results of Brazilian tensile strength tests of three rock types.

Rock Type	Average Diameter (mm)	Average Length (mm)	Average Density (g/cc)	Number of Samples	Brazilian Tensile Strength, σ_B (MPa)
Porphyritic andesite	53.66	26.72	2.83	10	17.0±1.6
Tuffaceous sandstone	53.66	27.37	2.65	10	13.1±3.3
Silicified tuffaceous sandstone	53.66	26.70	2.67	10	19.1±3.2

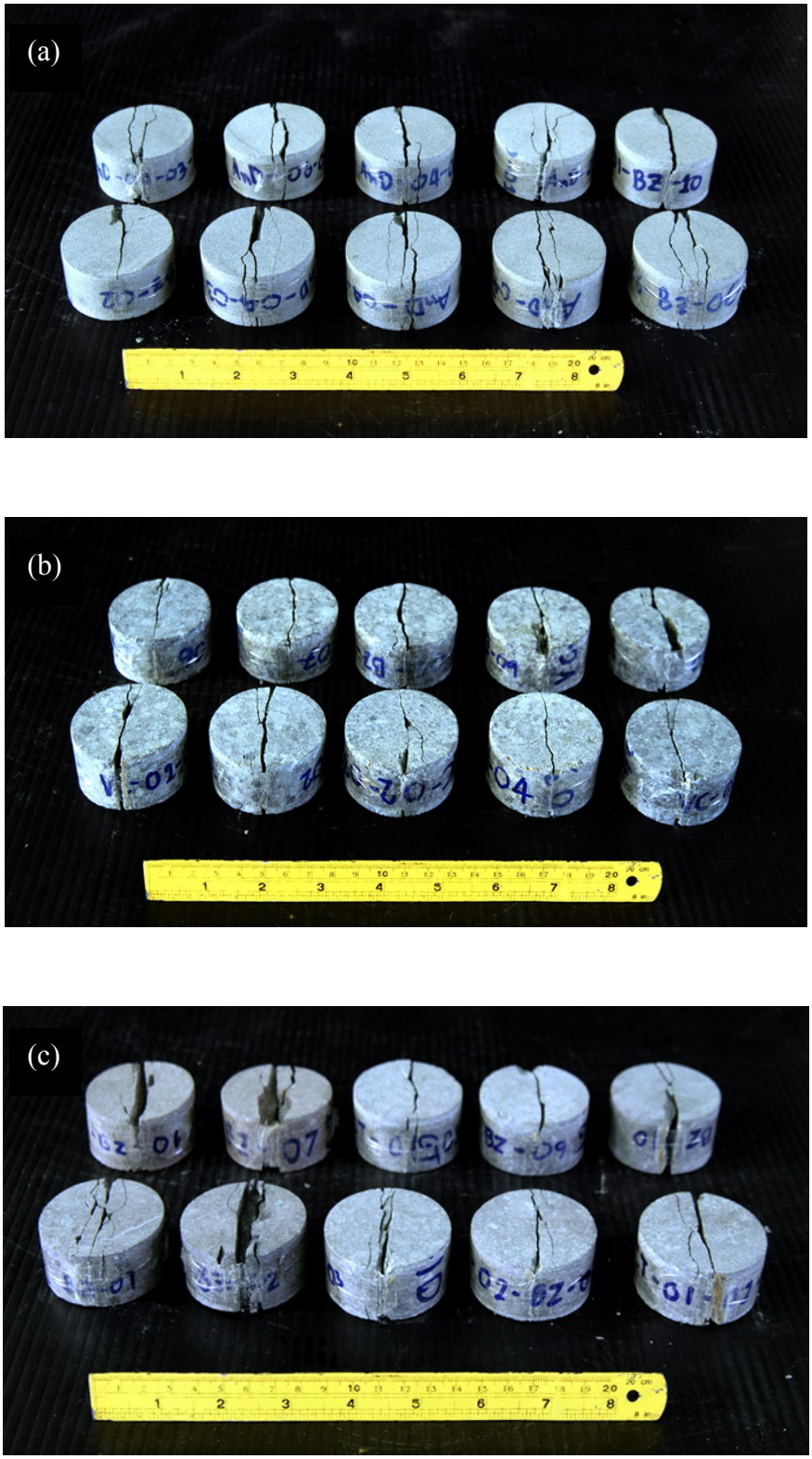

Figure 4.20 Post-test specimens (a) porphyritic andesite, (b) tuffaceous sandstone and (c) silicified tuffaceous sandstone

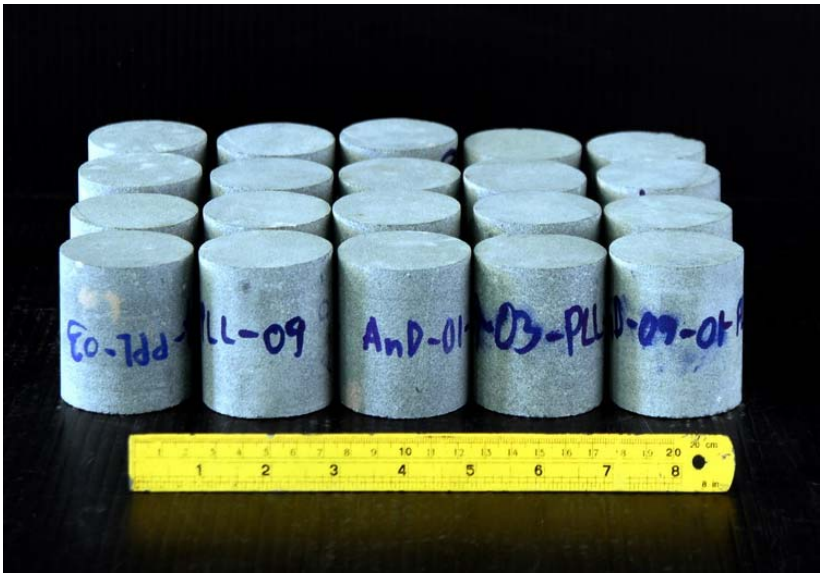

Figure 4.21 Pre-test samples of porphyritic andesite for conventional point load strength index test.

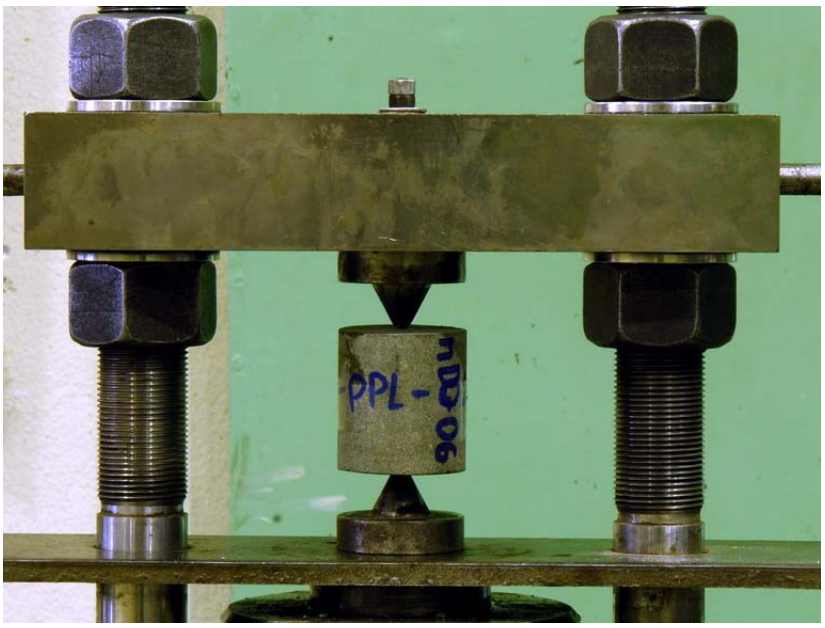

Figure 4.22 Conventional point load strength index test arrangement.

failures occur within 5-10 minutes. Post-failure characteristics are observed.

The point load strength index for axial loading (I_s) is calculated by the equation:

$$I_s = p_f / D_e^2 \tag{4.7}$$

where p_f is the load at failure, D_e is the equivalent core diameter (for axial loading, $D_e^2 = 4A/\pi$, and A=WD), A is the minimum cross-sectional area of a plane through the platen contact points, W is the specimen width (thickness of core), and D is the specimen diameter. The post-test specimens are shown in Figure 4.23.

The testing results of all three rock types are shown in Table 4.10. The point load strength index of andesite, pebbly tuffaceous sandstone, and silicified tuffaceous sandstone are average as 8.1 ± 1.2 , 10.2 ± 2.0, and 10.8 ± 2.2 MPa.

Table 4.10 Results of conventional point load strength index tests of three rock types.

Rock Types	Length (mm)	Diameter (mm)	Density (g/cc)	Point Load Strength Index, I_s (MPa)
Porphyritic Andesite	54.93	53.66	2.83	8.1±1.2
Tuffaceous Sandstone	55.45	53.66	2.65	10.2±2.0
Silicified Tuffaceous Sandstone	54.91	53.66	2.68	10.8±2.2

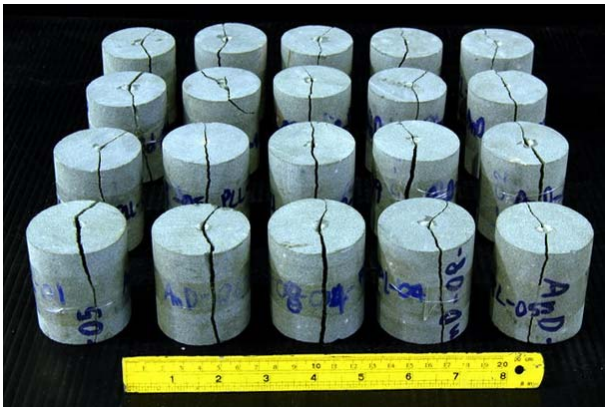

Figure 4.23 Post-Test rock specimens from conventional point load strength index tests. (a). porphyritic andesite (b). tuffaceous sandstone, and (c). silicified tuffaceous sandstone.

4.3 Modified point load (MPL) tests

The objectives of the modified point load (MPL) tests are to measure the strength of rock between the loading points and to produce failure stress results for various specimen sizes and shapes. The results are complied and evaluated to determine the mathematical relationship between the strengths and specimen dimensions, which are used to predict the elastic modulus and uniaxial and triaxial compressive strengths, and Brazilian tensile strength of the rocks.

The testing apparatus for the proposed MPL testing are similar to those of the conventional point load (CPL) test, except that the loading points are cylindrical shape and cut flat with the circular cross-sectional area instead of using half-spherical shape (Tepnarong, 2001). The loading platens used in this research are 7, 10, and 15 mm in diameter and the thickness-to-loading point diameter ratio (t/d) of about 2.5. The specimen diameter-to-loading point diameter is varying from 5 to 100. The load is applied at the rate of 200 N/s. Fifty specimens are prepared and tested for each rock type. The vertical deformations (δ) are monitored. One cycle of unloading and reloading is made at about 40% failure load. Then the load is increased to failure. The MPL strength (P_{MPL}) is calculated by:

$$P_{MPL} = p_f / ((\pi/4)(d^2)) \tag{4.8}$$

where p_f is the applied load at failure and d is the diameter of loading point. Figure 2.6 shows the example of post-test specimen, shear cone are usually formed underneath the loading points and two or three tension-induced cracks are commonly found across the specimens.

The MPL testing method is divided into 4 schemes based on its objective: elastic modulus, uniaxial and triaxial compressive strengths and Brazilian tensile strength determination.

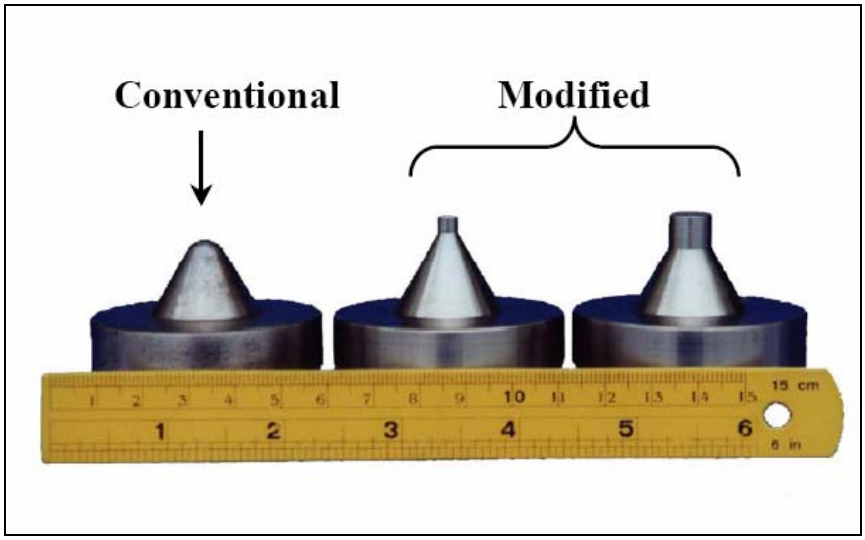

Figure 4.24 Conventional and modified loading points.(Tepnarong, 2006)

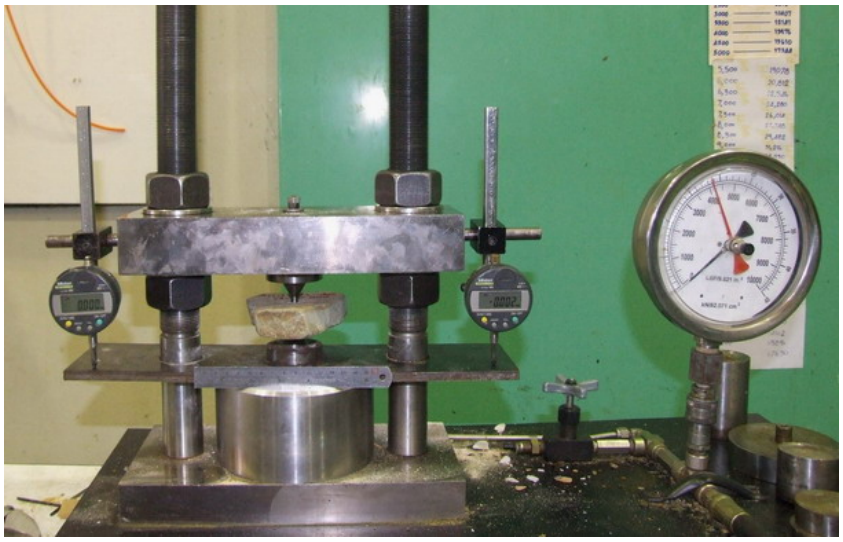

Figure 4.25 MPL testing arrangement.

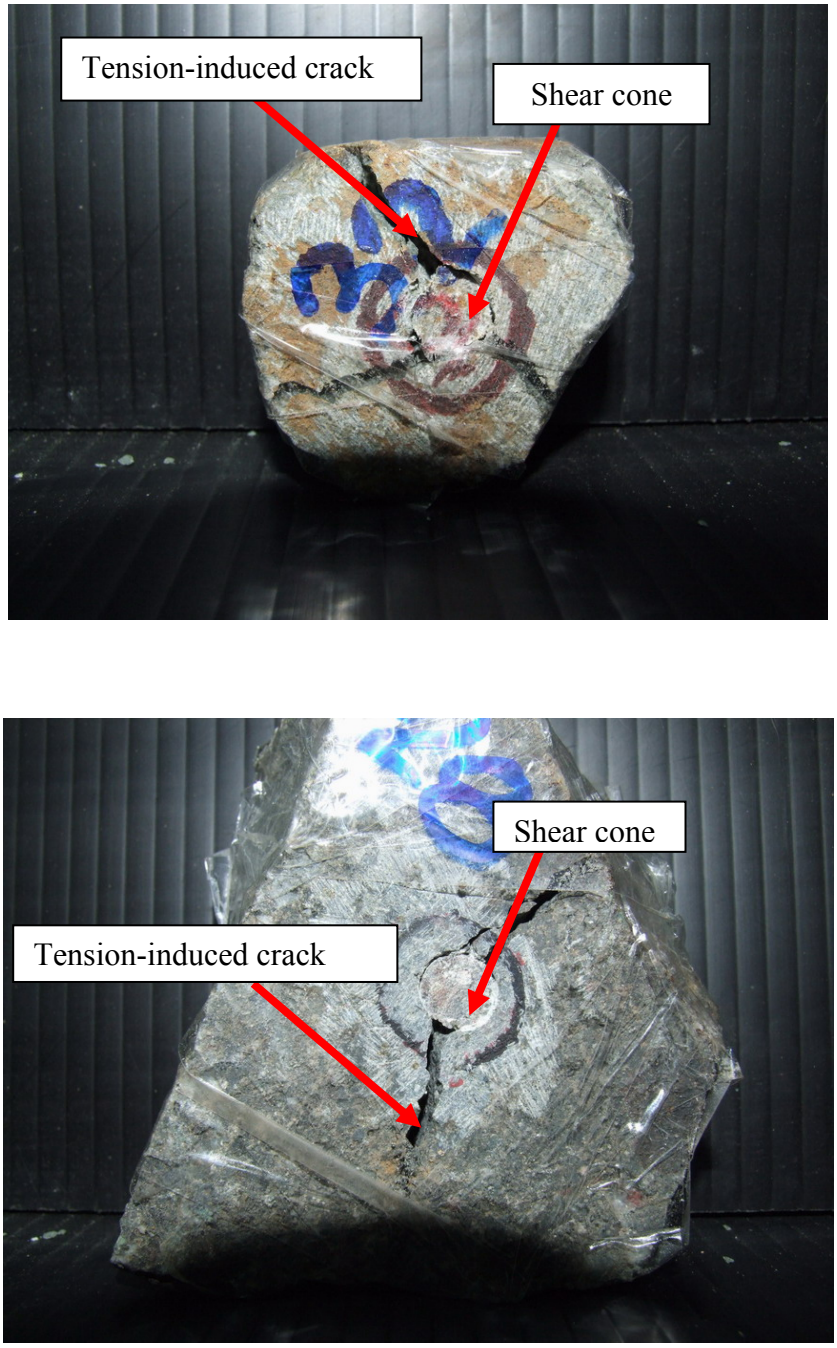

Figure 4.26 Post-test specimen, the tension-induced crack commonly found across the specimen and shear cone usually formed underneath the loading platens.

Table 4.11 Results of modified point load tests on porphyritic andesite

Specimen Number	t/d	D_e/d	Failure Load, p_f (kN)	$\Delta P/\Delta\delta$ (GPa/mm)	P_{mpl} (MPa)
And-MPL-01	2.46	5.43	28.0	1.25	159
And-MPL-02	3.51	6.32	37.0	1.80	471
And-MPL-03	2.36	6.34	15.0	1.70	191
And-MPL-04	2.66	9.60	25.0	2.34	319
And-MPL-05	2.84	9.03	37.0	3.69	471
And-MPL-06	2.45	7.93	28.0	1.82	357
And-MPL-07	2.63	8.74	26.0	2.34	331
And-MPL-08	2.61	9.80	21.0	1.71	268
And-MPL-09	2.80	7.77	27.0	0.56	344
And-MPL-10	2.44	5.69	28.0	1.24	159
And-MPL-11	2.51	6.13	65.0	1.38	368
And-MPL-12	2.26	6.31	60.0	1.89	340
And-MPL-13	2.33	11.26	18.0	1.51	468
And-MPL-14	2.79	12.03	22.0	1.65	572
And-MPL-15	2.39	5.03	40.0	0.11	227
And-MPL-16	2.81	4.74	30.0	0.12	170
And-MPL-17	3.05	8.61	39.0	0.21	497
And-MPL-18	2.33	6.53	50.0	0.08	283
And-MPL-19	2.94	13.86	38.0	2.00	484
And-MPL-20	2.65	8.60	41.0	0.17	522
And-MPL-21	2.38	4.25	55.0	0.87	311
And-MPL-22	2.30	4.17	45.0	0.87	255
And-MPL-23	2.23	5.57	50.0	2.31	283
And-MPL-24	2.50	7.60	55.0	1.12	311
And-MPL-25	2.59	12.43	18.0	5.85	468
And-MPL-26	3.03	5.60	31.0	1.43	395
And-MPL-27	2.73	16.40	39.0	1.56	497
And-MPL-28	2.82	9.06	22.0	2.00	280
And-MPL-29	3.11	9.34	29.0	1.56	369
And-MPL-30	2.46	13.14	25.0	6.50	650
And-MPL-31	2.62	9.82	20.0	1.75	255
And-MPL-32	2.60	11.47	18.0	1.56	468
And-MPL-33	2.40	7.00	45.0	1.01	255
And-MPL-34	3.04	8.00	24.0	1.35	306
And-MPL-35	2.50	4.55	22.0	1.27	280
And-MPL-36	2.43	16.97	12.0	2.92	312
And-MPL-37	3.33	15.20	31.0	1.56	395
And-MPL-38	2.38	6.61	17.0	2.60	442

Table 4.11 Results of modified point load tests on porphyritic andesite (Continued).

Specimen Number	t/d	D_e/d	Failure Load, p_f (kN)	$\Delta P/\Delta\delta$ (GPa/mm)	P_{mpl} (MPa)
And-MPL-39	3.18	3.47	13.0	1.86	338
And-MPL-40	2.45	5.51	15.0	2.60	390
And-MPL-41	2.07	5.61	15.0	3.25	390
And-MPL-42	2.23	4.25	50.0	2.31	283
And-MPL-43	2.07	5.61	15.0	3.46	390
And-MPL-44	3.24	3.40	31.0	2.34	395
And-MPL-45	2.75	4.26	24.0	1.69	306
And-MPL-46	3.02	3.97	13.0	1.75	166
And-MPL-47	2.55	3.14	10.0	1.70	127
And-MPL-48	2.57	2.20	25.0	0.94	142
And-MPL-49	2.56	2.14	13.0	0.57	74
And-MPL-50	2.43	1.66	18.0	0.78	102

Table 4.12 Results of modified point load tests on tuffaceous sandstone.

Specimen Number	t/d	D_e/d	Failure Load, p_f (kN)	$\Delta P/\Delta\delta$ (GPa/mm)	P_{mpl} (MPa)
TST -MPL-01	2.70	5.46	22.0	2.12	293
TST -MPL-02	2.58	7.87	23.0	3.26	293
TST -MPL-03	2.75	7.30	20.0	1.43	255
TST -MPL-04	2.82	7.15	40.0	1.43	510
TST -MPL-05	2.54	13.45	22.0	2.64	280
TST -MPL-06	2.92	8.93	20.0	1.43	255
TST -MPL-07	2.43	8.53	55.0	1.12	311
TST -MPL-08	2.87	10.47	21.0	3.19	268
TST -MPL-09	2.30	7.87	37.0	2.12	471
TST -MPL-10	2.30	4.27	26.0	1.32	147
TST -MPL-11	2.82	12.43	45.0	3.19	573
TST -MPL-12	2.54	6.04	20.0	1.27	255
TST -MPL-13	2.88	11.80	29.0	1.59	369
TST -MPL-14	2.51	6.31	41.0	1.70	232
TST -MPL-15	2.14	11.04	12.0	2.60	312
TST -MPL-16	2.29	4.86	38.0	1.02	215
TST -MPL-17	2.59	7.15	11.0	6.50	286
TST -MPL-18	2.43	2.85	18.0	0.73	102
TST -MPL-19	2.85	3.16	13.0	1.28	130
TST -MPL-20	2.41	2.95	18.0	1.70	102
TST -MPL-21	2.98	4.17	30.0	1.00	170
TST -MPL-22	2.65	6.42	30.0	0.88	170
TST -MPL-23	3.14	6.11	45.0	1.01	255
TST -MPL-24	3.03	4.81	65.0	1.24	368
TST -MPL-25	2.23	2.23	26.0	1.26	331
TST -MPL-26	2.73	6.52	26.0	1.78	331
TST -MPL-27	2.16	8.87	42.0	1.70	535
TST -MPL-28	3.19	7.18	29.0	1.64	369
TST -MPL-29	2.31	5.16	20.0	1.28	255
TST -MPL-30	2.60	6.41	38.0	2.80	484
TST -MPL-31	2.87	4.96	33.0	1.58	420
TST -MPL-32	2.64	3.68	23.0	1.70	293
TST -MPL-33	2.38	4.15	23.0	1.30	293
TST -MPL-34	2.71	8.24	14.0	2.60	364
TST -MPL-35	2.83	8.00	22.0	3.25	572
TST -MPL-36	2.42	10.13	18.0	3.25	468
TST -MPL-37	2.54	7.15	9.0	2.17	234
TST -MPL-38	2.10	7.55	15.0	5.20	390

Table 4.12 Results of modified point load tests on tuffaceous sandstone (Continued).

Specimen Number	t/d	D_e/d	Failure Load, p_f (kN)	$\Delta P/\Delta\delta$ (GPa/mm)	P_{mpl} (MPa)
TST -MPL-39	2.93	5.08	11.0	2.60	286
TST -MPL-40	2.73	4.10	10.0	3.47	260
TST -MPL-41	2.34	6.28	8.0	2.60	208
TST -MPL-42	2.59	4.33	13.0	2.60	338
TST -MPL-43	2.65	5.46	22.0	4.35	280
TST -MPL-44	2.55	8.29	26.0	2.22	147
TST -MPL-45	2.54	3.68	24.0	3.15	306
TST -MPL-46	2.93	6.95	37.0	2.22	210
TST -MPL-47	2.47	2.97	18.0	1.28	102
TST -MPL-48	3.10	6.11	30.0	2.37	170
TST -MPL-49	2.25	3.37	16.0	3.71	416
TST -MPL-50	2.59	4.10	12.0	3.94	312

Table 4.13 Results of modified point load tests on silicified tuffaceous sandstone.

Specimen Number	t/d	De/d	Failure Load, p_f (kN)	$\Delta P/\Delta\delta$ (GPa/mm)	P_{mpl} (MPa)
SST-MPL-01	3.00	7.82	17.0	2.80	442
SST-MPL-02	2.50	4.80	22.0	3.07	572
SST-MPL-03	3.14	4.24	34.0	3.56	433
SST-MPL-04	2.92	8.09	22.0	4.50	572
SST-MPL-05	2.75	11.42	30.0	5.32	780
SST -MPL-06	3.08	4.90	19.0	2.73	494
SST -MPL-07	3.17	6.11	28.0	4.18	728
SST -MPL-08	2.33	6.84	24.0	4.14	624
SST -MPL-09	2.55	4.80	23.0	3.71	598
SST -MPL-10	2.17	7.72	12.0	9.58	312
SST -MPL-11	3.12	9.03	27.0	4.00	702
SST -MPL-12	2.55	10.94	15.0	2.72	390
SST -MPL-13	2.86	7.42	40.0	4.08	510
SST -MPL-14	2.48	6.15	35.0	2.96	198
SST -MPL-15	2.53	8.05	21.0	2.82	546
SST -MPL-16	2.43	10.94	15.0	2.60	390

Table 4.13 Results of modified point load tests on silicified tuffaceous sandstone (Continued).

Specimen Number	t/d	D/d	Failure Load, p_f (kN)	$\Delta P/\Delta\delta$ (GPa/mm)	P_{mpl} (MPa)
SST-MPL-17	2.34	10.90	25.0	4.16	650
SST -MPL-18	2.53	13.71	24.0	4.73	624
SST -MPL-19	3.27	4.34	32.0	3.30	408
SST -MPL-20	2.70	3.10	39.0	2.78	497
SST -MPL-21	2.69	6.91	41.0	1.85	522
SST -MPL-22	3.12	5.04	38.0	1.82	484
SST -MPL-23	3.19	6.27	26.0	1.50	331
SST -MPL-24	2.81	6.89	33.0	2.95	420
SST -MPL-25	2.10	7.20	39.0	2.59	497
SST -MPL-26	3.03	7.75	37.0	2.21	471
SST -MPL-27	2.72	7.14	31.0	2.74	395
SST -MPL-28	2.92	8.55	60.0	2.09	764
SST -MPL-29	3.10	7.42	40.0	1.76	510
SST -MPL-30	2.84	8.47	41.0	1.58	522
SST -MPL-31	3.20	8.91	65.0	4.64	828
SST -MPL-32	2.61	2.56	40.0	1.78	226
SST -MPL-33	2.24	4.05	55.0	1.31	311
SST -MPL-34	2.31	3.79	45.0	2.15	255
SST -MPL-35	2.90	4.42	105.0	1.90	594
SST -MPL-36	2.41	5.21	50.0	1.02	283
SST -MPL-37	2.75	6.05	60.0	0.67	340
SST -MPL-38	2.63	6.16	65.0	1.27	368
SST -MPL-39	2.27	6.15	35.0	2.29	198
SST -MPL-40	2.36	5.08	55.0	0.90	311
SST -MPL-41	3.18	11.42	30.0	4.98	780
SST -MPL-42	3.03	8.09	21.0	3.92	546
SST -MPL-43	2.28	8.05	21.0	2.44	546
SST -MPL-44	2.83	11.42	30.0	5.71	780
SST -MPL-45	2.77	7.72	12.0	7.80	312
SST -MPL-46	2.88	12.06	28.0	4.11	728
SST -MPL-47	2.50	5.08	57.0	3.09	323
SST -MPL-48	2.75	4.42	105.0	3.38	594
SST -MPL-49	2.72	6.05	65.0	2.54	368
SST -MPL-50	2.60	8.05	20.0	3.60	520

4.3.1 Modified point load tests for elastic modulus measurement

The MPL tests are carried out with the measurement of axial deformation for use in elastic modulus estimation. Fifty irregular specimens for each rock type are tested. The specimen thickness-to-loading diameter (t/d) is about 2.5 and the specimen diameter -to-loading diameter (D/d) is varied from 25 to 50. Cyclic loading is performed while monitoring displacement (δ).

The testing apparatus used in this experiment includes the point load tester model SBEL PLT-75 and the modified point load platens. The displacement digital gages with a precision up to 0.001 mm are used to monitor the axial deformation of rock between the loading points as loading decreases. The cyclic load is applied along the specimen axis and is performed by systematically increasing and decreasing loads on the test specimen. After unloading, the axial load is increased until the failure occurs. Cyclic loading is performed on the specimens in an attempt at determining the elastic deformation. The ratio of change of stress to displacement ($\Delta P/\Delta\delta$) is measured from unloading curve. Post-failure characteristics are observed and recorded. Photographs are taken of the failed specimens.

The results of the deformation measurement by MPL tests are shown in Tables.4.11 through 4.13. The stresses (P) are plotted as a function of axial displacement (δ) and shown in Figures B.1 through B.150 (Appendix B). The results of $\Delta P/\Delta\delta$ are used to estimate the elastic modulus of the specimen.

The elastic modulus predictions from MPL results can be made by using the value of α_E plotted as a function of D_e/d for various t/d ratios as shown in Figure 4.27, and the MPL elastic modulus can be expressed as:

$$E_{mpl} = \left(\frac{t}{\alpha_E}\right)\left(\frac{\Delta P}{\Delta \delta}\right) \text{ (Tepnarong, 2006)} \quad (4.9)$$

where E_{mpl} is the elastic modulus predicted from MPL results, α_E is displacement function value from numerical analysis and $\Delta P/\Delta\delta$ is the ratio of change of stress to displacement which is measured from unloading curve of MPL tests and t is the specimen thickness. The value of α_E used in the calculation is 2.60 for t/d ratio equal to 2.5-3.0 (Tepnarong, 2006). The results of elastic modulus predictions from MPL tests are tabulated in Tables 4.14 through 4.16. Table 4.17 compares the elastic modulus obtained from standard uniaxial compressive strength test (ASTM D3148-96) with those predicted by MPL test.

The values of E_{mpl} for each specimen with P-δ curve are shown in Appendix B. The MPL method under-estimates the elastic modulus of all tested rocks. This is the primarily because the actual loaded area may be smaller than that used in the calculation due to the roughness of the specimen surfaces. As a result the contact area used to calculate P_{MPL} is larger than the actual. In addition the E_{MPL} tends to show a high intrinsic variation (high standard deviation). This is because the loading areas of MPL specimens are small. This phenomenon conforms by the test results obtained by Fuenkajorn and Deamen (1992). They conclude that smaller test specimens not only exhibit a higher strength than larger one (size effect), but also show a high intrinsic variability due to the heterogeneity of rock fabric, particularly at small sizes. This implied that to obtain a good prediction (accurate result) of the rock elasticity, a large amount of MPL specimens are desirable. This drawback may be compensated by the ease of testing and the low cost of sample preparation.

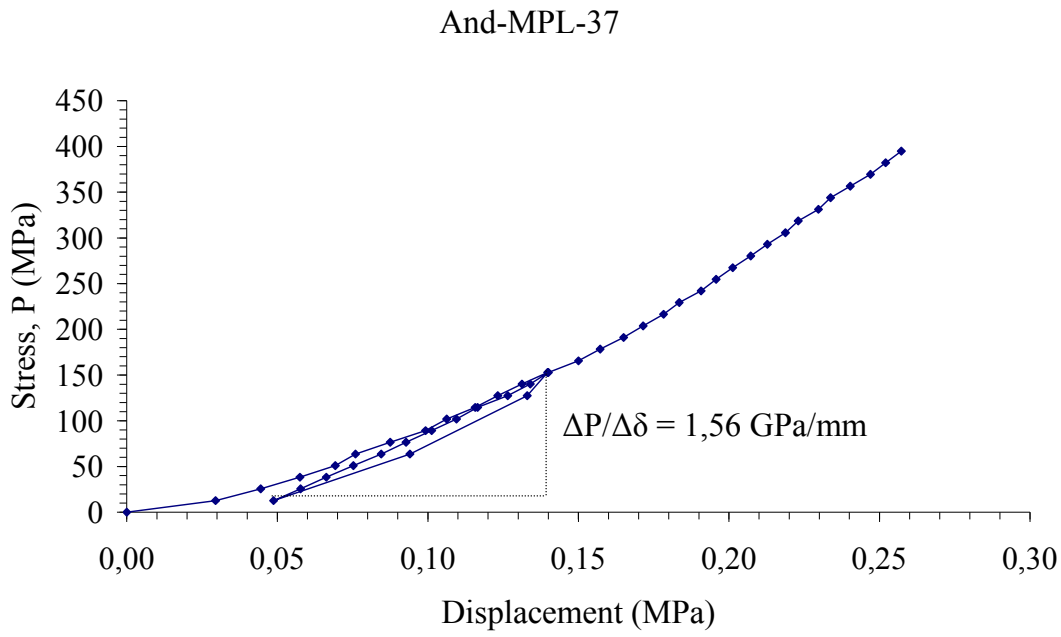

Figure 4.27 Example of P-δ curve for porphyritic andesite specimen. The ratio of ΔP/Δδ is used to predict the elastic modulus of MPL specimen (E_{mpl}).

Table 4.14 Results of elastic modulus calculation from MPL tests on porphyritic andesite.

Specimen Number	t/d	D_e/d	$\Delta P/\Delta\delta$ (GPa/mm)	α_E	$E_{mpl\ (GPa)}$
And-MPL-01	2.46	5.43	1.25	2.60	17.76
And-MPL-02	3.51	6.32	1.80	2.60	24.30
And-MPL-03	2.36	6.34	1.70	2.60	15.46
And-MPL-04	2.66	9.60	2.34	2.60	23.90
And-MPL-05	2.84	9.03	3.69	2.60	40.31
And-MPL-06	2.45	7.93	1.82	2.60	17.12
And-MPL-07	2.63	8.74	2.34	2.60	23.67
And-MPL-08	2.61	9.80	1.71	2.60	17.17
And-MPL-09	2.80	7.77	0.56	2.60	6.03
And-MPL-10	2.44	5.69	1.24	2.60	17.48
And-MPL-11	2.51	6.13	1.38	2.60	20.01
And-MPL-12	2.26	6.31	1.89	2.60	24.64
And-MPL-13	2.33	11.26	1.51	2.60	9.47
And-MPL-14	2.79	12.03	1.65	2.60	12.39
And-MPL-15	2.39	5.03	0.11	2.60	1.51
And-MPL-16	2.81	4.74	0.12	2.60	1.95
And-MPL-17	3.05	8.61	0.21	2.60	2.47
And-MPL-18	2.33	6.53	0.08	2.60	1.08
And-MPL-19	2.94	13.86	2.00	2.60	22.63
And-MPL-20	2.65	8.60	0.17	2.60	1.73
And-MPL-21	2.38	4.25	0.87	2.60	11.95
And-MPL-22	2.30	4.17	0.87	2.60	11.54
And-MPL-23	2.23	5.57	2.31	2.60	29.76
And-MPL-24	2.50	7.60	1.12	2.60	16.15
And-MPL-25	2.59	12.43	5.85	2.60	40.73
And-MPL-26	3.03	5.60	1.43	2.60	16.67
And-MPL-27	2.73	16.40	1.56	2.60	16.39
And-MPL-28	2.82	9.06	2.00	2.60	21.72
And-MPL-29	3.11	9.34	1.56	2.60	18.68
And-MPL-30	2.46	13.14	6.50	2.60	43.10
And-MPL-31	2.62	9.82	1.75	2.60	17.66
And-MPL-32	2.60	11.47	1.56	2.60	10.93
And-MPL-33	2.40	7.00	1.01	2.60	13.98
And-MPL-34	3.04	8.00	1.35	2.60	15.76
And-MPL-35	2.50	4.55	1.27	2.60	12.21
And-MPL-36	2.43	16.97	2.92	2.60	19.09
And-MPL-37	3.33	15.20	1.56	2.60	20.00
And-MPL-38	2.38	6.61	2.60	2.60	16.65
And-MPL-39	3.18	3.47	1.86	2.60	15.92
And-MPL-40	2.45	5.51	2.60	2.60	17.12

And-MPL-41	2.07	5.61	3.25	2.60	18.15

Table 4.14 Results of elastic modulus calculation from MPL tests on porphyritic andesite (continued).

Specimen Number	t/d	D_e/d	$\Delta P/\Delta\delta$ (GPa/mm)	α_E	$E_{mpl\ (GPa)}$
And-MPL-42	2.23	4.25	2.31	2.60	29.76
And-MPL-43	2.07	5.61	3.46	2.60	19.32
And-MPL-44	3.24	3.40	2.34	2.60	29.12
And-MPL-45	2.75	4.26	1.69	2.60	17.85
And-MPL-46	3.02	3.97	1.75	2.60	20.33
And-MPL-47	2.55	3.14	1.70	2.60	16.67
And-MPL-48	2.57	2.20	0.94	2.60	13.93
And-MPL-49	2.56	2.14	0.57	2.60	8.43
And-MPL-50	2.43	1.66	0.78	2.60	10.94
				Average	**17.43**
				Standard Deviation	**9.10**

Table 4.15 Results of elastic modulus calculation from MPL tests on silicified tuffaceous sandstone.

Specimen Number	t/d	D_e/d	$\Delta P/\Delta\delta$ (GPa/mm)	α_E	$E_{mpl\ (GPa)}$
SST -MPL-01	3.00	7.82	2.80	2.60	22.62
SST -MPL-02	2.50	4.80	3.07	2.60	20.66
SST -MPL-03	3.14	4.24	3.56	2.60	43.02
SST -MPL-04	2.92	8.09	4.50	2.60	35.33
SST -MPL-05	2.75	11.42	5.32	2.60	39.39
SST -MPL-06	3.08	4.90	2.73	2.60	22.66
SST -MPL-07	3.17	6.11	4.18	2.60	35.72
SST -MPL-08	2.33	6.84	4.14	2.60	25.95
SST -MPL-09	2.55	4.80	3.71	2.60	25.46
SST -MPL-10	2.17	7.72	9.58	2.60	55.93
SST -MPL-11	3.12	9.03	4.00	2.60	33.60
SST -MPL-12	2.55	10.94	2.72	2.60	18.64
SST -MPL-13	2.86	7.42	4.08	2.60	44.35
SST -MPL-14	2.48	6.15	2.96	2.60	42.35
SST -MPL-15	2.53	8.05	2.82	2.60	19.18
SST -MPL-16	2.43	10.94	2.60	2.60	16.98
SST -MPL-17	2.34	10.90	4.16	2.60	26.21
SST -MPL-18	2.53	13.71	4.73	2.60	32.24
SST -MPL-19	3.27	4.34	3.30	2.60	41.53
SST -MPL-20	2.70	3.10	2.78	2.60	28.63

Table 4.15 Results of elastic modulus calculation from MPL tests on silicified tuffaceous sandstone (continued).

Specimen Number	t/d	D_e/d	$\Delta P/\Delta\delta$ (GPa/mm)	α_E	$E_{mpl\ (GPa)}$
SST -MPL-21	2.69	6.91	1.85	2.60	19.14
SST -MPL-22	3.12	5.04	1.82	2.60	21.83
SST -MPL-23	3.19	6.27	1.50	2.60	18.39
SST -MPL-24	2.81	6.89	2.95	2.60	31.93
SST -MPL-25	2.10	7.20	2.59	2.60	20.90
SST -MPL-26	3.03	7.75	2.21	2.60	25.77
SST -MPL-27	2.72	7.14	2.74	2.60	28.62
SST -MPL-28	2.92	8.55	2.09	2.60	23.50
SST -MPL-29	3.10	7.42	1.76	2.60	20.97
SST -MPL-30	2.84	8.47	1.58	2.60	17.28
SST -MPL-31	3.20	8.91	4.64	2.60	57.07
SST -MPL-32	2.61	2.56	1.78	2.60	26.78
SST -MPL-33	2.24	4.05	1.31	2.60	16.90
SST -MPL-34	2.31	3.79	2.15	2.60	28.63
SST -MPL-35	2.90	4.42	1.90	2.60	31.74
SST -MPL-36	2.41	5.21	1.02	2.60	14.16
SST -MPL-37	2.75	6.05	0.67	2.60	10.64
SST -MPL-38	2.63	6.16	1.27	2.60	19.26
SST -MPL-39	2.27	6.15	2.29	2.60	30.05
SST -MPL-40	2.36	5.08	0.90	2.60	12.26
SST -MPL-41	3.18	11.42	4.98	2.60	42.64
SST -MPL-42	3.03	8.09	3.92	2.60	31.96
SST -MPL-43	2.28	8.05	2.44	2.60	15.00
SST -MPL-44	2.83	11.42	5.71	2.60	43.48
SST -MPL-45	2.77	7.72	7.80	2.60	58.26
SST -MPL-46	2.88	12.06	4.11	2.60	31.84
SST -MPL-47	2.50	5.08	3.09	2.60	44.64
SST -MPL-48	2.75	4.42	3.38	2.60	53.64
SST -MPL-49	2.72	6.05	2.54	2.60	39.81
SST -MPL-50	2.60	8.05	3.60	2.60	25.23
				Average	**29.86**
			Standard Deviation		**11.90**

Table 4.16 Results of elastic modulus calculation from MPL tests on tuffaceous sandstone.

Specimen Number	t/d	D_e/d	$\Delta P/\Delta\delta$ (GPa/mm)	α_E	$E_{mpl\ (GPa)}$
TST -MPL-01	2.70	5.46	2.12	2.60	22.02
TST -MPL-02	2.58	7.87	3.26	2.60	32.32
TST -MPL-03	2.75	7.30	1.43	2.60	15.13
TST -MPL-04	2.82	7.15	1.43	2.60	15.51
TST -MPL-05	2.54	13.45	2.64	2.60	25.79
TST -MPL-06	2.92	8.93	1.43	2.60	16.06
TST -MPL-07	2.43	8.53	1.12	2.60	22.73
TST -MPL-08	2.87	10.47	3.19	2.60	35.21
TST -MPL-09	2.30	7.87	2.12	2.60	18.75
TST -MPL-10	2.30	4.27	1.32	2.60	17.52
TST -MPL-11	2.82	12.43	3.19	2.60	34.55
TST -MPL-12	2.54	6.04	1.27	2.60	12.41
TST -MPL-13	2.88	11.80	1.59	2.60	17.64
TST -MPL-14	2.51	6.31	1.70	2.60	24.65
TST -MPL-15	2.14	11.04	2.60	2.60	15.00
TST -MPL-16	2.29	4.86	1.02	2.60	13.45
TST -MPL-17	2.59	7.15	6.50	2.60	45.30
TST -MPL-18	2.43	2.85	0.73	2.60	10.25
TST -MPL-19	2.85	3.16	1.28	2.60	21.05
TST -MPL-20	2.41	2.95	1.70	2.60	23.60
TST -MPL-21	2.98	4.17	1.00	2.60	17.22
TST -MPL-22	2.65	6.42	0.88	2.60	8.96
TST -MPL-23	3.14	6.11	1.01	2.60	18.30
TST -MPL-24	3.03	4.81	1.24	2.60	21.66
TST -MPL-25	2.23	2.23	1.26	2.60	10.83
TST -MPL-26	2.73	6.52	1.78	2.60	18.69
TST -MPL-27	2.16	8.87	1.70	2.60	20.65
TST -MPL-28	3.19	7.18	1.64	2.60	20.11
TST -MPL-29	3.10	7.42	1.28	2.60	11.36
TST -MPL-30	2.60	6.41	2.80	2.60	28.00
TST -MPL-31	2.87	4.96	1.58	2.60	17.42
TST -MPL-32	2.64	3.68	1.70	2.60	17.25
TST -MPL-33	2.38	4.15	1.30	2.60	11.92
TST -MPL-34	2.71	8.24	2.60	2.60	19.42
TST -MPL-35	2.83	8.00	3.25	2.60	24.78
TST -MPL-36	2.42	10.13	3.25	2.60	21.15
TST -MPL-37	2.54	7.15	2.17	2.60	14.84
TST -MPL-38	2.10	7.55	5.20	2.60	29.44
TST -MPL-39	2.93	5.08	2.60	2.60	20.52
TST -MPL-40	2.73	4.10	3.47	2.60	25.52

Table 4.16 Results of elastic modulus calculation from MPL tests on tuffaceous sandstone (continued).

Specimen Number	t/d	D_e/d	$\Delta P/\Delta\delta$ (GPa/mm)	α_E	$E_{mpl\ (GPa)}$
TST -MPL-41	2.34	6.28	2.60	2.60	16.38
TST -MPL-42	2.59	4.33	2.60	2.60	18.14
TST -MPL-43	2.65	5.46	4.35	2.60	44.40
TST -MPL-44	2.55	8.29	2.22	2.60	32.65
TST -MPL-45	2.54	3.68	3.15	2.60	30.75
TST -MPL-46	2.93	6.95	2.22	2.60	25.02
TST -MPL-47	2.47	2.97	1.28	2.60	18.27
TST -MPL-48	3.10	6.11	2.37	2.60	42.40
TST -MPL-49	2.25	3.37	3.71	2.60	22.52
TST -MPL-50	2.59	4.10	3.94	2.60	27.46
				Average	**21.90**
				Standard Deviation	**8.30**

Table 4.17 Comparisons of elastic modulus results obtained from uniaxial compressive strength tests and those from modified point load tests.

Rock Type	Tangential Elastic Modulus from UCS tests, E_t (GPa)	Elastic Modulus from MPL tests, E_{mpl} (GPa)
Porphyritic andesite	43.0±3.4	17.4±9.1
Silicified tuffaceous sandstone	63.3±8.0	29.9±11.9
tuffaceous sandstone	51.3±5.3	21.9±8.3

4.3.2 Modified point load tests predicting uniaxial compressive strength.

The uniaxial compressive strength of MPL specimens can be predicted by plotting P_{mpl} as a function of diameter ratio, D_e/d as shown in Figures 4.28 through 4.30. At diameter ratio equal to unity the P_{mpl} represents the uniaxial compressive strength of rock. The uniaxial compressive strength predicted from MPL tests compared with those from CPL test and UCS standard test is shown in Table 4.18.

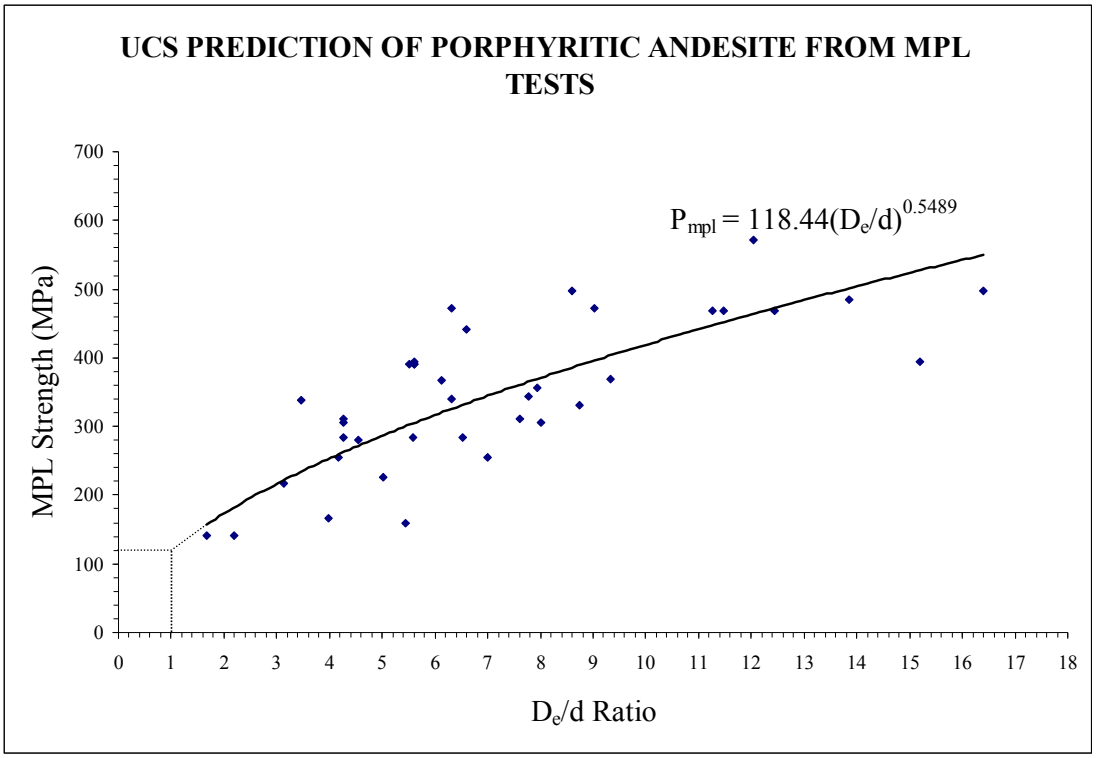

Figure 4.28 Uniaxial compressive strength predicted for porphyritic andesite from MPL tests.

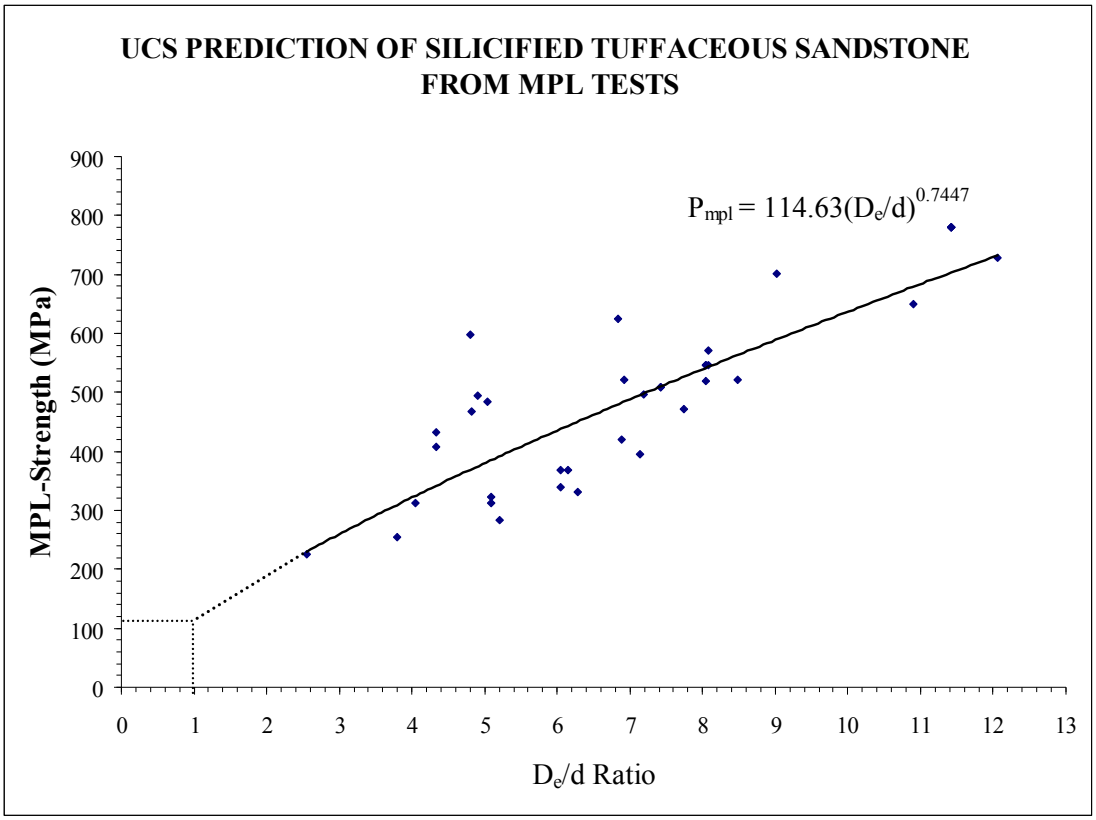

Figure 4.29 Uniaxial compressive strength predicted for silicified tuffaceous sandstone from MPL tests.

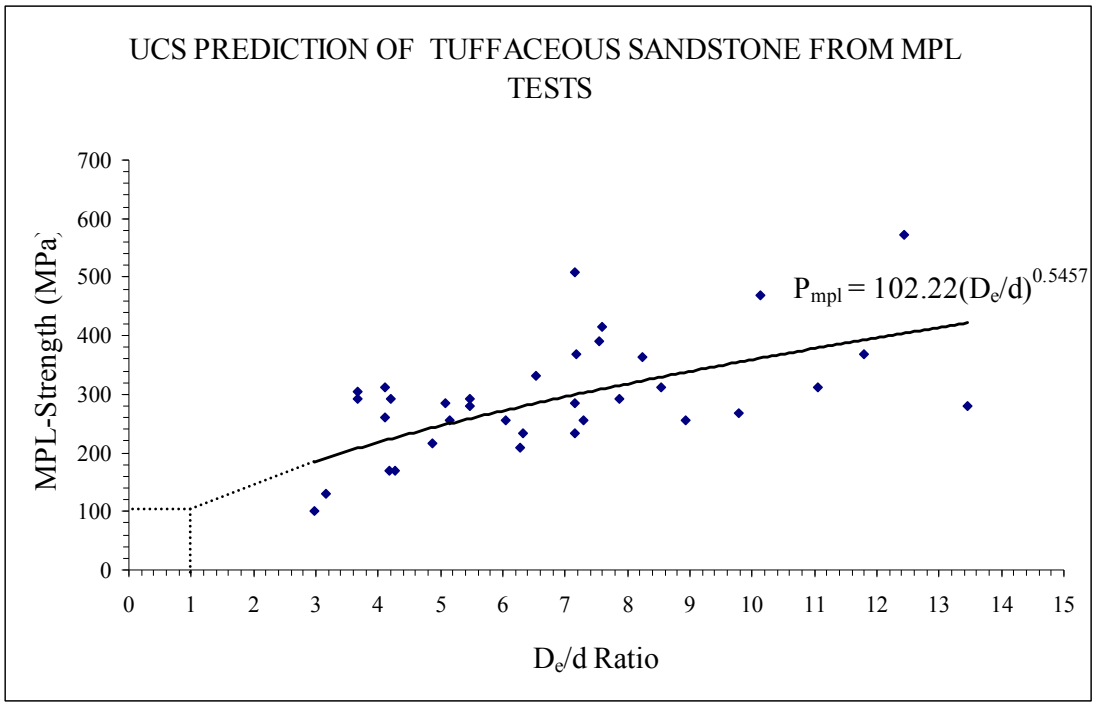

Figure 4.30 Uniaxial compressive strength predicted for tuffaceous sandstone from MPL tests.

Table 4.18 Comparison the test results between UCS, CPL, Brazilian tensile strength and MPL tests.

Rock Type	Uniaxial Compressive Strength (MPa)			Tensile Strength (MPa)	
	UCS Testing	CPL Prediction	MPL Prediction	Brazilian Testing	MPL Prediction
And	115.0	194.4 ±1.2	100.5	17.0±1.6	13.9±4.3
TST	111.4	244.8±2.0	130.8	13.1±3.3	12.1±7.3
SST	120.7	259.2±2.2	102.2	19.1±3.2	17.1±12.6

4.3.3 Modified Point Load Tests for Tensile Strength Predictions

The MPL results determine the rock tensile strength by using the relationship of the failure stresses (P_{mpl}) as a function of specimen thickness to

loading diameter ratio (t/d). The tensile strength from MPL prediction can be expressed as an empirical equation (Tepnarong, 2001):

$$\sigma_{t,\,mpl} = P_{mpl} / (\alpha_T \ln (t/d) + \beta_T) \quad (4.10)$$

where $\alpha_T = 13.3 \ln (D_e/d) - 7.56$ and $\beta_T = -7.0 \ln (D_e/d) + 19.52$.

The results of tensile strengths of all rock types are shown in Tables 4.19.through 4.21. The predicted tensile strengths are compared with the Brazilian tensile strengths for the three rock types in Table 4.18. A close agreement of the results obtained between two methods. The discrepancies of the results are less than the standard deviation of the results.

Table 4.19 Results of tensile strengths of porphyritic andesite predicted from MPL tests

Specimen Number	t/d	D_e/d	P_{mpl} (MPa)	α_T	β_T	$\sigma_{t,\,mpl}$ (MPa)
And-MPL-01	2.46	5.43	159	14.95	7.67	7.50
And-MPL-02	3.51	6.32	471	16.97	6.61	16.88
And-MPL-03	2.36	6.34	191	17.01	6.59	9.00
And-MPL-04	2.66	9.60	319	22.52	3.69	12.40
And-MPL-05	2.84	9.03	471	21.70	4.12	17.61
And-MPL-06	2.45	7.93	357	19.99	5.02	15.58
And-MPL-07	2.63	8.74	331	21.27	4.35	13.30
And-MPL-08	2.61	9.80	268	22.79	3.55	10.53
And-MPL-09	2.80	7.77	344	19.71	5.17	13.51
And-MPL-10	2.44	5.69	159	15.57	7.34	7.46
And-MPL-11	2.51	6.13	368	16.56	6.83	16.66
And-MPL-12	2.26	6.31	340	16.95	6.62	16.62
And-MPL-13	2.33	11.26	468	24.64	2.57	20.00
And-MPL-14	2.79	12.03	572	25.52	2.11	20.22
And-MPL-15	2.39	5.03	227	13.92	8.22	11.14
And-MPL-16	2.81	4.74	170	13.14	8.63	7.65
And-MPL-17	3.05	8.61	497	21.08	4.45	17.76
And-MPL-18	2.33	6.53	283	17.40	6.38	13.40
And-MPL-19	2.94	13.86	484	27.41	1.12	15.77
And-MPL-20	2.65	8.60	522	21.06	4.46	20.91

And-MPL-21	2.38	4.25	311	11.69	9.39	15.95
And-MPL-22	2.30	4.17	255	11.42	9.53	13.38
And-MPL-23	2.23	5.57	283	15.29	7.49	14.31
And-MPL-24	2.50	7.60	311	19.41	5.32	13.47
And-MPL-25	2.59	12.43	468	25.96	1.88	17.63
And-MPL-26	3.03	5.60	395	15.35	7.46	16.13

Table 4.19 Results of tensile strengths of porphyritic andesite predicted from MPL tests (continued).

Specimen Number	t/d	D_e/d	P_{mpl} (MPa)	α_T	β_T	$\sigma_{t, mpl}$ (MPa)
And-MPL-27	2.73	16.40	497	29.64	-0.06	16.71
And-MPL-28	2.82	9.06	280	22.52	3.69	10.35
And-MPL-29	3.11	9.34	369	22.16	3.88	12.72
And-MPL-30	2.46	13.14	650	26.70	1.49	25.43
And-MPL-31	2.62	9.82	255	22.82	3.53	9.97
And-MPL-32	2.60	11.47	468	24.88	2.44	17.83
And-MPL-33	2.40	7.00	255	18.32	5.90	11.61
And-MPL-34	3.04	8.00	306	20.10	4.96	11.21
And-MPL-35	2.50	4.55	280	12.59	8.91	13.70
And-MPL-36	2.43	16.97	312	30.10	-0.30	11.81
And-MPL-37	3.33	15.20	395	28.63	0.47	11.30
And-MPL-38	2.38	6.61	442	17.55	6.30	20.54
And-MPL-39	3.18	3.47	338	8.97	10.82	15.94
And-MPL-40	2.45	5.51	390	15.13	7.58	18.47
And-MPL-41	2.07	5.61	390	15.37	7.45	20.89
And-MPL-42	2.23	4.25	283	11.69	9.39	15.07
And-MPL-43	2.07	5.61	390	15.37	7.45	20.89
And-MPL-44	3.24	3.40	395	8.71	10.96	18.64
And-MPL-45	2.75	4.26	306	11.72	9.37	14.41
And-MPL-46	3.02	3.97	166	10.79	9.86	7.60
And-MPL-47	2.55	3.14	127	7.66	11.51	11.59
And-MPL-48	2.57	2.20	142	2.91	14.01	8.45
And-MPL-49	2.56	2.14	74	2.57	14.19	4.43
And-MPL-50	2.43	1.66	102	-0.78	15.95	9.28
					Average	**14.27**
					Standard Deviation	**4.4**

Table 4.20 Results of tensile strengths of silicified tuffaceous sandstone predicted from MPL tests.

Specimen Number	t/d	D_e/d	P_{mpl} (MPa)	α_T	β_T	$\sigma_{t, mpl}$ (MPa)
SST -MPL-01	3.00	7.82	442	13.36	8.51	20.18
SST -MPL-02	2.50	4.80	572	13.31	8.53	27.59
SST -MPL-03	3.14	4.24	433	11.96	9.24	18.88
SST -MPL-04	2.92	8.09	572	20.24	4.89	21.55
SST -MPL-05	2.75	11.42	780	24.83	2.47	28.27
SST -MPL-06	3.08	4.90	494	13.57	8.40	20.86
SST -MPL-07	3.17	6.11	728	16.51	6.85	28.08
SST -MPL-08	2.33	6.84	624	18.00	6.06	29.32
SST -MPL-09	2.55	4.80	598	13.31	8.53	28.49
SST -MPL-10	2.17	7.72	312	19.62	5.22	15.29
SST -MPL-11	3.12	9.03	702	21.70	4.12	24.36
SST -MPL-12	2.55	10.94	390	24.26	2.77	15.33
SST -MPL-13	2.86	7.42	510	19.10	5.49	20.11
SST -MPL-14	2.48	6.15	198	16.61	6.80	9.05
SST -MPL-15	2.53	8.05	546	20.17	4.92	23.12
SST -MPL-16	2.43	10.94	390	24.26	2.77	16.07
SST -MPL-17	2.34	10.90	650	24.21	2.80	27.80
SST -MPL-18	2.53	13.71	624	27.26	1.20	23.54
SST -MPL-19	3.27	4.34	408	11.96	9.24	17.40
SST -MPL-20	2.70	3.10	497	7.48	11.60	26.18
SST -MPL-21	2.69	6.91	522	18.16	5.99	21.81
SST -MPL-22	3.12	5.04	484	13.94	8.21	20.12
SST -MPL-23	3.19	6.27	331	16.86	6.67	12.63
SST -MPL-24	2.81	6.89	420	18.12	6.01	16.99
SST -MPL-25	2.10	7.20	497	18.69	5.70	25.41
SST -MPL-26	3.03	7.75	471	19.68	5.19	17.45
SST -MPL-27	2.72	7.14	395	18.59	5.76	16.23
SST -MPL-28	2.92	8.55	764	20.98	4.50	28.30
SST -MPL-29	3.10	7.42	510	19.10	5.49	18.81
SST -MPL-30	2.84	8.47	522	20.87	4.56	19.81
SST -MPL-31	3.20	8.91	828	21.53	4.21	28.32
SST -MPL-32	2.61	2.56	226	4.92	12.95	12.82
SST -MPL-33	2.24	4.05	311	11.06	9.72	16.72
SST -MPL-34	2.31	3.79	255	10.17	10.19	13.63
SST -MPL-35	2.90	4.42	594	12.21	9.12	26.90
SST -MPL-36	2.41	5.21	283	14.39	7.97	13.74
SST -MPL-37	2.75	6.05	340	16.39	6.92	14.45
SST -MPL-38	2.63	6.16	368	16.61	6.80	16.11

Table 4.20 Results of tensile strengths of silicified tuffaceous sandstone predicted from MPL tests (continued).

Specimen Number	t/d	D_e/d	P_{mpl} (MPa)	α_T	β_T	$\sigma_{t, mpl}$ (MPa)
SST -MPL-39	2.27	6.15	198	16.61	6.80	9.69
SST -MPL-40	2.36	5.08	311	14.06	8.14	15.40
SST -MPL-41	3.18	11.42	780	24.83	2.47	25.00
SST -MPL-42	3.03	8.09	546	20.24	4.89	19.99
SST -MPL-43	2.28	8.05	546	20.17	4.92	25.30
SST -MPL-44	2.83	11.42	780	24.83	2.47	27.57
SST -MPL-45	2.77	7.72	312	19.62	5.22	12.36
SST -MPL-46	2.88	12.06	728	25.55	2.09	25.02
SST -MPL-47	2.50	5.08	323	14.06	8.14	15.33
SST -MPL-48	2.75	4.42	594	12.21	9.12	27.69
SST -MPL-49	2.72	6.05	368	16.39	6.92	15.80
SST -MPL-50	2.60	8.05	520	20.17	4.92	21.47
					Average	**20.45**
					Standard Deviation	**5.6**

Table 4.21 Results of tensile strengths of tuffaceous sandstone predicted from MPL tests.

Specimen Number	t/d	D_e/d	P_{mpl} (MPa)	α_T	β_T	$\sigma_{t, mpl}$ (MPa)
TST -MPL-01	2.70	5.46	293	15.02	7.63	12.99
TST -MPL-02	2.58	7.87	293	19.88	5.08	12.26
TST -MPL-03	2.75	7.30	255	18.88	5.60	10.31
TST -MPL-04	2.82	7.15	510	18.60	5.75	20.35
TST -MPL-05	2.54	13.45	280	27.01	1.33	10.58
TST -MPL-06	2.92	8.93	255	21.56	4.20	9.33
TST -MPL-07	2.43	8.53	311	20.95	4.51	13.46
TST -MPL-08	2.87	10.47	268	22.79	3.55	9.70
TST -MPL-09	2.30	7.87	471	19.88	5.08	21.79
TST -MPL-10	2.30	4.27	147	11.76	9.35	7.69
TST -MPL-11	2.82	12.43	573	25.96	1.88	19.94
TST -MPL-12	2.54	6.04	255	16.36	6.93	11.49
TST -MPL-13	2.88	11.80	369	25.27	2.24	12.74
TST -MPL-14	2.51	6.31	232	16.95	6.62	10.44
TST -MPL-15	2.14	11.04	312	24.38	2.71	14.65
TST -MPL-16	2.29	4.86	215	13.47	8.45	10.98
TST -MPL-17	2.59	7.15	286	18.61	5.75	12.20
TST -MPL-18	2.43	2.85	102	6.37	12.19	5.71
TST -MPL-19	2.85	3.16	130	7.76	11.46	6.65
TST -MPL-20	2.41	2.95	102	6.85	11.94	5.68
TST -MPL-21	2.98	4.17	170	11.43	9.52	7.71
TST -MPL-22	2.65	6.42	170	11.78	9.34	10.59
TST -MPL-23	3.14	6.11	255	16.52	6.85	9.89
TST -MPL-24	3.03	4.81	368	14.23	8.05	15.45
TST -MPL-25	2.23	2.23	331	3.13	13.89	20.18
TST -MPL-26	2.73	6.52	331	17.38	6.40	13.89
TST -MPL-27	2.16	8.87	535	21.46	4.24	18.50
TST -MPL-28	3.19	7.18	369	18.66	5.72	13.50
TST -MPL-29	2.31	5.16	255	14.25	8.04	12.76
TST -MPL-30	2.60	6.41	484	17.15	6.51	21.14
TST -MPL-31	2.87	4.96	420	13.73	8.32	18.46
TST -MPL-32	2.64	3.68	293	9.76	10.41	14.75
TST -MPL-33	2.38	4.15	293	11.51	9.48	15.04
TST -MPL-34	2.71	8.24	364	20.49	4.76	14.18
TST -MPL-35	2.83	8.00	572	20.10	4.96	22.10
TST -MPL-36	2.42	10.13	468	23.24	3.31	19.65
TST -MPL-37	2.54	7.15	234	18.61	5.75	10.13
TST -MPL-38	2.10	7.55	390	19.32	5.37	19.76

Table 4.21 Results of tensile strengths of tuffaceous sandstone predicted from MPL tests (continued).

Specimen Number	t/d	D_e/d	P_{mpl} (MPa)	α_T	β_T	$\sigma_{t,\ mpl}$ (MPa)
TST -MPL-39	2.93	5.08	286	14.06	8.14	12.29
TST -MPL-40	2.73	4.10	260	11.24	9.63	12.43
TST -MPL-41	2.34	6.28	208	16.88	6.66	9.90
TST -MPL-42	2.59	4.33	338	11.94	9.26	16.39
TST -MPL-43	2.65	5.46	280	15.02	7.63	12.57
TST -MPL-44	2.55	8.29	147	20.57	4.72	6.14
TST -MPL-45	2.54	3.68	306	9.76	10.41	15.68
TST -MPL-46	2.93	6.95	210	18.22	5.95	18.46
TST -MPL-47	2.47	2.97	102	6.91	11.90	5.61
TST -MPL-48	3.10	6.11	170	16.52	6.85	6.65
TST -MPL-49	2.25	3.37	416	19.39	5.33	19.72
TST -MPL-50	2.59	4.10	312	11.20	9.65	15.37
					Average	**13.36**
					Standard Deviation	**5.6**

4.3.4 Modified point load tests for triaxial compressive strength predictions

The objective of this section is to predict the triaxial compressive strength of intact rock specimens by using the MPL results (modified point load strength, P_{mpl}). It is speculated that increase of applied load (σ_1) will invoke a confining pressure (σ_3) on the imaginary cylindrical profile between the two loading points. This is due to the effect of Poisson's ratio (ν) which causing a potential expansion of rock in this cylinder. The greater the σ_1, the greater the σ_3. in addition, Poisson's ratios also affect the magnitude of σ_3. The magnitude of σ_3 also depends on the specimen shape, particularly the D_e/d ratio. In principle, σ_3 will equal zero for D_e/d ratio equal to unity. But when D_e/d ratio is very large, approaching infinity, σ_3 will reach its maximum. This maximum value of σ_3 will also depend on the rock Poisson's ratio. From computer simulation of t/d =2.5, the variation of $\sigma_1/\ \sigma_3$ ratio can be simply expressed by Tepnarong (2006) as.

$$(\sigma_1/\ \sigma_3) = 2/\ ((\nu\ /\ (1–\nu)\ (1-(d/D_e)^2)) \quad (4.11)$$

where ν is the Poisson's ratio of rock specimen, d is the modified point load diameter and D_e is the equivalent diameter of the specimen. The Poisson's ratio of rock specimen used in equation 4.11 can be assumed to be 2.5. The $\sigma_1/\ \sigma_3$ ratio tends to be independent of D_e/d for D_e/d greater than 10. This implies that when MPL specimen diameter is more than 10 times of the loading point diameter, the magnitude of σ_3 is approaching its maximum value (Tepnarong, 2006).

It should be pointed out that approach used here to determine σ_3 assumes that there is no shear stress (τ_{rz}) along the imagination cylinder. As a result, the magnitude of σ_3 determined here would be higher than the actual σ_3 applied in the true triaxial test specimen. This mean that the $\sigma_1/\ \sigma_3$ ratios at failure obtained from MPL tests will be lower than the actual failure stress ratio from the true triaxial tests.

From the concept of $\sigma_1/\ \sigma_3$-D_e/d relation proposed, the major and minor principal stresses at failure (σ_1, σ_3) can be predicted from the measured MPL failure stress. P_{mpl} and D_e/d ratio The Poisson's ratio used here is equal to 0.25.

Comparison between the failure stress (σ_1, σ_3) obtained from the standard triaxial compressive strength testing (ASTM D7012-07) and those predicted from MPL test results are made graphically in Figures 4.31 through 4.33, for ν =0.25. The figures are plotted the maximum shear stress ($½(\sigma_1-\sigma_3)$) as a function of mean shear stress ($½(\sigma_1+\sigma_3)$) indicating that the predicted failure stresses under-estimate the value obtained from the standard testing. This is because of the assumption of no shear stresses developed on the surface of the imaginary cylinder. The under prediction may be due to the intrinsic variability of the rocks. The predictions are also sensitive to assumed Poisson's ratio. The Poisson's ratio of the tested specimens

may be lower than the assumed value of 0.25. This comparison implies that the triaxial strength predicted from MPL test will be more conservative than those from the standard testing method.

Table 4.22 Results of triaxial strengths of porphyritic andesite predicted from MPL tests.

Specimen Number	t/d	D_e/d	σ_1 (MPa)	σ_3 (MPa)	Maximum shear stress (MPa)	Mean stress (MPa)
And-MPL-01	2.46	5.43	159	25.27	66.63	91.90
And-MPL-02	3.51	6.32	471	75.83	197.76	273.58
And-MPL-03	2.36	6.34	191	30.75	80.17	110.91
And-MPL-04	2.66	9.60	319	51.98	133.25	185.22
And-MPL-05	2.84	9.03	471	76.82	197.26	274.08
And-MPL-06	2.45	7.93	357	57.92	149.38	207.30
And-MPL-07	2.63	8.74	331	53.93	138.64	192.57
And-MPL-08	2.61	9.80	268	43.68	111.92	155.60
And-MPL-09	2.80	7.77	344	55.81	144.07	199.88
And-MPL-10	2.44	5.69	159	25.35	66.59	91.94
And-MPL-11	2.51	6.13	368	59.11	154.45	213.56
And-MPL-12	2.26	6.31	340	54.65	142.53	197.17
And-MPL-13	2.33	11.26	468	76.60	195.68	272.28
And-MPL-14	2.79	12.03	572	93.72	239.11	332.83
And-MPL-15	2.39	5.03	227	35.89	95.29	131.18
And-MPL-16	2.81	4.74	170	26.78	71.54	98.31
And-MPL-17	3.05	8.61	497	80.87	207.97	288.84
And-MPL-18	2.33	6.53	283	45.61	118.74	164.35
And-MPL-19	2.94	13.86	484	79.46	202.31	281.77
And-MPL-20	2.65	8.60	522	85.01	218.64	303.65
And-MPL-21	2.38	4.25	311	48.54	131.43	179.97
And-MPL-22	2.30	4.17	255	39.62	107.58	147.20
And-MPL-23	2.23	5.57	283	45.21	118.94	164.15
And-MPL-24	2.50	7.60	311	50.49	130.45	180.94
And-MPL-25	2.59	12.43	468	76.71	195.62	272.34
And-MPL-26	3.03	5.60	395	63.08	165.91	228.99
And-MPL-27	2.73	16.40	497	81.67	207.57	289.24
And-MPL-28	2.82	9.06	280	45.74	117.26	163.00
And-MPL-29	3.11	9.34	369	60.26	154.59	214.84
And-MPL-30	2.46	13.14	650	106.6	271.66	378.28
And-MPL-31	2.62	9.82	255	41.60	106.59	148.19
And-MPL-32	2.60	11.47	468	76.63	195.67	272.29

And-MPL-33	2.40	7.00	255	41.18	106.80	147.98
And-MPL-34	3.04	8.00	306	49.66	128.04	177.70

Table 4.22 Results of triaxial strengths of porphyritic andesite predicted from MPL tests (continued).

Specimen Number	t/d	D_e/d	σ_1 (MPa)	σ_3 (MPa)	Maximum shear stress (MPa)	Mean stress (MPa)
And-MPL-35	2.50	4.55	280	44.01	118.12	162.13
And-MPL-36	2.43	16.97	312	51.30	130.34	181.63
And-MPL-37	3.33	15.20	395	64.88	165.01	229.89
And-MPL-38	2.38	6.61	442	71.25	185.35	256.61
And-MPL-39	3.18	3.47	338	51.12	143.42	194.55
And-MPL-40	2.45	5.51	390	62.22	163.87	226.09
And-MPL-41	2.07	5.61	390	62.30	163.83	226.13
And-MPL-42	2.23	4.25	283	44.13	119.48	163.61
And-MPL-43	2.07	5.61	390	62.30	163.83	226.13
And-MPL-44	3.24	3.40	395	59.52	167.69	227.21
And-MPL-45	2.75	4.26	306	47.67	129.03	176.70
And-MPL-46	3.02	3.97	166	25.59	70.01	95.60
And-MPL-47	2.55	3.14	127	32.11	92.23	124.33
And-MPL-48	2.57	2.20	142	18.52	61.51	80.03
And-MPL-49	2.56	2.14	74	9.50	32.05	41.55
And-MPL-50	2.43	1.66	102	14.93	63.31	78.23

Table 4.23 Results of triaxial strengths of silicified tuffaceous sandstone predicted from MPL tests.

Specimen Number	t/d	D_e/d	σ_1 (MPa)	σ_3 (MPa)	Maximum shear stress (MPa)	Mean stress (MPa)
SST -MPL-01	3.00	7.82	442	73.89	197.03	270.92
SST -MPL-02	2.50	4.80	572	90.28	240.83	331.12
SST -MPL-03	3.14	4.24	433	67.67	182.73	250.40
SST -MPL-04	2.92	8.09	572	92.93	239.51	332.44
SST -MPL-05	2.75	11.42	780	127.7	326.11	453.82
SST -MPL-06	3.08	4.90	494	78.11	207.92	286.03
SST -MPL-07	3.17	6.11	728	116.9	305.52	422.41
SST -MPL-08	2.33	6.84	624	100.8	261.60	362.35
SST -MPL-09	2.55	4.80	598	94.39	251.78	346.17
SST -MPL-10	2.17	7.72	312	50.61	130.68	181.29
SST -MPL-11	3.12	9.03	702	114.4	293.77	408.17
SST -MPL-12	2.55	10.94	390	63.81	163.08	226.89
SST -MPL-13	2.86	7.42	510	82.55	213.50	296.05
SST -MPL-14	2.48	6.15	198	31.83	83.16	115.00

Table 4.23 Results of triaxial strengths of silicified tuffaceous sandstone predicted from MPL tests (continued).

Specimen Number	t/d	D_e/d	σ_1 (MPa)	σ_3 (MPa)	Maximum shear stress (MPa)	Mean stress (MPa)
SST -MPL-15	2.53	8.05	546	88.69	228.63	317.32
SST -MPL-16	2.43	10.94	390	63.81	163.08	226.89
SST -MPL-17	2.34	10.90	650	106.3	271.80	378.14
SST -MPL-18	2.53	13.71	624	102.4	260.77	363.17
SST -MPL-19	3.27	4.34	408	63.69	171.98	235.67
SST -MPL-20	2.70	3.10	497	73.44	211.69	285.13
SST -MPL-21	2.69	6.91	522	84.38	218.96	303.33
SST -MPL-22	3.12	5.04	484	76.72	203.68	280.40
SST -MPL-23	3.19	6.27	331	56.26	138.97	192.24
SST -MPL-24	2.81	6.89	420	67.90	176.24	244.14
SST -MPL-25	2.10	7.20	497	80.39	208.21	288.60
SST -MPL-26	3.03	7.75	471	76.48	197.43	273.91
SST -MPL-27	2.72	7.14	395	63.88	165.51	229.39
SST -MPL-28	2.92	8.55	764	124.4	319.97	444.36
SST -MPL-29	3.10	7.42	510	82.55	213.50	296.05
SST -MPL-30	2.84	8.47	522	84.98	218.66	303.64
SST -MPL-31	3.20	8.91	828	134.9	346.56	481.46
SST -MPL-32	2.61	2.56	226	31.65	97.41	129.06
SST -MPL-33	2.24	4.05	311	48.25	131.57	179.82
SST -MPL-34	2.31	3.79	255	39.12	107.83	146.95
SST -MPL-35	2.90	4.42	594	93.07	250.71	343.77
SST -MPL-36	2.41	5.21	283	44.99	119.05	164.04
SST -MPL-37	2.75	6.05	340	54.52	142.59	197.11
SST -MPL-38	2.63	6.16	368	59.12	154.45	213.57
SST -MPL-39	2.27	6.15	198	31.83	83.16	115.00
SST -MPL-40	2.36	5.08	311	49.39	131.00	180.39
SST -MPL-41	3.18	11.42	780	127.7	326.11	453.82
SST -MPL-42	3.03	8.09	546	88.70	228.62	317.33
SST -MPL-43	2.28	8.05	546	88.69	228.63	317.32
SST -MPL-44	2.83	11.42	780	127.7	326.11	453.82
SST -MPL-45	2.77	7.72	312	50.61	130.68	181.29
SST -MPL-46	2.88	12.06	728	119.3	304.33	423.61
SST -MPL-47	2.50	5.08	323	51.19	135.77	186.95
SST -MPL-48	2.75	4.42	594	93.07	250.71	343.77
SST -MPL-49	2.72	6.05	368	59.06	154.47	213.54
SST -MPL-50	2.60	8.05	520	84.47	217.74	302.21

Table 4.24 Results of triaxial strengths of tuffaceous sandstone predicted from MPL tests.

Specimen Number	t/d	D_e/d	σ_1 (MPa)	σ_3 (MPa)	Maximum shear stress (MPa)	Mean stress (MPa)
TST -MPL-01	2.70	5.46	293	46.72	123.13	169.86
TST -MPL-02	2.58	7.87	293	47.56	122.72	170.28
TST -MPL-03	2.75	7.30	255	41.25	106.76	148.01
TST -MPL-04	2.82	7.15	510	82.43	213.56	295.99
TST -MPL-05	2.54	13.45	280	45.99	117.13	163.12
TST -MPL-06	2.92	8.93	255	41.51	106.63	148.14
TST -MPL-07	2.43	8.53	311	50.67	130.36	181.03
TST -MPL-08	2.87	10.47	268	43.68	111.92	155.60
TST -MPL-09	2.30	7.87	471	76.51	197.41	273.93
TST -MPL-10	2.30	4.27	147	22.96	62.12	85.08
TST -MPL-11	2.82	12.43	573	93.97	239.64	333.61
TST -MPL-12	2.54	6.04	255	40.89	106.95	147.83
TST -MPL-13	2.88	11.80	369	60.52	154.45	214.97
TST -MPL-14	2.51	6.31	232	37.34	97.39	134.74
TST -MPL-15	2.14	11.04	312	51.05	130.46	181.51
TST -MPL-16	2.29	4.86	215	34.00	90.57	124.57
TST -MPL-17	2.59	7.15	286	46.26	119.86	166.12
TST -MPL-18	2.43	2.85	102	14.74	43.58	58.33
TST -MPL-19	2.85	3.16	130	19.34	55.44	74.78
TST -MPL-20	2.41	2.95	102	14.89	43.51	58.40
TST -MPL-21	2.98	4.17	170	26.41	71.72	98.13
TST -MPL-22	2.65	6.42	170	26.50	71.68	98.17
TST -MPL-23	3.14	6.11	255	40.91	106.93	147.84
TST -MPL-24	3.03	4.81	368	58.43	154.76	213.22
TST -MPL-25	2.23	2.23	331	43.70	143.76	187.45
TST -MPL-26	2.73	6.52	331	53.36	138.92	192.29
TST -MPL-27	2.16	8.87	535	87.16	223.94	311.09
TST -MPL-28	3.19	7.18	369	59.77	154.83	214.60
TST -MPL-29	2.31	5.16	255	40.46	107.16	147.62
TST -MPL-30	2.60	6.41	484	77.93	203.07	281.00
TST -MPL-31	2.87	4.96	420	66.54	176.92	243.46
TST -MPL-32	2.64	3.68	293	44.77	124.11	168.88
TST -MPL-33	2.38	4.15	293	45.60	123.70	169.30
TST -MPL-34	2.71	8.24	364	59.17	152.40	211.57
TST -MPL-35	2.83	8.00	572	92.90	239.53	332.42
TST -MPL-36	2.42	10.13	468	76.46	195.75	272.21
TST -MPL-37	2.54	7.15	234	37.85	98.06	135.92
TST -MPL-38	2.10	7.55	390	63.21	163.38	226.59

Table 4.24 Results of triaxial strengths of tuffaceous sandstone predicted from MPL tests (continued).

Specimen Number	t/d	D_e/d	σ_1 (MPa)	σ_3 (MPa)	Maximum shear stress (MPa)	Mean stress (MPa)
TST -MPL-39	2.93	5.08	286	45.36	120.31	165.67
TST -MPL-40	2.73	4.10	260	40.36	109.81	150.17
TST -MPL-41	2.34	6.28	208	33.45	87.27	120.71
TST -MPL-42	2.59	4.33	338	52.79	142.59	195.38
TST -MPL-43	2.65	5.46	280	44.69	117.78	162.47
TST -MPL-44	2.55	8.29	147	23.94	61.63	85.57
TST -MPL-45	2.54	3.68	306	46.71	129.51	176.22
TST -MPL-46	2.93	6.95	210	76.16	197.59	273.75
TST -MPL-47	2.47	2.97	102	14.91	43.59	58.41
TST -MPL-48	3.10	6.11	170	27.28	71.29	98.70
TST -MPL-49	2.25	3.37	416	67.44	174.26	241.70
TST -MPL-50	2.59	4.10	312	48.41	131.78	180.19

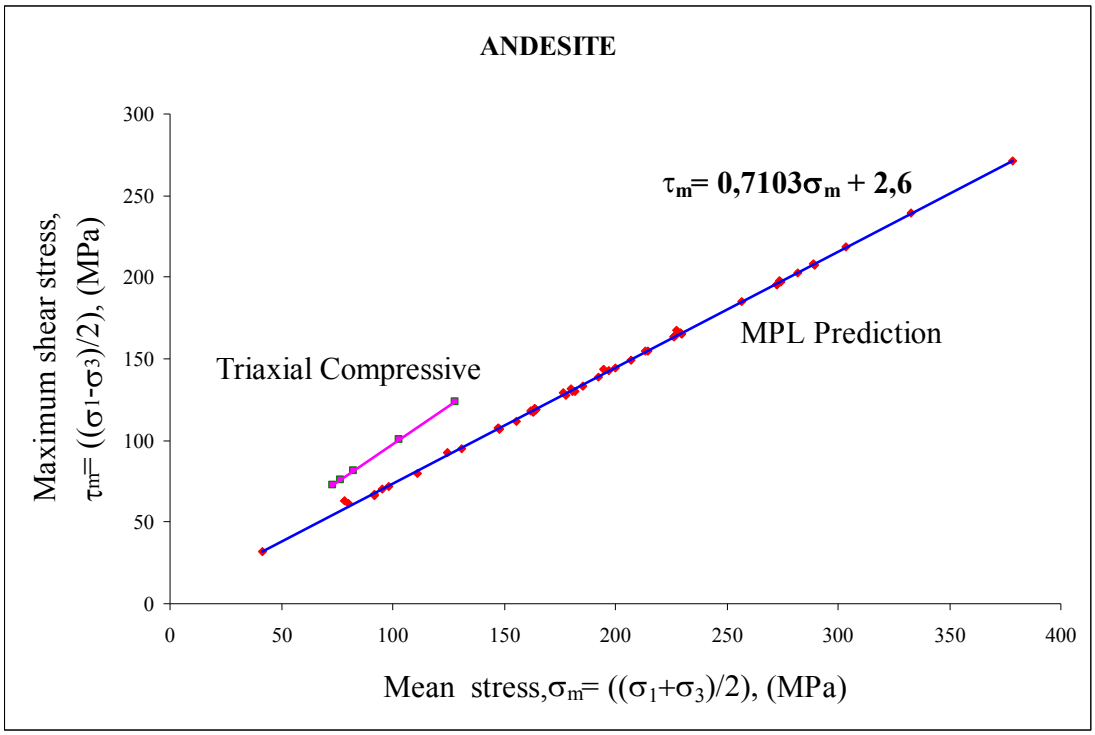

Figure 4.31 Comparisons of triaxial compressive strength criterion of porphyritic andesite between the triaxial compressive strength test and MPL test.

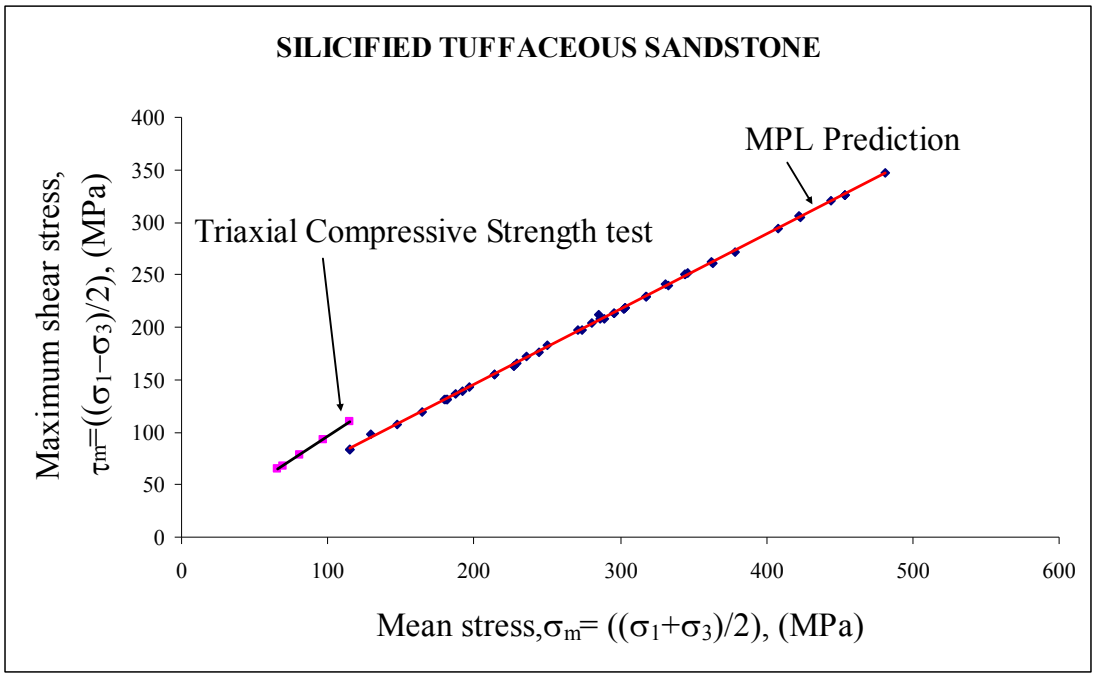

Figure 4.32 Comparisons of triaxial compressive strength criterion of silicified tuffaceous sandstone between the triaxial compressive strength test and MPL test

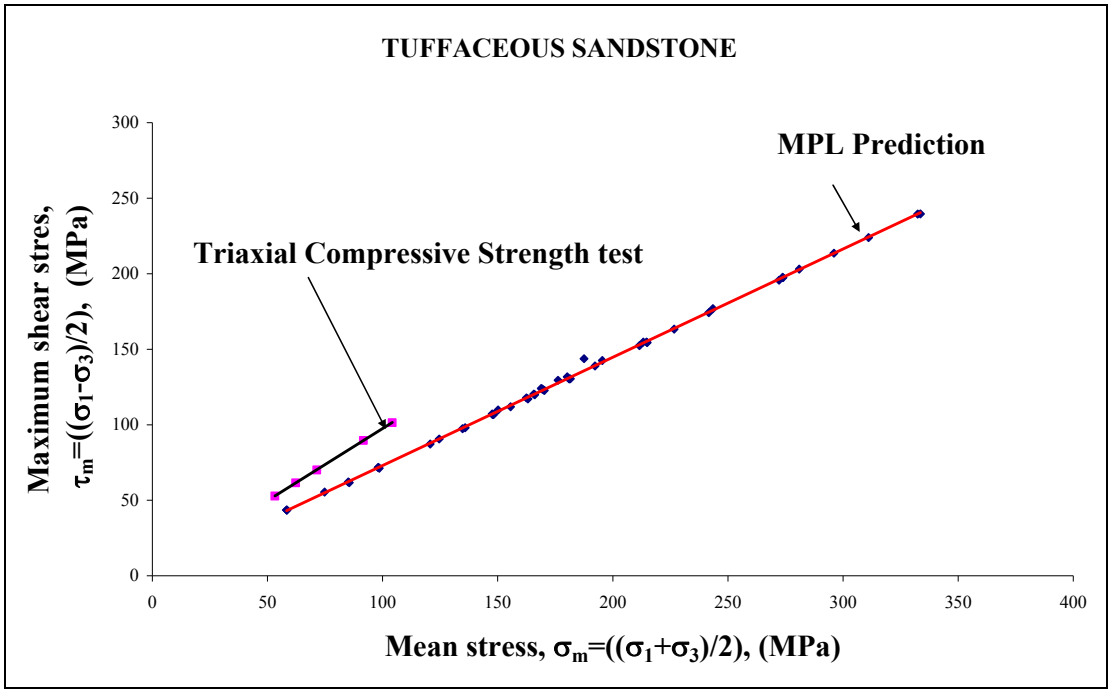

Figure 4.33 Comparisons of triaxial compressive strength criterion of tuffaceous sandstone between the triaxial compressive strength test and MPL test.

Table 4.25 compares the triaxial test results in terms of the cohesion, c and internal friction angle, ϕ_i by assuming the failure mode follows the Coulomb's criterion. The c and ϕ_i values are calculated from the test results and the predicted results by the assumption of Coulomb's criterion (Jaeger and Cook, 1978). Table 4.25 shows that the strengths predicted by MPL testing of all rock types under-estimate those obtained from the standard triaxial testing. This is probably the actual Poisson's ratio of the rock specimens are probably lower than those assumed in the model simulation which is assumed the Poisson's ratio as 0.25.

Table 4.25 Comparisons of the internal friction angle and cohesion between MPL predictions and triaxial compressive strength tests.

Rock Type	Triaxial Compressive Strength Test		MPL Predictions (ν=0.25)	
	c (MPa)	**ϕ_i (degrees)**	**c (MPa)**	**ϕ_i (degrees)**
Porphyritic Andesite	12	69	4	45
Silicified Tuffaceous Sandstone	13	65	3	46
Tuffaceous Sandstone	7	73	2	46

CHAPTER V

FINITE DIFFERENCE ANALYSES

5.1 Objectives

The objective of the finite difference analyses is to verify that the equivalent diameter of rock specimens used in the MPL strength prediction is appropriate. The finite difference analyses using FLAC software is made to determine the MPL strength for various specimen diameters (D) with a constant cross-sectional area.

5.2 Model characteristics

The analyses are made in axis symmetry. Four specimen models with the constant thickness of 3.18 cm are loaded with 1.0 cm diameter loading point. The diameter of the specimen (D) models is varied from 5.08 cm to 7.62 cm. Each specimen has a constant cross-sectional area of 16.13 cm^2 as shown in Figure 5.1 through 5.5. The load is applied to the specimens until failure occurs and then the failure loads (P) are recorded.

5.3 Results of finite difference analyses

The results of numerical simulation are shown in Table 5.1. The results suggest that the MPL strength remains roughly constant when the same equivalent diameter (D_e) is used. It can be concluded that the equivalent diameter used in this research is appropriate to predict the MPL strength.

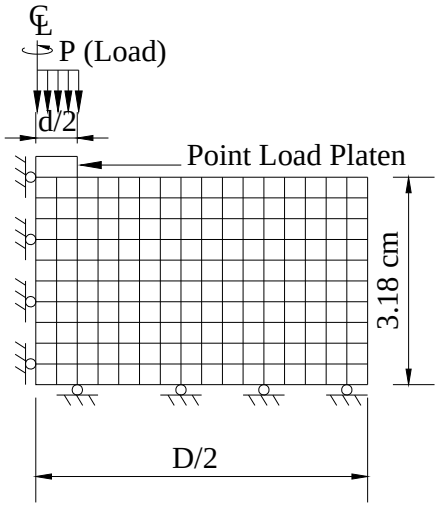

Figure 5.1 Simulation model No.1, t= 3.18 cm, D= 5.08 cm, d=10 mm

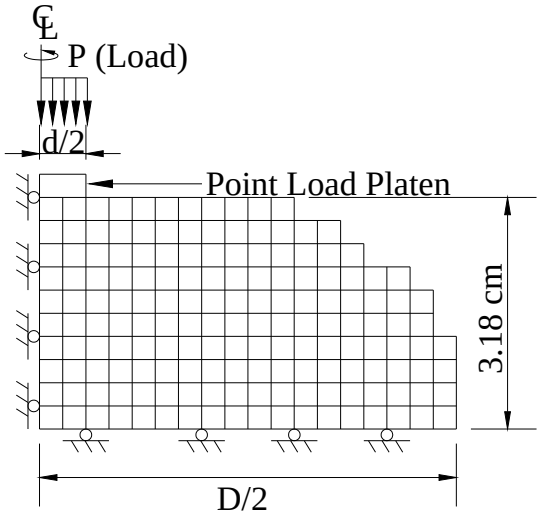

Figure 5.2 Simulation model No.2, t= 3.18 cm, D= 5.72 cm, d=10 mm

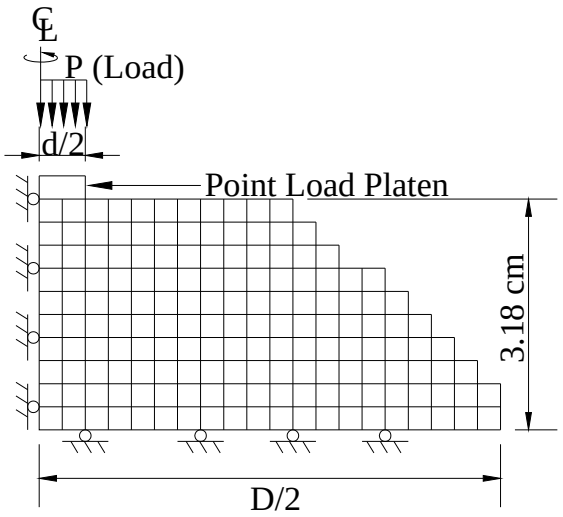

Figure 5.3 Simulation model No.3, t= 3.18 cm, D= 6.35 cm, d=10 mm

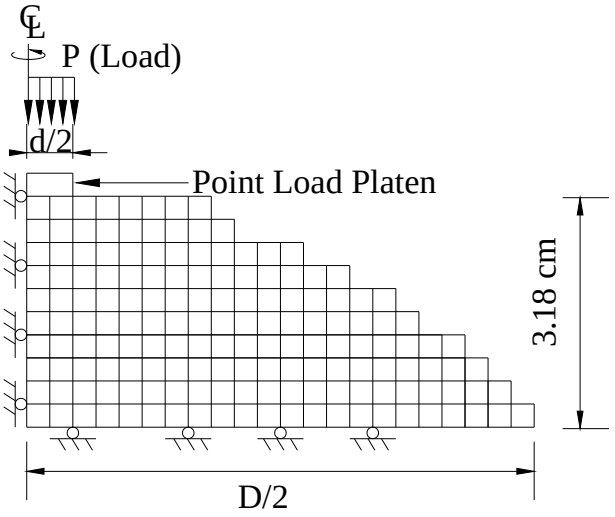

Figure 5.4 Simulation model No.4, t= 3.18 cm, D= 6.98 cm, d=10 mm

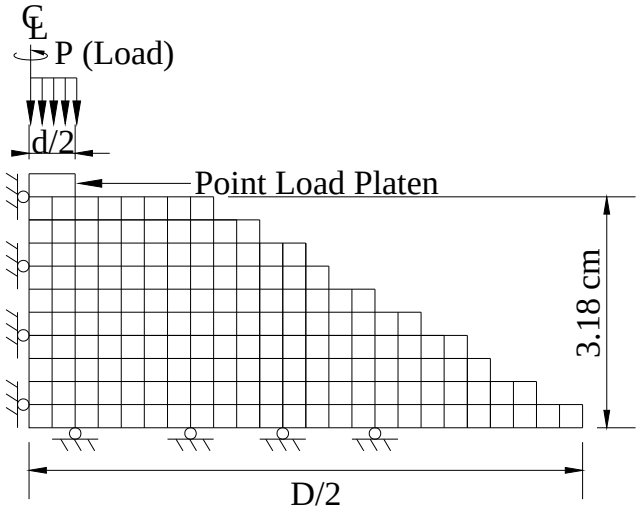

Figure 5.5 Simulation model No.5, t= 3.18 cm, D= 7.62 cm, d=10 mm

Table 5.1 Summary of the results from numerical simulations.

Model Number	Specimen Thickness, t (cm)	Specimen Diameter, D (cm)	Cross-Sectional Are of Specimen, A (cm^2)	Equivalent Diameter, D_e (cm)	Failure Load, P (kN)
1	3.18	5.08	16.13	5.08	44.85
2	3.18	5.72	16.13	5.08	46.30
3	3.18	6.35	16.13	5.08	46.14
4	3.18	6.98	16.13	5.08	46.27
5	3.18	7.62	16.13	5.08	45.90

CHAPTER VI

DISCUSSIONS, CONCLUSIONS AND RECOMMENDATIONS

This chapter discusses various aspects of the proposed MPL testing technique for determining the elastic modulus, uniaxial and triaxial compressive strengths, and tensile strength of intact rock specimens. The discussed issues include reliability of the testing results, validity, scope and limitations of the proposed method of calculations, and accuracy of the predicted rock properties.

6.1 Discussions

1) For selection of rock specimens for MPL testing in this research, an attempt has been made to select the specimens, particularly in obtaining a high degree of uniformity of rock matrix so as to reduce the intrinsic variability of the mechanical test results, and hence clearly reveals of the relation between the standard test results with the MPL test results. Nevertheless, a high degree of intrinsic variability remains, as evidenced from the results of the characterization testing. For all tested rock types here, the igneous rocks are normally heterogeneous. The high intrinsic variability is caused by the degree of weathering among specimens and the distribution of rock fragments in the groundmass which promotes the different orientations of cleavage planes and pore spaces to become a weak plane in rock specimens. Silicified tuffaceous sandstone, the high standard deviation may be caused by the silicified degree in rock specimens.

2) For prediction of elastic modulus of rock specimens, the effects of the heterogeneity that cause the selective weak planes are enhanced during the MPL testing. This is because the applied loading areas are much smaller than those under standard uniaxial compressive strength testing. This load condition yields a high degree of intrinsic variability of the MPL testing results. The standard deviation of the elastic modulus predicted from MPL results are in the range between 35-50%. This means that in order to obtain the accurate prediction, a large number of rock specimens is necessary for each rock types and that the MPL testing is more applicable in fine-grained rocks than coarse-grained rocks. Another factor is the uneven contacts between the loading platens and the rock surfaces which caused the elastic modulus of all rock types that predicted from MPL testing to be lower compared with those from the uniaxial compressive strength .

3) Equivalent diameter used to define the rock specimen width (perpendicular to the loading direction) seems adequate for use in MPL predictions of rock compressive and tensile strengths.

4) Determination of σ_3 at failure for the MPL testing is the empirical. In fact results from the numerical simulation indicate that σ_3 distribution along the imaginary cylinder between the loading points is not uniform particularly for low t/d ratio (lower than 2.5). Along this cylinder σ_3 is tension near the loading point and becomes compression in the mid-length of the MPL specimen. There are also shear stresses along the imaginary cylinder. The induced stress states along the assume cylinder in MPL specimen are therefore different from those the actual triaxial strength testing specimen. The MPL method can not satisfactorily predict the triaxial compressive strength of all tested rock types, primarily due to the heterogeneity of

rock specimens that is the different sizes of phenocrysts in igneous rock in lateral and horizontal directions. This promotes the different failure formations.

6.2 Conclusions

The objective of this research is to determine the elastic modulus, uniaxial compressive strength, tensile strength and triaxial compressive strength of rock specimens by using the modified point load (MPL) test method. Three rock types used in this research are porphyritic andesite, silicified tuffaceous sandstone and tuffaceous sandstone. Prior to performing the modified point load testing, the standard characterization testing is carried out on these rock types to obtain the data basis for use to compare the results from MPL testing. The MPL specimens are irregular-shaped with the specimen thickness to loading platen diameter (t/d) varies from 2.5-3.5 and the equivalent diameter of specimen to loading platen diameter (D_e/d) varies from 1.5 to 20. Loading platen diameters used in this research are 7, 10 and 15 mm. Finite different analysis is used to verify the equivalent diameter that use to calculate rock properties from MPL tests.

The research results illustrate that the elastic modulus estimated from MPL tests under-estimates those obtained from the ASTM standard test with the standard deviation of 40% for porphyritic andesite, 48% for silicified tuffaceous sandstone and 43% for tuffaceous sandstone. The MPL test method can satisfactorily predict the uniaxial compressive strength and tensile strength of all rock types tested here. The conventional point load test method over-predicts the actual strength results by much as 100%. The MPL method however can not predict the triaxial compressive strengths for three rock types tested here, primarily due to heterogeneous and different

weathering degree of rock specimens and uneven surface of rock specimens. This suggests that the smooth and parallel contact surfaces on opposite side of the loading points are important for determining the strength of rock specimens for MPL method.

6.3 Recommendations

The assessment of predictive capability of the proposed MPL testing technique has been limited to three rock types. More testing is needed to confirm the applicability and limitations of the proposed method. Some obvious future research needs are summarized as follows.

1) More testing is required for elastic modulus and triaxial compressive strength on different rock types. Smooth and parallel of rock specimen surfaces in the opposite sides should be prepared for all rock types. The results may also reveal the impacts of grain size on elasticity and strength of obtained under different loading areas. And the effects of size of the areas underneath the applied load should be further investigated.

2) To truly confirm the validity of MPL predictions for the elastic modulus and strength of rocks may be desirable to obtain the actual Poisson's ratio of all rock types. The results could reveal the accuracy of the predicted elastic modulus under the assumed Poisson's ratio of 0.25. Comparison between the elastic modulus obtained from the actual Poisson's ratio may show the validity of assumption of the Poisson's ratio posed here.

3) All tests made in this research are on dry specimens, the results of pore pressure and degree of saturation have not been investigated. It is desirable to learn also the proposed MPL testing technique can yield the intact rock properties under different degree of saturation.

REFERENCES

ASTM D2664-86. Standard test method for triaxial compressive strength of undrained rock core specimens without pore pressure measurements. In **Annual Book of ASTM Standards** (Vol. 04.08). Philadelphia: American Society for Testing and Materials.

ASTM D7012-07. Standard test method for compressive strength and elastic moduli of intact rock core specimens under varying states of stress and temperatures. In **Annual Book of ASTM Standards** (Vol. 04.08). West Conshohocken American Society for Testing and Materials.

ASTM D3967-81. Standard test method for splitting tensile strength of intact rock core specimens. In **Annual Book of ASTM Standards** (Vol. 04.08). Philadelphia: American Society for Testing and Materials.

ASTM D4543-85. Standard test method for preparing rock core specimens and determining dimensional and shape tolerances. In **Annual Book of ASTM Standards** (Vol. 04.08). Philadelphia: American Society for Testing and Materials.

ASTM D5731-95. Standard test method for determination of point load strength index of rock. In **Annual Book of ASTM Standards** (Vol. 04.08). Philadelphia: American Society for Testing and Materials.

Bieniawski, Z. T. (1974). Estimating of the strength of rock materials. **J. Inst. Min. Metall.** 7: 123-137.

Bieniawski, Z. T. (1975). The point-load test in geotechnical practice. **Engng. Geol.** 9: 1-11.

Bieniawski, Z. T. and Bernede, M. J. (1979). Suggested methods for determining the uniaxial compressive strength and deferability of rock material, for ISRM Commission on Standardization of Laboratory and Field test. **Int. J. Rock Mech. Min. Sci.** 16 (2).xx?xx (page no.?)

Bray, J. W. (1987). Some applications of elastic theory. In E. T. Brown (ed.). **Analytical and Computational Methods in Engineering Rock Mechanics** (pp 32-94). Allen & Unwin, London.

Broch, E. and Franklin J. A. (1972). The point-load test**. Int. J. Rock Mech. Min. Sci.** 9: 669-697.

Book, N. (1977). The use of irregular specimens for rock strength tests. **Int. J. Rock Mech. Min. Sci. & Geomech. Abstr**. 14: 193-202.

Book, N. (1979). Estimating the triaxial strength of rocks. **Int. J. Rock Mech. Min. Sci. & Geomech. Abstr**. 16: 261-264.

Book, N. (1980). Size correction for point load testing. **Int. J. Rock Mech. Min. Sci.** 17:231-235 [Technical note].

Book, N. (1985). The equivalent core diameter method of size and shape correction in point load testing. **Int. J. Rock Mech. Min. Sci. & Geomech. Abstr**. 22: 61-70.

Brown, E. T. (1981). **Rock characterization Testing and Monitoring: ISRM Suggestion Methods.** New York: International Society for Rock Mechanics, Pergamon Press.

Butenuth, C. (1997). Comparison of tensile strength values of rocks determined by point load and direct tensile tests. **Rock Mech. Rock Engng**. 30: 65-72.

Cargill, J. S. and Shakoor, A. (1992). Evaluation of empirical methods for measuring the uniaxial compressive strength. **Int. J. Rock Mech. Min. Sci.** 27: 495-503.

Chau, K.T. (1997). Young's modulus interpreted from compression tests with end friction. **J. Engng. Mech**. January: 1-7. plat. Ann Inst Tech Trav Publics. 58: 967-971.

Chau, K.T. and Wei, X. X. (1999). A new analytic solution for the diametral point load strength test on finite solid circular cylinders. **Int. J. Solids and Structures**. 38(9): 1459-1481.

Chau, K.T. and Wong, R. H.C. (1996). Uniaxial compressive strength and point load strength. **Int. J. Rock Mech. Min. Sci.** 33:183-188.

Davis, R. O. and Selvadurai, A.P.S. (1996). **Elasticity and Geomechanics**. New York: Cambridge University Press. 198 p.

Deere, D.U. and Miller, R. P. (1966). **Engineering Classification and Index Properties for Intact Rock.** US Air Force Weapons Lab. Rep., AFWL-TR-65-116.

Durelli, A. J. and Parks, V. (1962). Relationship of size and stress gradient to brittle failure stress. In **Proceeding of the 4th US National Cong. Of Appl. Mech.** (pp 931-938).

Evans, I. (1961). The tensile strength of coal. Colliery Eng. 38: 428-434.

Fairhurst, C. (1961). Laboratory measurement of some physical properties of rock. In **Proceeding of the 4th Symp. Rock. Mech**. (pp 105-118). Penn. State. University.

Farmer, I. (1983). **Engineering Behavior of Rocks**. New York: Chapman and Hall. 208 p.

Forster, I. R. (1983). The influence of core sample geometry on axial load test. **Int. J. Rock Mech. Min. Sci.** 20: 291-295.

Fuenkajorn, K. (2002). Modified point load test determining uniaxial compressive strength of intact rock. In **Proceeding of 5th North American Rock Mechanics Symposium and the 17th Tunneling Association of Canada Conference (NARMS-TAC 2002)** (pp **?**)**.** Toronto.

Fuenkajorn, K. and Daemen, J. J. K. (1986). Shape effect on ring test tensile strength. In **Key to Energy Production: Proceeding of the 27th US Symposium on Rock Mechanics** (pp 155-163). Tuscaloosa: University of Alabama.

Fuenkajorn, K. and Daemen, J. J. K. (1991b). An empirical strength criterion for heterogeneous welded tuff. In **ASME Applied Mechanics and Biomechanics Summer Conference.** Columbus: Ohio University.

Fuenkajorn, K. and Daemen, J. J. K. (1992). An empirical strength criterion for heterogeneous tuff. **Int. J. Engineering Geology**. 32: 209-223.

Fuenkajorn, K. and Tepnarong, P. (2001). Size and stress gradient effects on the modified point load strength of Saraburi Marble. In the **6th Mining, Metallurgical, and Petroleum Engineering Conference.** Bangkok, Thailand.(pp.?)

Ghosh, A., Fuenkajorn, K., and Daemen, J. J. K. (1995). Tensile strength of welded Apache Leap tuff: investigation for scale effects. In Proceeding **of the 35th US Rock Mech. Symposium** (pp 459-646). University of Navada, Reno.

Goodman, R. E. (1980). **Methods of Geological Engineering in Discontinuous Rock**. New York: Wiley and Sons.

Greminger, M. (1982). Experimental studies of the influence of rock anisotropy on size and shape effects in point-load testing. **Int. J. Rock Mech. Min. Sci.** 19: 241-246.

Gunsallus, K. L. and Kulhawy, F. H. (1984). A comparative evaluation of rock strength measures. **Int. J. Rock Mech. Min. Sci.** 21: 233-248.

Hassani, F. P.., Scoble, M. J., and Whittaker, B. N. (1980). Application of point load index test to strength determination of rock and proposals for new size-correction chart (pp 543-564). Rolla.

Hiramatsu, Y. and Oka, Y. (1966). Determination of tensile strength of rock by a compression test of irregular test piece. **Int. J. Rock Mech. Min. Sci**. 3: 89-99.

Hoek, E. (1990). Estimating Mohr-Coulomb friction and cohesion values from the Hoek-Brown falure criterion-Technical note. **Int. J. Rock Mech. Min. Sci**. **& Geomech. Abstr.** 27: 227-229.

Hoek, E. and Brown, E. T. (1980a). Empirical strength criterion for rock masses. **J. Geotech. Eng. Div.** 106 (GT9): 1013-1035.

Hondros, G. (1959). The evaluation of Poisson's ratio and modulus of material of a low tensile resistance by the Brazilian (indirect tensile) test with particular reference to concrete. **Aust. J. Appl. Sci.** 10: 243-264.

Horii, H. and Nemat-Nasser, S. (1985). Compression-induced microcrack growth in brittle solids: axial splitting and shear failure. **J. Geophts. Res.** 90: 3105-3125.

Hudson, J. A.., Brown, E. T., and Fairhurst, C. (1971). Shape of the complete stress-strain curve for rock. In **Proceeding of the 13th US Symp. Rock Mech** (pp 773-795). Urbana.

ISRM. (1985). Suggested method for determining point load strength. **Int. J. Rock Mech. Min. Sci**. **& Geomech. Abstr.** 22: 53-60.

ISRM. (1985). Suggested methods for deformability determination using a flexible dilatometer. **Int. J. Rock Mech. Min. Sci**. **& Geomech. Abstr.** 24: 123-134.

Jaeger, J. C. and Cook, N. G. W. (1979). **Fundamentals of Rock Mechanics**. London: Chapman and Hall. 593 p.

Kaczynski, R R. (1986). Scale effect during compressive strength of rocks. In **Proceeding of 5th Int. Assoc. Eng. Geol. Congr.**, p. 371-373.

Lama, R. D. and Vutukuri, V. S. (1978). Testing techniques and results. In **Handbook on Mechanical Properties of Rock.** Vol. III, No. 2, Trans Tech Publications, (International Standard Book Number 0-87849-022-1, Clausthal, Germany).

Lonborg, N. (1967). The strength-size relation of granite. **Int. J. Rock Mech. Min. Sci**. 4: 269-272.

Miller, R. P. (1965). **Engineering Classification and Index Properties for Intact Rock.** Ph.D. Dissertation., Univ. Of Illinois, Urbana, III., 92 p.

Nimick, F. B. (1988). Empirical relations between porosity and the mechanical properties of tuff. In **Key Questions in Rock Mechanics** (pp 741-742). Balkema, Rotterdam.

Obert, L. and Stephenson, D. E. (1965). Stress conditions under which core disking occurs. **Trans Soc. Min. Eng. AIME**. 232: 227-235.

Panek, L. A. and Fannon, T. A. (1992). Size and shape effects in point load tests of irregular rock fragments. **J Rock Mechanics and Rock Engineering.** 25: 109-140.

Pells, P. J. N. (1975). The use of point load test in predicting the compressive strength of rock material. **Aust Geotech** (pp 54-56). G5(N1).

Reichmuth, D. R. (1968). Point-load testing of brittle materials to determine the tensile strength and relative brittleness. In **Proceeding of the 9th US Symp. Rock Mech** (pp 134-159). University of Colorado.

Sammis, C. G. and Ashby, M. F. (1986). The failure of brittle porous solid under compressive stress state. **Acta Metall**. 34: 511-526.

Serata, S. and Fuenkajorn, K. (1992a). Finite element progam 'GEO' for modeling brittle-ductile deterioration of aging earth structures. In **SMRI Paper, Presented at the Solution Mining Research Institute**, Fall Meeting, October 19-22. Houston, Texas. 24p.

Sheorey, P. R., Biswas, A. K., and Choubey, V. D. (1989). An empirical failure criterion of rocks and jointed rock masses. **Eng. Geol.** 26: 141-159.

Stowe, R. L. (1969**). Strength and deformation properties of granite, basalt, limestone, and tuff.** US Army Corps of Engineers, WES Misc. Paper C-69-1.

Taliercio, A. and Sacchi Landrianni, G. (1988). Failure criterion for layered rock. **Int. J. Rock Mech. Min. Sci**. **& Geomech. Abstr.** 25: 299-305.

Tepnarong, P. (2001). **Theoretical and experimental studies to determine compressive and tensile strengths of rocks, using modified point load testing**. M. Eng. Thesis, Suranaree University of Technology, Thailand.

Tepnarong, P. (2006). **Theoretical and experimental studies to determine elastic modulus and triaxial compressive strength of intact rocks, by modified point load testing**. Ph.D. Eng. Thesis, Suranaree University of Technology, Thailand.

Tepnarong, P. and Fuenkajorn, K. (2004). Determining of elasticity and strengths of intact rocks using modified point load test. In **Proceeding of the ISRM International Symposium 3rd ASRM,** Vol. 2 (pp 397-392).

Timoshenko, S. (1958**). Strength of materials I, Element Theory and Problems**. (3rd ed.). Princeton, N. J. D. Van Nostard.

Timoshenko, S. and Goodier, J. N. (1951). **Theory of Elasticity.** (2nd ed.) New York: McGraw-Hill.

Truk, N. and Dearman, W. R. (1985). Improvements in the determination of point load strength. **Bull Int Assoc Eng Geol**. 31: 137-142.

Truk, N. and Dearman, W. R. (1986). A correction equation on the influence of length-to-diameter ratio on uniaxial compressive strength of rocks. **J. Eng. Geol.** 22: 293-300.

Wei, X. X. and Chau, K. T. (2002). Analytic solution for finite transversely isotropic circular cylinder under the axial point load test. **J. Eng. Mech** (pp 209-219).Vol.?

Wei, X. X. and Chau, K. T. and Wong, R. H. C. (1999). Analytic solution for axial point load strength test on solid circular cylinders. **J. Eng. Mech** (pp 1349-1357). Vol.?

Wijk, G. (1978). Some new theoretical aspects of indirect measurements of the tensile strength of rocks. **Int. J. Rock Mech. Min. Sci**. **& Geomech. Abstr.** 15: 149-160.

Wijk, G. (1980). The point load test for the tensile strength of rock. **Geotech. Test, ASTM.** 3: 49-54.

APPENDIX A

CHARACTERIZATION TEST RESULTS

Table A-1 Results of conventional point load strength index test on porphyritic andesite.

Sample No.	Length (mm)	Diameter (mm)	Density (g/cc)	Point Load Strength Index Test, I_s (MPa)
And-06-05-CPL-01	53.97	53.66	2.84	5.2
And-06-05-CPL-02	53.32	53.66	2.83	7.8
And-08-04-CPL-03	54.32	53.66	2.84	9.0
And-08-04-CPL-04	54.82	53.66	2.86	8.7
And-06-01-CPL-05	53.30	53.66	2.85	7.6
And-06-01-CPL-06	56.13	53.66	2.84	7.6
And-04-04-CPL-07	56.17	53.66	2.81	7.5
And-04-05-CPL-08	55.25	53.66	2.82	7.5
And-03-02-CPL-09	55.95	53.66	2.80	8.5
And-03-02-CPL-10	55.35	53.66	2.83	8.5
And-06-06-CPL-11	54.75	53.66	2.83	7.5
And-09-01-CPL-12	55.52	53.66	2.86	9.0
And-09-01-CPL-13	55.03	53.66	2.83	9.0
And-02-04-CPL-14	55.42	53.66	2.82	8.5
And-09-03-CPL-15	56.07	53.66	2.82	8.5
And-09-03-CPL-16	54.52	53.66	2.85	9.6
And-01-03-CPL-17	55.30	53.66	2.83	8.7
And-01-03-CPL-18	53.13	53.66	2.83	9.0
And-01-04-CPL-19	54.65	53.66	2.84	5.6
And-01-04-CPL-20	55.72	53.66	2.83	9.7
			Average	**8.1±1.2**

Table A-2 Results of conventional point load strength index test on silicified tuffaceous sand stone.

Sample No.	Length (mm)	Diameter (mm)	Density (g/cc)	Point Load Strength Index Test, I_s (MPa)
SST-02-03-CPL-01	53.73	53.66	2.68	12.5
SST-06-04-CPL-02	54.69	53.66	2.68	7.0
SST-02-07-CPL-03	55.05	53.66	2.69	7.0
SST-02-06-CPL-04	55.18	53.66	2.67	13.0
SST-02-04-CPL-05	56.26	53.66	2.67	12.5
SST-02-03-CPL-06	51.39	53.66	2.70	13.2
SST-02-03-CPL-07	54.83	53.66	2.71	7.1
SST-02-05-CPL-08	53.40	53.66	2.66	12.5
SST-02-05-CPL-09	53.99	53.66	2.65	7.0
SST-07-05-CPL-10	56.43	53.66	2.63	9.9
SST-07-05-CPL-11	53.81	53.66	2.66	10.6
SST-05-02-CPL-12	54.39	53.66	2.74	10.4
SST-05-02-CPL-13	54.91	53.66	2.71	10.4
SST-03-04-CPL-14	54.30	53.66	2.63	11.3
SST-03-04-CPL-15	55.56	53.66	2.63	10.6
SST-09-03-CPL-16	54.91	53.66	2.72	12.5
SST-09-03-CPL-17	57.03	53.66	2.71	12.5
SST-01-01-CPL-18	57.05	53.66	2.67	13.2
SST-02-07-CPL-19	55.96	53.66	2.69	11.1
SST-02-07-CPL-20	55.27	53.66	2.71	11.8
			Average	**10.8±2.2**

Table A-3 Results of conventional point load strength index test on tuffaceous sand stone.

Sample No.	Length (mm)	Diameter (mm)	Density (g/cc)	Point Load Strength Index Test, I_s (MPa)
TST-06-05-CPL-01	56.57	53.66	2.63	12.5
TST-06-05-CPL-02	57.81	53.66	2.64	10.9
TST-02-05-CPL-03	56.86	53.66	2.63	10.6
TST-02-05-CPL-04	57.47	53.66	2.64	8.0
TST-08-03-CPL-05	56.06	53.66	2.68	11.5
TST-08-03-CPL-06	55.74	53.66	2.66	11.8
TST-08-01-CPL-07	54.91	53.66	2.68	11.1
TST-08-01-CPL-08	54.78	53.66	2.68	11.5
TST-04-02-CPL-09	54.22	53.66	2.63	10.3
TST-04-02-CPL-10	53.87	53.66	2.64	11.1
TST-08-04-CPL-11	53.71	53.66	2.67	11.5
TST-08-04-CPL-12	54.63	53.66	2.67	11.3
TST-06-07-CPL-13	55.45	53.66	2.67	10.8
TST-04-01-CPL-14	57.29	53.66	2.61	5.9
TST-06-06-CPL-15	54.57	53.66	2.61	9.9
TST-06-06-CPL-16	54.69	53.66	2.63	10.9
TST-06-06-CPL-17	54.97	53.66	2.66	12.2
TST-04-03-CPL-18	55.50	53.66	2.61	8.7
TST-04-03-CPL-19	55.21	53.66	2.62	5.2
TST-04-05-CPL-20	54.77	53.66	2.64	8.7
			Average	**10.2±2.0**

Table A-4 Results of uniaxial compressive strength tests and elastic modulus measurements on porphyritic andesite.

Sample No.	Length (mm)	Diameter (mm)	Density (g/cc)	σ_c (MPa)	E (GPa)
And-02-02-UCS-01	134.86	53.66	2.82	132.7	45.1
And -06-03-UCS-02	134.94	53.66	2.83	110.6	39.7
And -02-01-UCS-03	134.85	53.66	2.80	106.1	47.0
And -08-03-UCS-04	134.17	53.66	2.84	128.2	39.2
And -04-04-UCS-05	134.64	53.66	2.85	97.3	43.8
			Average	**115±15.0**	**43.0±3.4**

Table A-5 Results of uniaxial compressive strength tests and elastic modulus measurements on silicified tuffaceous sandstone.

Sample No.	Length (mm)	Diameter (mm)	Density (g/cc)	σ_c (MPa)	E (GPa)
SST-02-01-UCS-01	133.09	53.66	2.71	119.4	65.69
SST-07-01-UCS-02	135.47	53.66	2.67	93.0	63.2
SST-07-03-UCS-03	130.95	53.66	2.68	119.4	50.3
SST-02-06-UCS-04	134.75	53.66	2.69	161.4	66.1
SST-06-02-UCS-05	135.77	53.66	2.70	110.6	71.3
			Average	**120.7±25.2**	**63.3±8.0**

Table A-6 Results of uniaxial compressive strength tests and elastic modulus measurements on tuffaceous sandstone.

Sample No.	Length (mm)	Diameter (mm)	Density (g/cc)	σ_c (MPa)	E (GPa)
TST-08-02-UCS-01	138.10	53.66	2.66	101.7	53.8
TST-01-02-UCS-02	132.36	53.66	2.68	123.8	54.5
TST-02-04-UCS-03	135.58	53.66	2.64	97.3	44.1
TST-06-09-UCS-04	135.15	53.66	2.67	145.9	47.5
TST-02-02-UCS-05	137.45	53.66	2.63	88.4	56.6
			Average	**111.4±23.3**	**51.3±5.3**

Table A-7 Results of Brazilian tensile strength tests on porphyritic andesite.

Sample No.	Thickness (mm)	Diameter (mm)	Density (g/cc)	Failure Load (kN)	σ_B (MPa)
And-04-03-BZ-01	26.28	53.66	2.81	39.5	17.8
And-04-03-BZ-02	25.51	53.66	2.79	35.0	16.3
And-04-03-BZ-03	27.55	53.66	2.85	38.0	16.4
And-04-03-BZ-04	26.69	53.66	2.79	41.5	18.4
And-04-06-BZ-05	26.86	53.66	2.80	32.0	14.1
And-04-06-BZ-06	26.99	53.66	2.86	41.5	18.2
And-04-06-BZ-07	26.49	53.66	2.82	39.5	17.7
And-04-06-BZ-08	26.42	53.66	2.86	34.0	15.3
And-06-01-BZ-09	26.78	53.66	2.86	43.5	19.3
And-06-01-BZ-10	27.58	53.66	2.85	38.5	16.6
				Average	**17.0±1.6**

Table A-8 Results of Brazilian tensile strength tests on silicified tuffaceous sandstone.

Sample No.	Thickness (mm)	Diameter (mm)	Density (g/cc)	Failure Load (kN)	σ_B (MPa)
SST-02-02-BZ-01	25.07	53.66	2.65	45.0	21.3
SST-01-06-BZ-02	26.64	53.66	2.64	52.0	23.2
SST-01-02-BZ-03	25.95	53.66	2.62	40.0	18.3
SST-01-02-BZ-04	25.93	53.66	2.61	32.0	14.6
SST-01-02-BZ-05	26.08	53.66	2.66	50.0	22.8
SST-02-01-BZ-06	27.10	53.66	2.66	50.0	22.0
SST-02-01-BZ-07	26.54	53.66	2.62	45.0	20.1
SST-01-05-BZ-08	27.78	53.66	2.68	35.0	15.0
SST-01-05-BZ-09	27.93	53.66	2.66	40.0	17.0
SST-01-05-BZ-10	27.95	53.66	2.66	40.0	17.0
				Average	**19.1±3.2**

Table A-9 esults of Brazilian tensile strength tests on tuffaceous sandstone.

Sample No.	Thickness (mm)	Diameter (mm)	Density (g/cc)	Failure Load (kN)	σ_B (MPa)
TST-02-03-BZ-01	28.11	53.66	2.60	36.0	15.2
TST-02-03-BZ-02	27.57	53.66	2.60	25.5	11.0
TST-02-03-BZ-03	27.39	53.66	2.62	32.5	14.1
TST-02-03-BZ-04	26.88	53.66	2.63	17.5	7.7
TST-06-04-BZ-05	27.65	53.66	2.66	45.0	19.3
TST-06-04-BZ-06	27.29	53.66	2.64	28.0	12.2
TST-06-04-BZ-07	27.30	53.66	2.60	23.0	10.0
TST-06-02-BZ-08	27.48	53.66	2.64	28.5	12.3
TST-06-02-BZ-09	27.43	53.66	2.61	29.0	12.5
TST-06-02-BZ-10	26.58	53.66	2.65	37.0	16.5
				Average	**13.1±3.3**

Table A-10 esults of triaxial compressive strength tests on porphyritic andesite.

Sample No.	Length (mm)	Diameter (mm)	Density (g/cc)	σ_3 (MPa)	σ_1 (MPa
And-02-02-UCS-01	134.86	53.66	2.82	132.7	45.1
And -06-03-UCS-02	134.94	53.66	2.83	110.6	39.7
And -02-01-UCS-03	134.85	53.66	2.80	106.1	47.0
And -08-03-UCS-04	134.17	53.66	2.84	128.2	39.2
And -04-04-UCS-05	134.64	53.66	2.85	97.3	43.8
			Average	**115±15.0**	**43.0±3.4**

Table A-11 Results of triaxial compressive strength tests on silicified tuffaceous sandstone.

Sample No.	Length (mm)	Diameter (mm)	Density (g/cc)	σ_3 (MPa)	σ_1 (MPa
SST-02-01-UCS-01	133.09	53.66	2.71	119.4	65.69
SST-07-01-UCS-02	135.47	53.66	2.67	93.0	63.2
SST-07-03-UCS-03	130.95	53.66	2.68	119.4	50.3
SST-02-06-UCS-04	134.75	53.66	2.69	161.4	66.1
SST-06-02-UCS-05	135.77	53.66	2.70	110.6	71.3
			Average	**120.7±25.2**	**63.3±8.0**

Table A-12 Results of triaxial compressive strength tests on tuffaceous sandstone.

Sample No.	Length (mm)	Diameter (mm)	Density (g/cc)	σ_3 (MPa)	σ_1 (MPa
TST-08-02-UCS-01	138.10	53.66	2.66	101.7	53.8
TST-01-02-UCS-02	132.36	53.66	2.68	123.8	54.5
TST-02-04-UCS-03	135.58	53.66	2.64	97.3	44.1
TST-06-09-UCS-04	135.15	53.66	2.67	145.9	47.5
TST-02-02-UCS-05	137.45	53.66	2.63	88.4	56.6
			Average	**111.4±23.3**	**51.3±5.3**

APPENDIX B

MODIFIED POINT LOAD TEST RESULTS FOR ELASTIC MODULUS PREDICTION

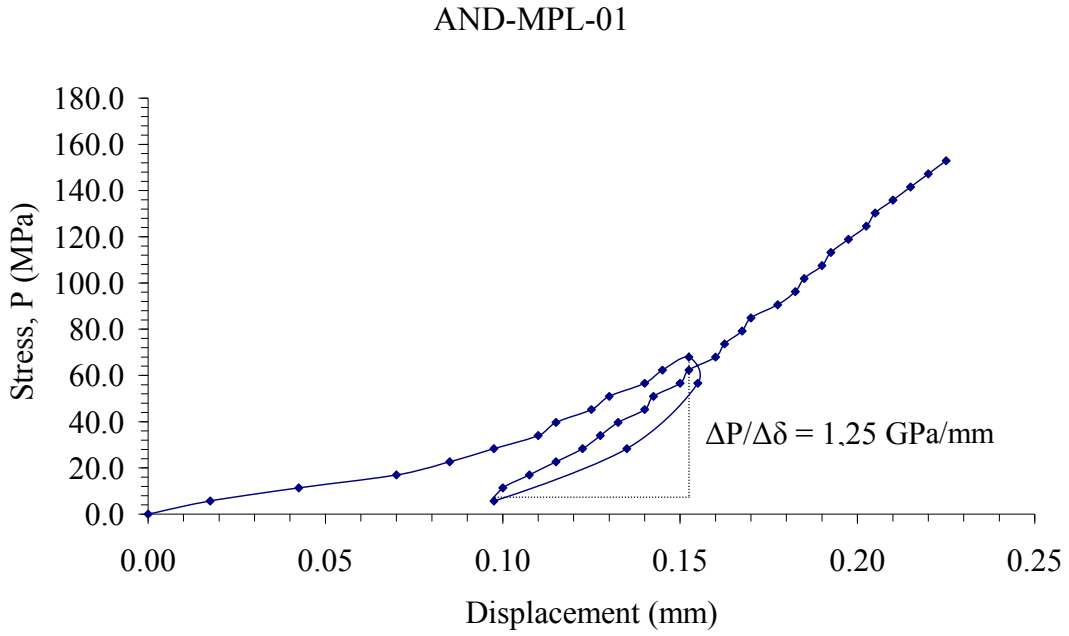

Figure B.1 Applied stress (P) as a function of displacement (δ) for specimen no. And-MPL-01.

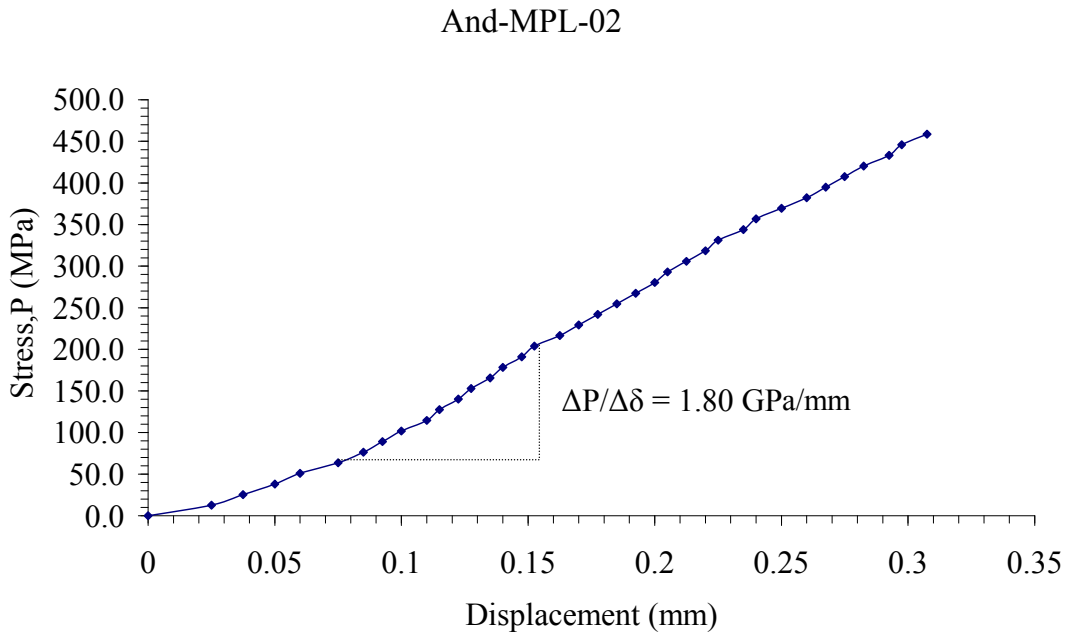

Figure B.2 Applied stress (P) as a function of displacement (δ) for specimen no. And-MPL-02.

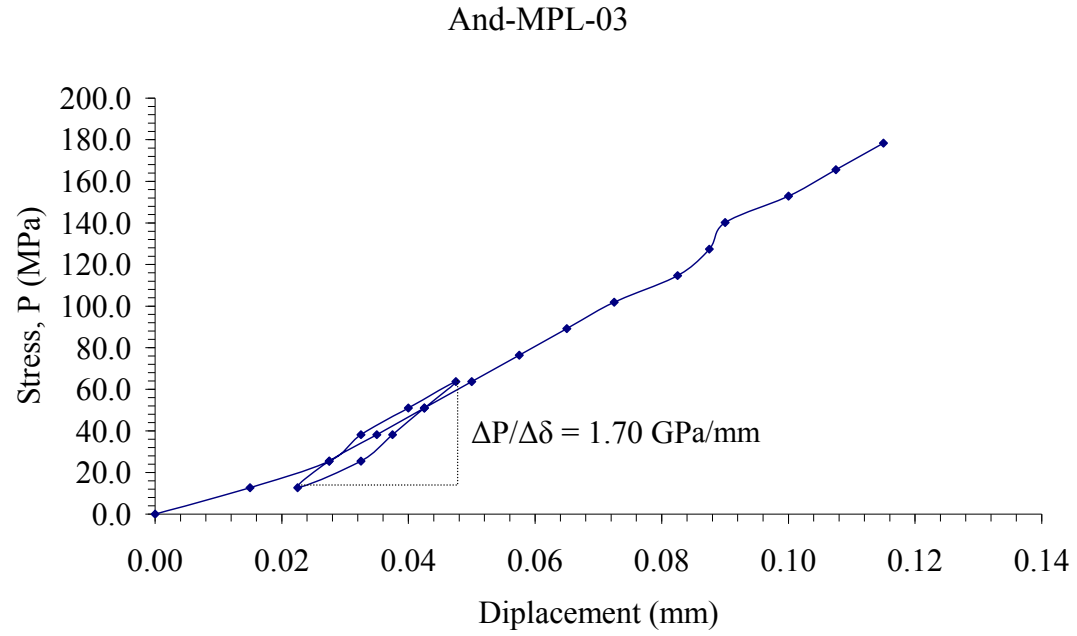

Figure B.3 Applied stress (P) as a function of displacement (δ) for specimen no. And-MPL-03.

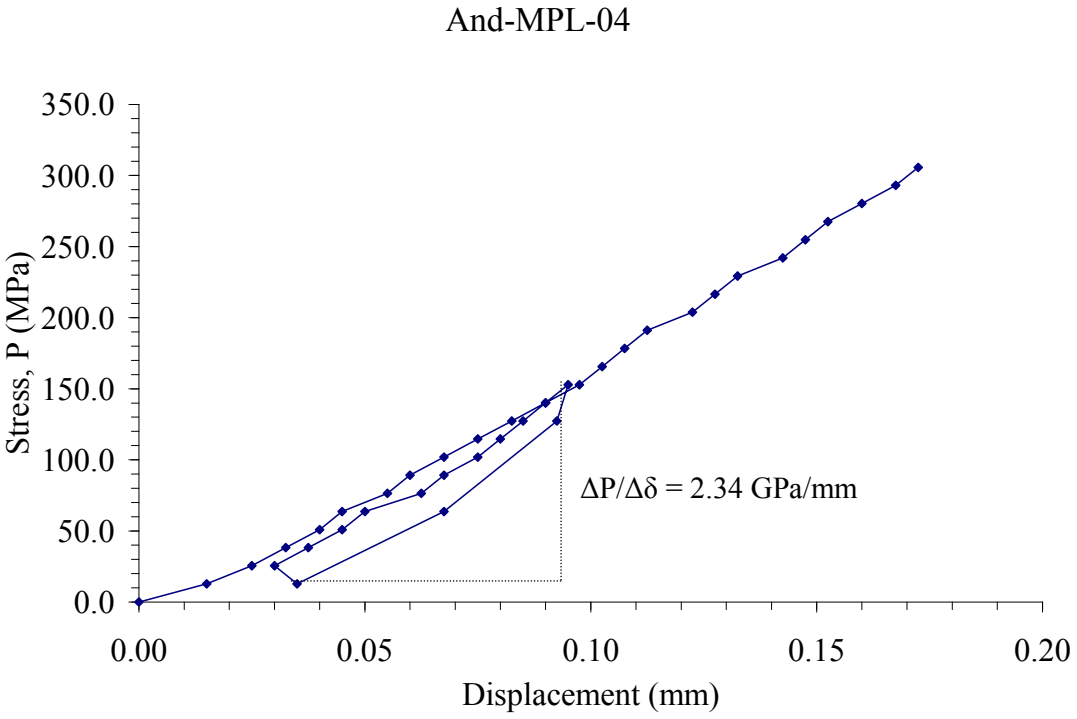

Figure B.4 Applied stress (P) as a function of displacement (δ) for specimen no. And-MPL-04.

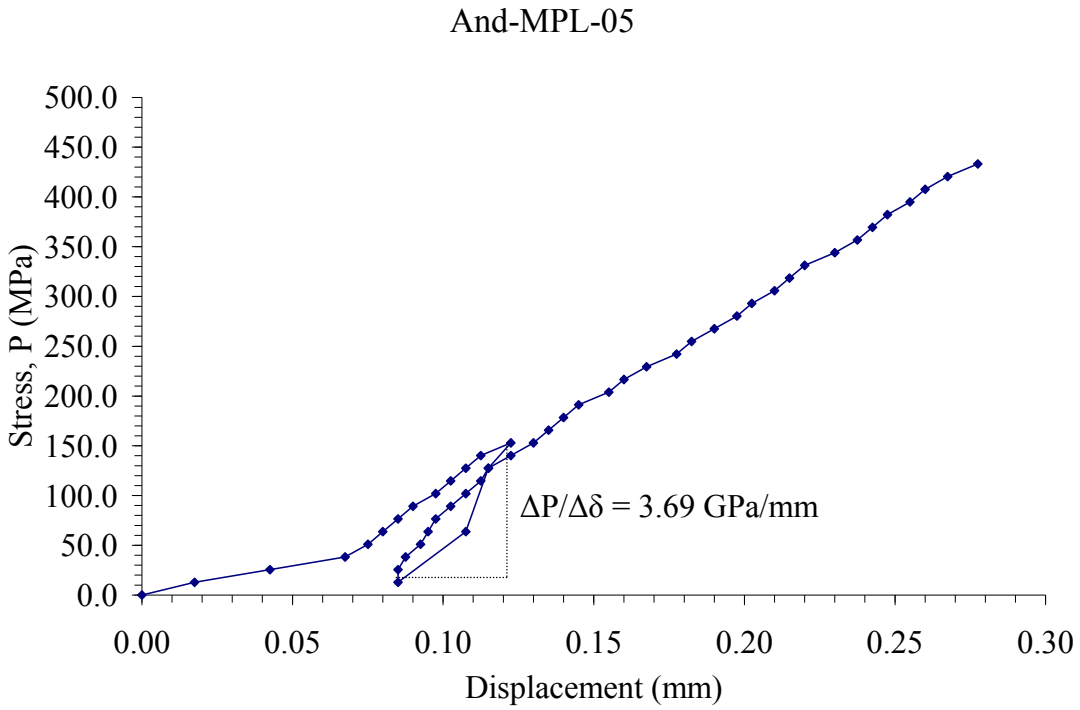

Figure B.5 Applied stress (P) as a function of displacement (δ) for specimen no. And-MPL-05.

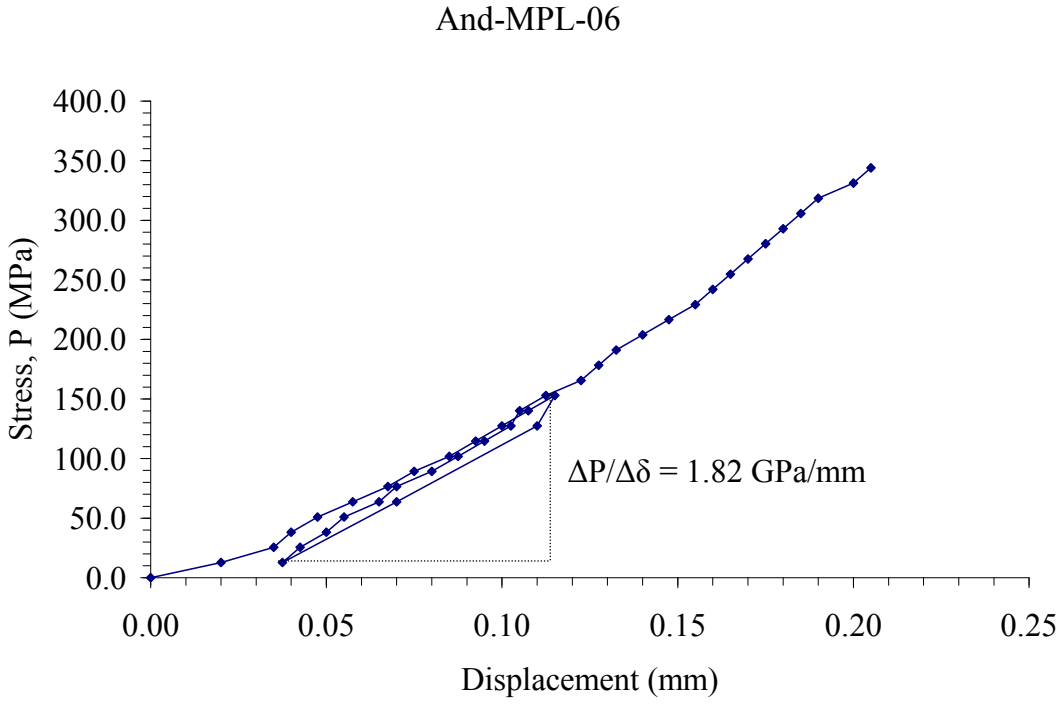

Figure B.6 Applied stress (P) as a function of displacement (δ) for specimen no. And-MPL-06.

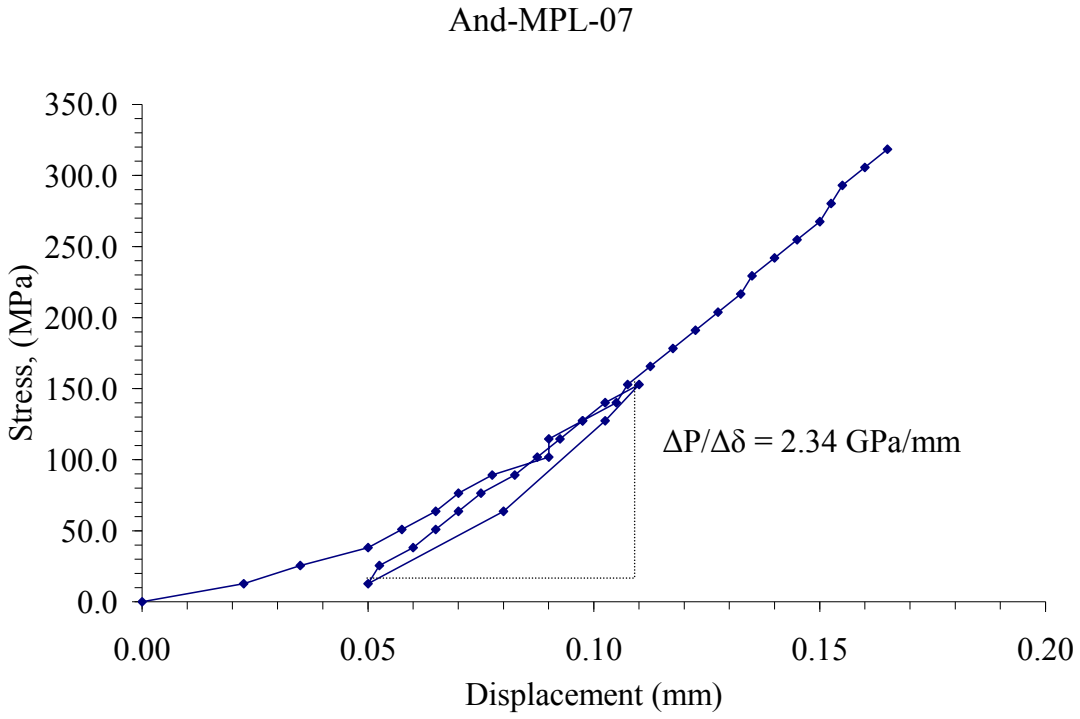

Figure B.7 Applied stress (P) as a function of displacement (δ) for specimen no. And-MPL-07.

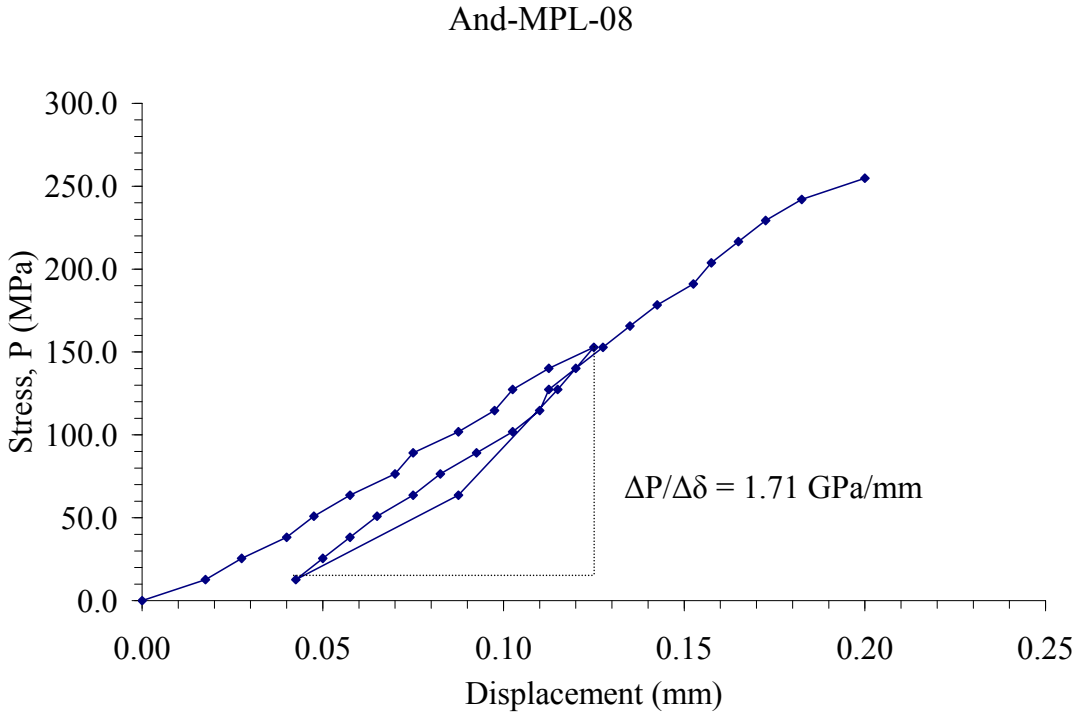

Figure B.8 Applied stress (P) as a function of displacement (δ) for specimen no. And-MPL-08.

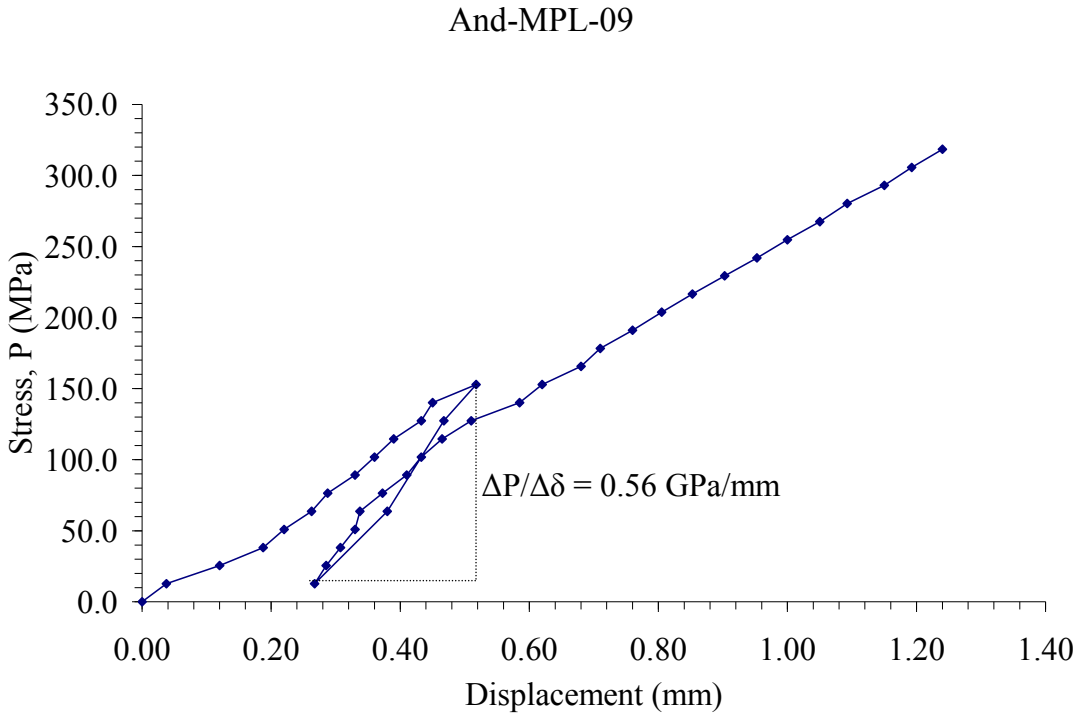

Figure B.9 Applied stress (P) as a function of displacement (δ) for specimen no. And-MPL-09.

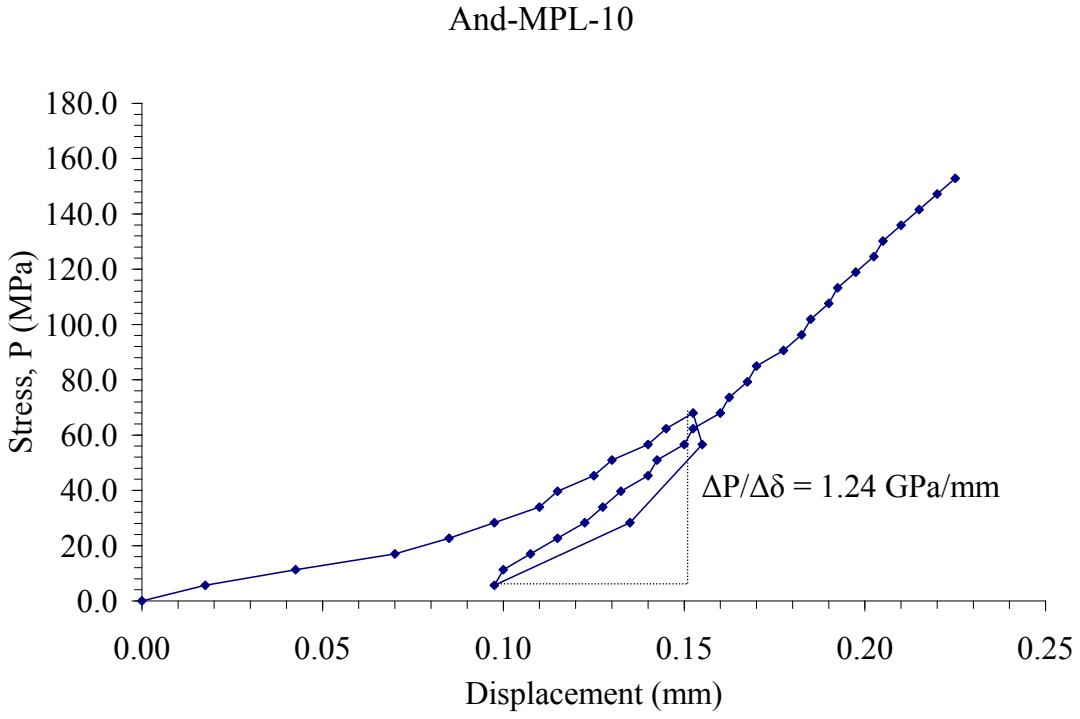

Figure B.10 Applied stress (P) as a function of displacement (δ) for specimen no. And-MPL-10.

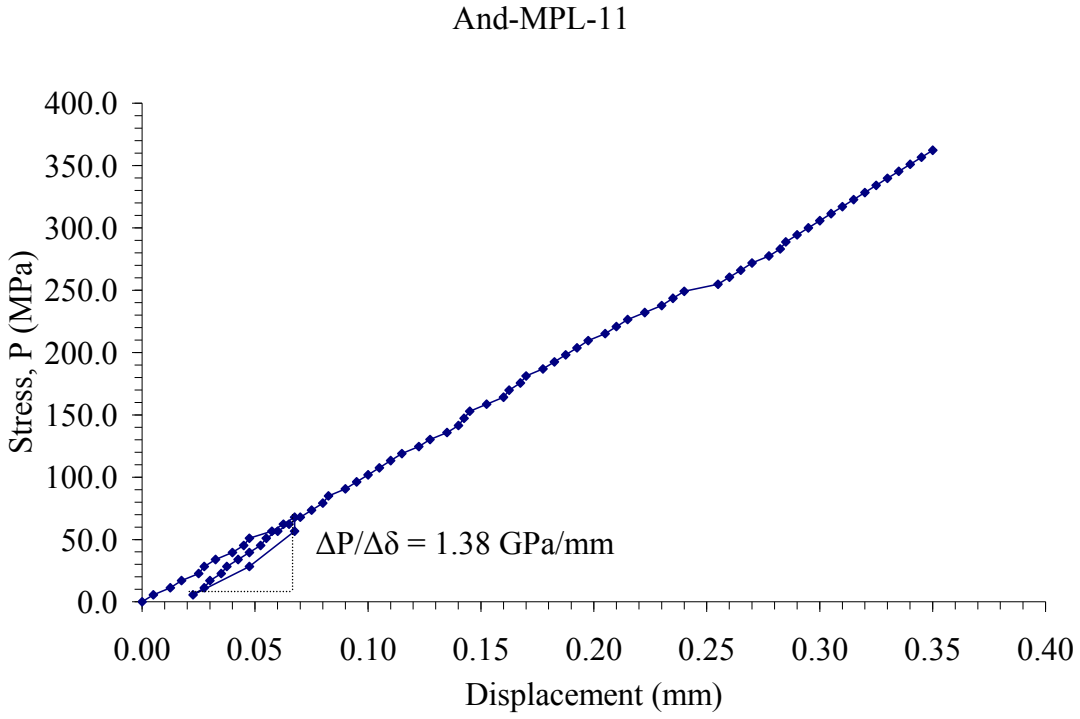

Figure B.11 Applied stress (P) as a function of displacement (δ) for specimen no. And-MPL-11.

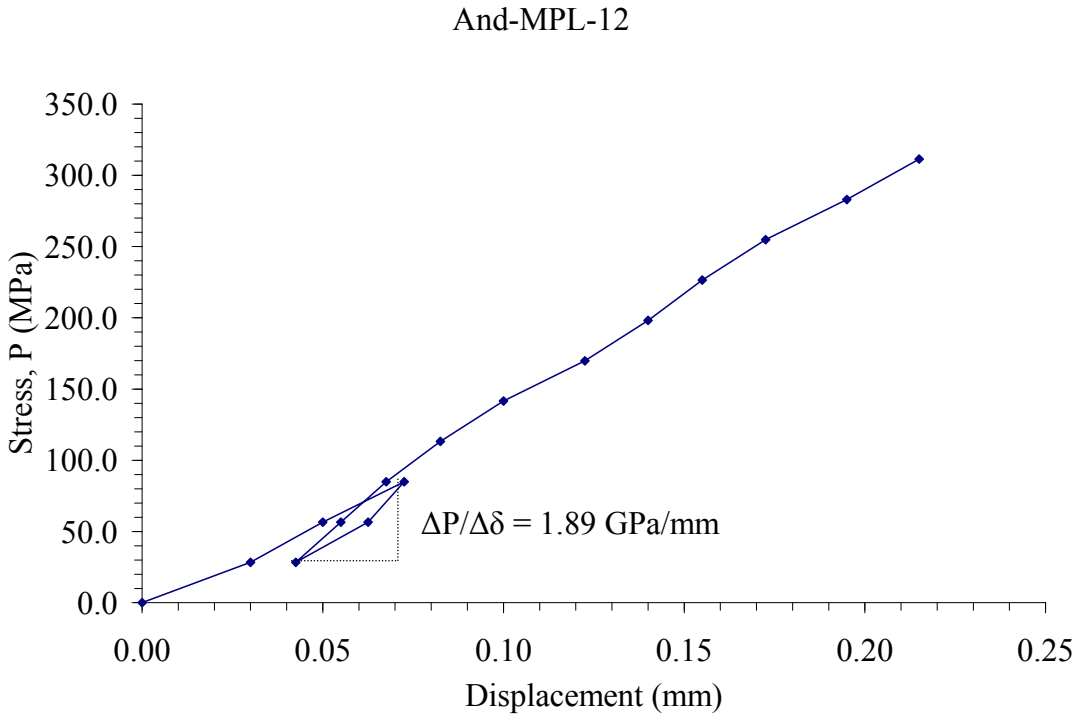

Figure B.12 Applied stress (P) as a function of displacement (δ) for specimen no. And-MPL-12.

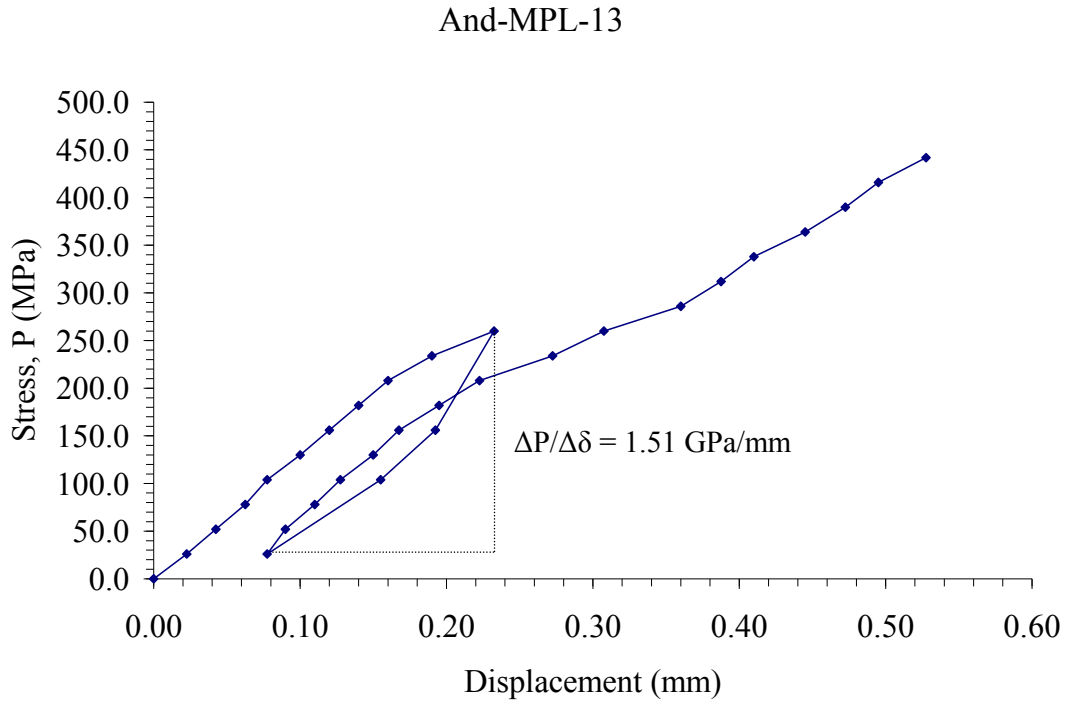

Figure B.13 Applied stress (P) as a function of displacement (δ) for specimen no. And-MPL-13.

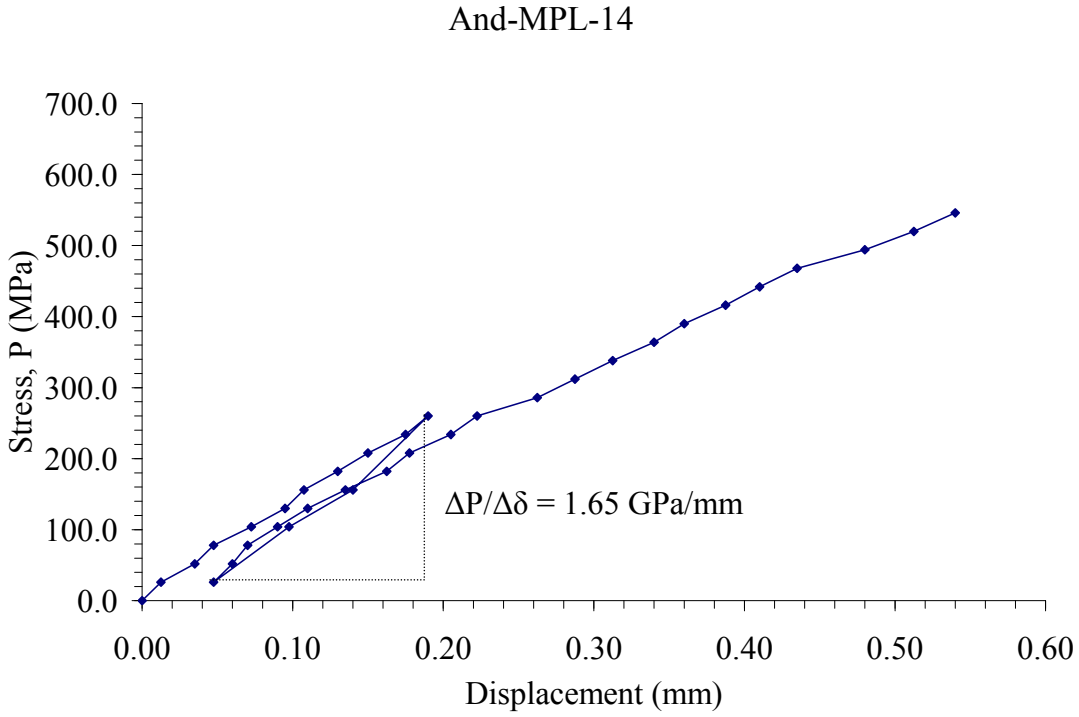

Figure B.14 Applied stress (P) as a function of displacement (δ) for specimen no. And-MPL-14.

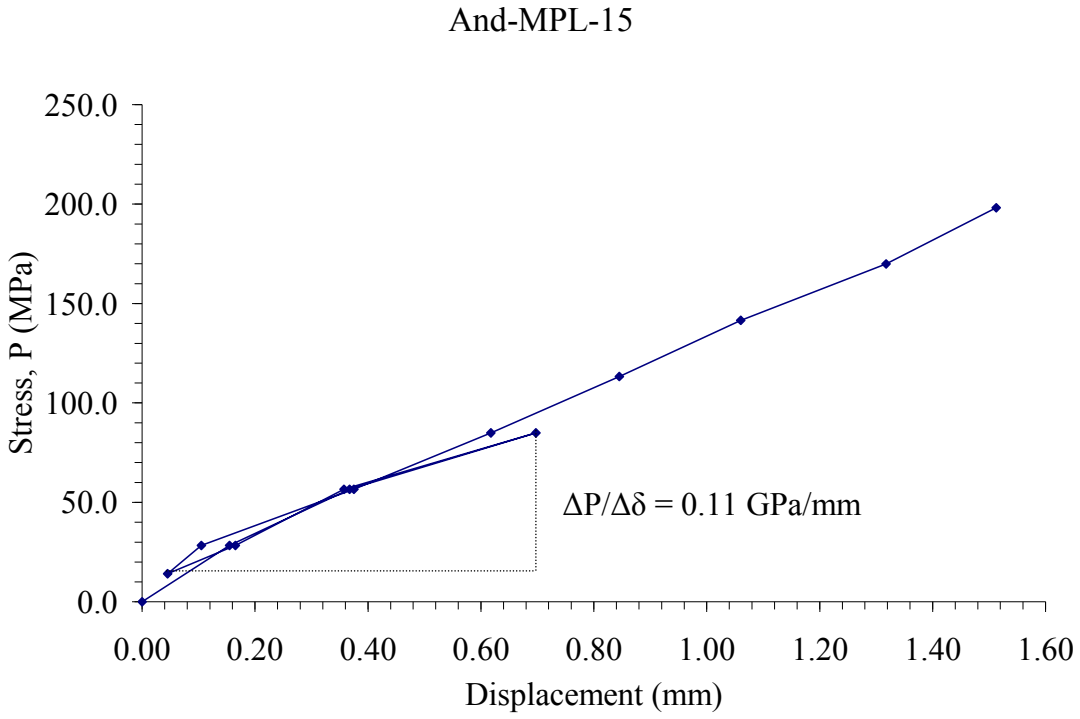

Figure B.15 Applied stress (P) as a function of displacement (δ) for specimen no. And-MPL-15.

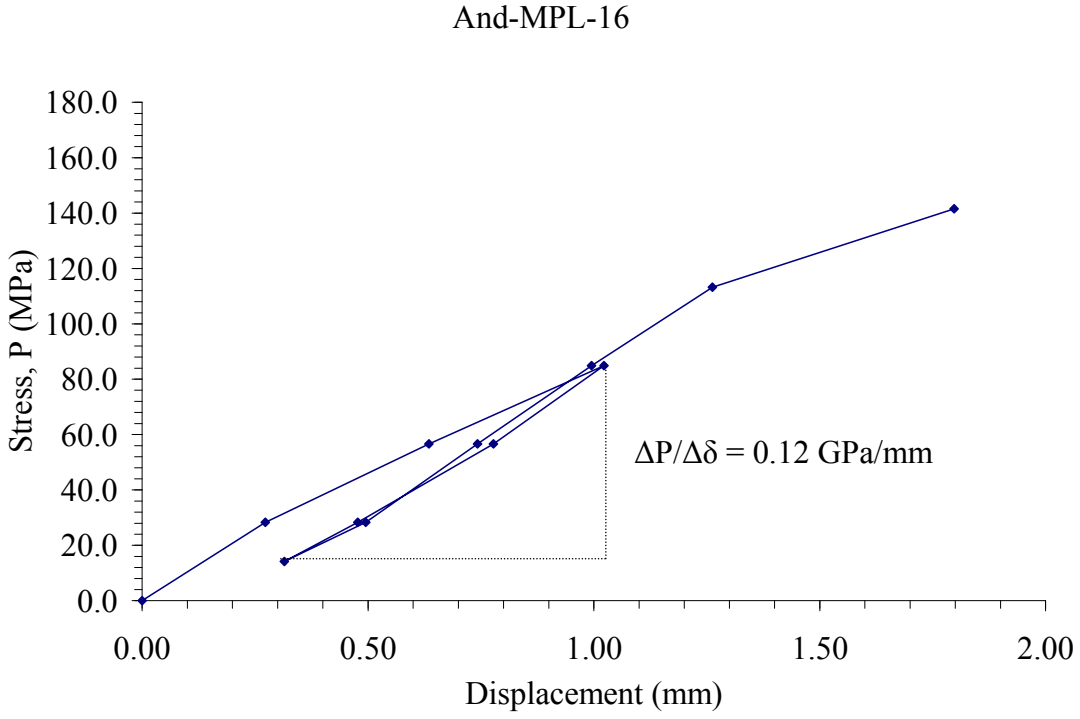

Figure B.16 Applied stress (P) as a function of displacement (δ) for specimen no. And-MPL-16.

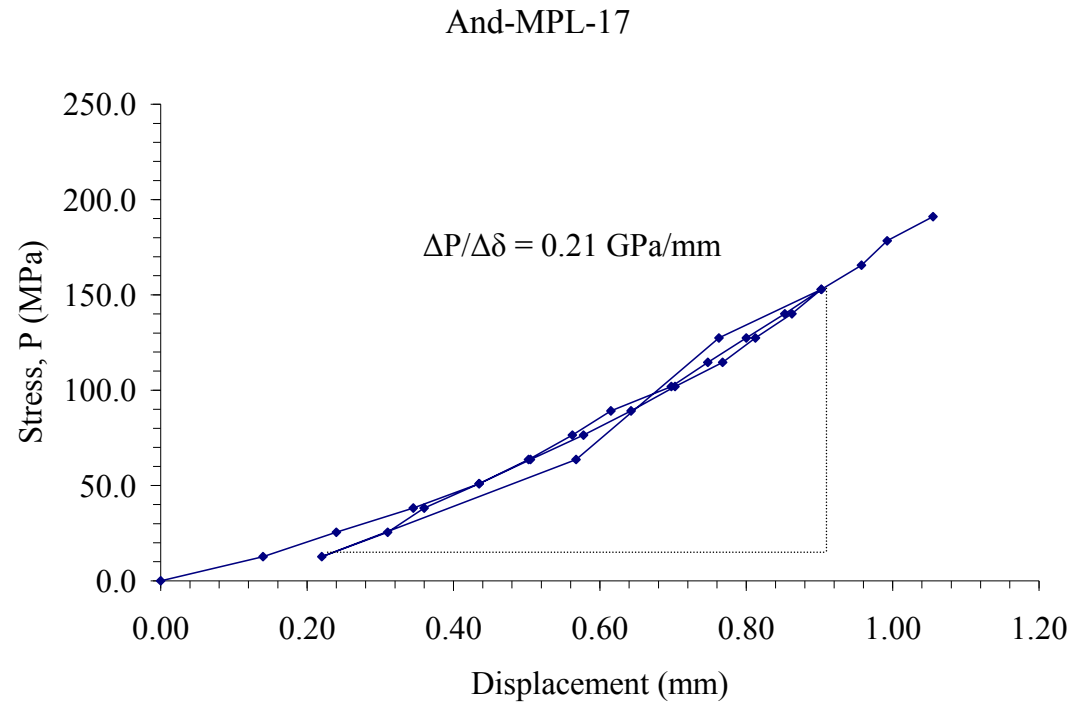

Figure B.17 Applied stress (P) as a function of displacement (δ) for specimen no. And-MPL-17.

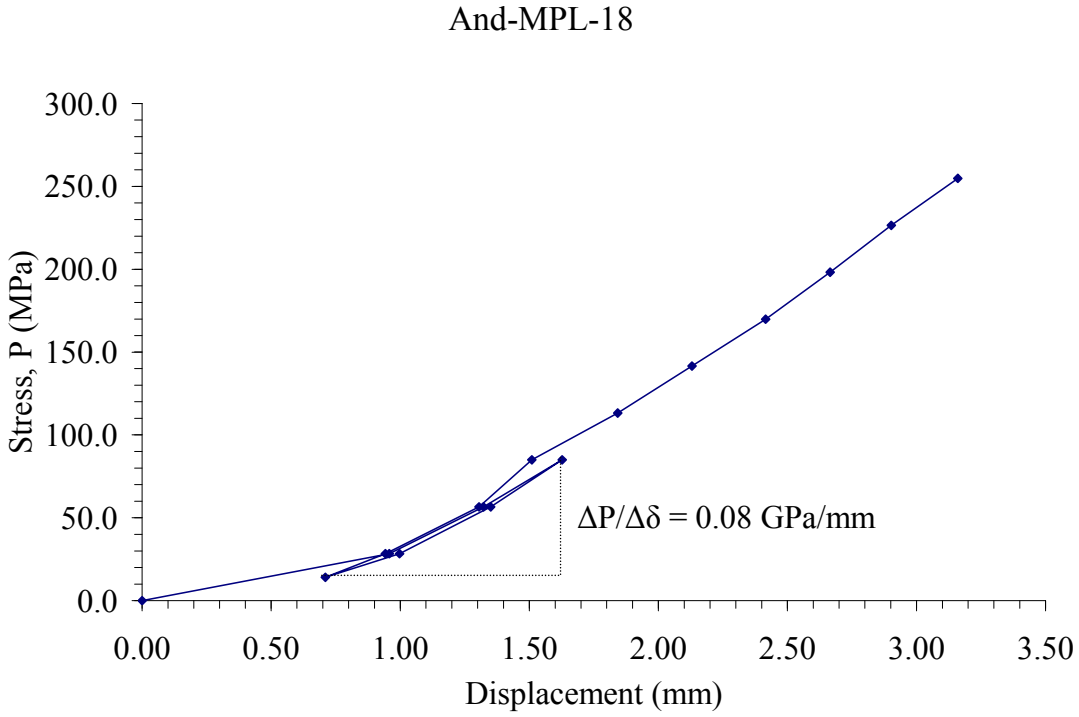

Figure B.18 Applied stress (P) as a function of displacement (δ) for specimen no. And-MPL-18.

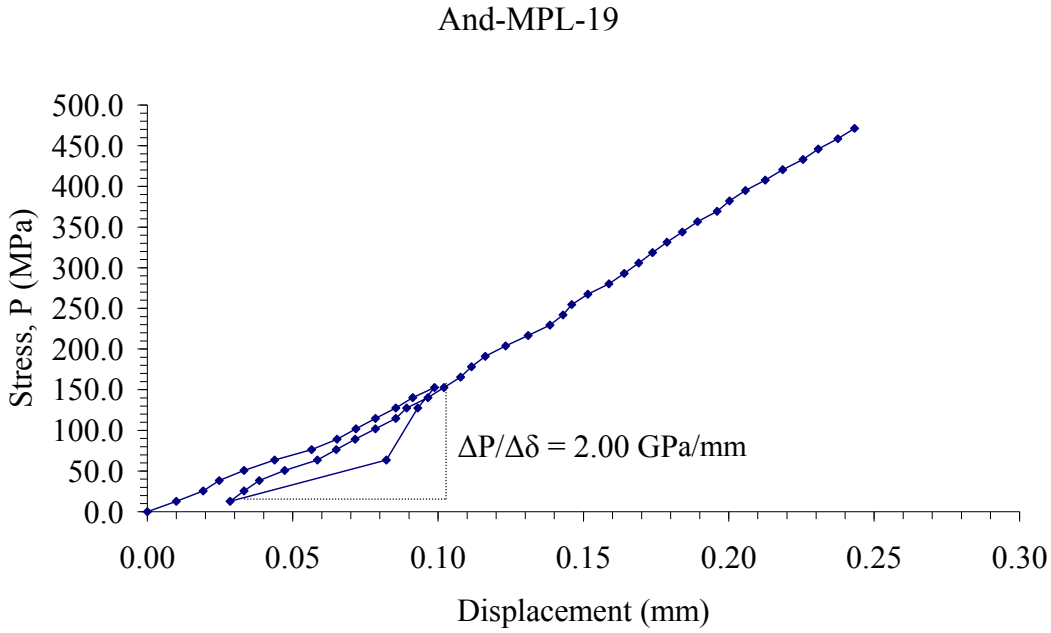

Figure B.19 Applied stress (P) as a function of displacement (δ) for specimen no. And-MPL-19.

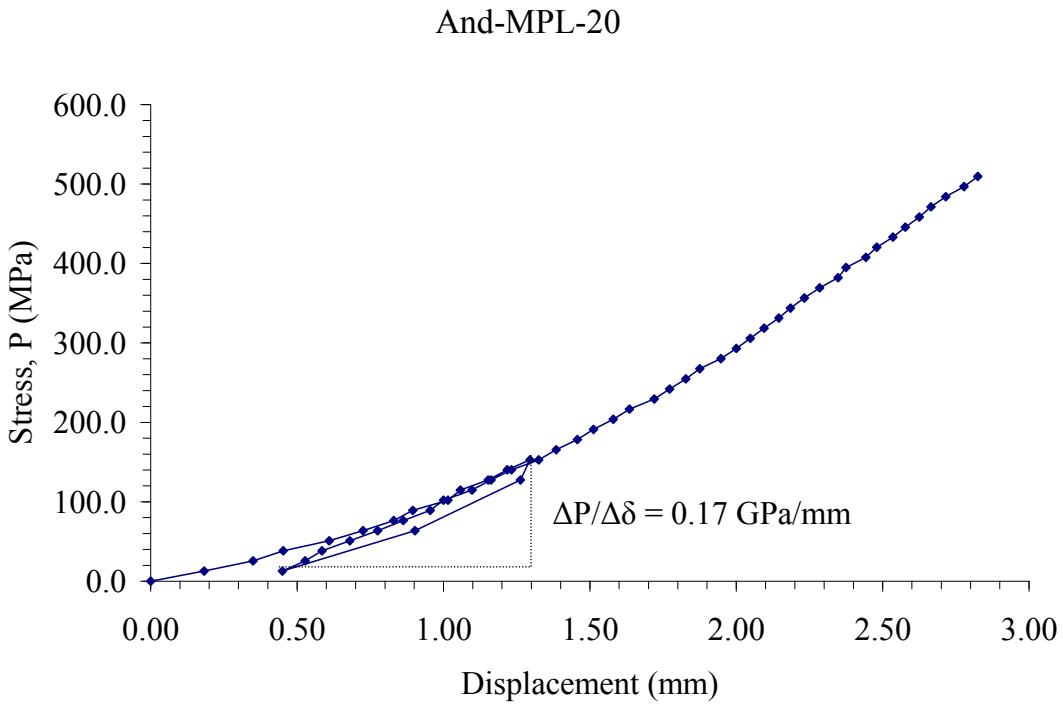

Figure B.20 Applied stress (P) as a function of displacement (δ) for specimen no. And-MPL-20.

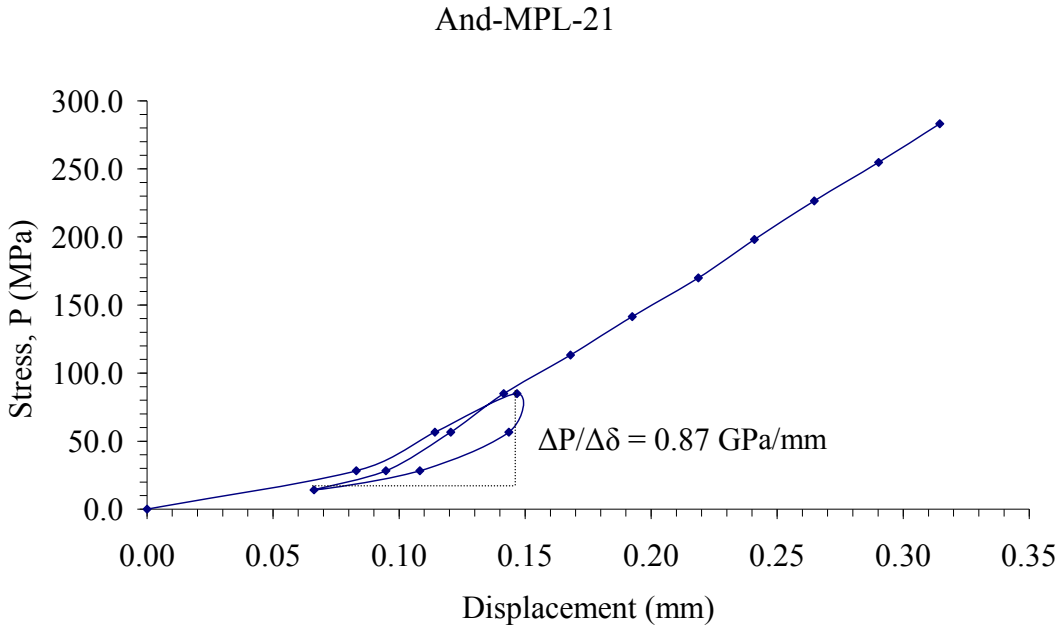

Figure B.21 Applied stress (P) as a function of displacement (δ) for specimen no. And-MPL-21.

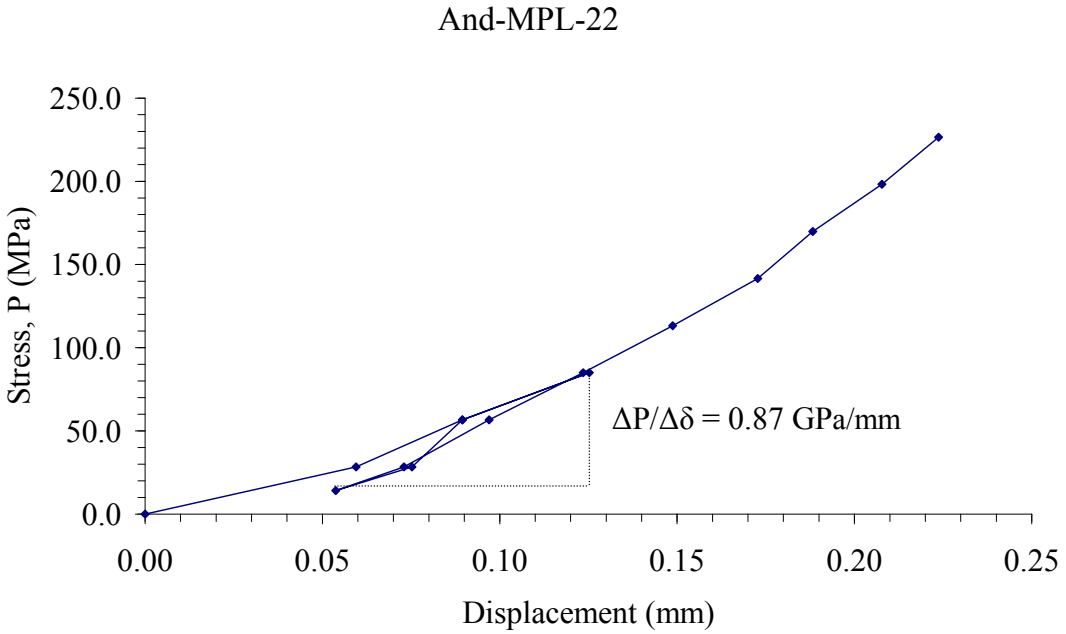

Figure B.22 Applied stress (P) as a function of displacement (δ) for specimen no. And-MPL-22.

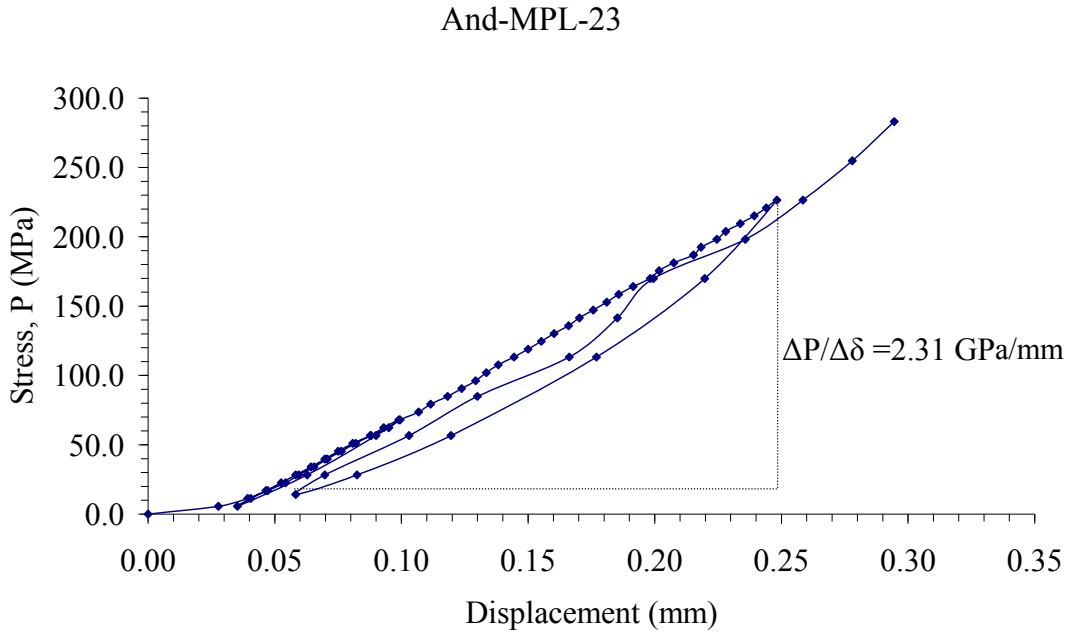

Figure B.23 Applied stress (P) as a function of displacement (δ) for specimen no. And-MPL-23.

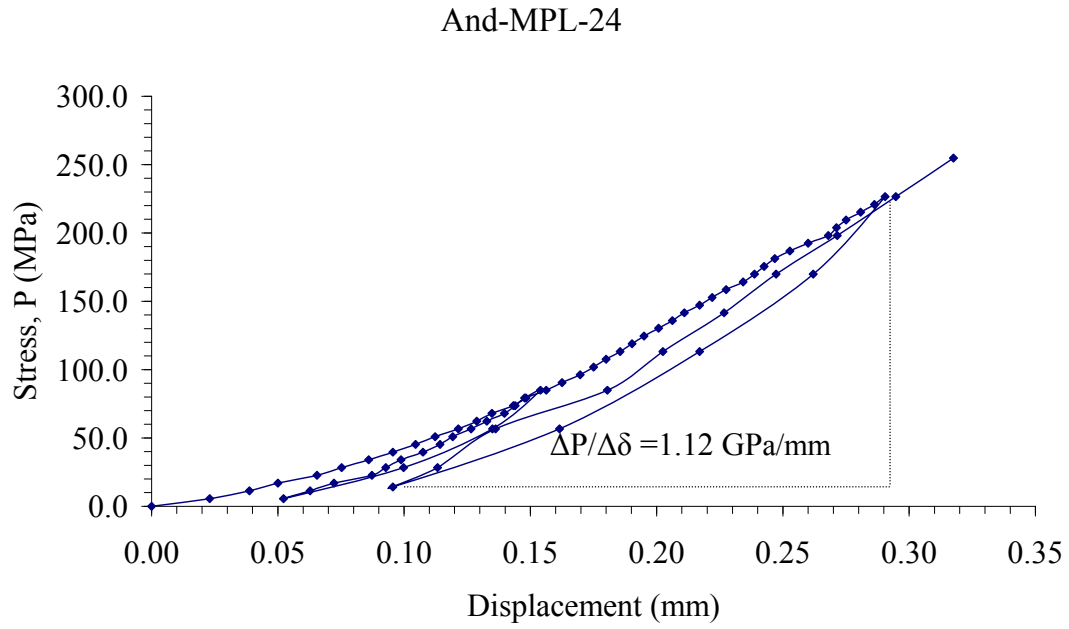

Figure B.24 Applied stress (P) as a function of displacement (δ) for specimen no. And-MPL-24.

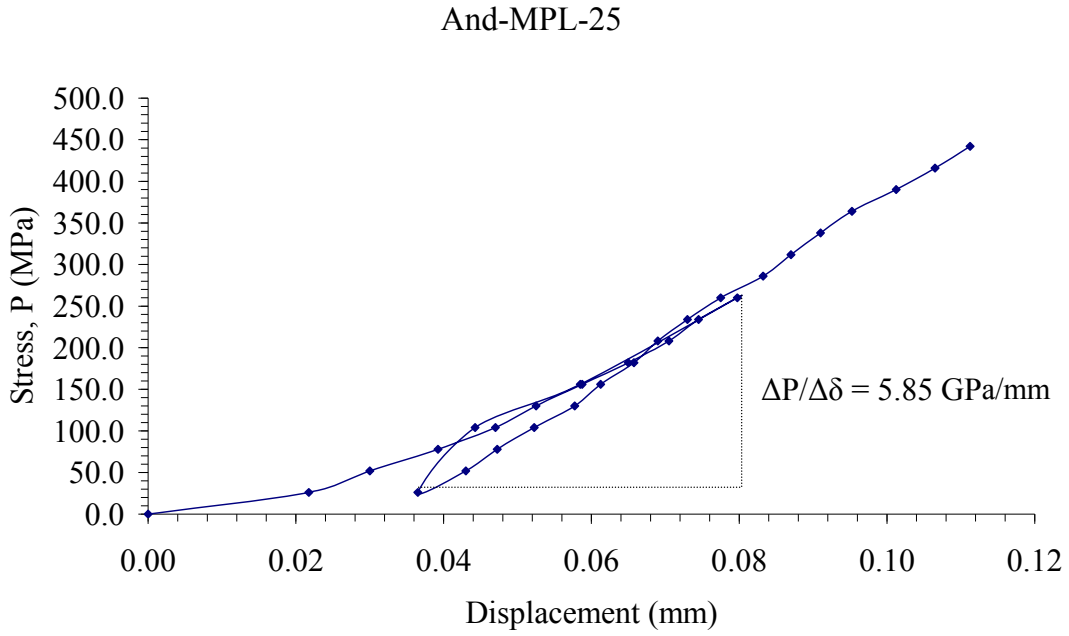

Figure B.25 Applied stress (P) as a function of displacement (δ) for specimen no. And-MPL-25.

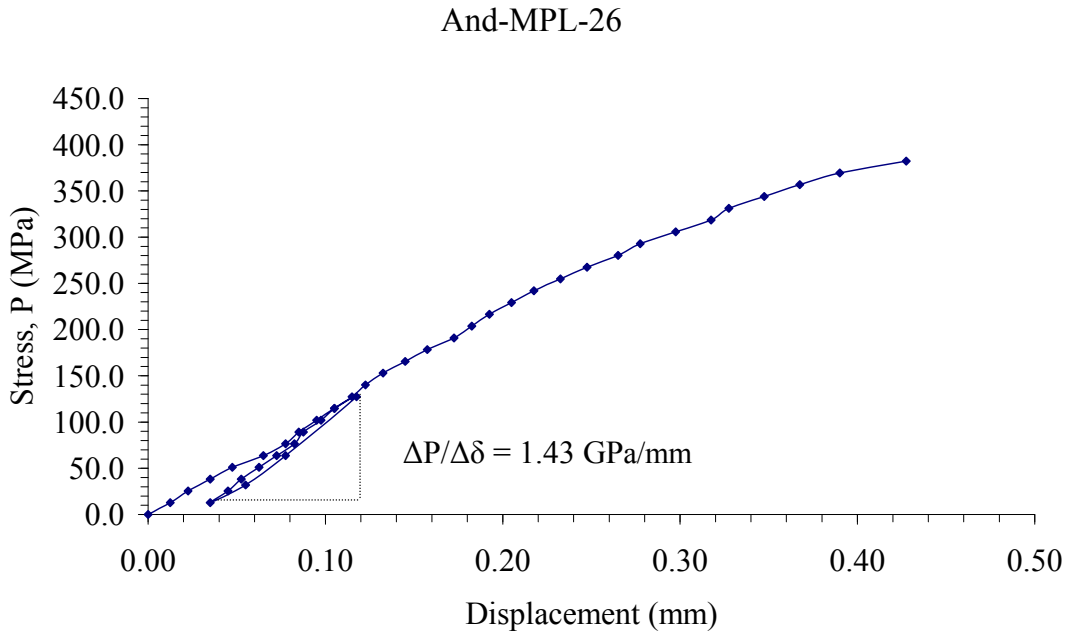

Figure B.26 Applied stress (P) as a function of displacement (δ) for specimen no. And-MPL-26.

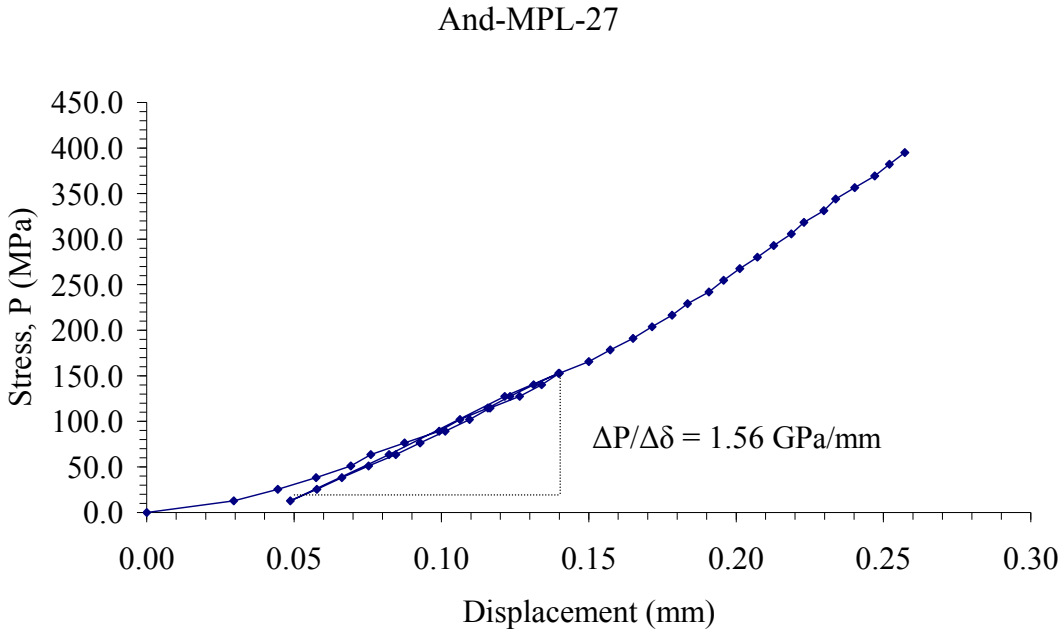

Figure B.27 Applied stress (P) as a function of displacement (δ) for specimen no. And-MPL-27.

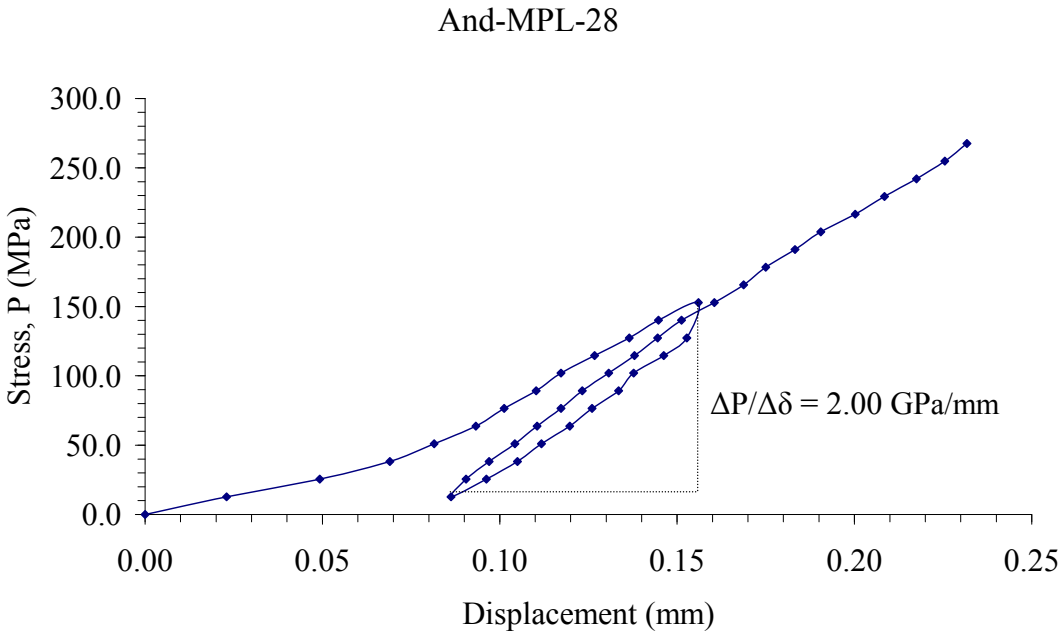

Figure B.28 Applied stress (P) as a function of displacement (δ) for specimen no. And-MPL-28.

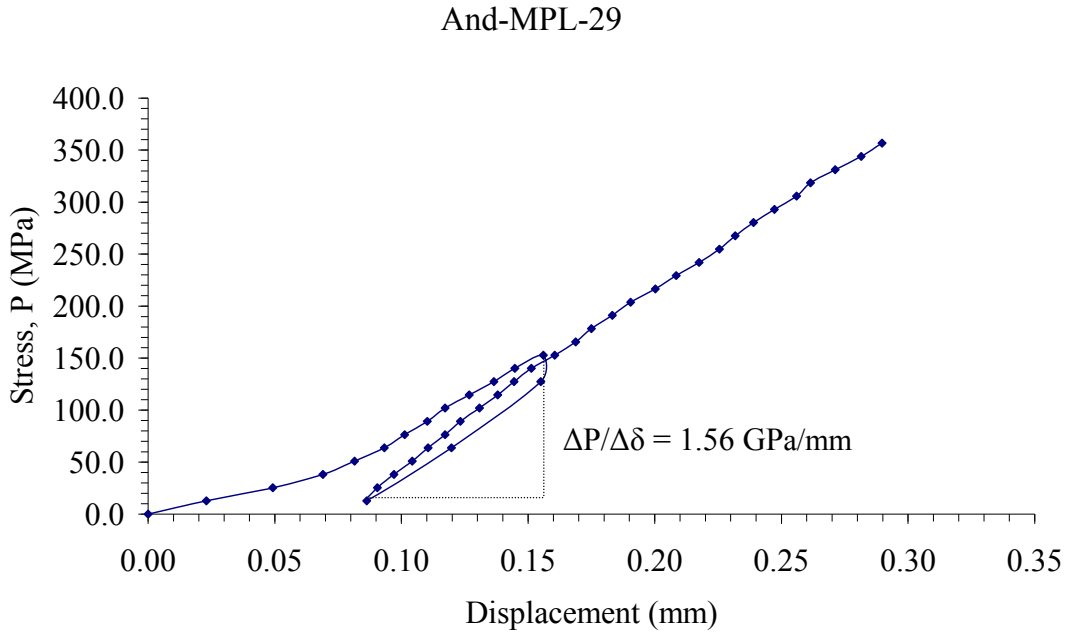

Figure B.29 Applied stress (P) as a function of displacement (δ) for specimen no. And-MPL-29.

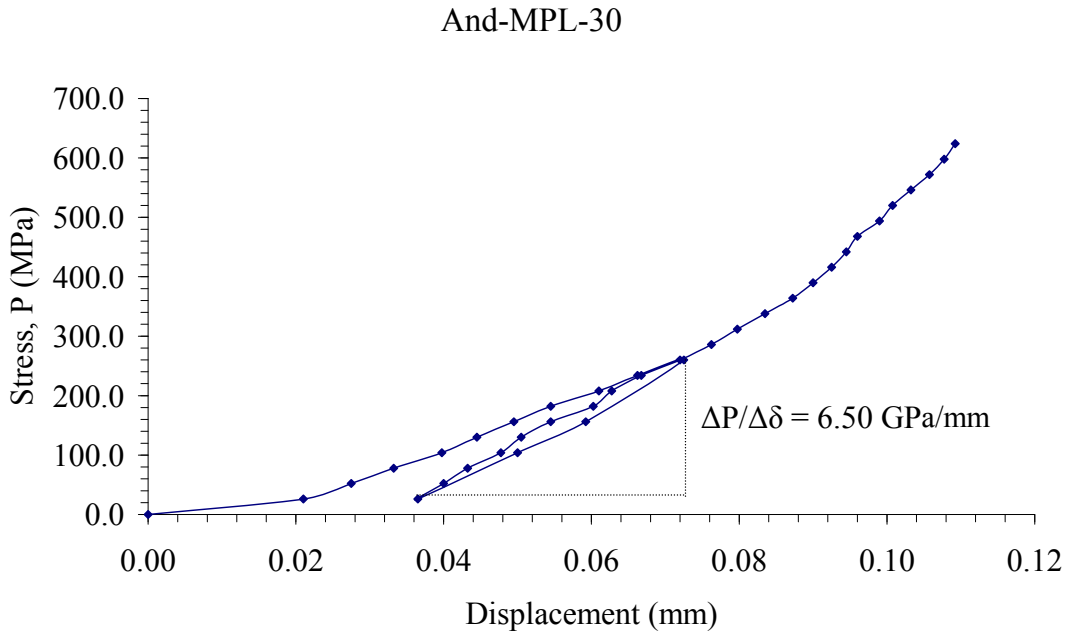

Figure B.30 Applied stress (P) as a function of displacement (δ) for specimen no. And-MPL-30.

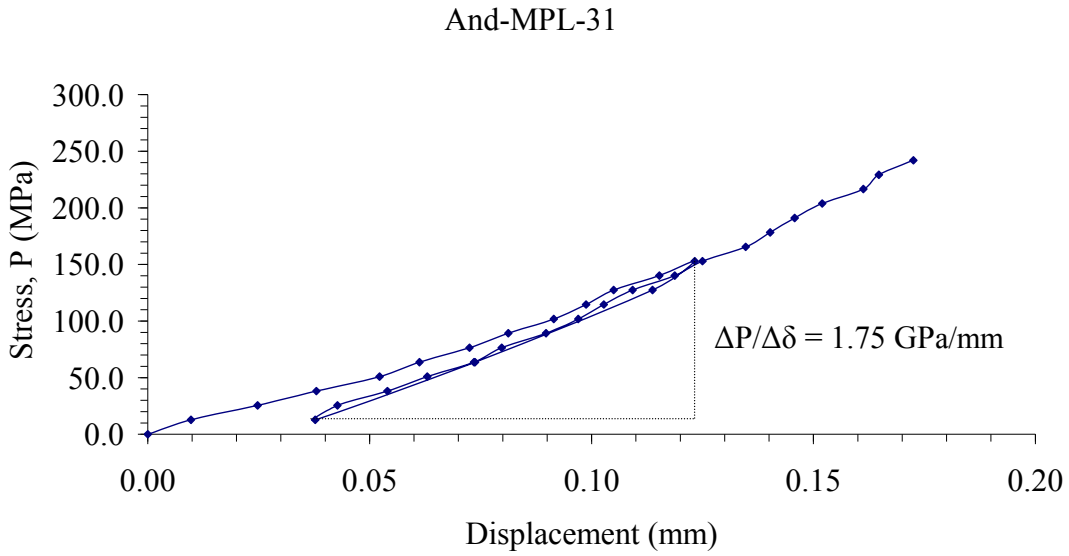

Figure B.31 Applied stress (P) as a function of displacement (δ) for specimen no. And-MPL-31.

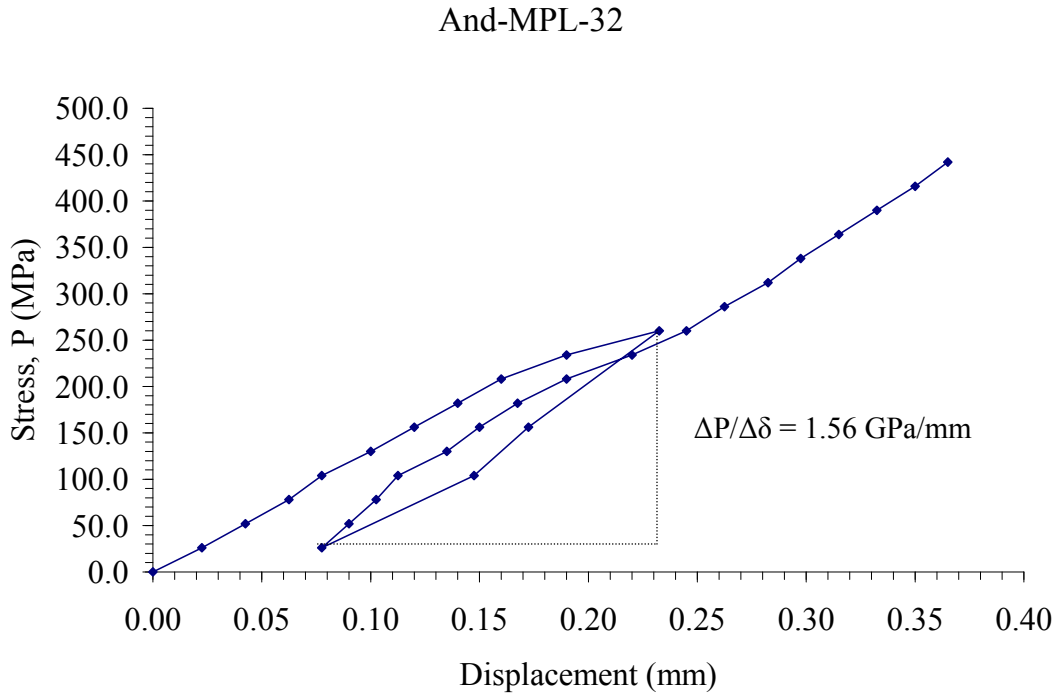

Figure B.32 Applied stress (P) as a function of displacement (δ) for specimen no. And-MPL-32.

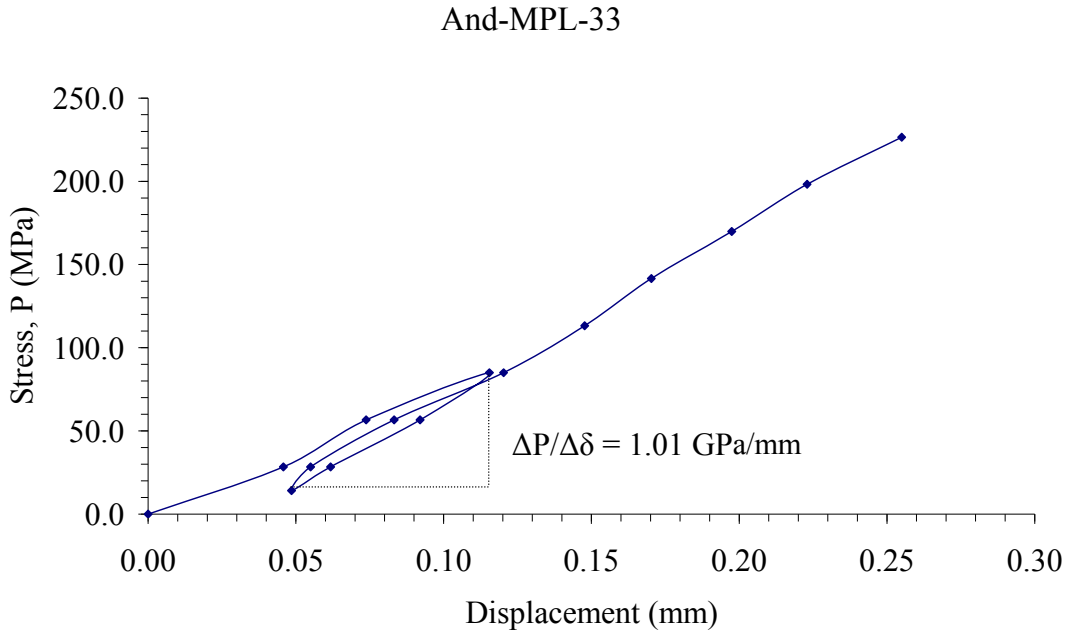

Figure B.33 Applied stress (P) as a function of displacement (δ) for specimen no. And-MPL-33.

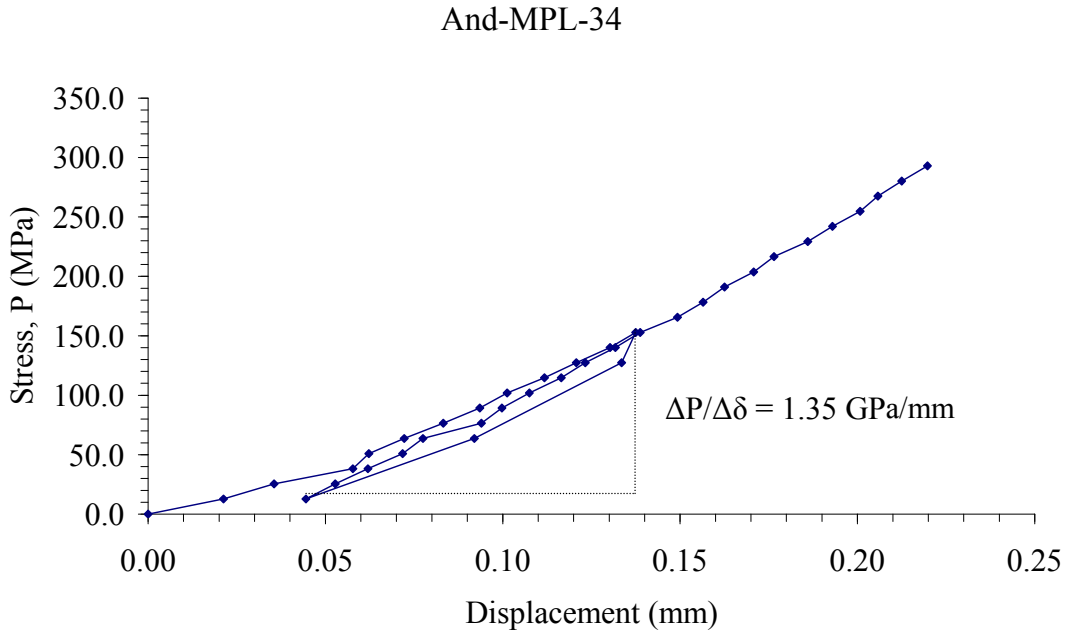

Figure B.34 Applied stress (P) as a function of displacement (δ) for specimen no. And-MPL-34.

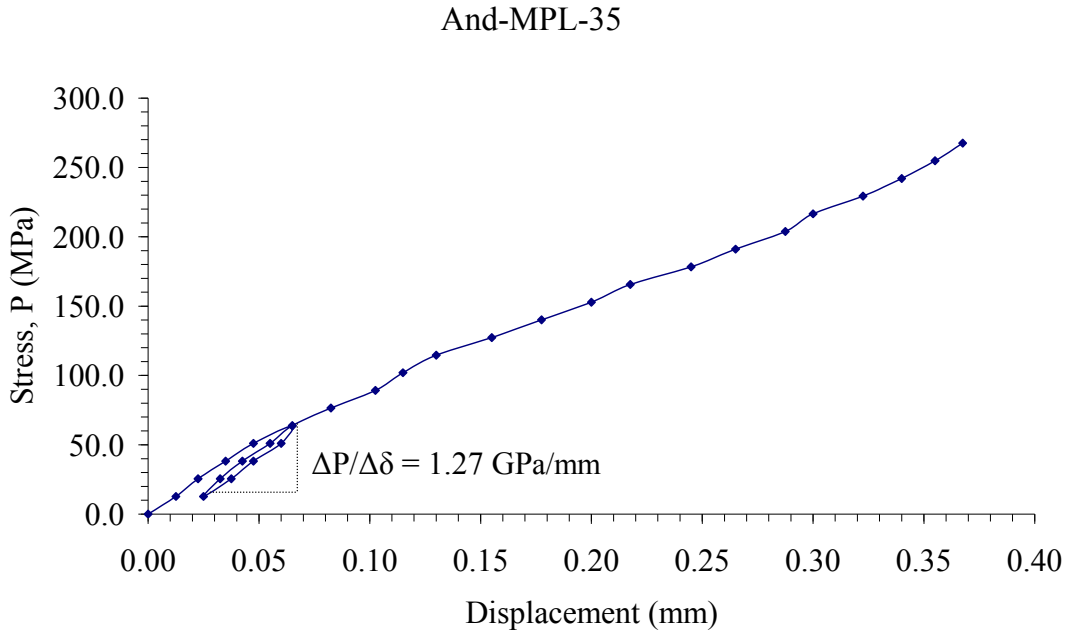

Figure B.35 Applied stress (P) as a function of displacement (δ) for specimen no. And-MPL-35.

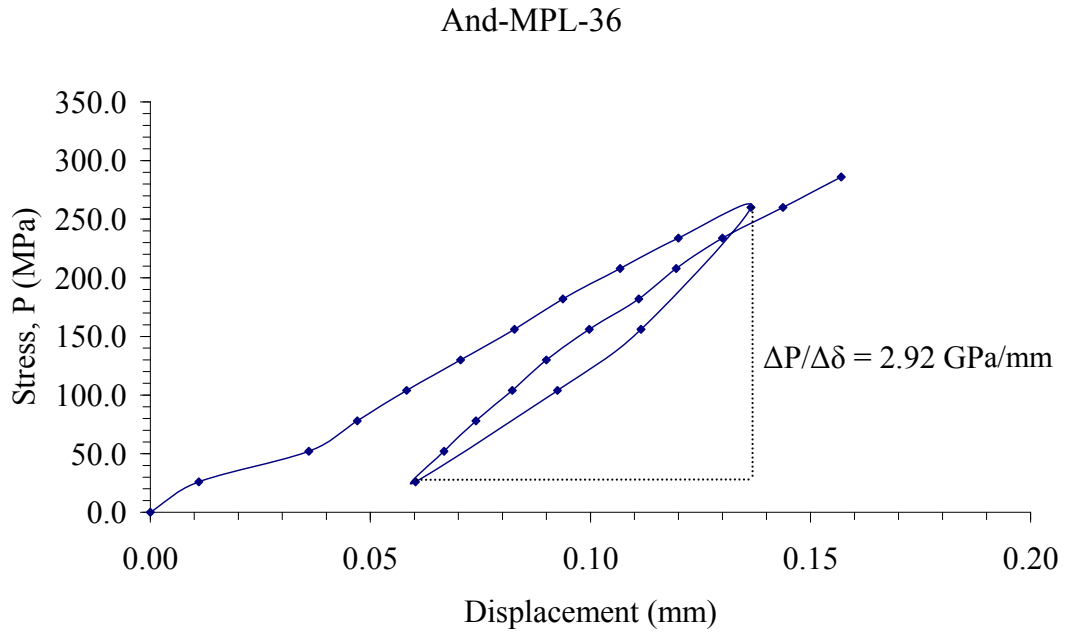

Figure B.36 Applied stress (P) as a function of displacement (δ) for specimen no. And-MPL-36

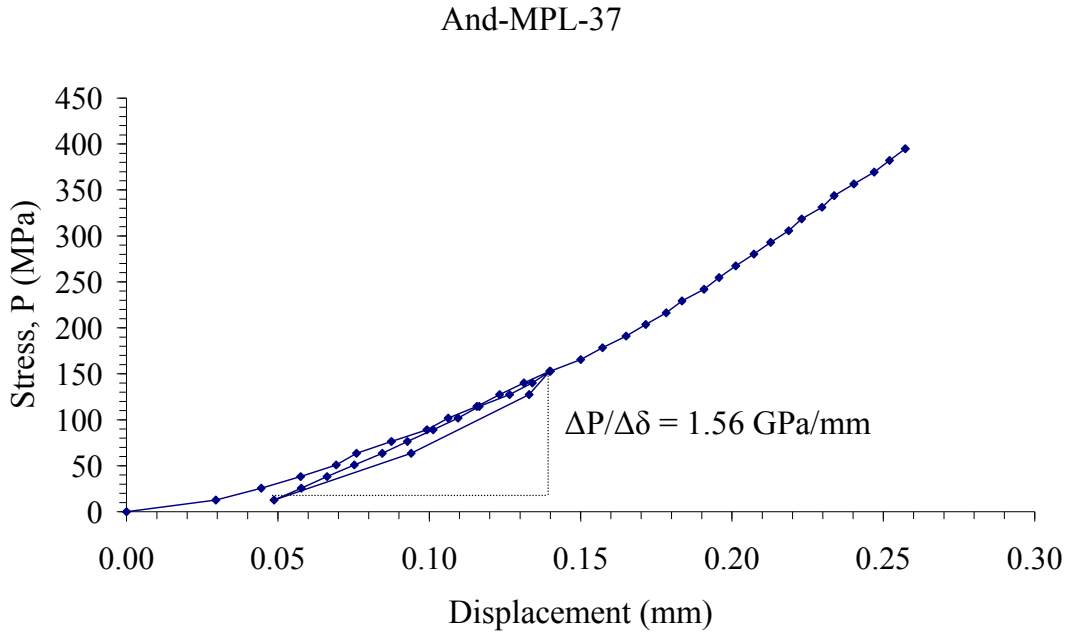

Figure B.37 Applied stress (P) as a function of displacement (δ) for specimen no. And-MPL-37

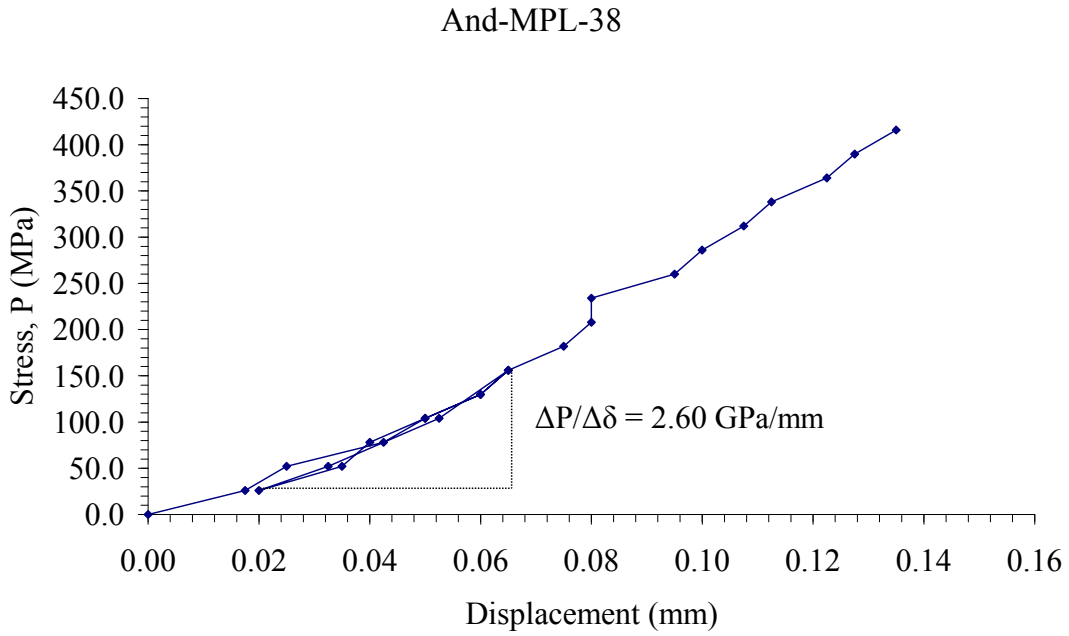

Figure B.38 Applied stress (P) as a function of displacement (δ) for specimen no. And-MPL-38

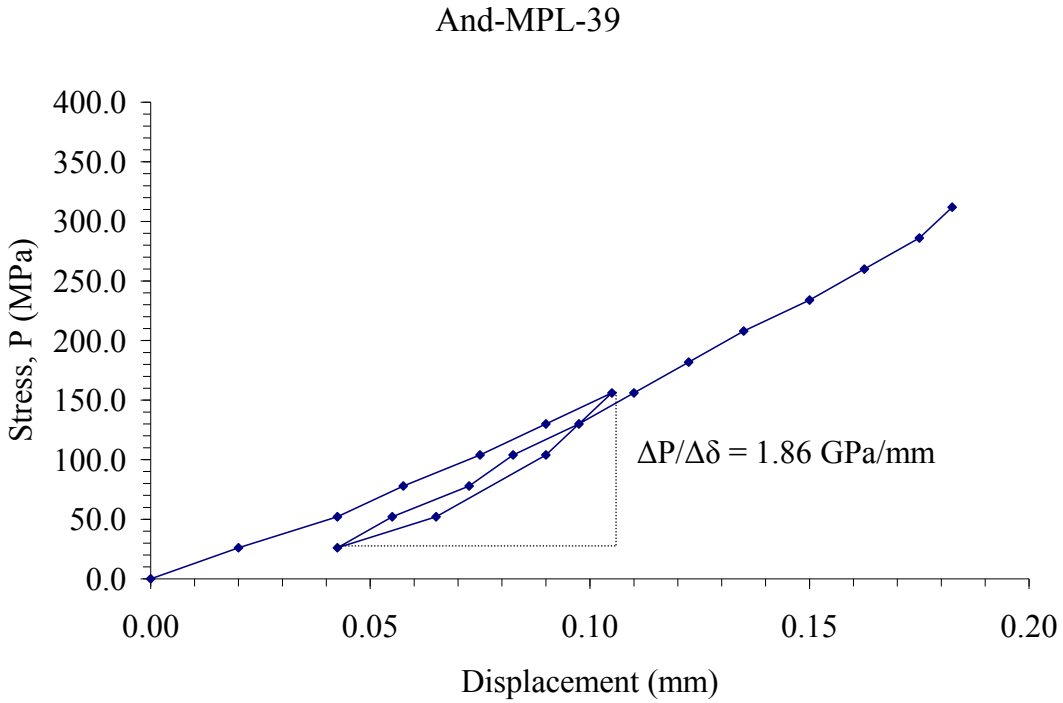

Figure B.39 Applied stress (P) as a function of displacement (δ) for specimen no. And-MPL-39.

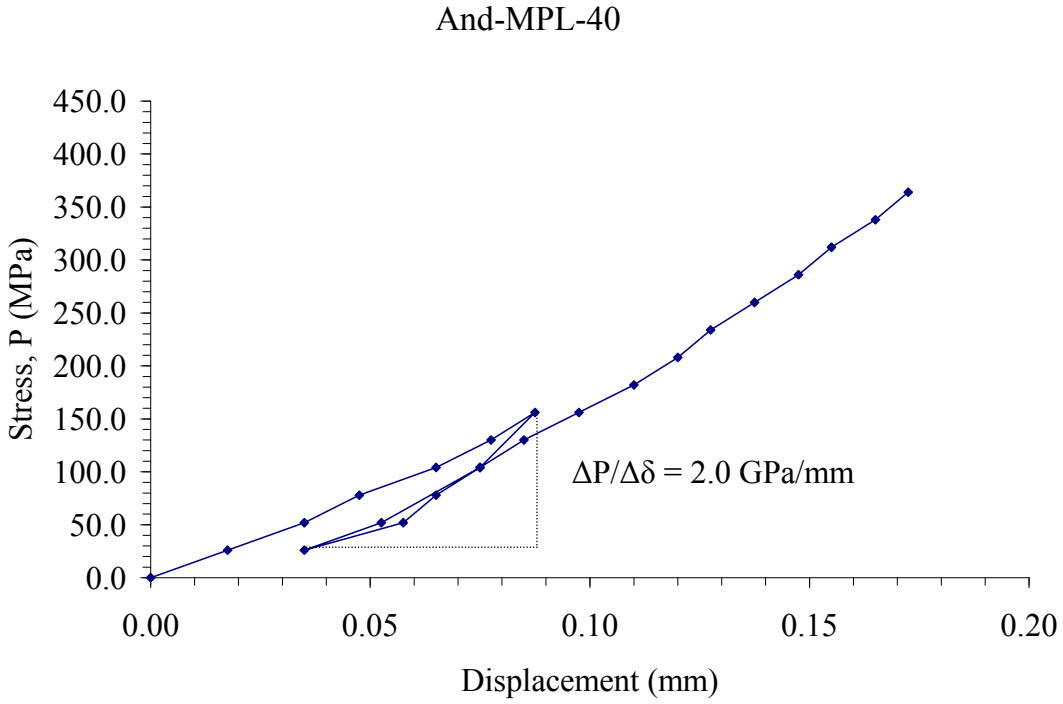

Figure B.40 Applied stress (P) as a function of displacement (δ) for specimen no. And-MPL-40.

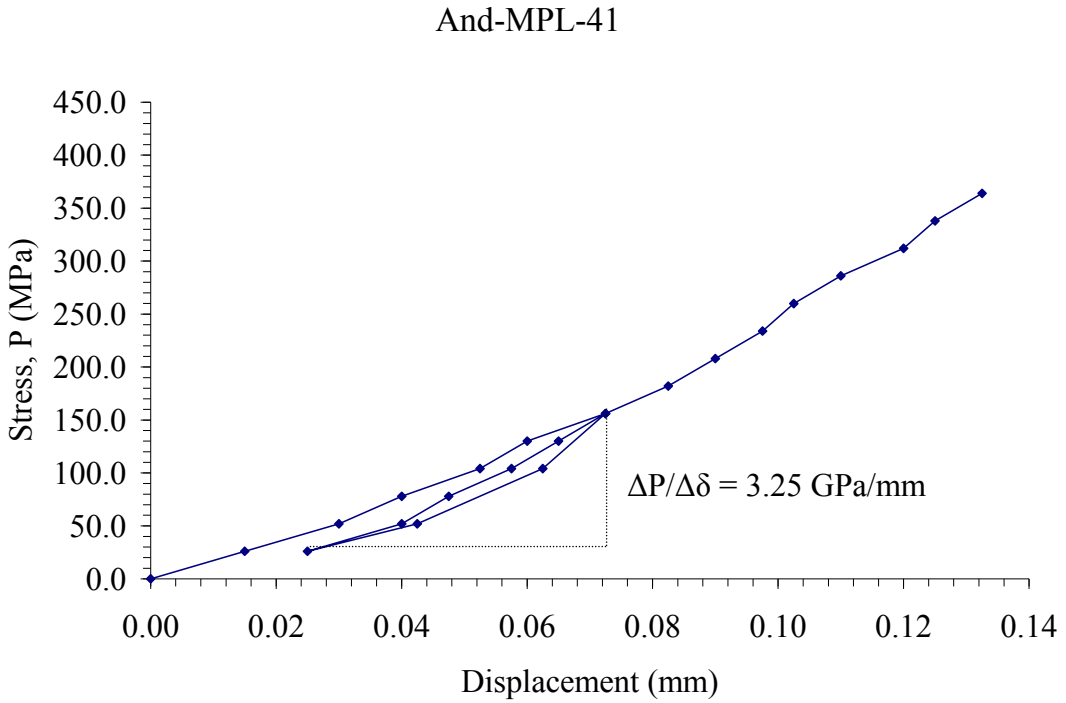

Figure B.41 Applied stress (P) as a function of displacement (δ) for specimen no. And-MPL-41.

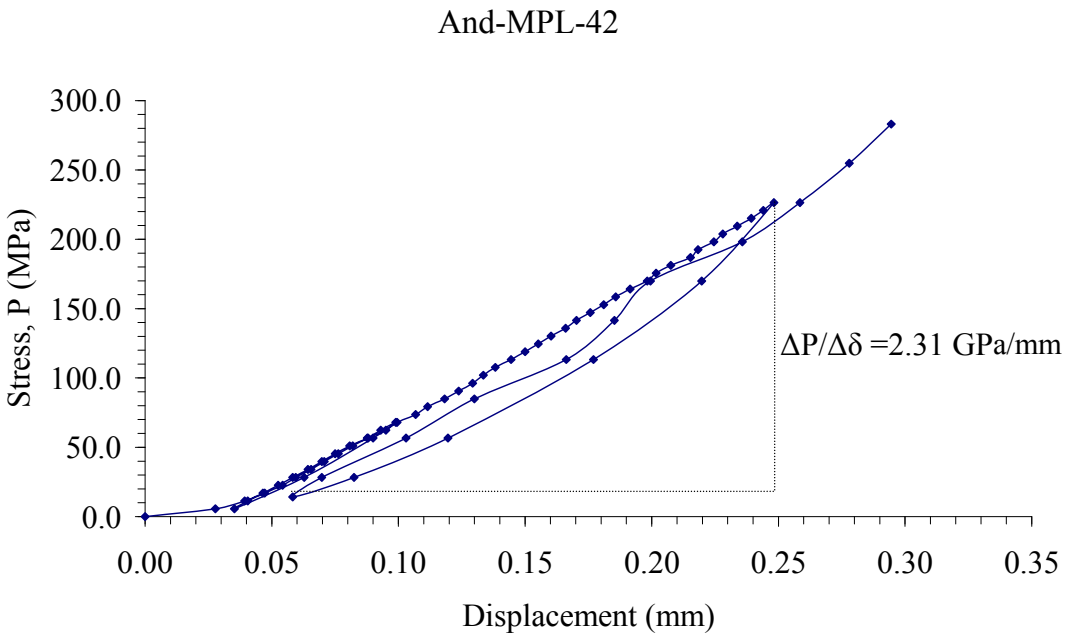

Figure B.42 Applied stress (P) as a function of displacement (δ) for specimen no. And-MPL-42.

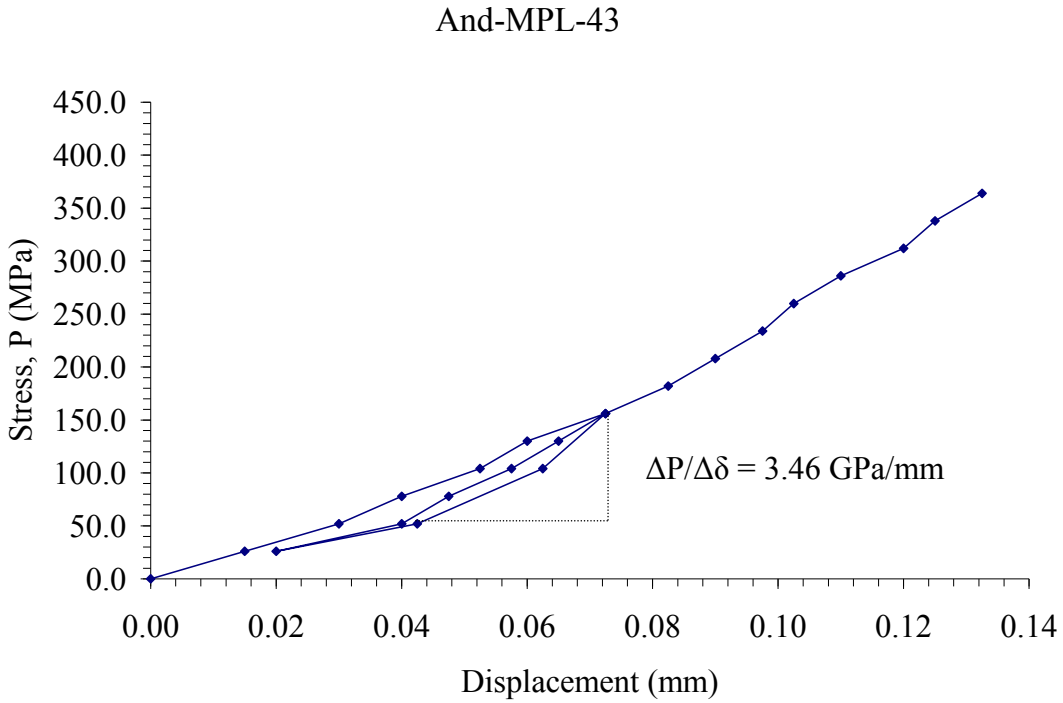

Figure B.43 Applied stress (P) as a function of displacement (δ) for specimen no. And-MPL-43.

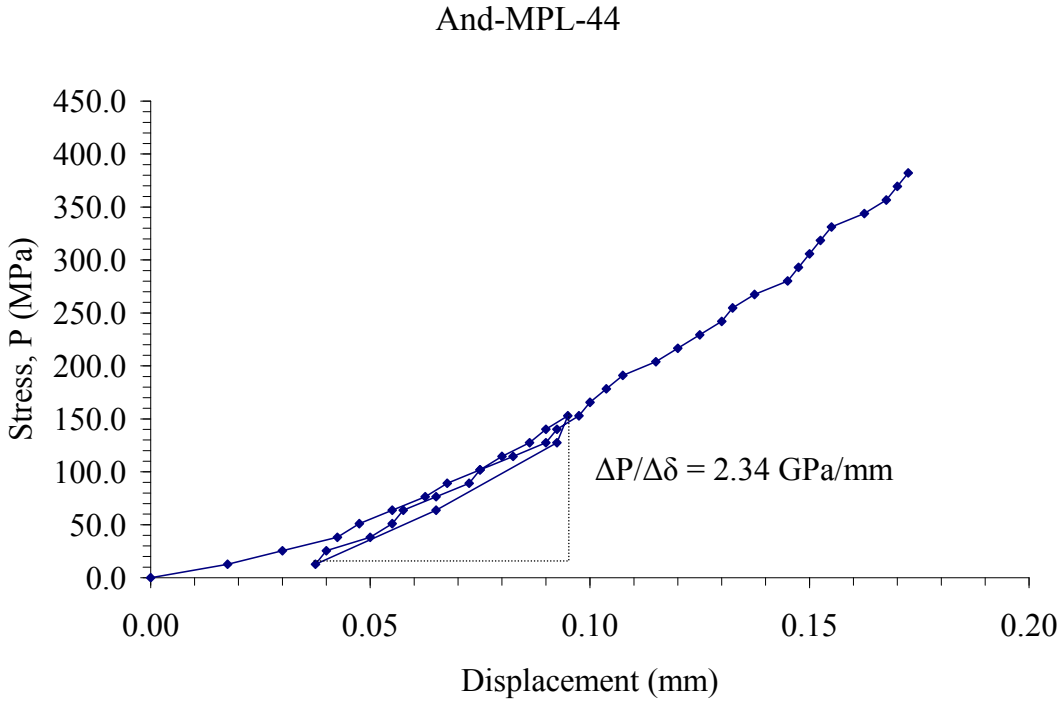

Figure B.44 Applied stress (P) as a function of displacement (δ) for specimen no. And-MPL-44.

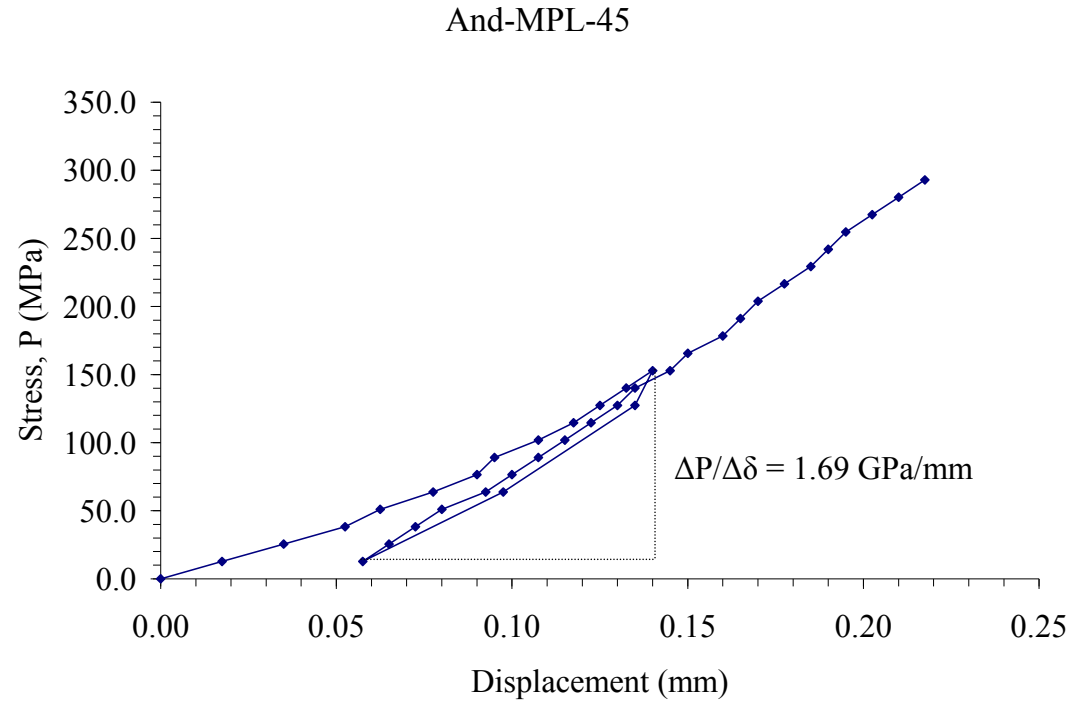

Figure B.45 Applied stress (P) as a function of displacement (δ) for specimen no. And-MPL-45.

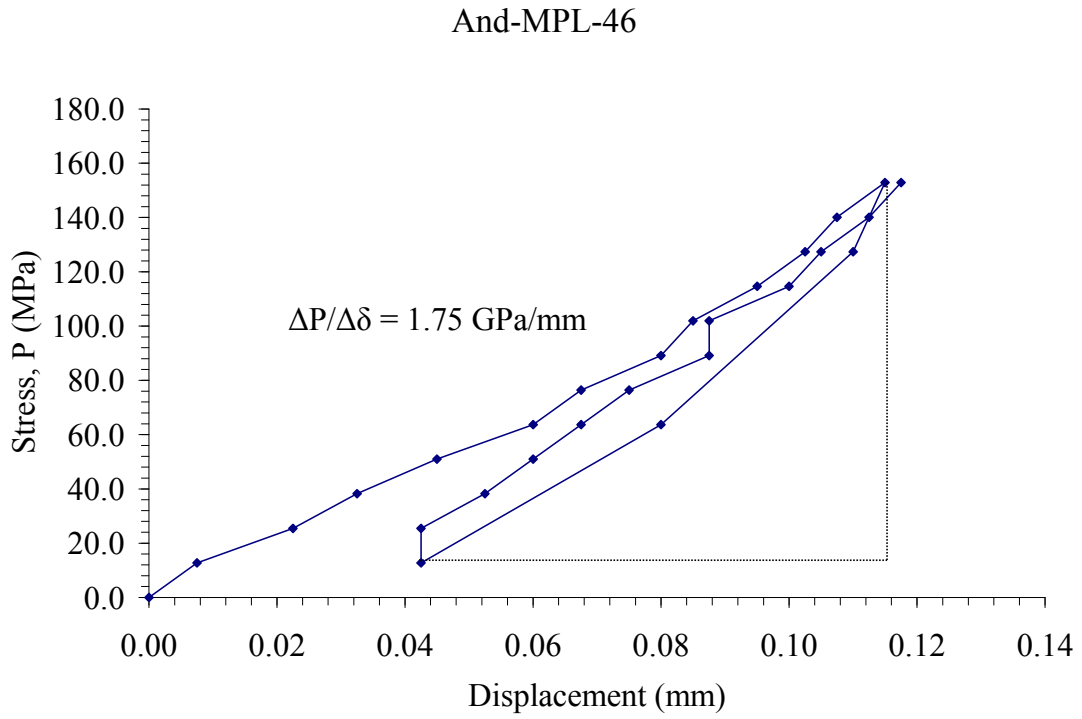

Figure B.46 Applied stress (P) as a function of displacement (δ) for specimen no. And-MPL-46.

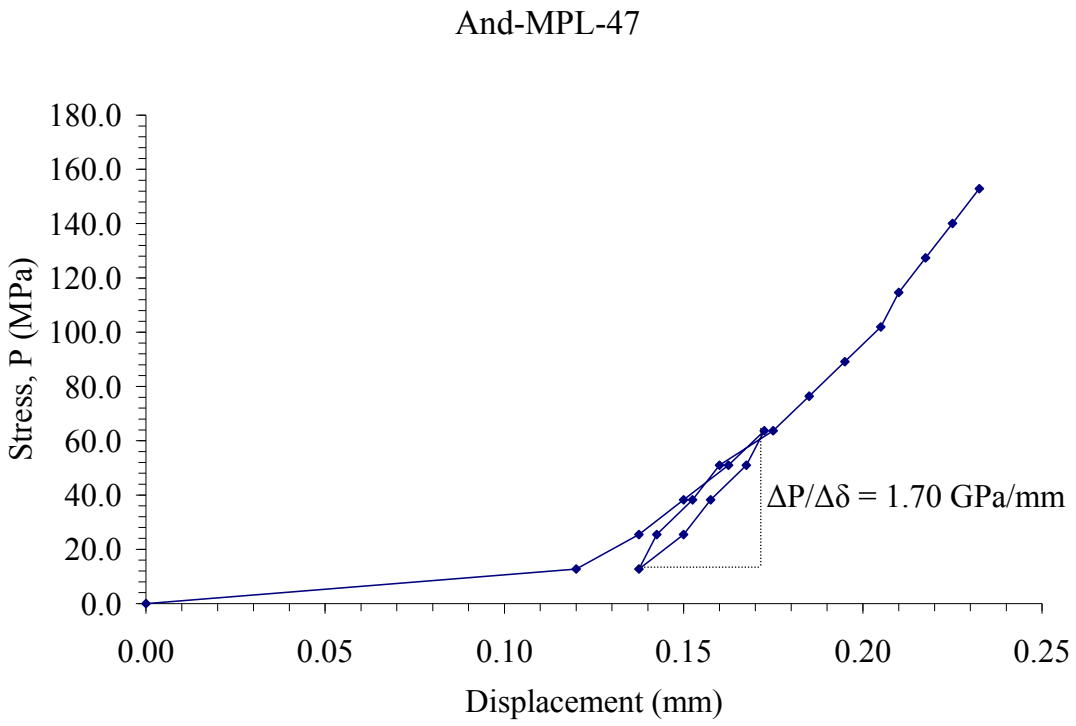

Figure B.47 Applied stress (P) as a function of displacement (δ) for specimen no. And-MPL-47.

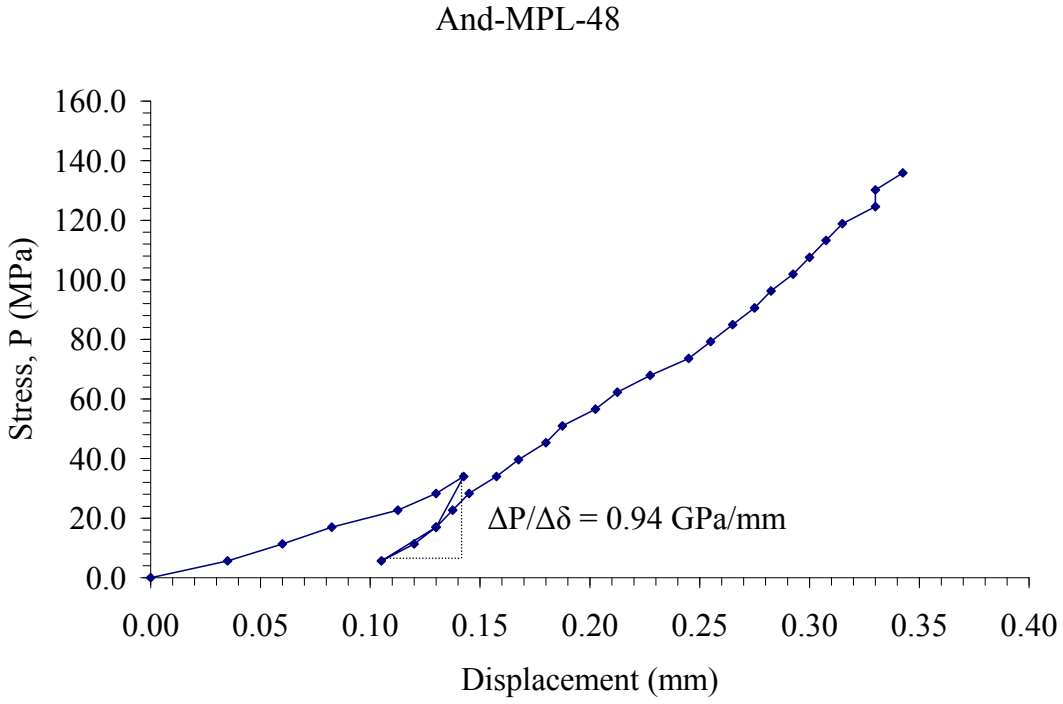

Figure B.48 Applied stress (P) as a function of displacement (δ) for specimen no. And-MPL-48.

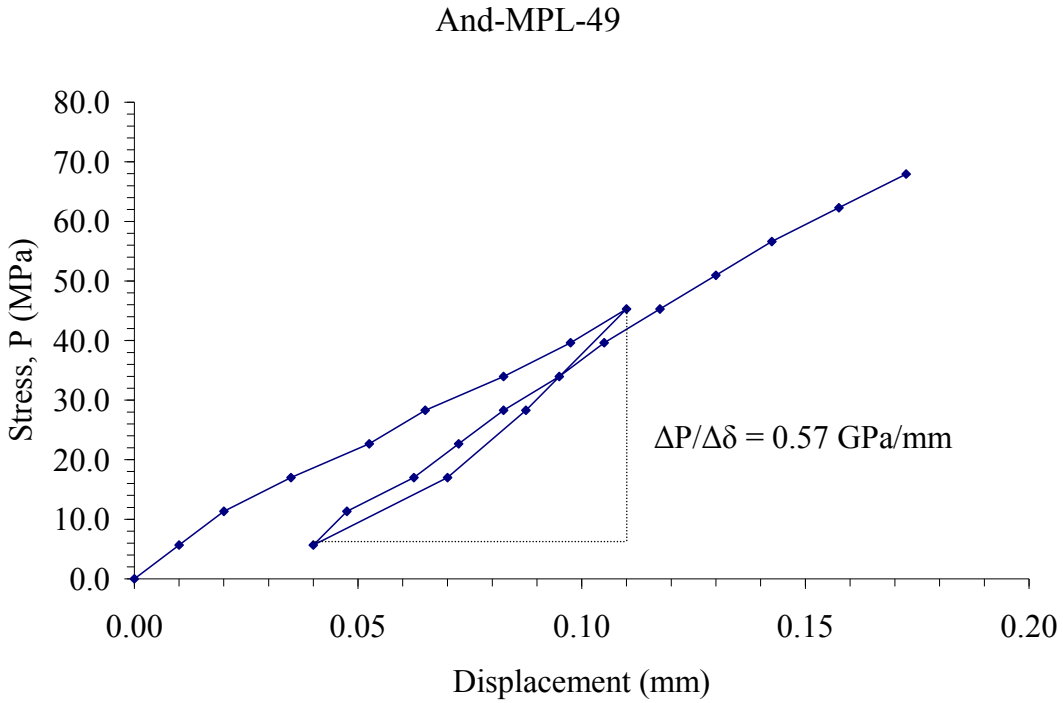

Figure B.49 Applied stress (P) as a function of displacement (δ) for specimen no. And-MPL-49.

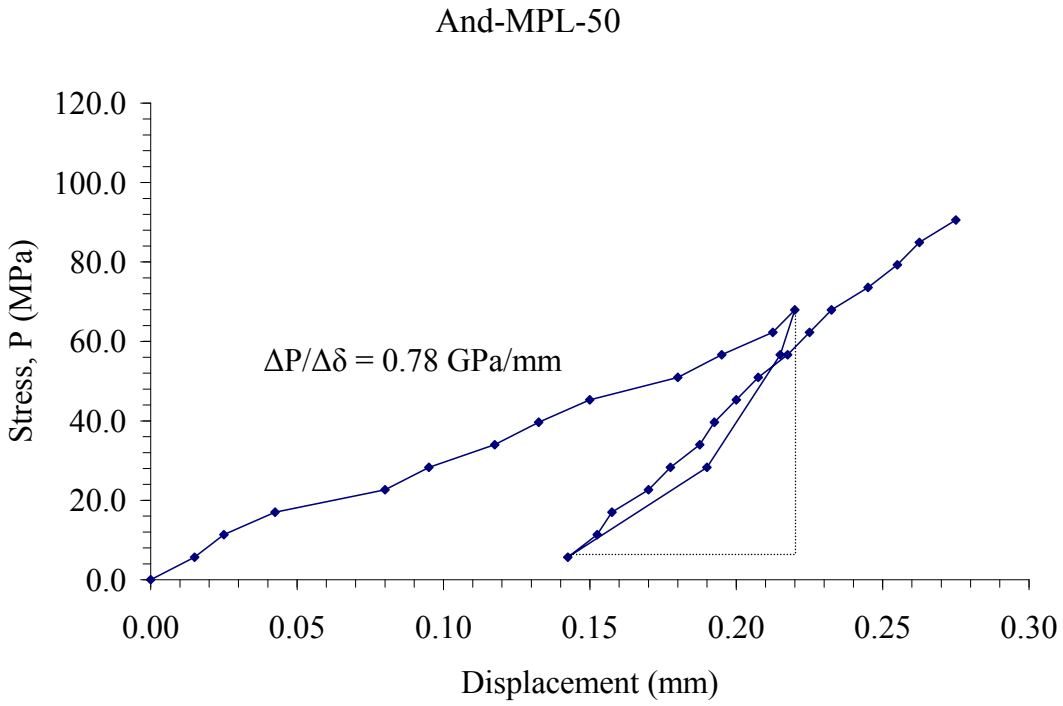

Figure B.50 Applied stress (P) as a function of displacement (δ) for specimen no. And-MPL-50.

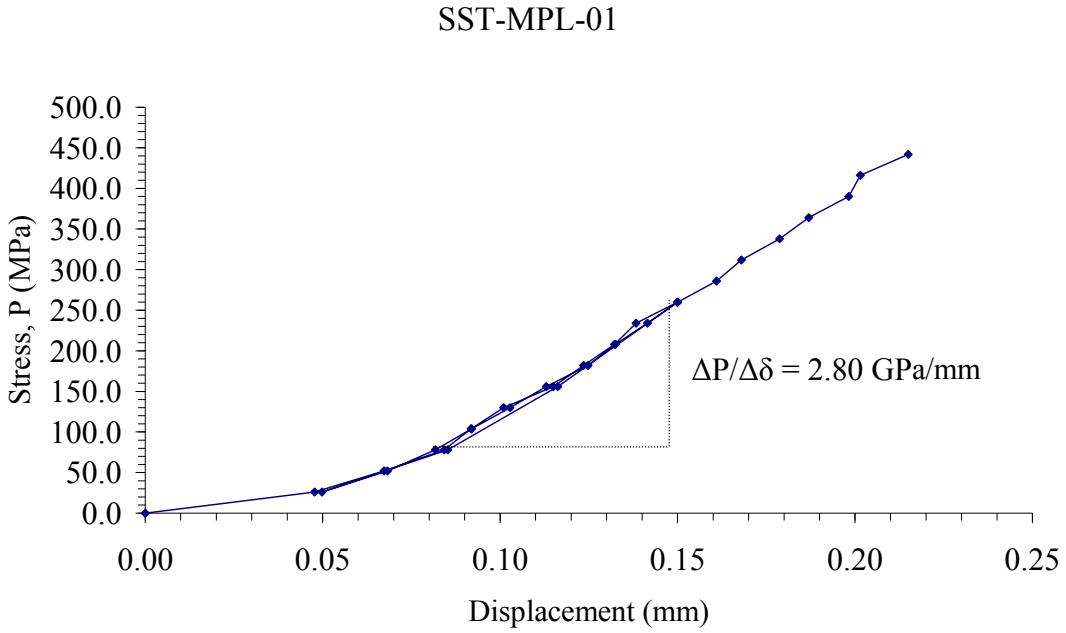

Figure B.51 Applied stress (P) as a function of displacement (δ) for specimen no. SST-MPL-01.

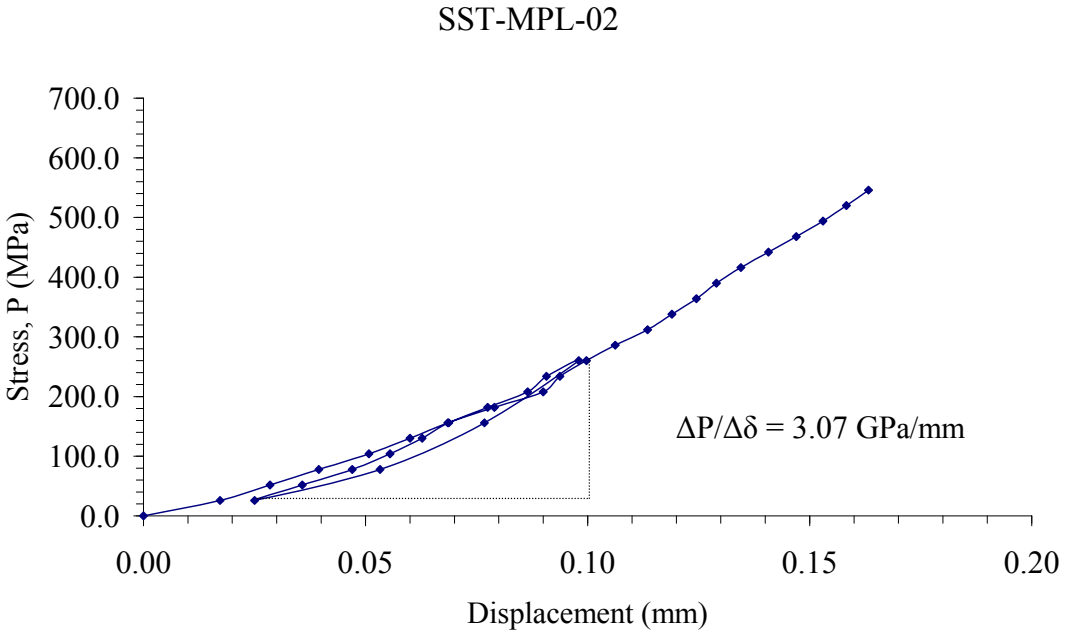

Figure B.52 Applied stress (P) as a function of displacement (δ) for specimen no. SST-MPL-02.

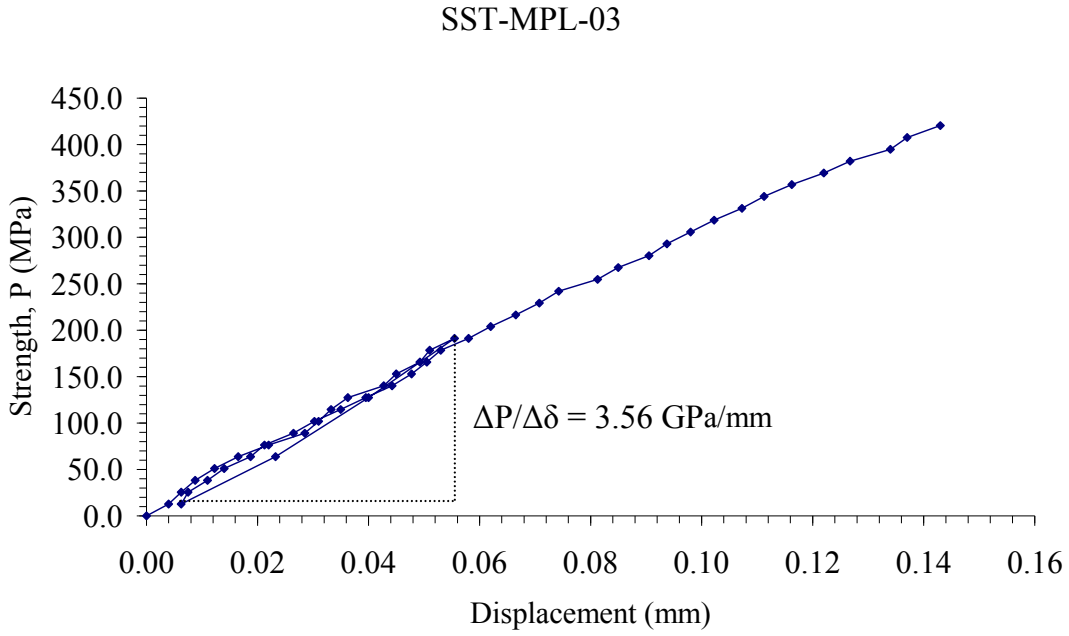

Figure B.53 Applied stress (P) as a function of displacement (δ) for specimen no. SST-MPL-03.

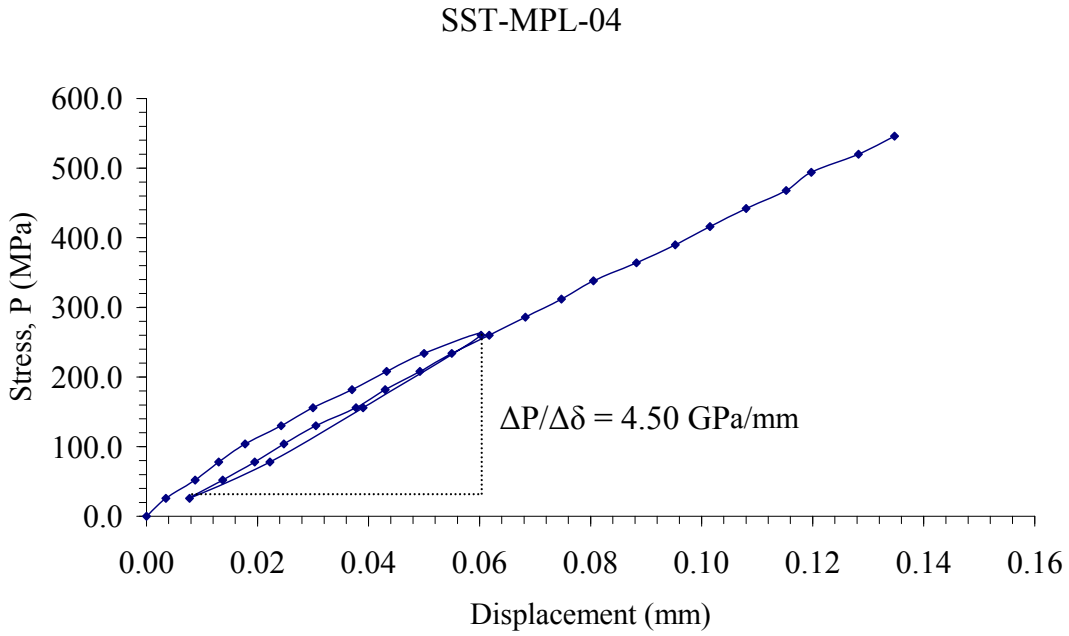

Figure B.54 Applied stress (P) as a function of displacement (δ) for specimen no. SST-MPL-04.

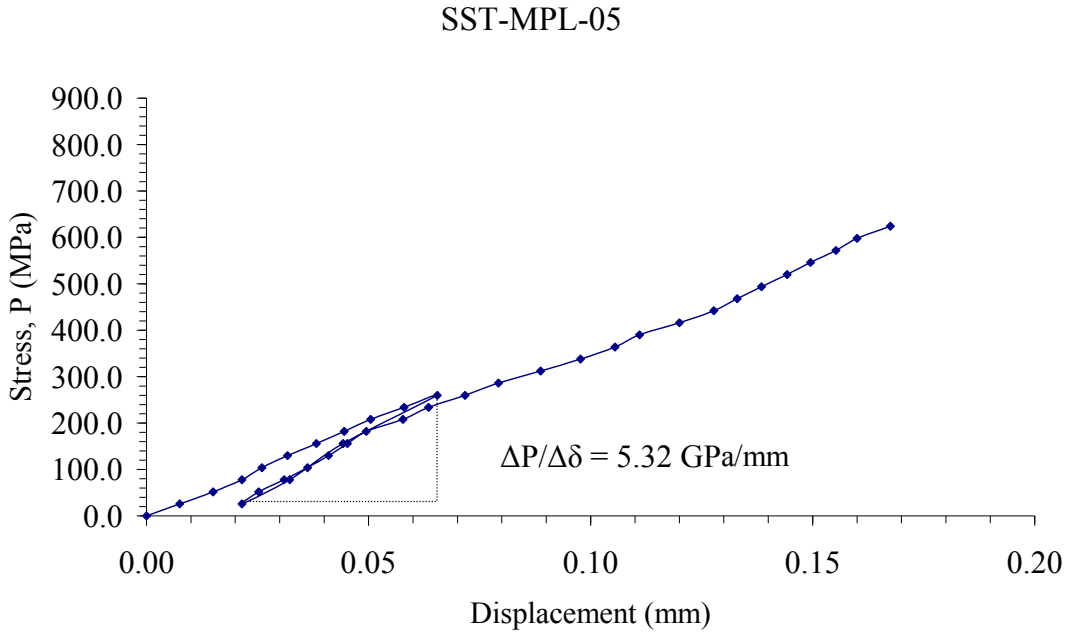

Figure B.55 Applied stress (P) as a function of displacement (δ) for specimen no. SST-MPL-05.

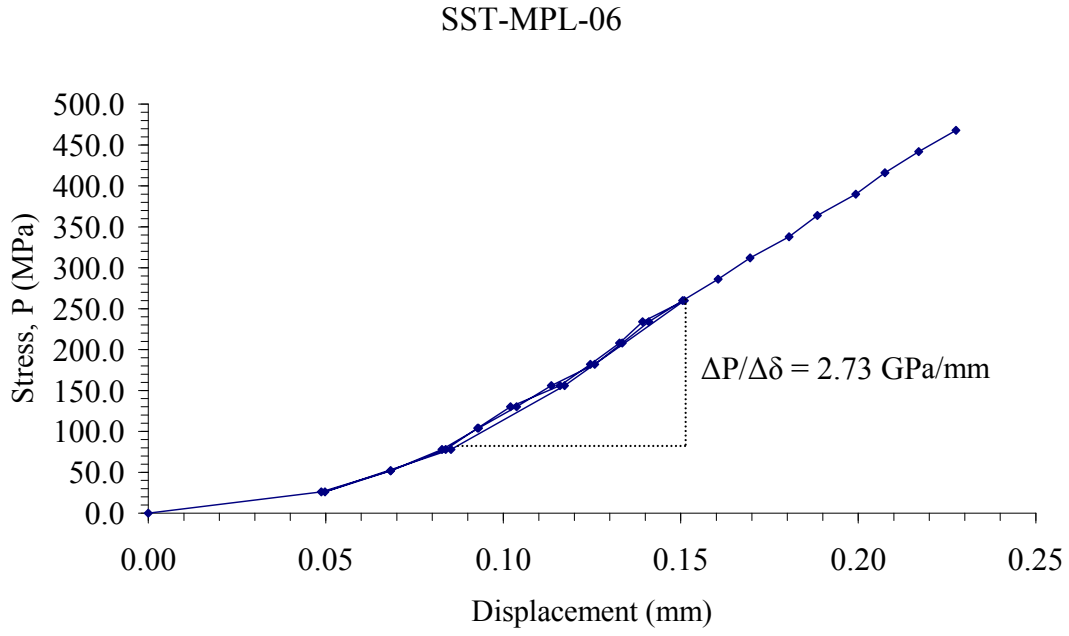

Figure B.56 Applied stress (P) as a function of displacement (δ) for specimen no. SST-MPL-06.

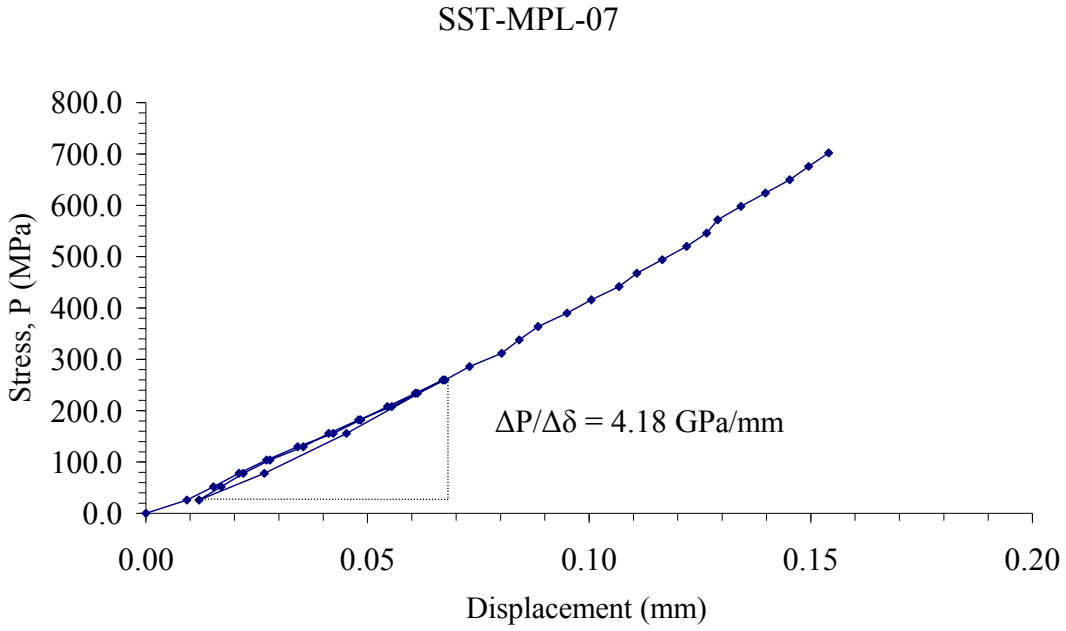

Figure B.57 Applied stress (P) as a function of displacement (δ) for specimen no. SST-MPL-07.

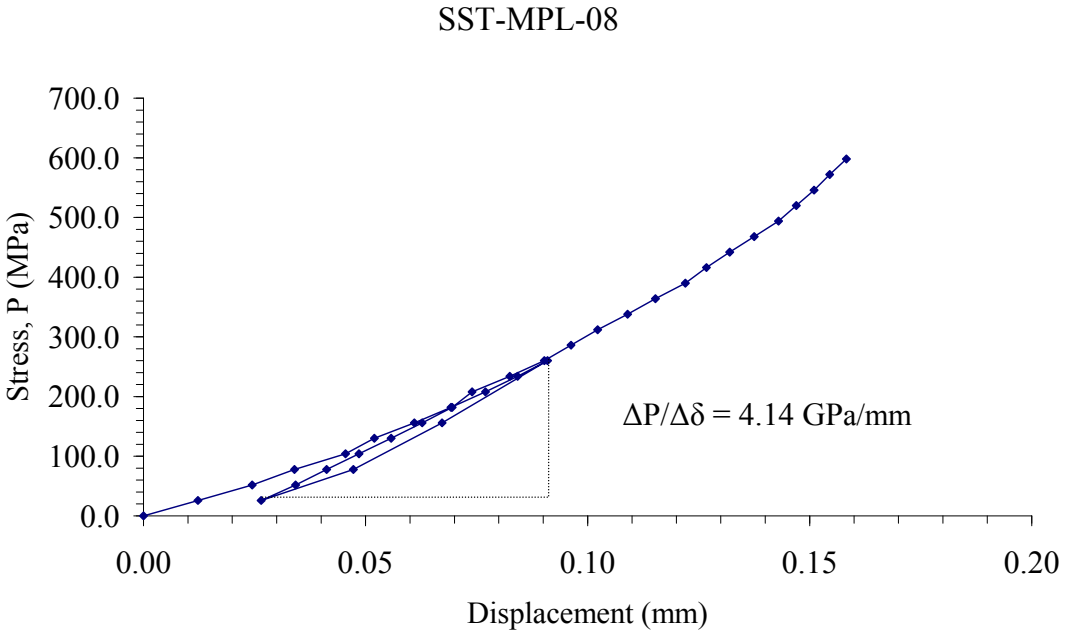

Figure B.58 Applied stress (P) as a function of displacement (δ) for specimen no. SST-MPL-08.

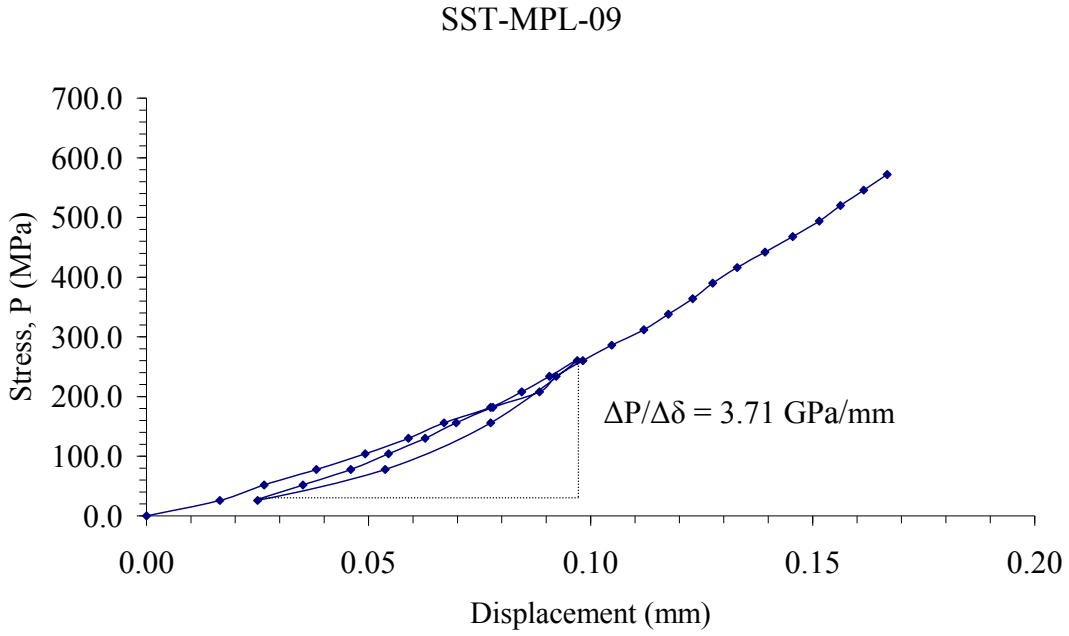

Figure B.59 Applied stress (P) as a function of displacement (δ) for specimen no. SST-MPL-09.

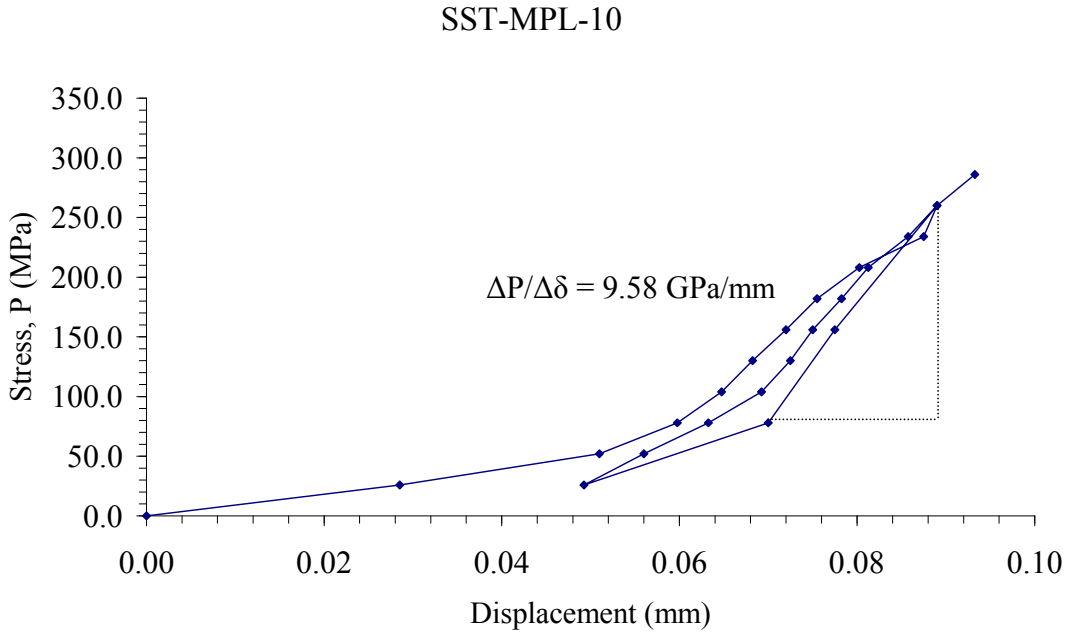

Figure B.60 Applied stress (P) as a function of displacement (δ) for specimen no. SST-MPL-10.

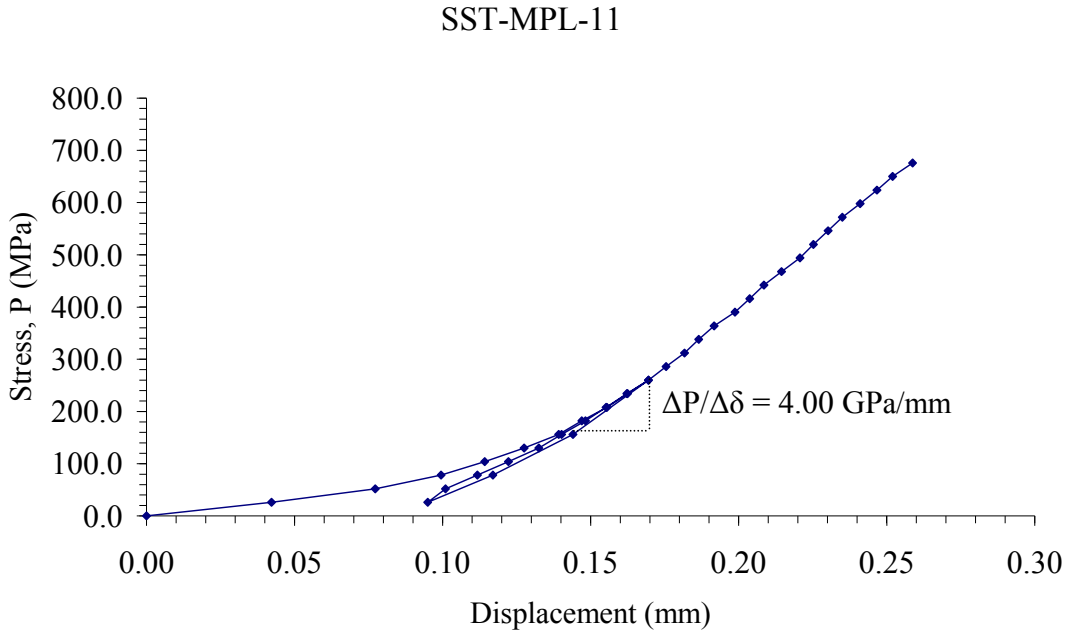

Figure B.61 Applied stress (P) as a function of displacement (δ) for specimen no. SST-MPL-11.

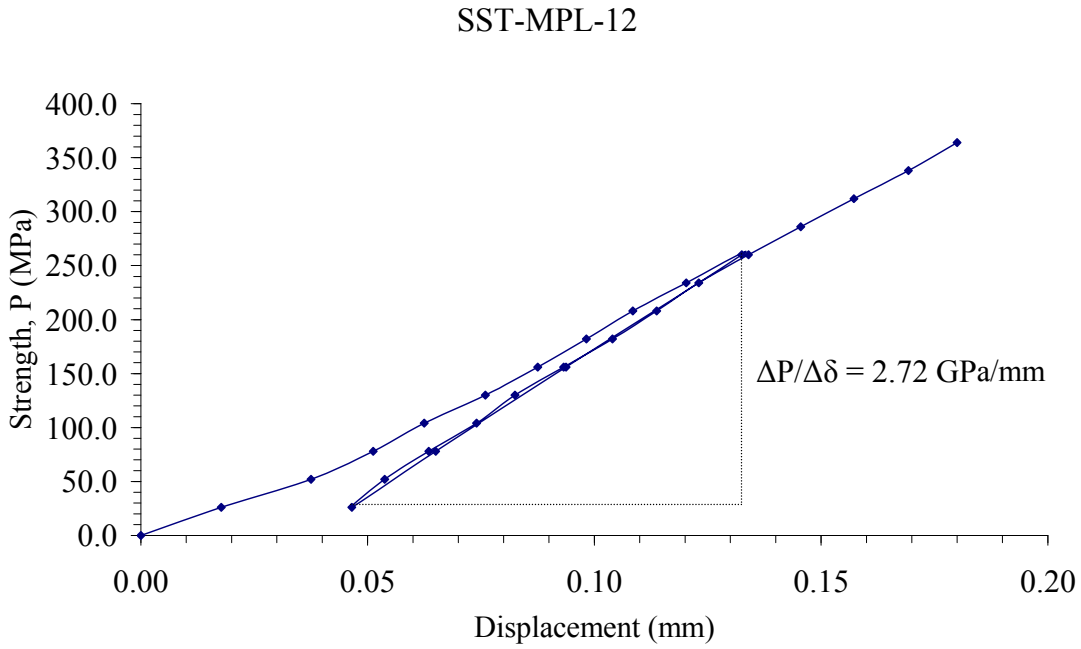

Figure B.62 Applied stress (P) as a function of displacement (δ) for specimen no. SST-MPL-12.

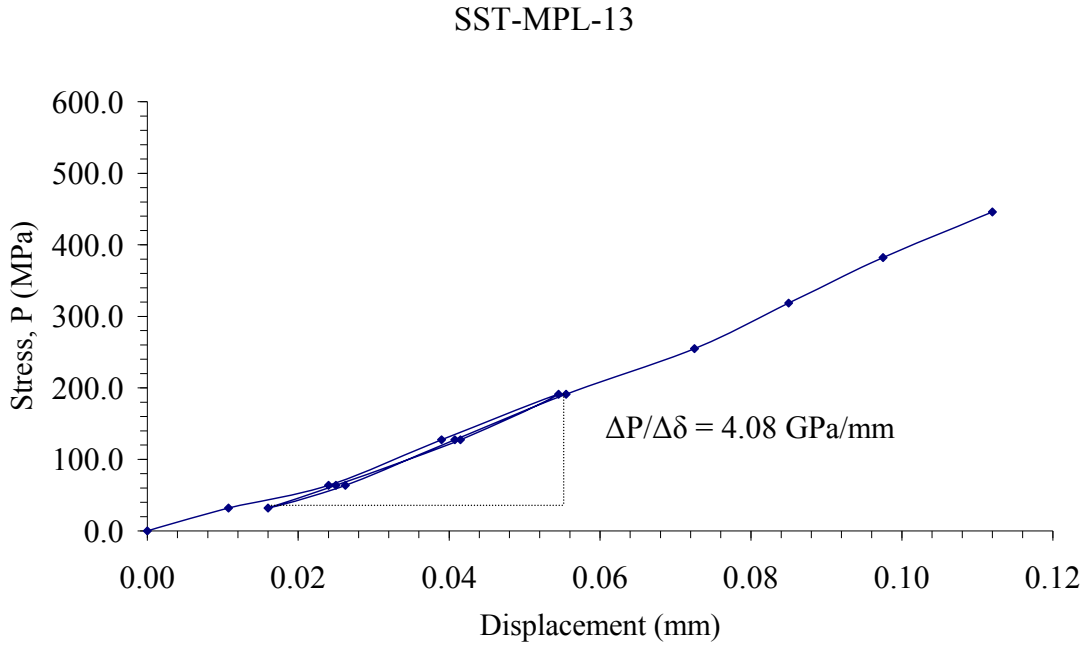

Figure B.63 Applied stress (P) as a function of displacement (δ) for specimen no. SST-MPL-13.

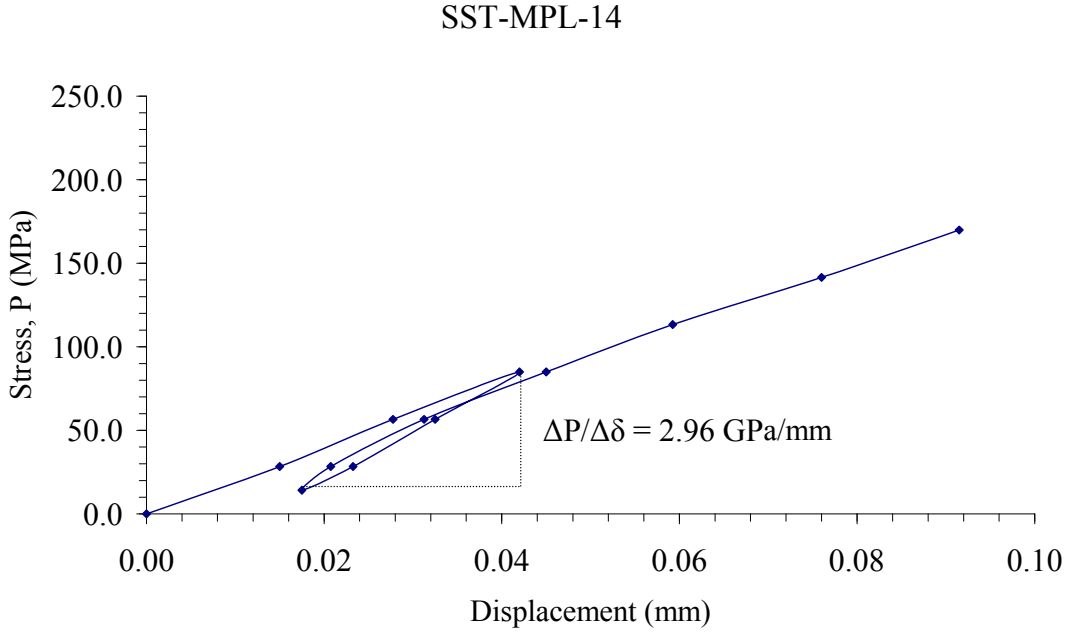

Figure B.64 Applied stress (P) as a function of displacement (δ) for specimen no. SST-MPL-14.

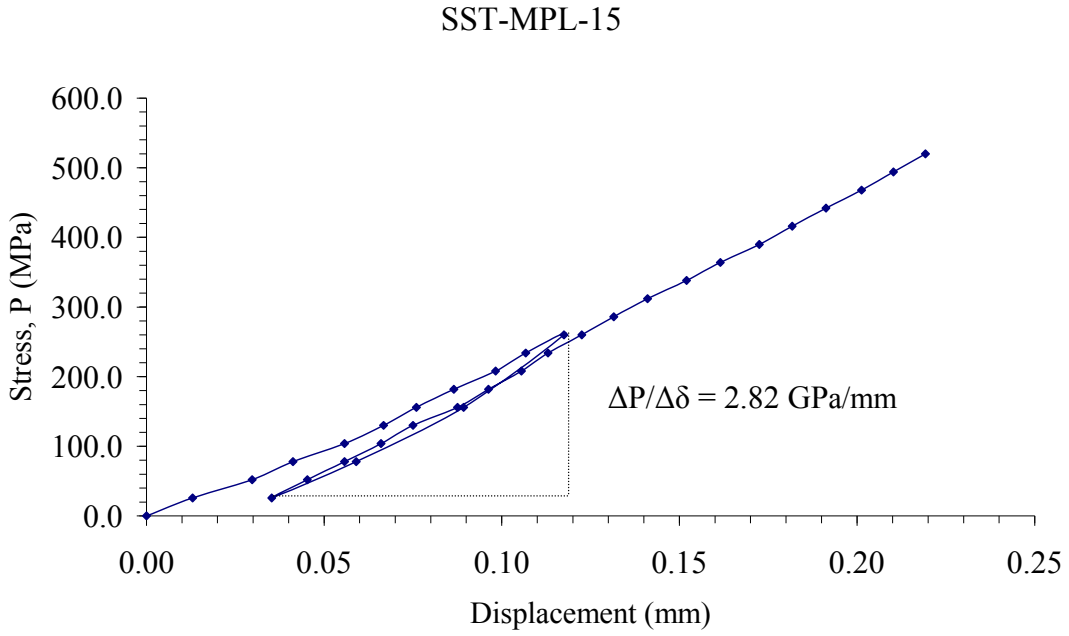

Figure B.65 Applied stress (P) as a function of displacement (δ) for specimen no. SST-MPL-15.

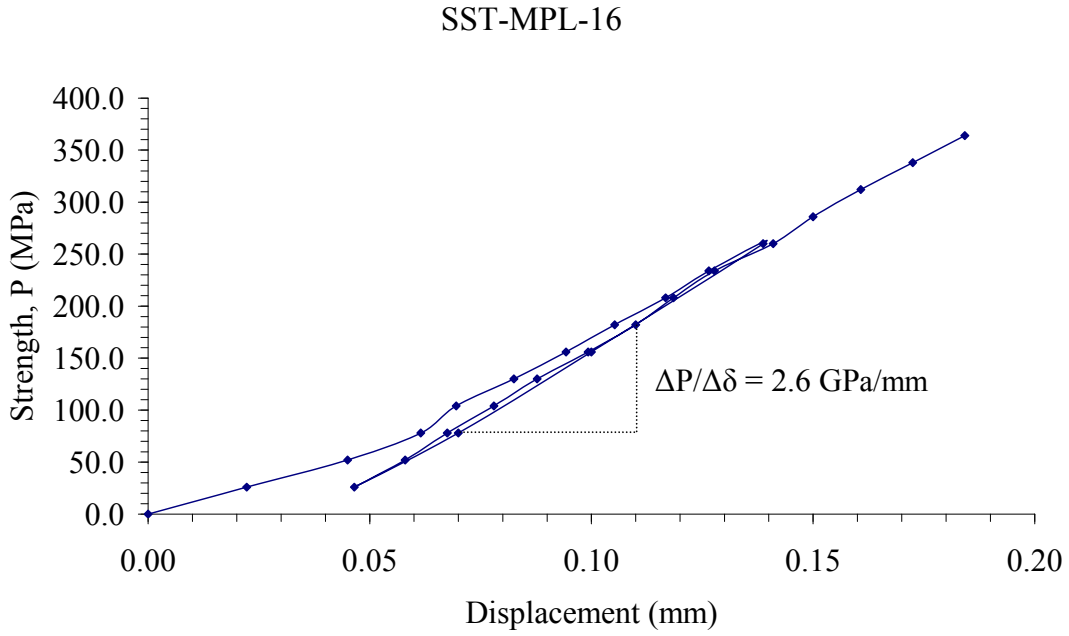

Figure B.66 Applied stress (P) as a function of displacement (δ) for specimen no. SST-MPL-16.

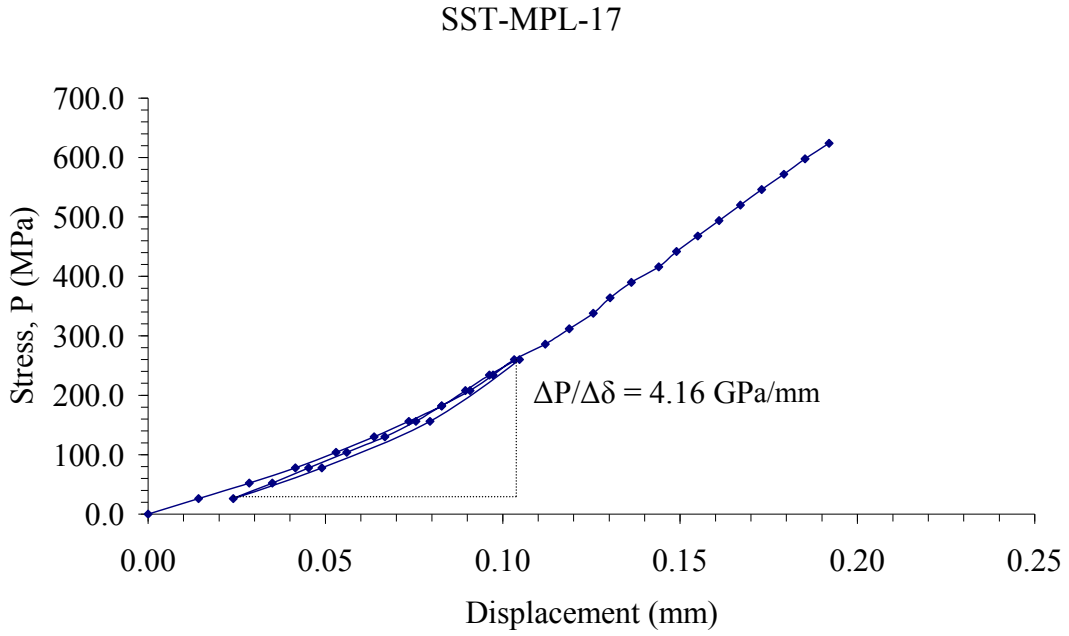

Figure B.67 Applied stress (P) as a function of displacement (δ) for specimen no. SST-MPL-17.

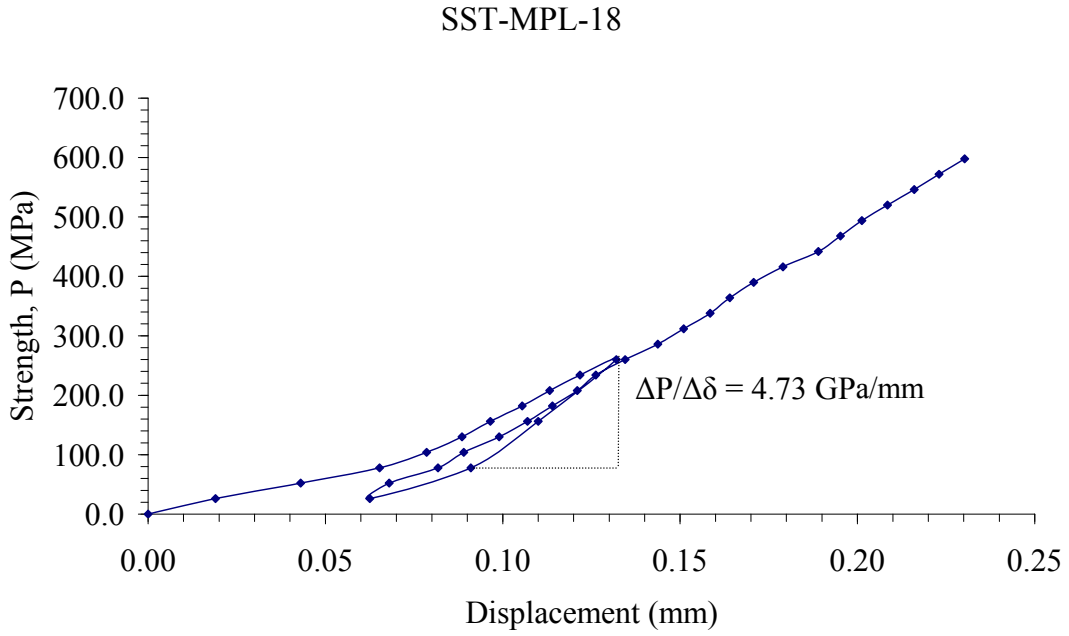

Figure B.68 Applied stress (P) as a function of displacement (δ) for specimen no. SST-MPL-18.

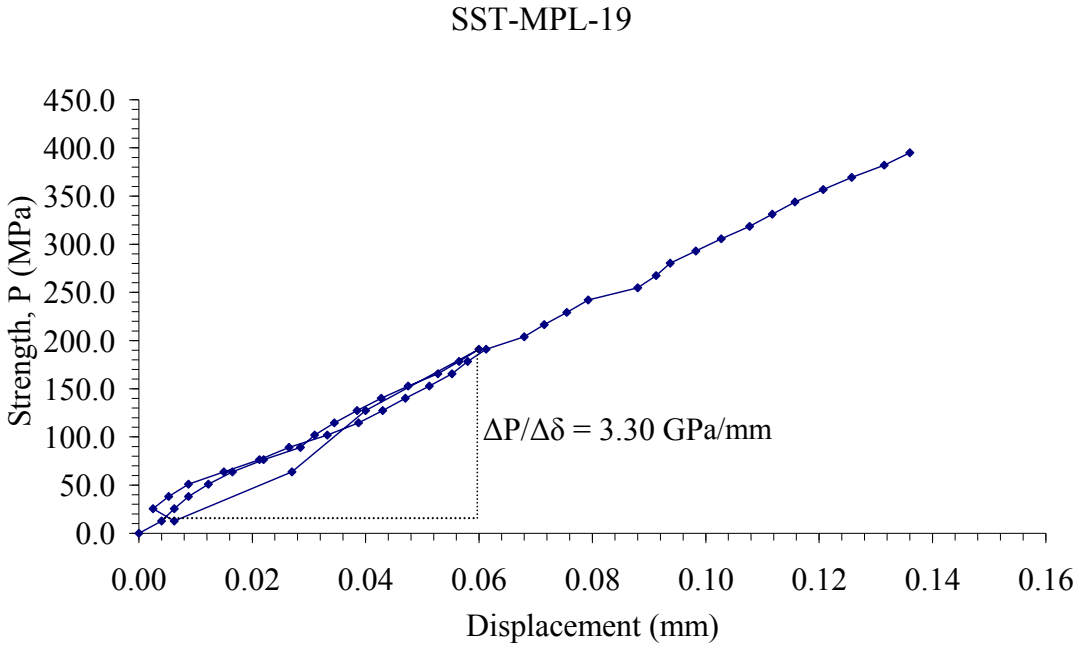

Figure B.69 Applied stress (P) as a function of displacement (δ) for specimen no. SST-MPL-19.

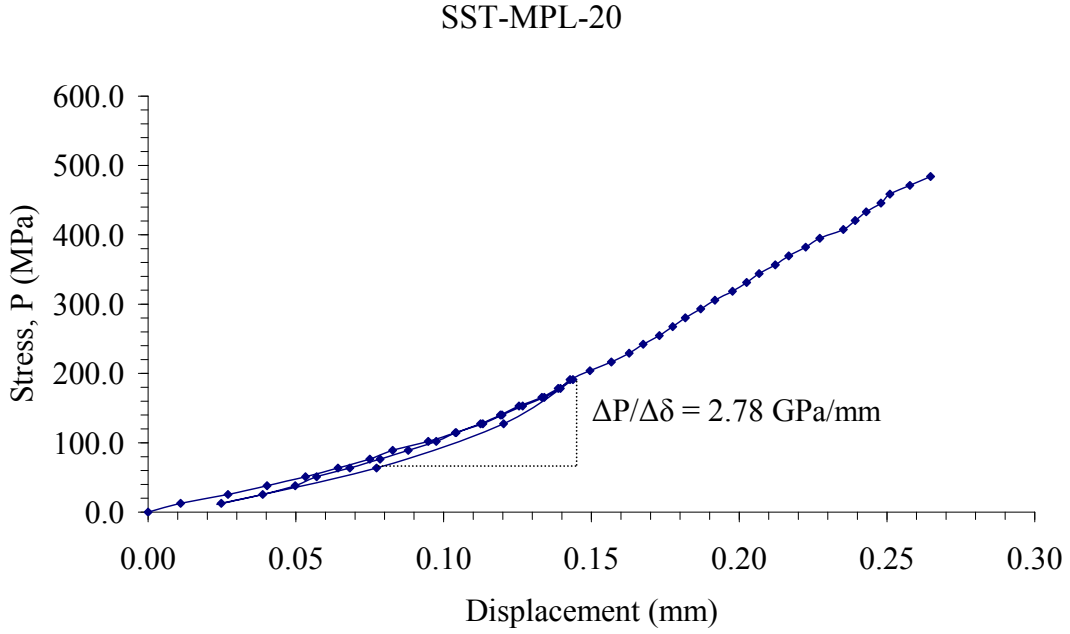

Figure B.70 Applied stress (P) as a function of displacement (δ) for specimen no. SST-MPL-20.

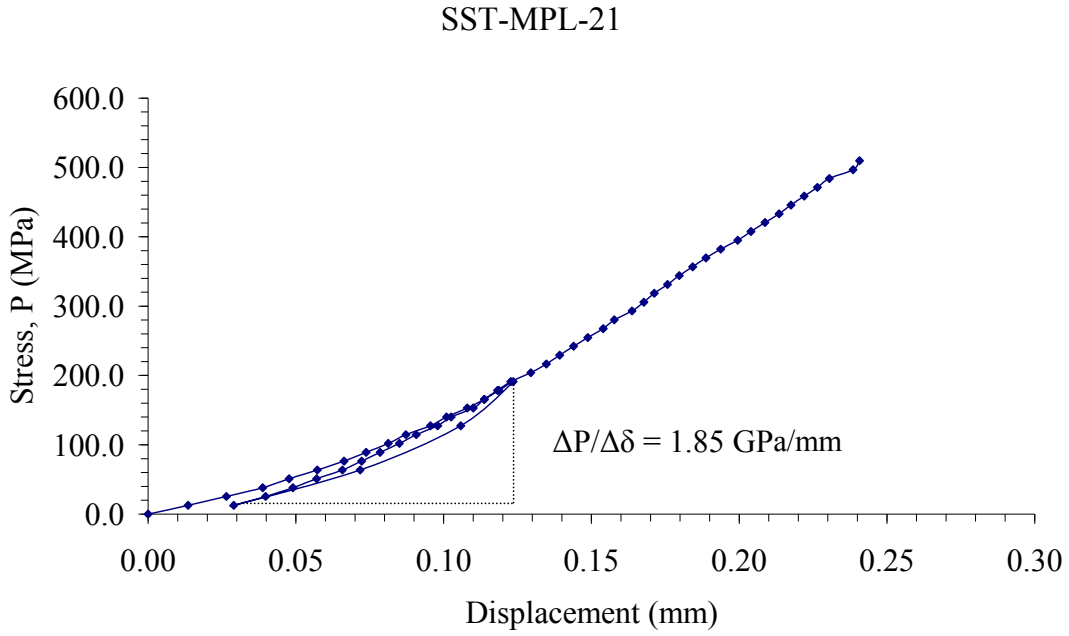

Figure B.71 Applied stress (P) as a function of displacement (δ) for specimen no. SST-MPL-21.

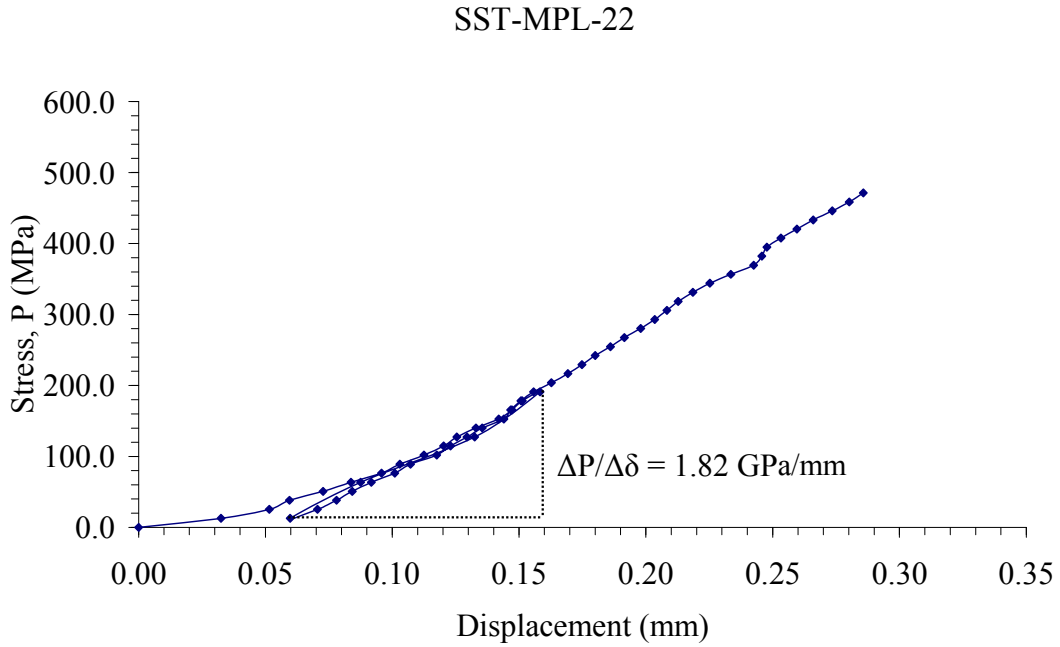

Figure B.72 Applied stress (P) as a function of displacement (δ) for specimen no. SST-MPL-22.

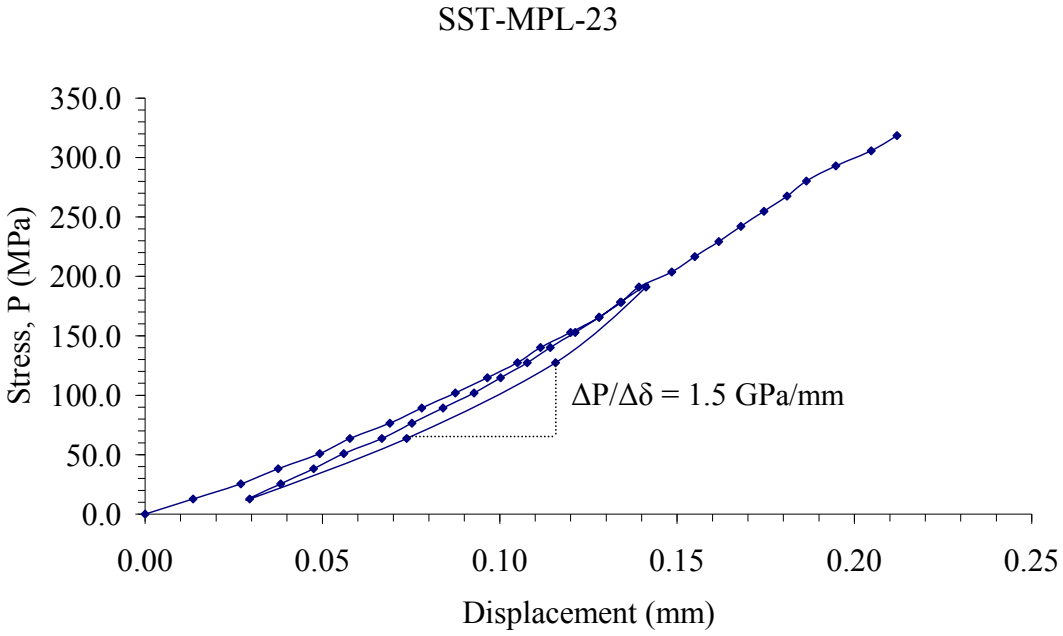

Figure B.73 Applied stress (P) as a function of displacement (δ) for specimen no. SST-MPL-23.

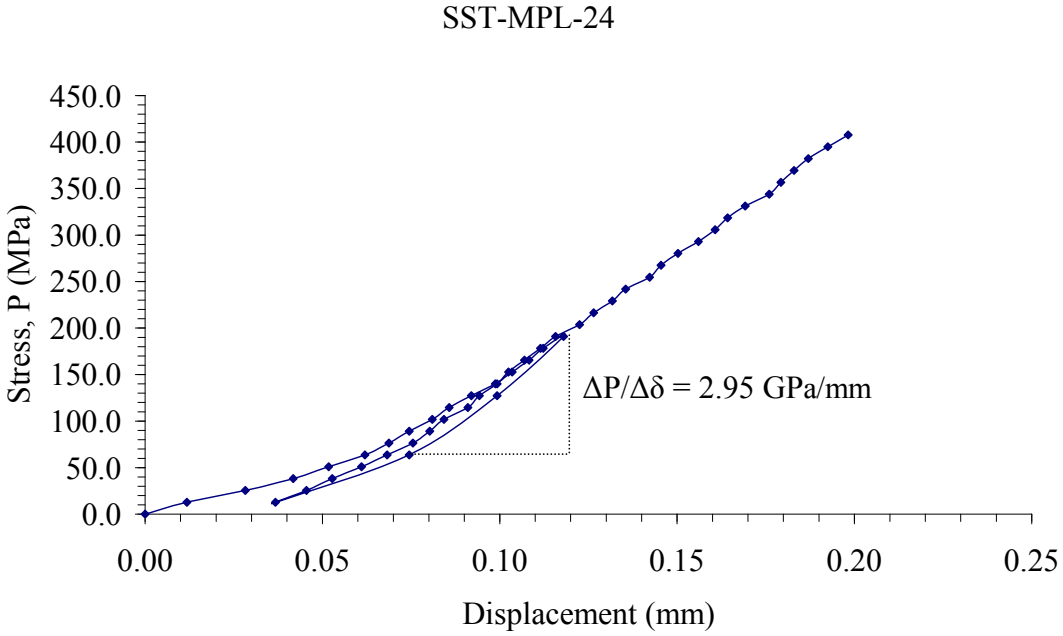

Figure B.74 Applied stress (P) as a function of displacement (δ) for specimen no. SST-MPL-24.

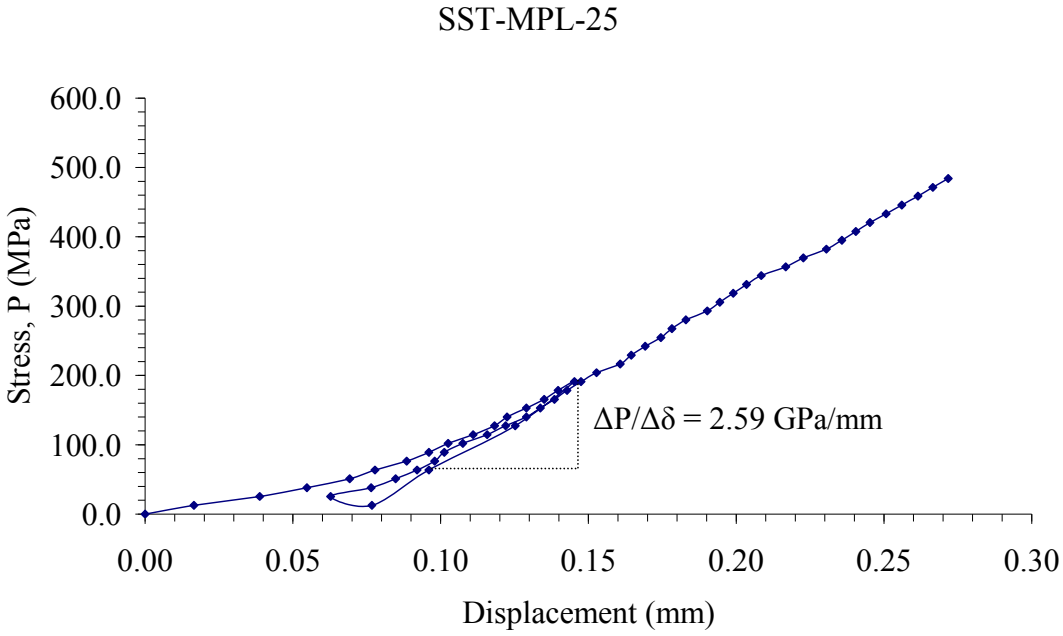

Figure B.75 Applied stress (P) as a function of displacement (δ) for specimen no. SST-MPL-25.

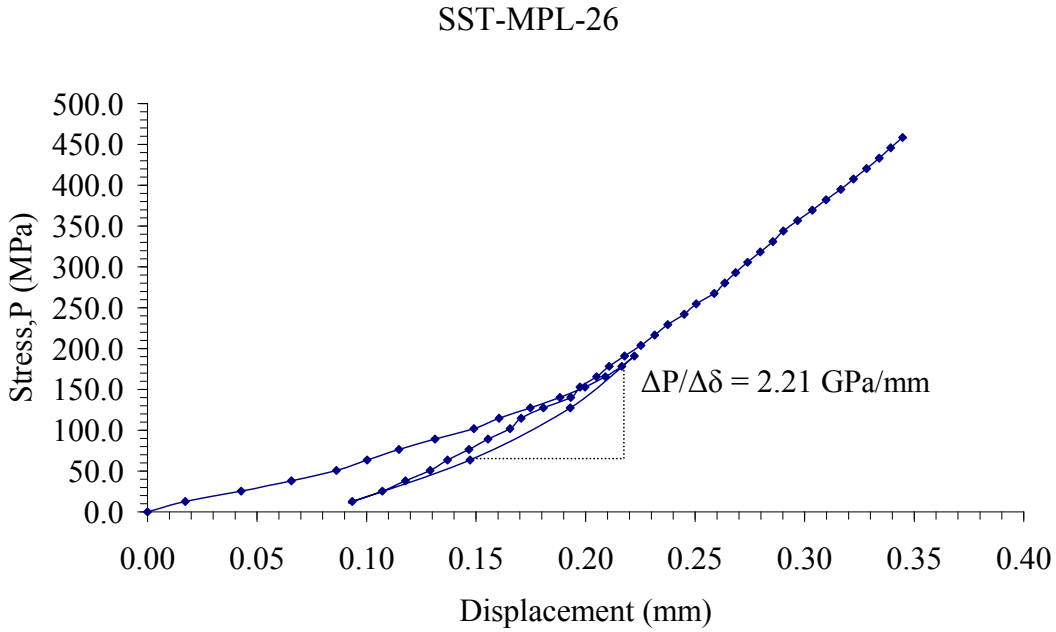

Figure B.76 Applied stress (P) as a function of displacement (δ) for specimen no. SST-MPL-26.

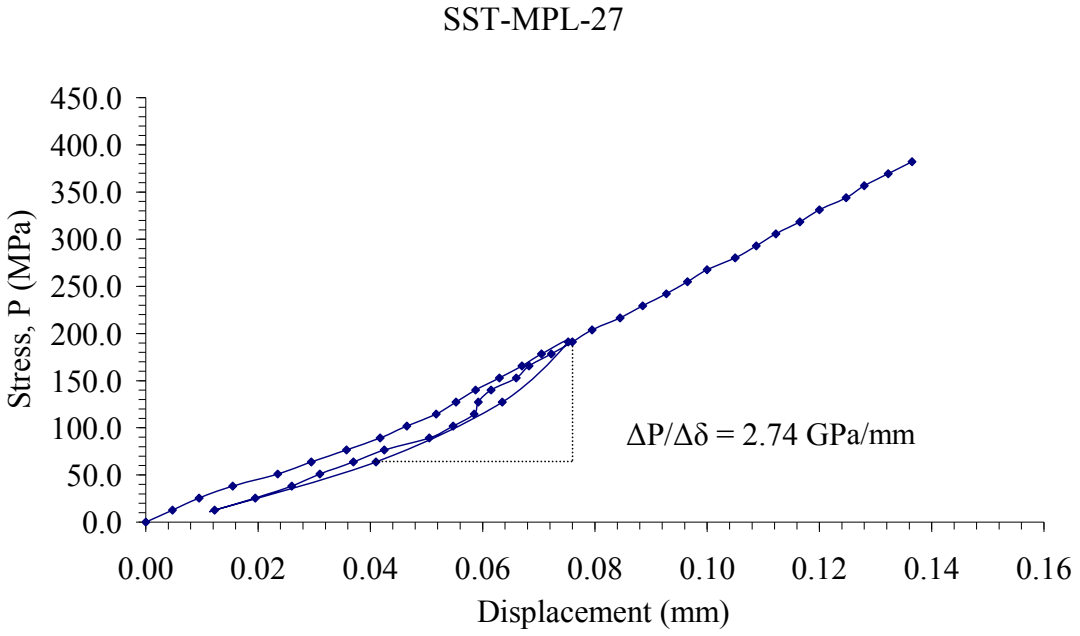

Figure B.77 Applied stress (P) as a function of displacement (δ) for specimen no. SST-MPL-27.

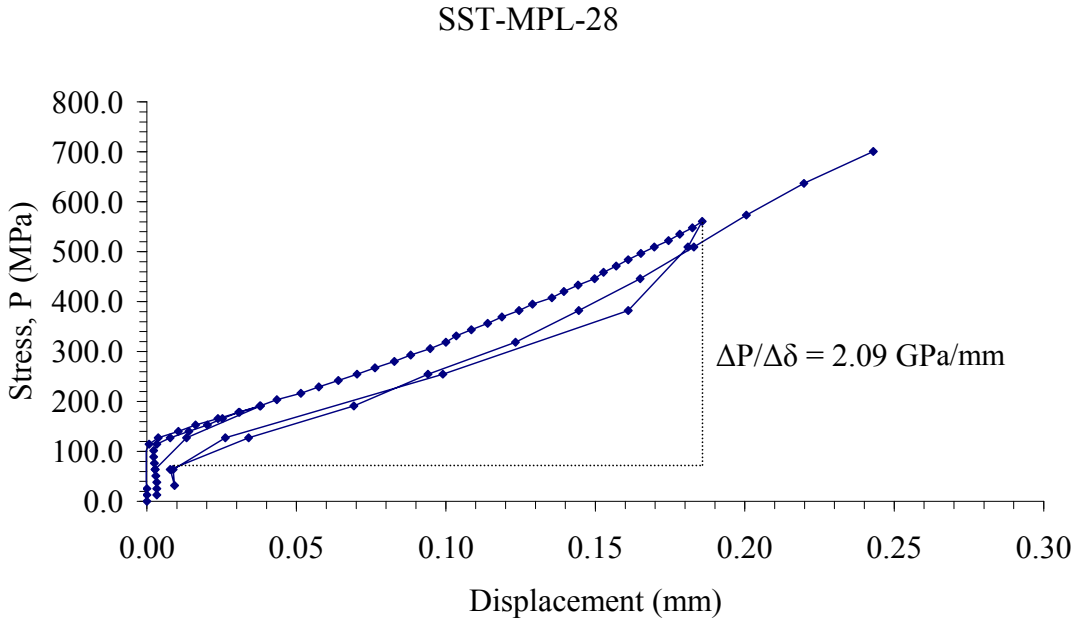

Figure B.78 Applied stress (P) as a function of displacement (δ) for specimen no. SST-MPL-28.

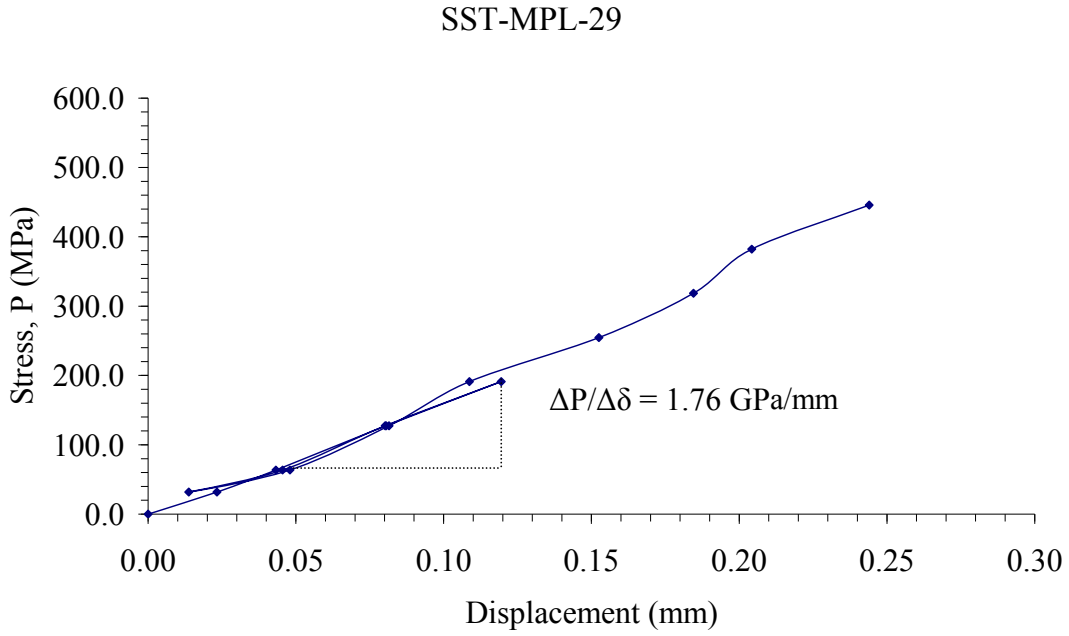

Figure B.79 Applied stress (P) as a function of displacement (δ) for specimen no. SST-MPL-29.

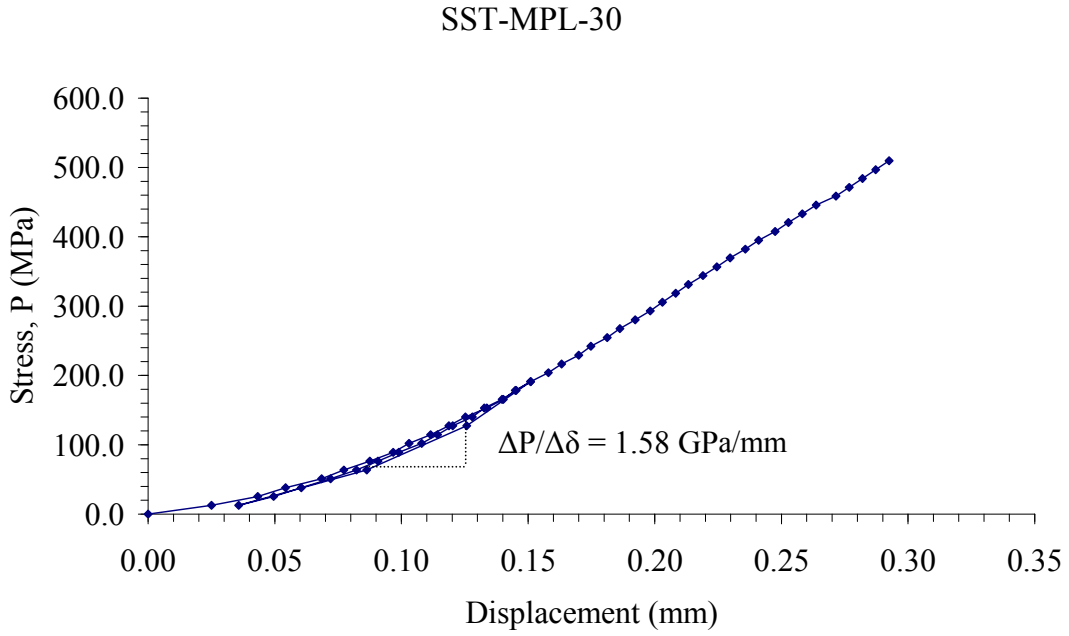

Figure B.80 Applied stress (P) as a function of displacement (δ) for specimen no. SST-MPL-30.

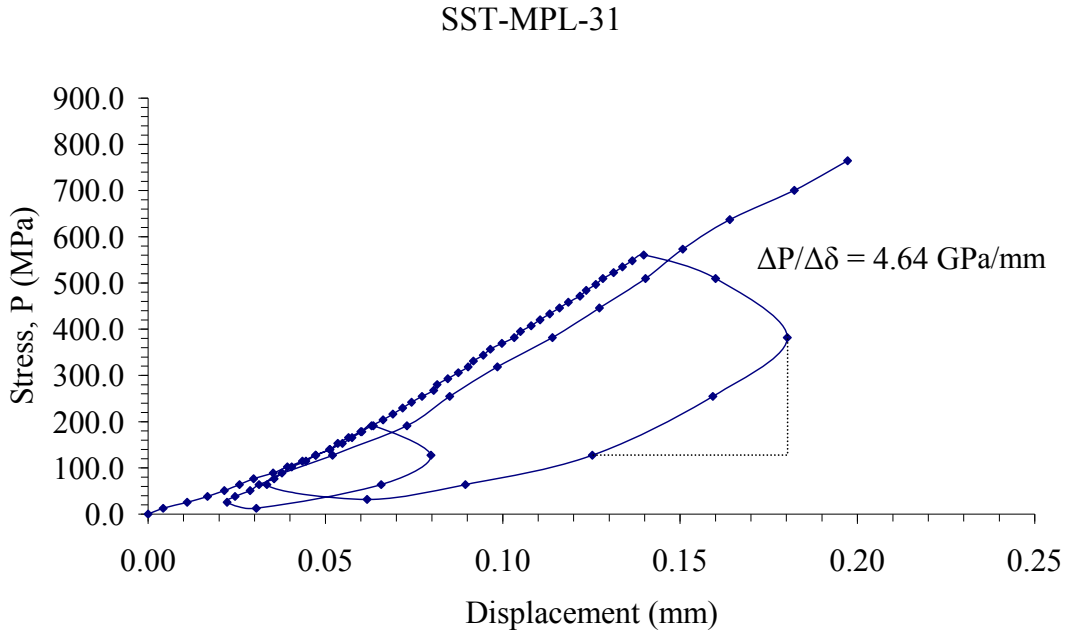

Figure B.81 Applied stress (P) as a function of displacement (δ) for specimen no. SST-MPL-31.

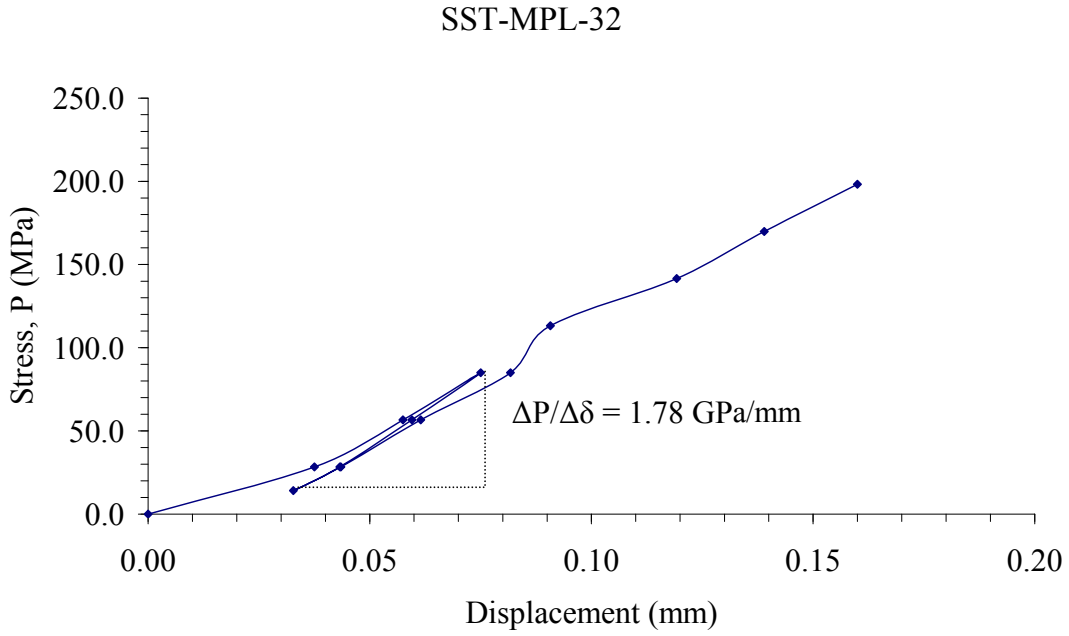

Figure B.82 Applied stress (P) as a function of displacement (δ) for specimen no. SST-MPL-32.

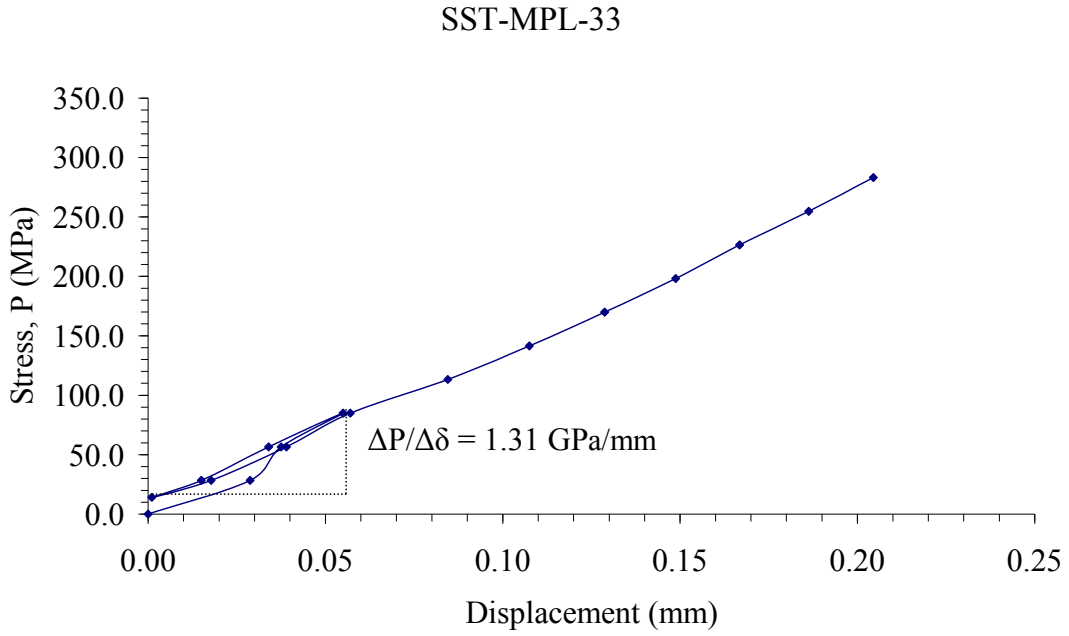

Figure B.83 Applied stress (P) as a function of displacement (δ) for specimen no. SST-MPL-33.

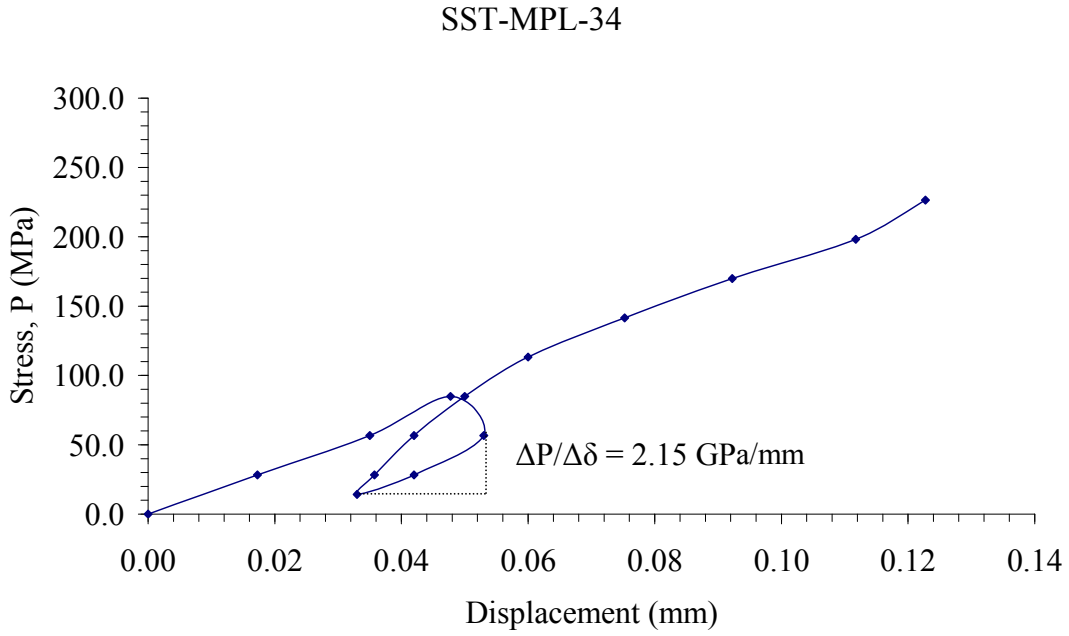

Figure B.84 Applied stress (P) as a function of displacement (δ) for specimen no. SST-MPL-34.

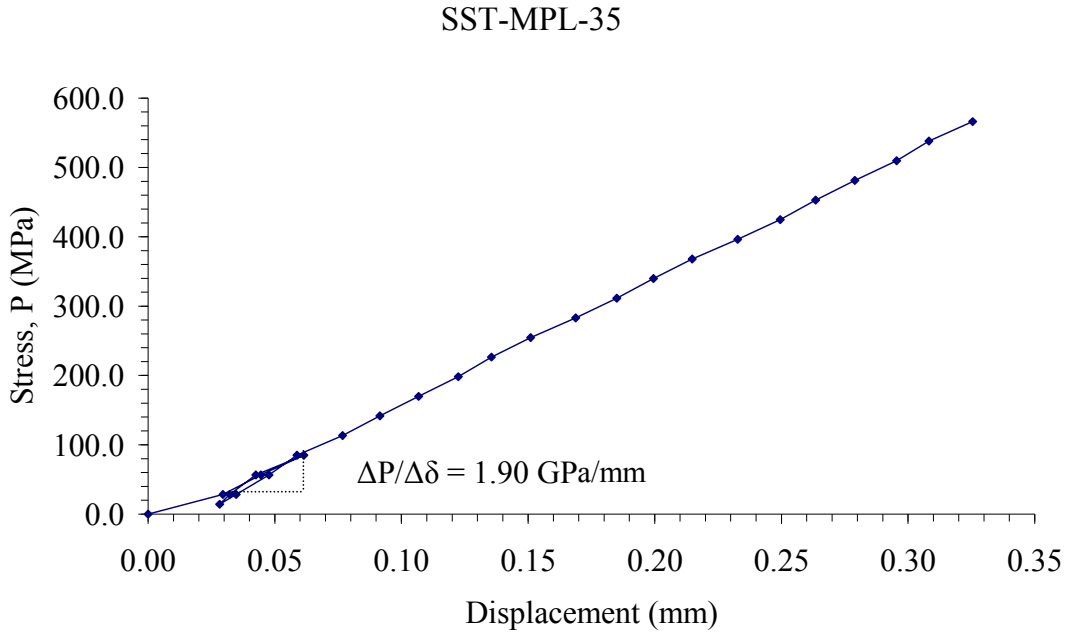

Figure B.85 Applied stress (P) as a function of displacement (δ) for specimen no. SST-MPL-35.

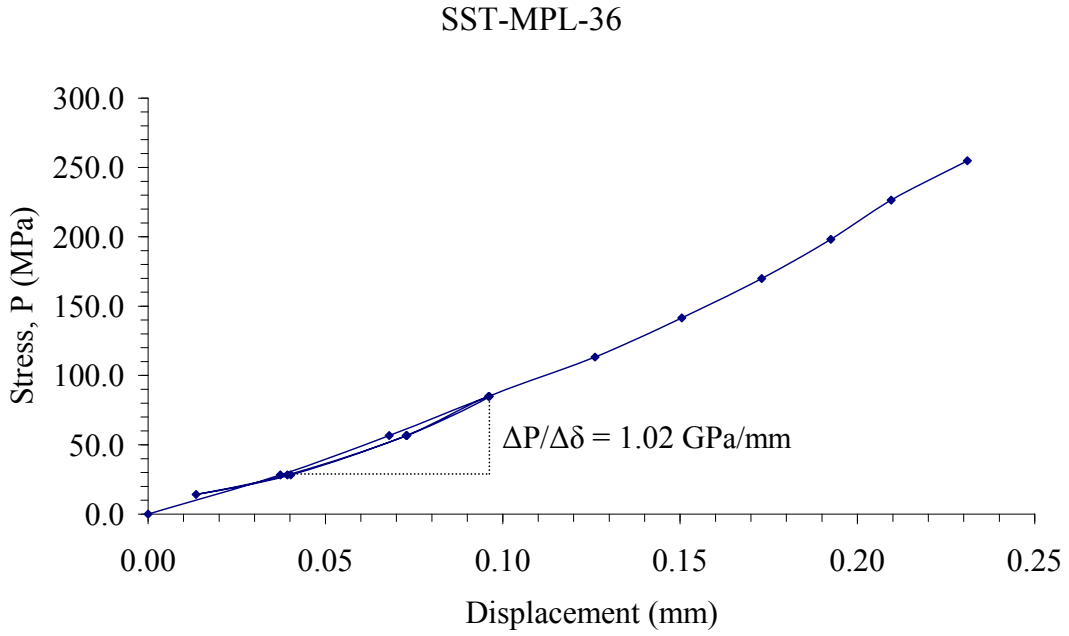

Figure B.86 Applied stress (P) as a function of displacement (δ) for specimen no. SST-MPL-36.

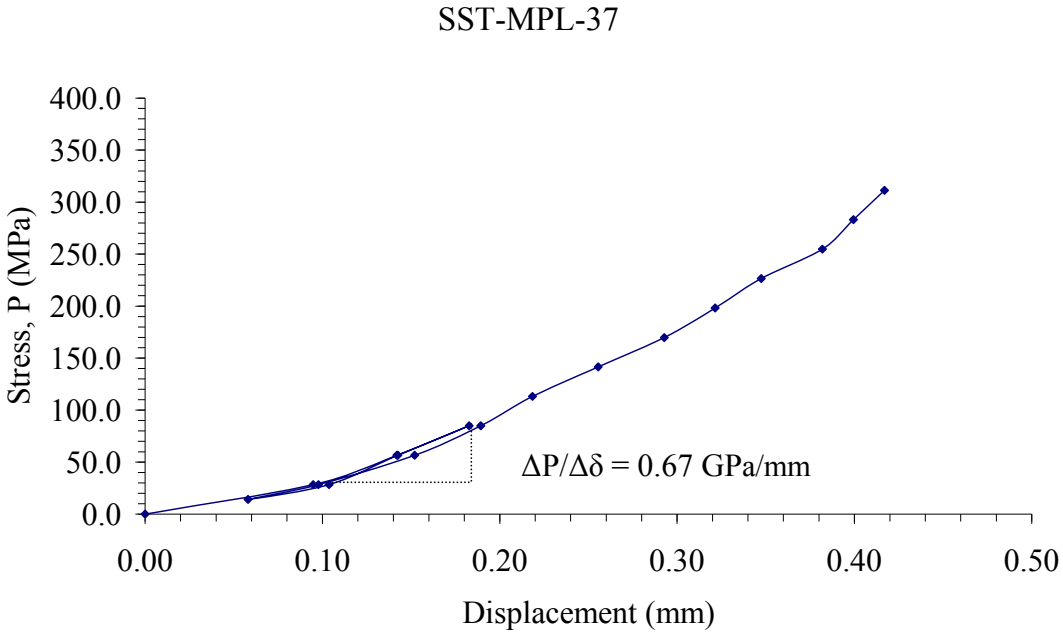

Figure B.87 Applied stress (P) as a function of displacement (δ) for specimen no. SST-MPL-37.

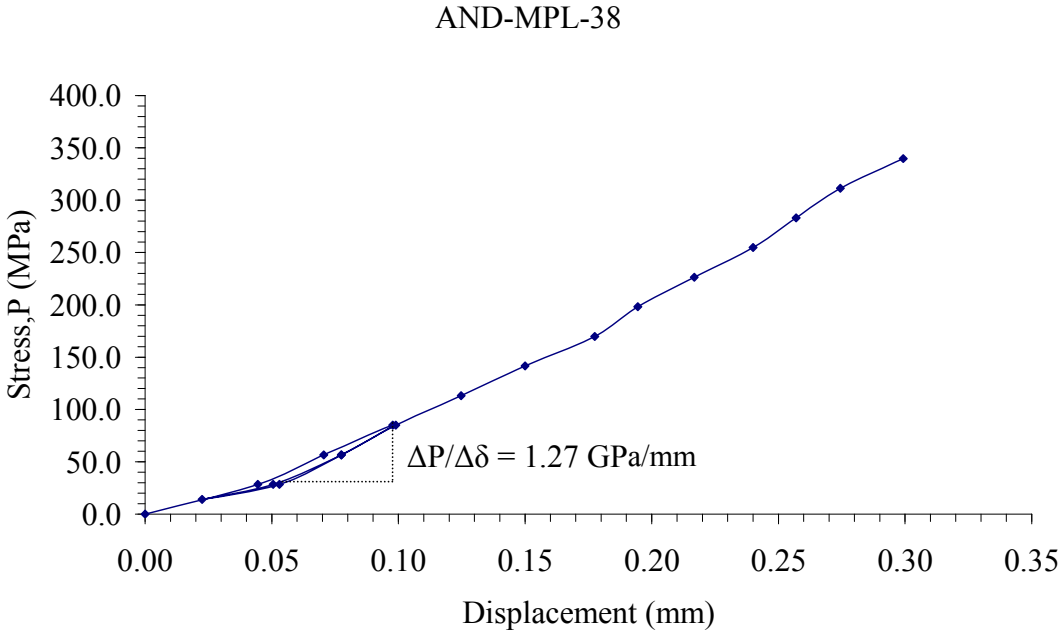

Figure B.88 Applied stress (P) as a function of displacement (δ) for specimen no. SST-MPL-38.

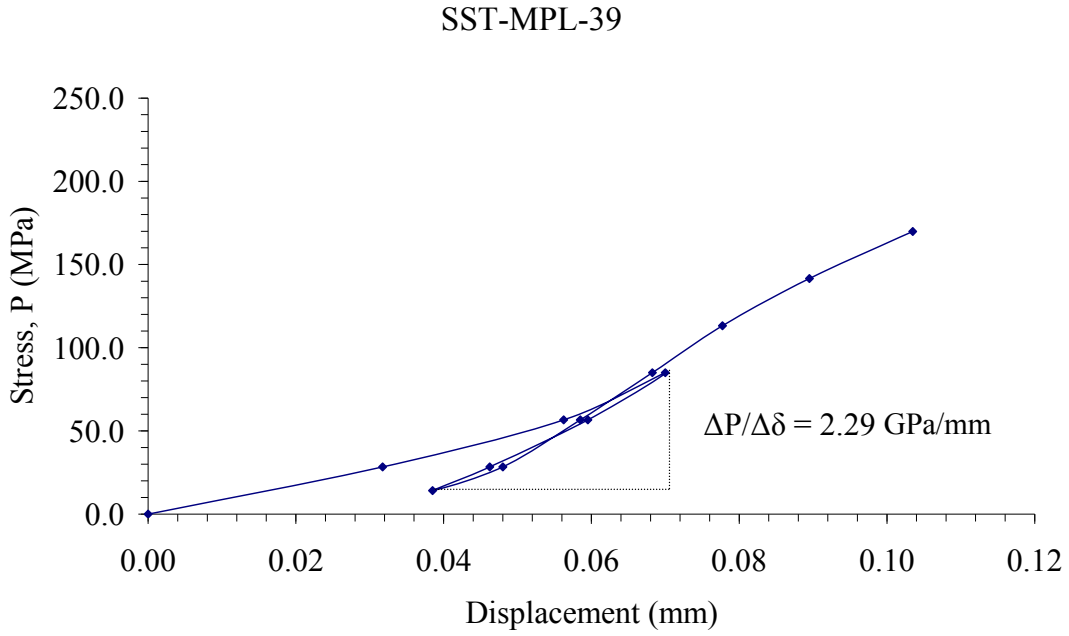

Figure B.89 Applied stress (P) as a function of displacement (δ) for specimen no. SST-MPL-39.

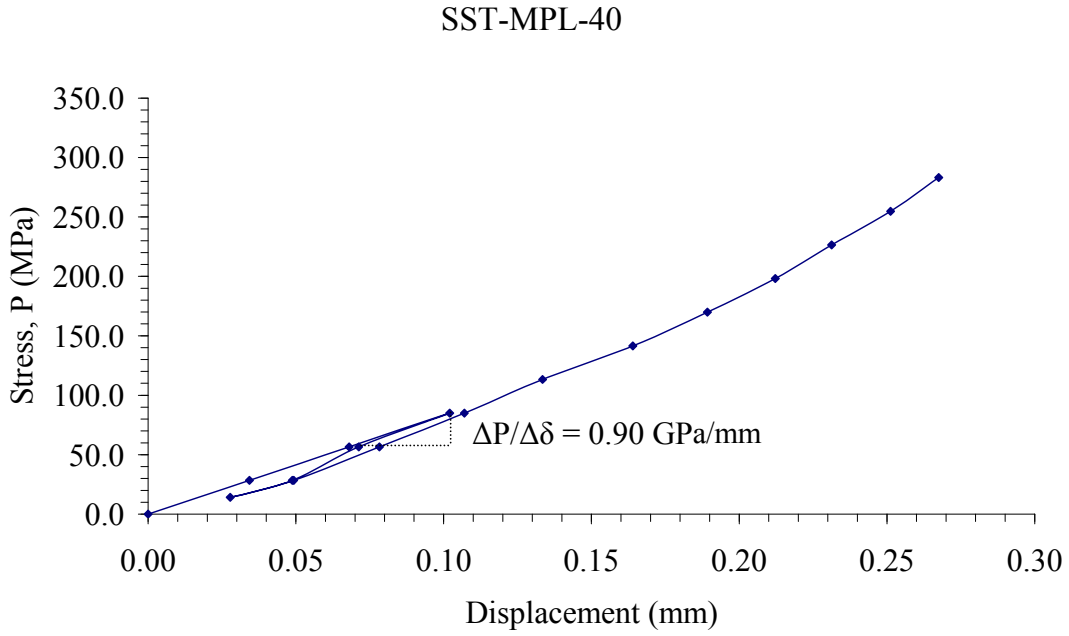

Figure B.90 Applied stress (P) as a function of displacement (δ) for specimen no. SST-MPL-40.

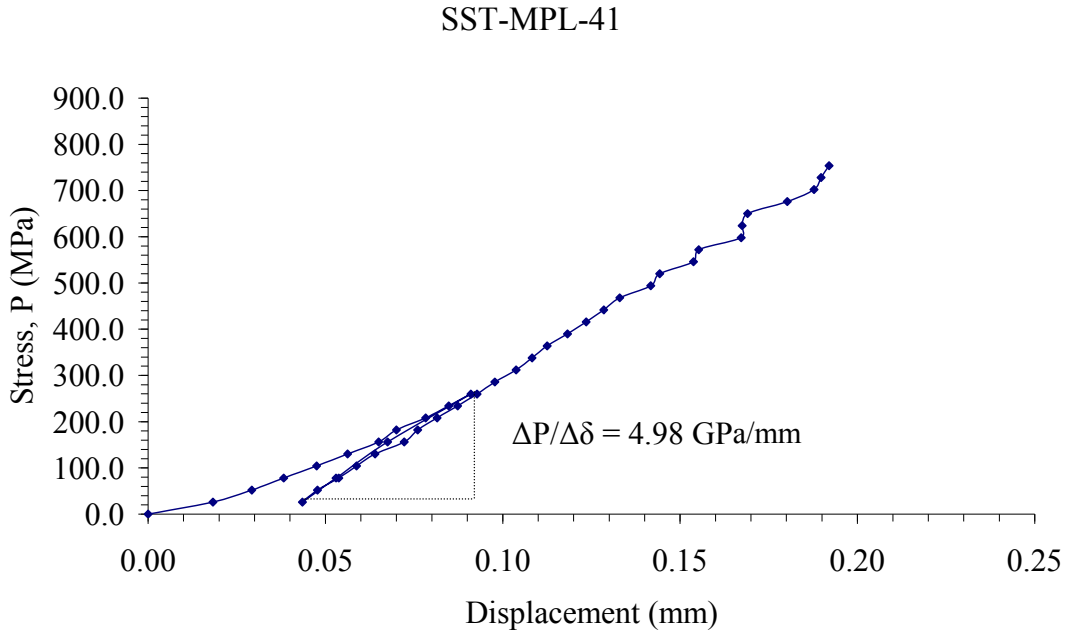

Figure B.91 Applied stress (P) as a function of displacement (δ) for specimen no. SST-MPL-41.

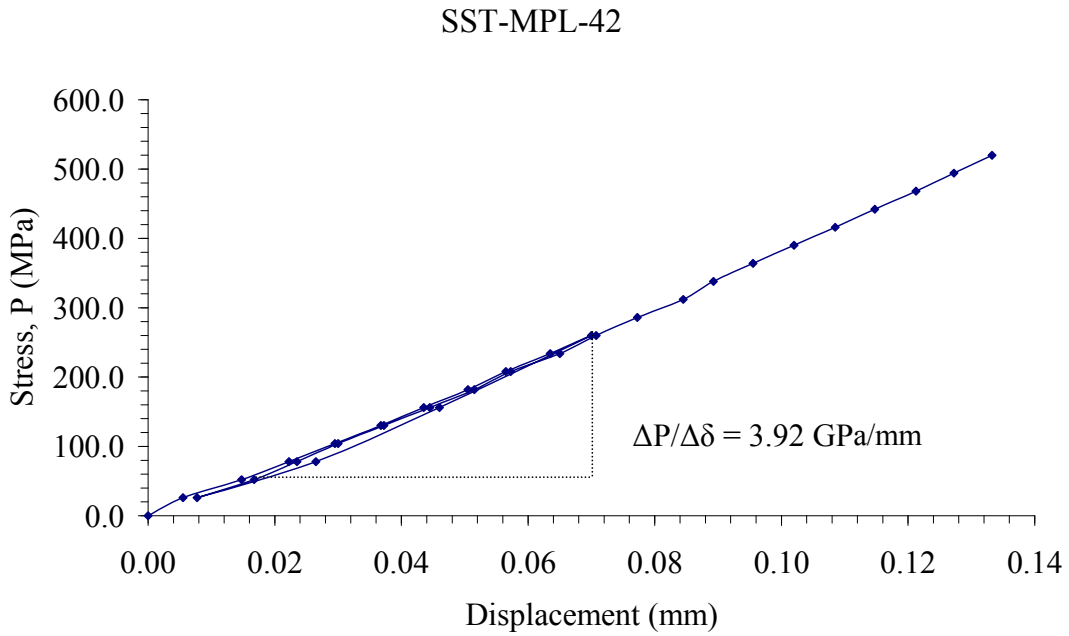

Figure B.92 Applied stress (P) as a function of displacement (δ) for specimen no. SST-MPL-42.

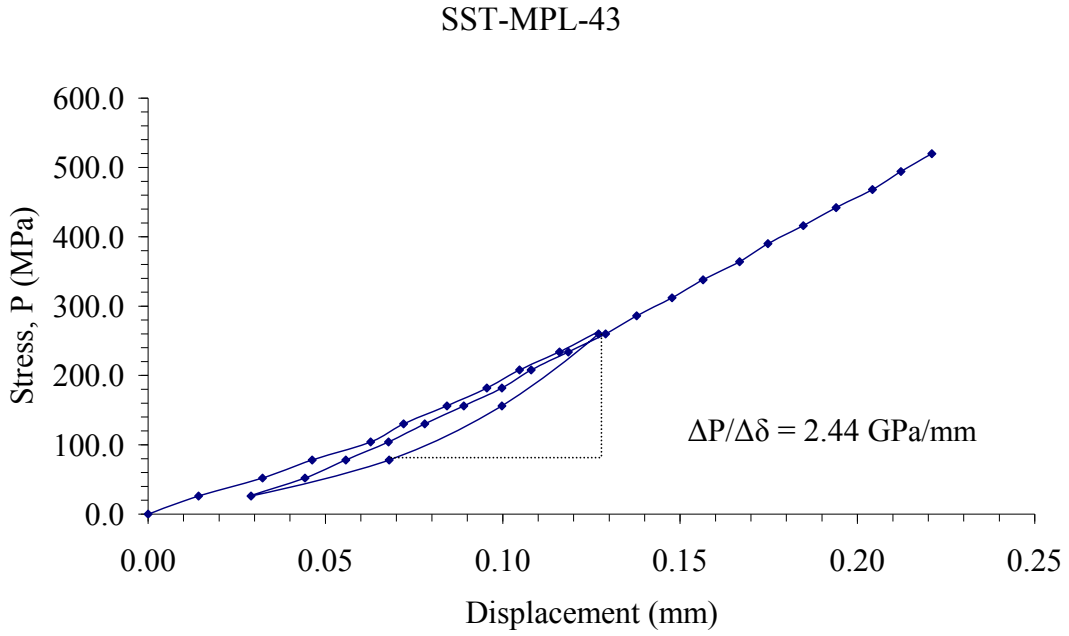

Figure B.93 Applied stress (P) as a function of displacement (δ) for specimen no. SST-MPL-43.

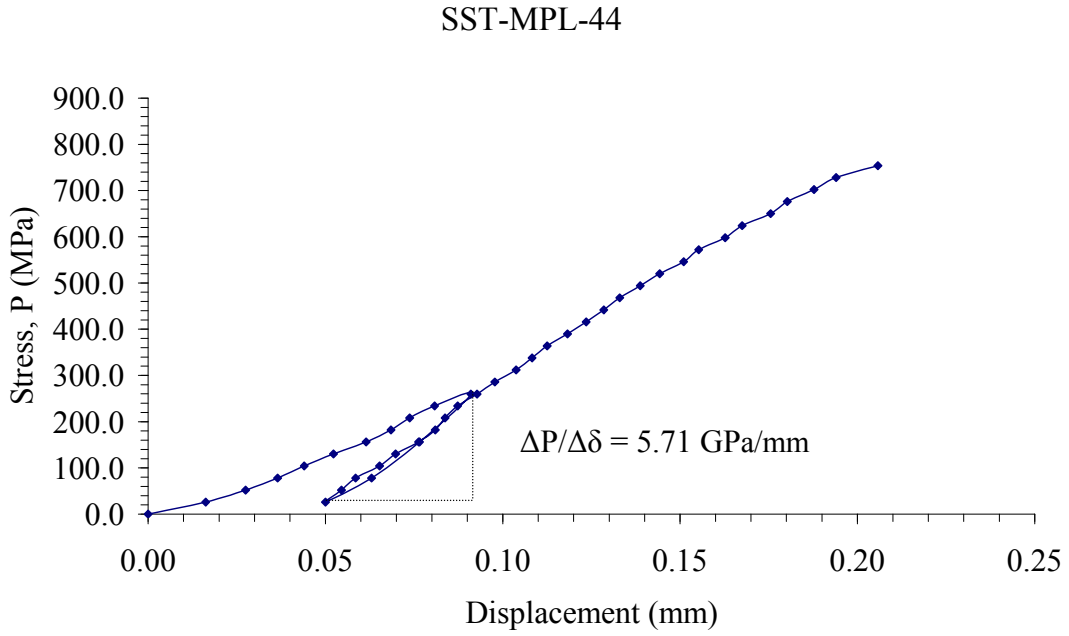

Figure B.94 Applied stress (P) as a function of displacement (δ) for specimen no. SST-MPL-44.

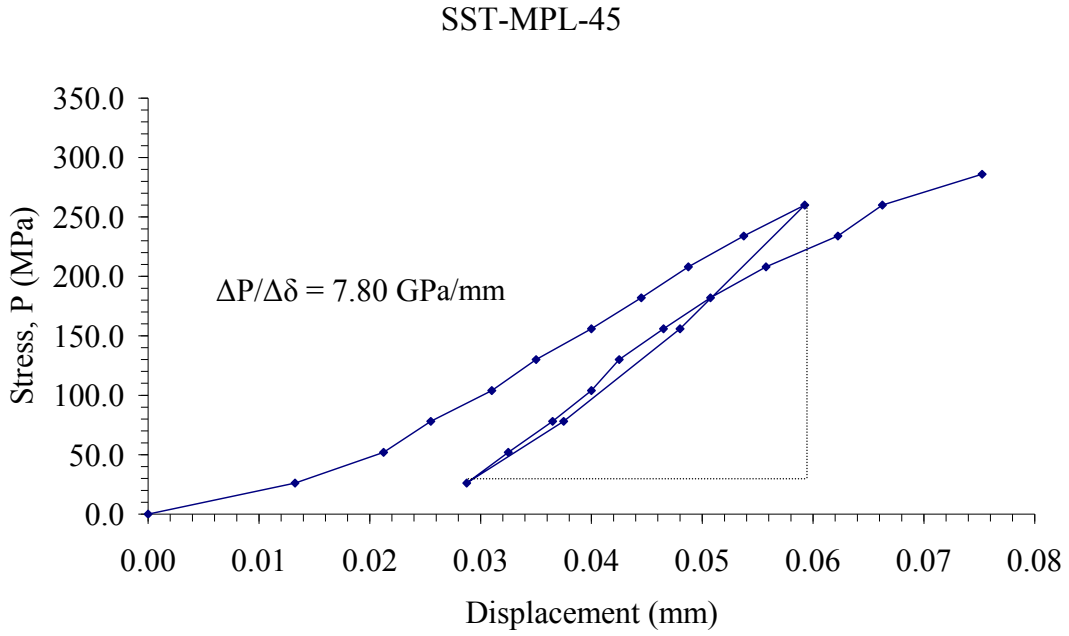

Figure B.95 Applied stress (P) as a function of displacement (δ) for specimen no. SST-MPL-45.

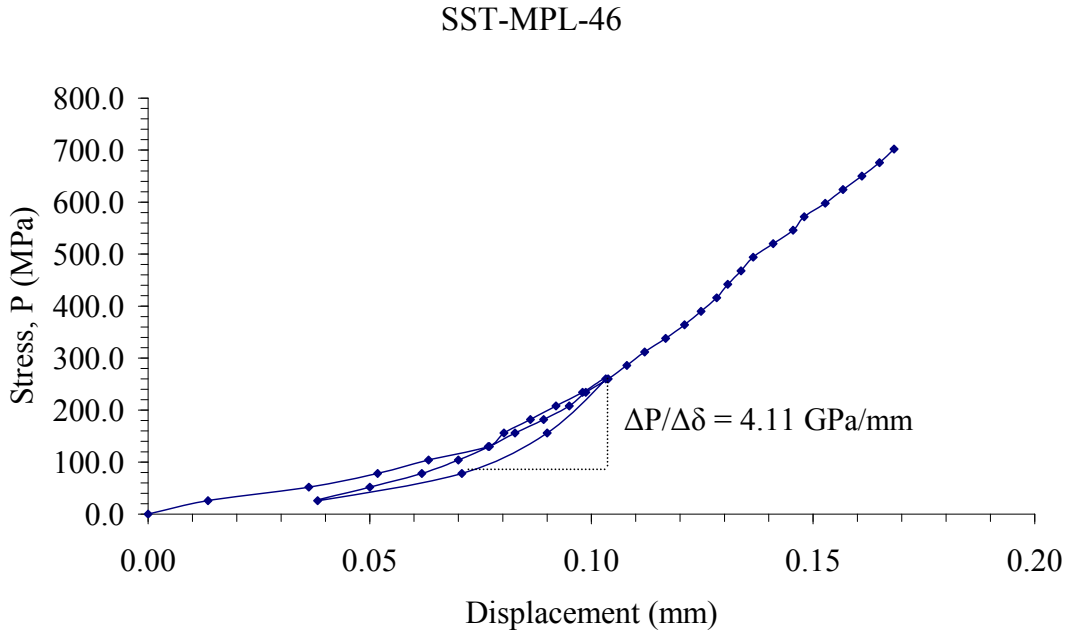

Figure B.96 Applied stress (P) as a function of displacement (δ) for specimen no. SST-MPL-46.

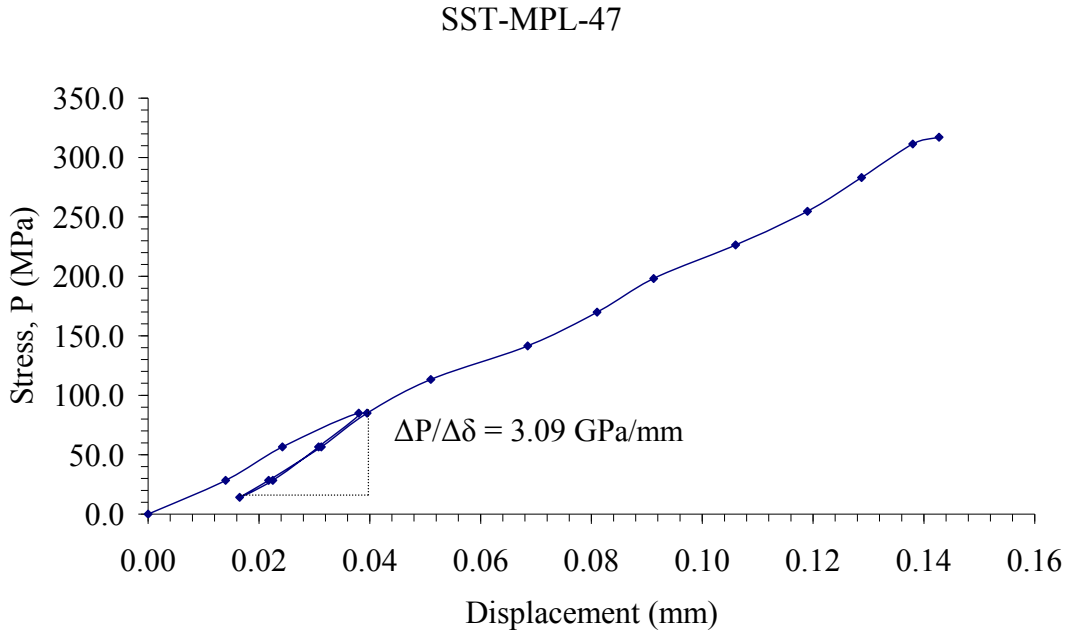

Figure B.97 Applied stress (P) as a function of displacement (δ) for specimen no. SST-MPL-47.

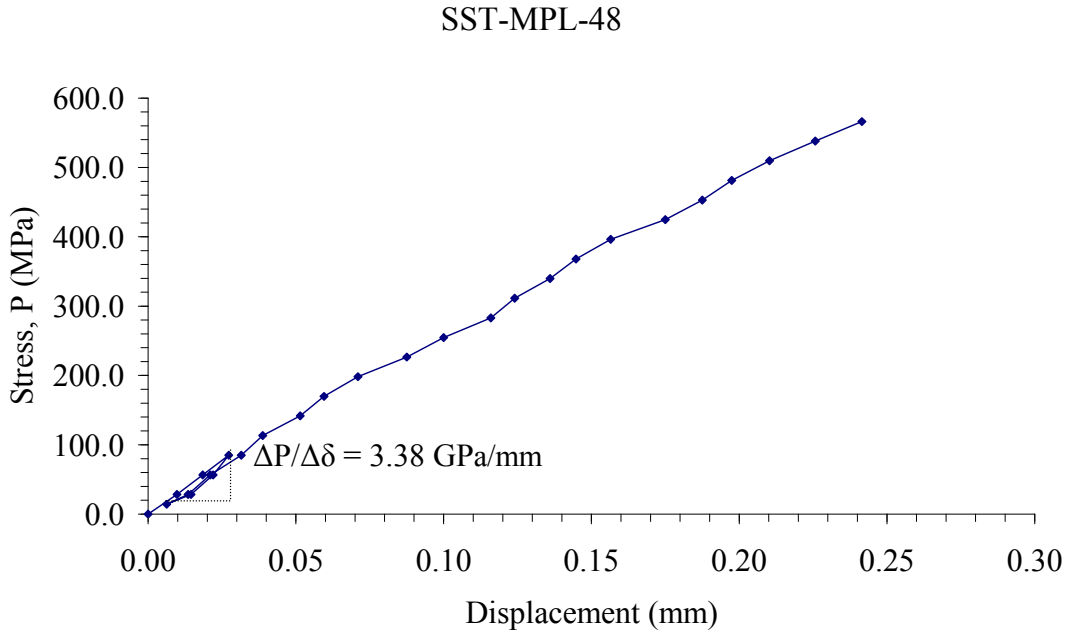

Figure B.98 Applied stress (P) as a function of displacement (δ) for specimen no. SST-MPL-48.

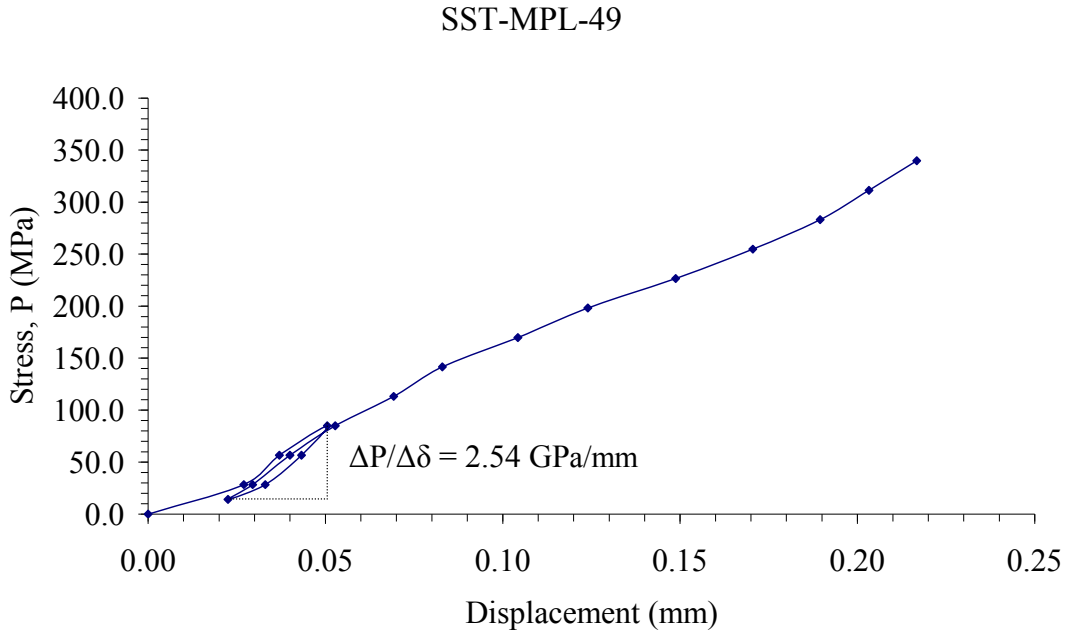

Figure B.99 Applied stress (P) as a function of displacement (δ) for specimen no. SST-MPL-49.

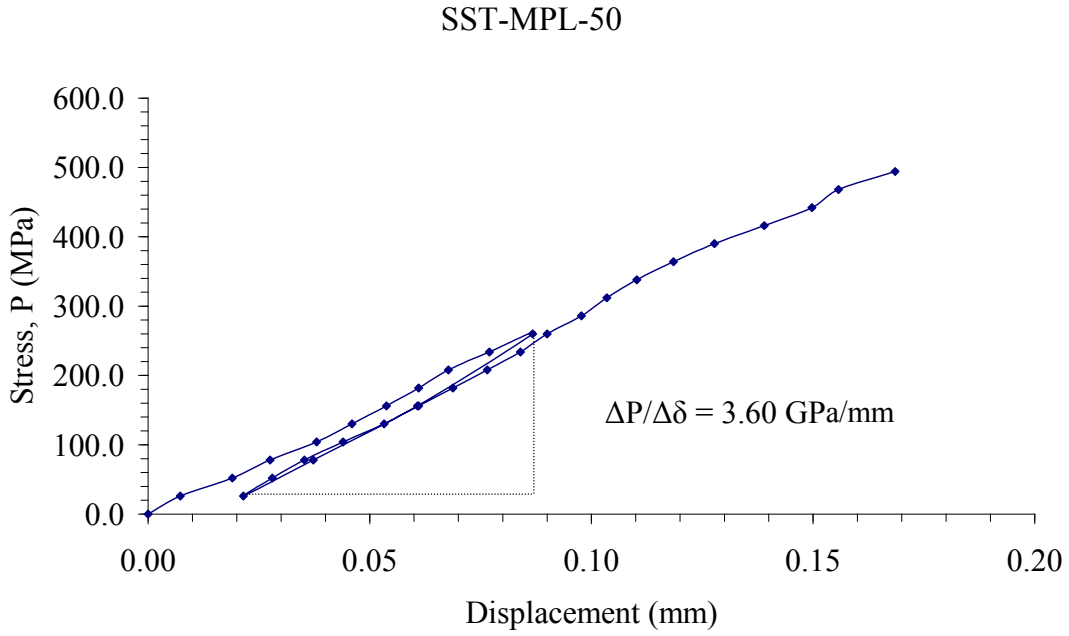

Figure B.100 Applied stress (P) as a function of displacement (δ) for specimen no. SST-MPL-50.

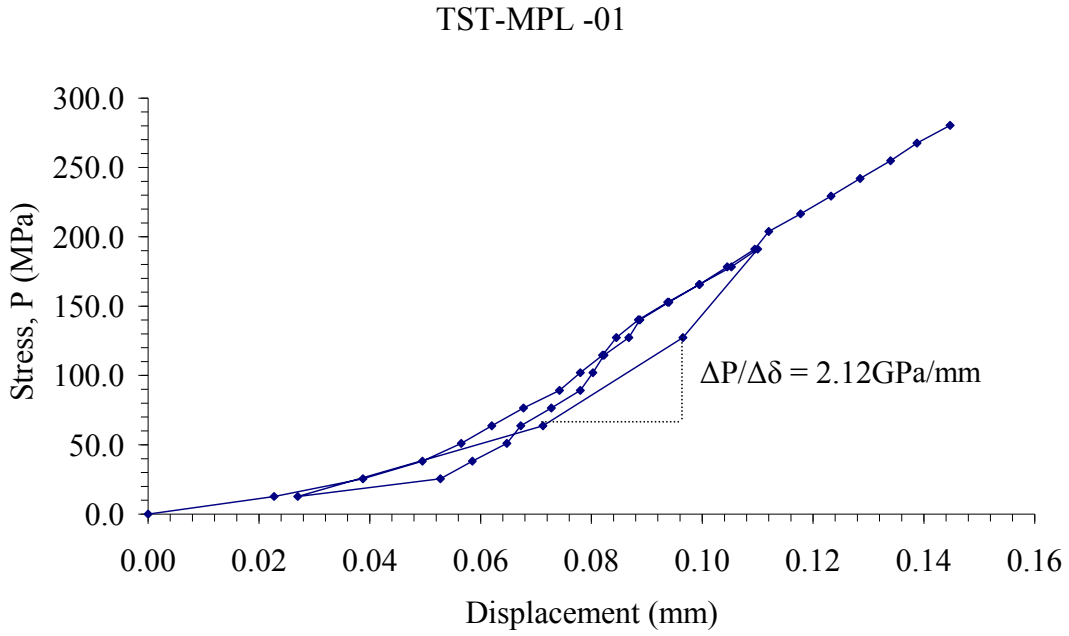

Figure B.101 Applied stress (P) as a function of displacement (δ) for specimen no. TST-MPL-01.

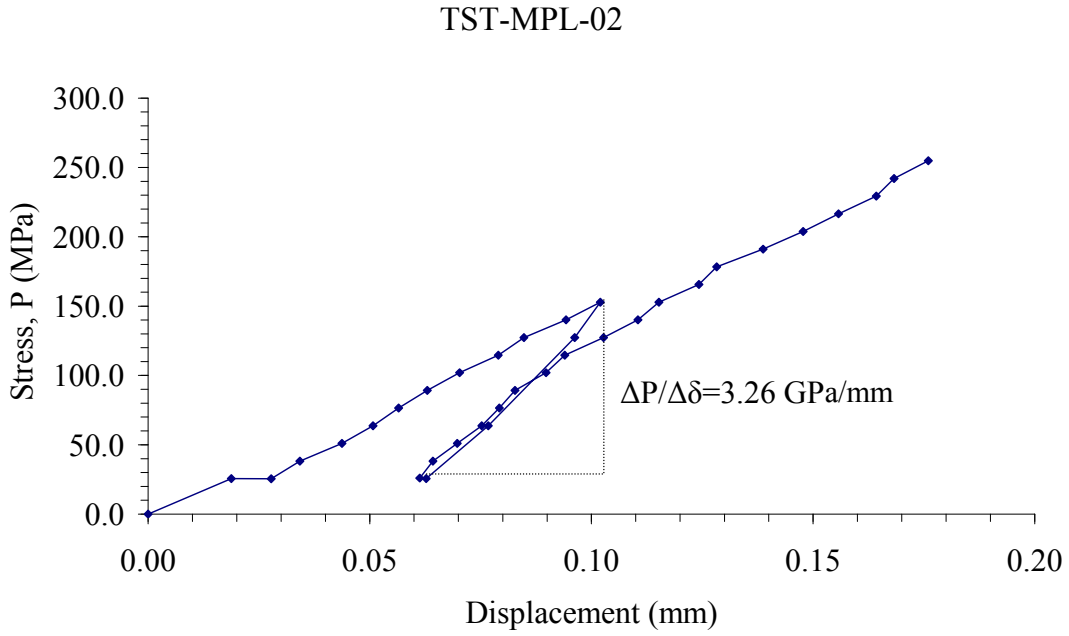

Figure B.102 Applied stress (P) as a function of displacement (δ) for specimen no. TST-MPL-02.

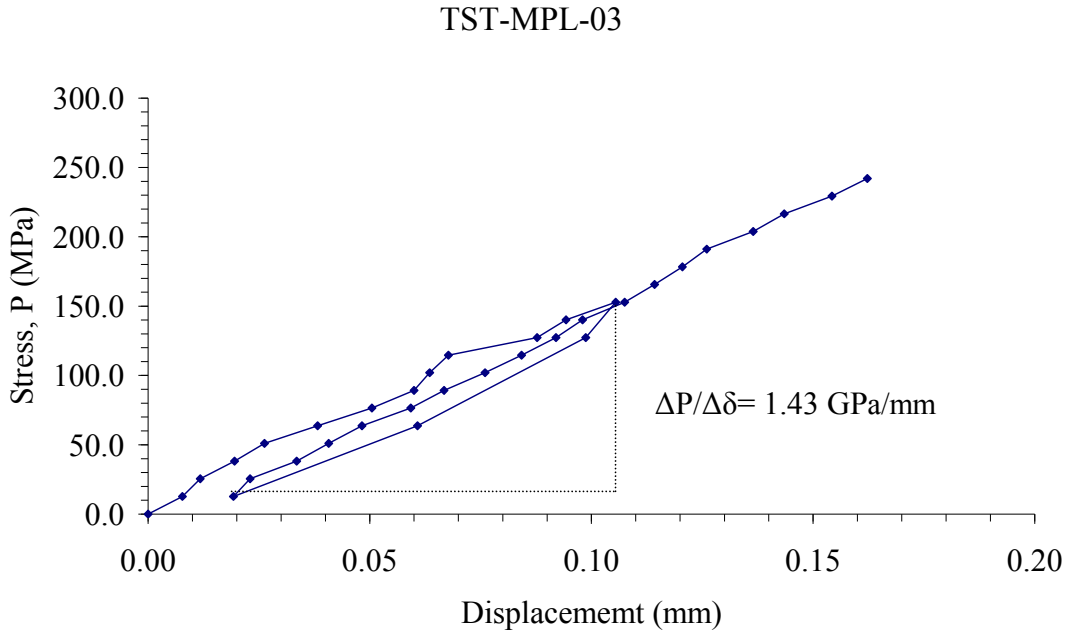

Figure B.103 Applied stress (P) as a function of displacement (δ) for specimen no. TST-MPL-03.

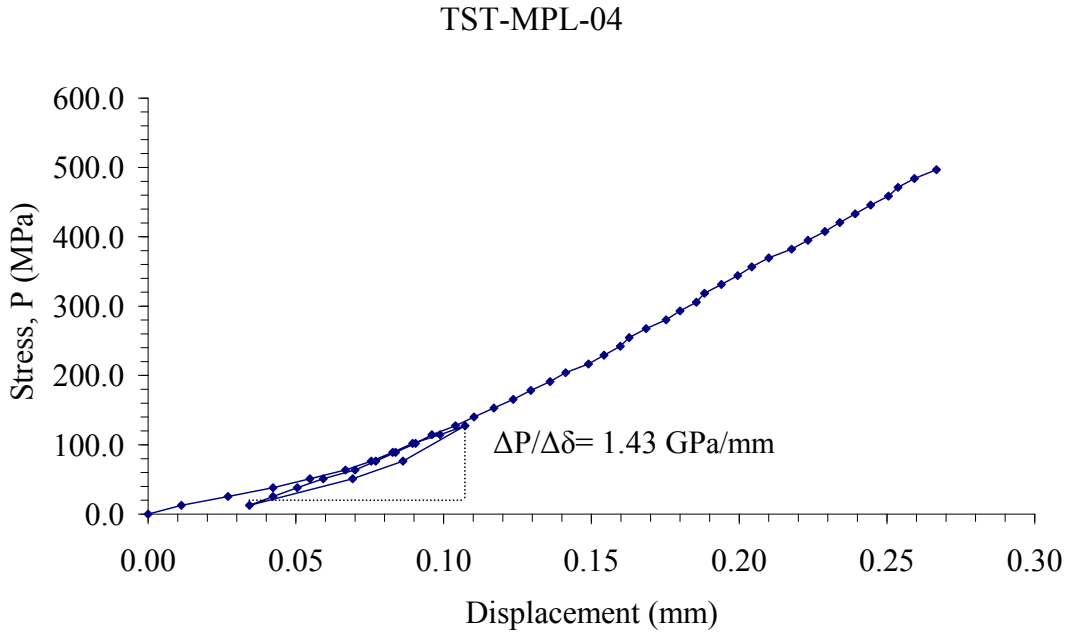

Figure B.104 Applied stress (P) as a function of displacement (δ) for specimen no. TST-MPL-04.

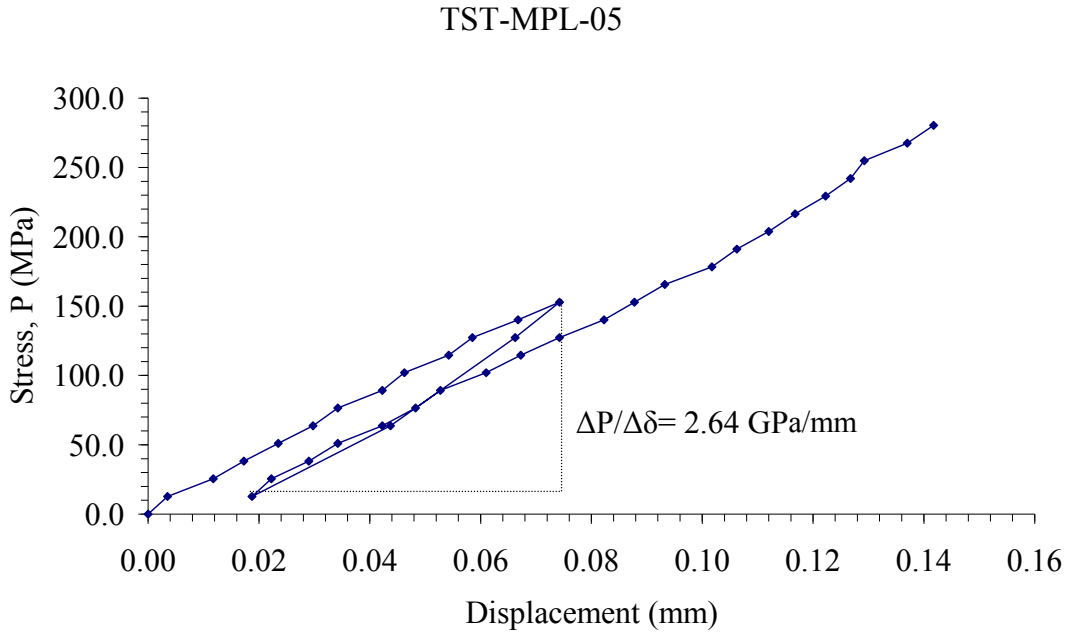

Figure B.105 Applied stress (P) as a function of displacement (δ) for specimen no. TST-MPL-05.

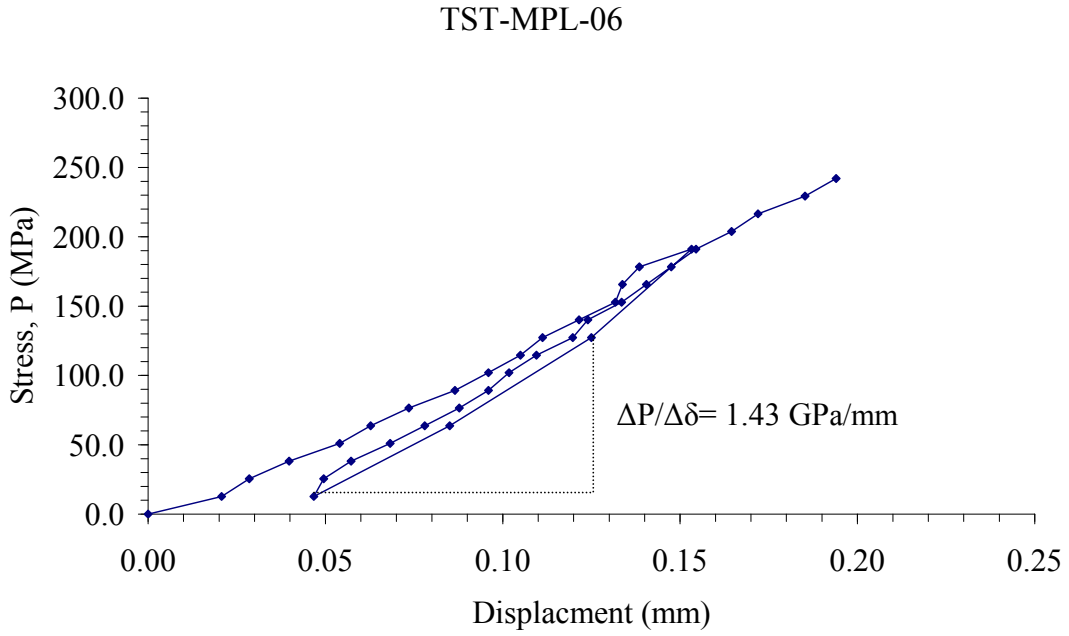

Figure B.106 Applied stress (P) as a function of displacement (δ) for specimen no. TST-MPL-06.

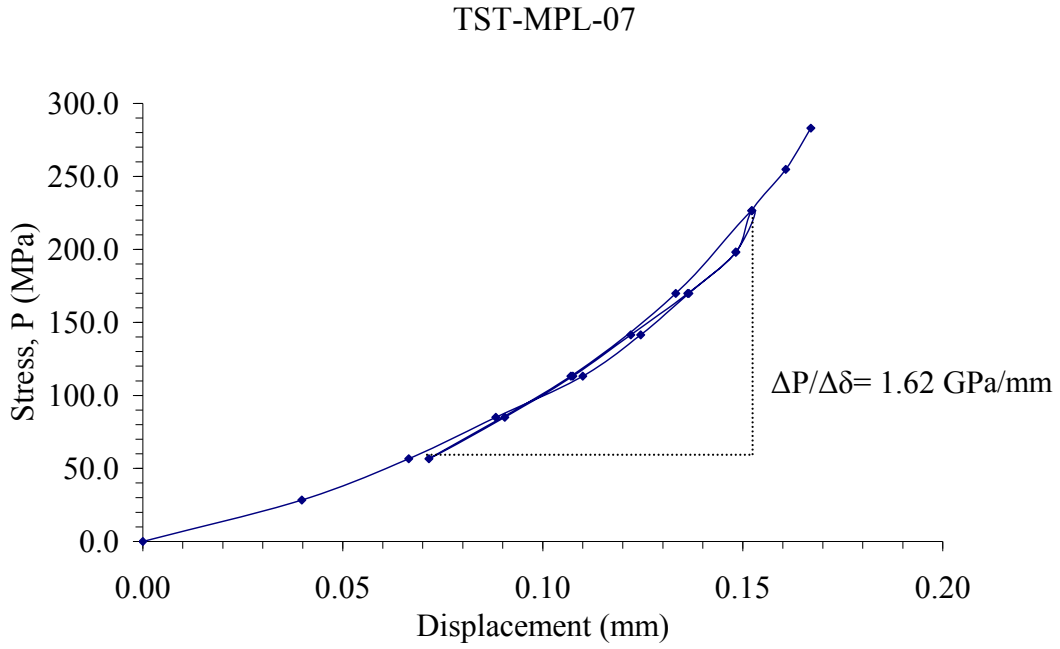

Figure B.107 Applied stress (P) as a function of displacement (δ) for specimen no. TST-MPL-07.

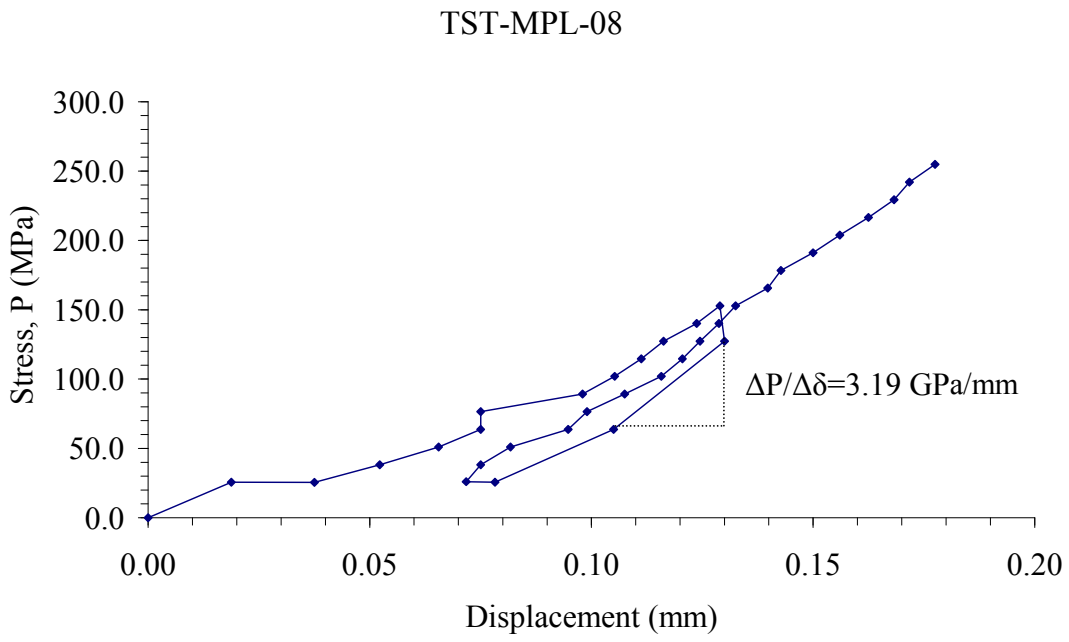

Figure B.108 Applied stress (P) as a function of displacement (δ) for specimen no. TST-MPL-08.

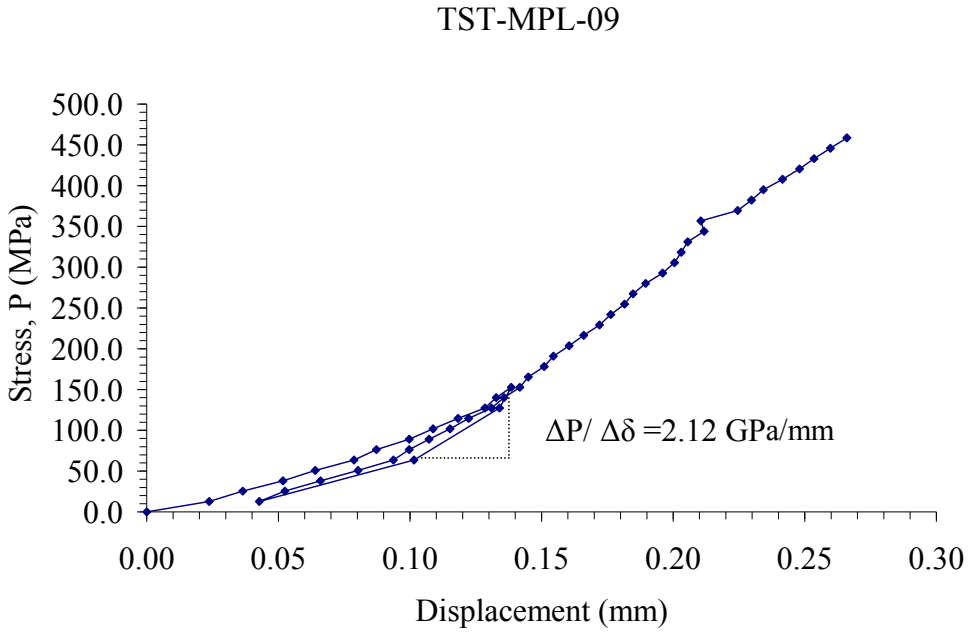

Figure B.109 Applied stress (P) as a function of displacement (δ) for specimen no. TST-MPL-09.

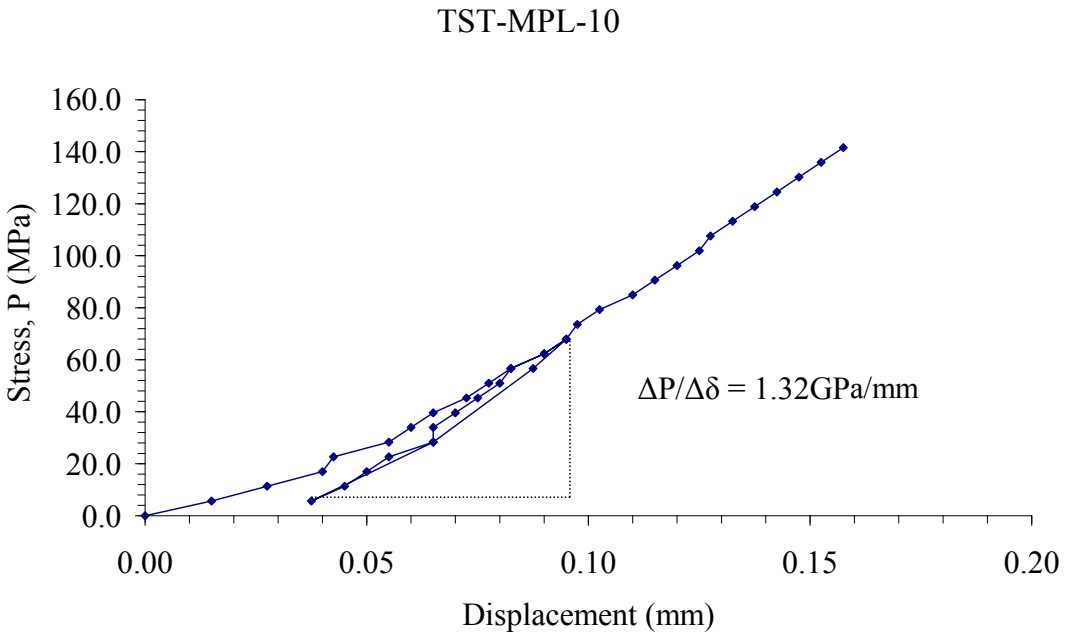

Figure B.110 Applied stress (P) as a function of displacement (δ) for specimen no. TST-MPL-10.

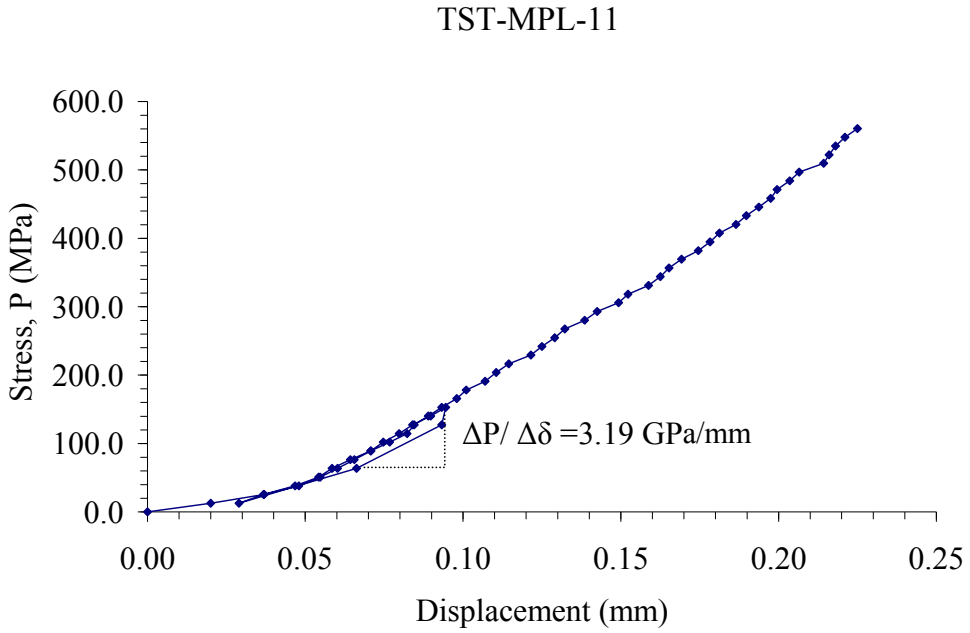

Figure B.111 Applied stress (P) as a function of displacement (δ) for specimen no. TST-MPL-11.

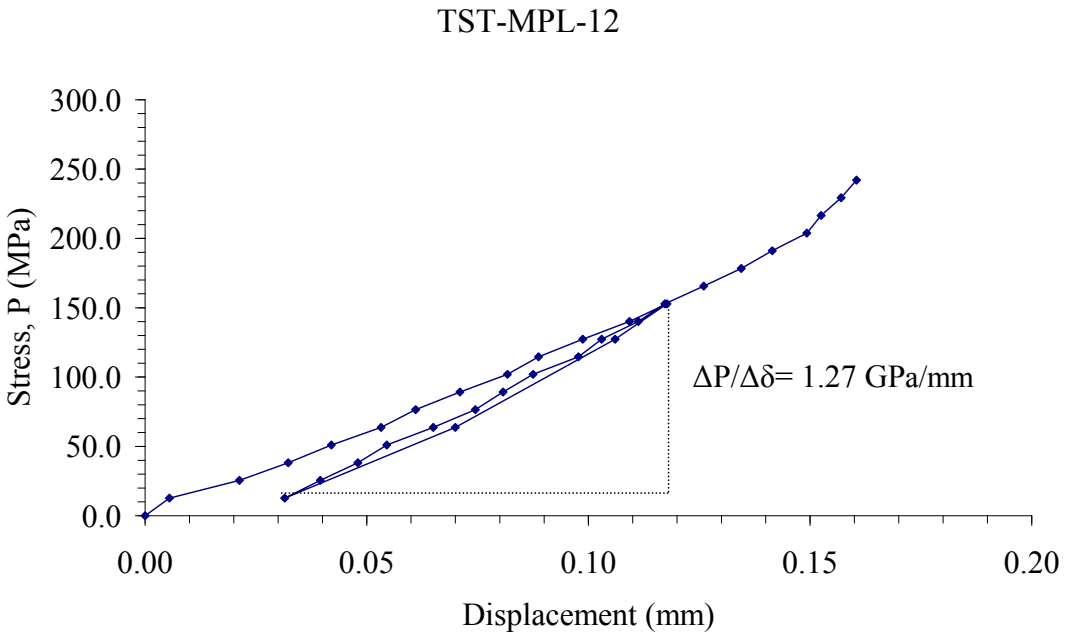

Figure B.112 Applied stress (P) as a function of displacement (δ) for specimen no. TST-MPL-12.

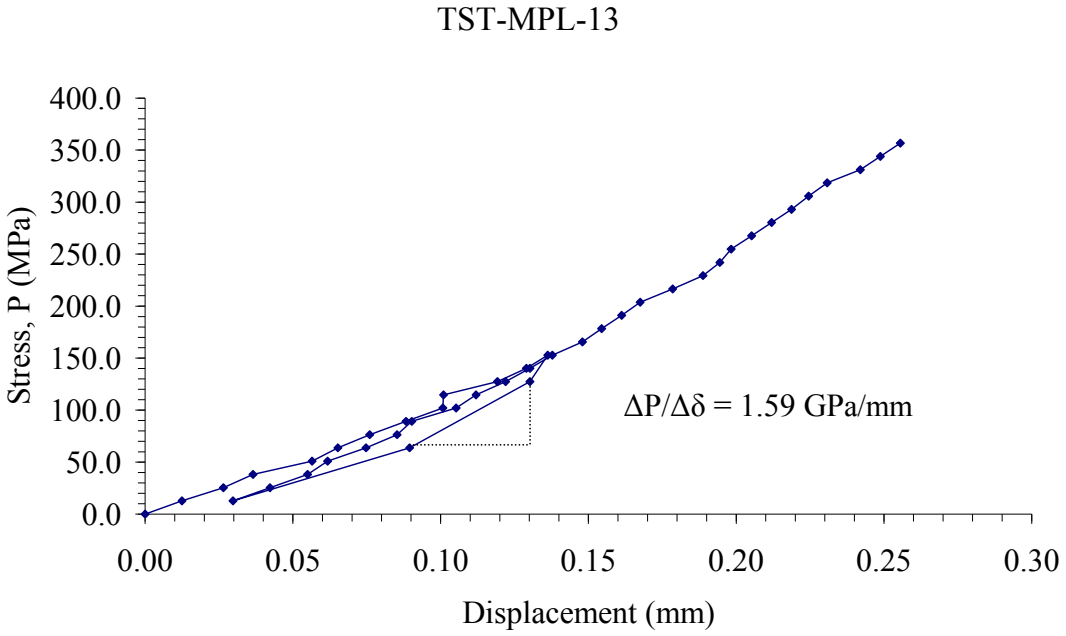

Figure B.113 Applied stress (P) as a function of displacement (δ) for specimen no. TST-MPL-13.

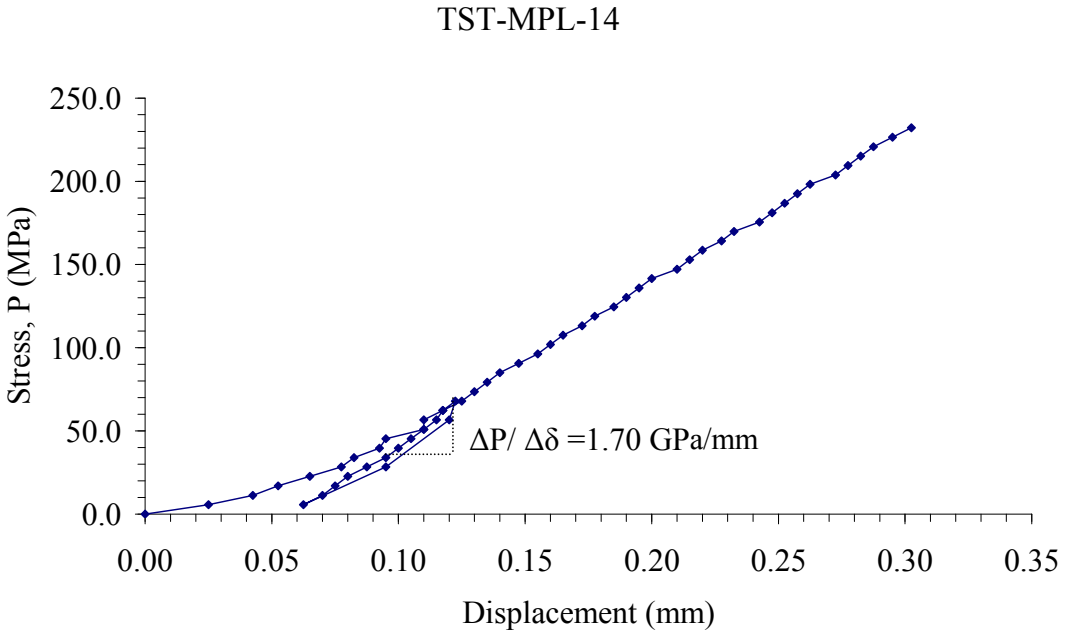

Figure B.114 Applied stress (P) as a function of displacement (δ) for specimen no. TST-MPL-14.

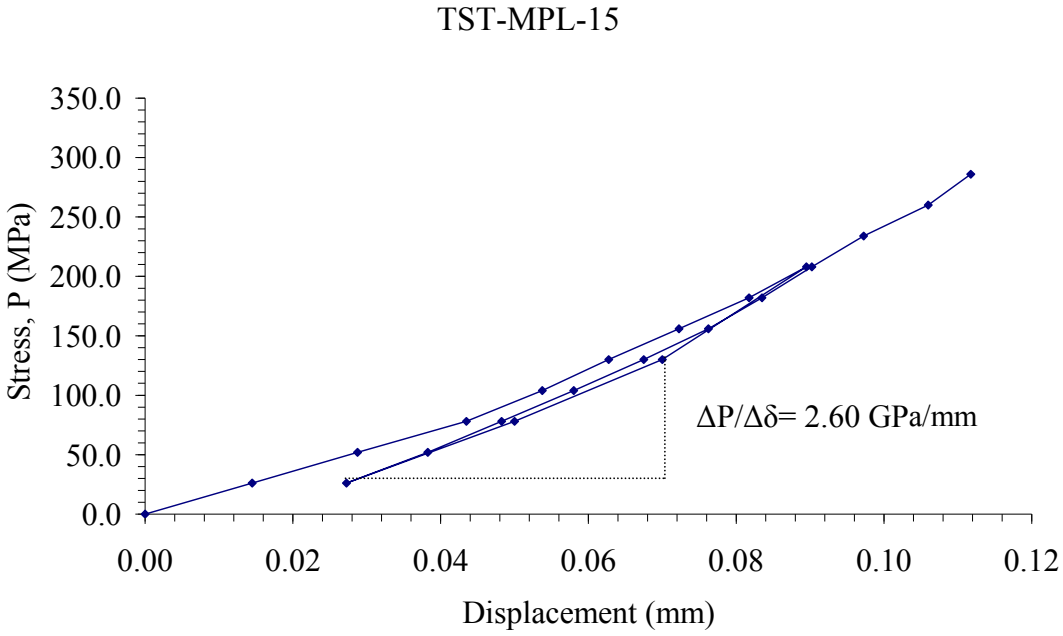

Figure B.115 Applied stress (P) as a function of displacement (δ) for specimen no. TST-MPL-15.

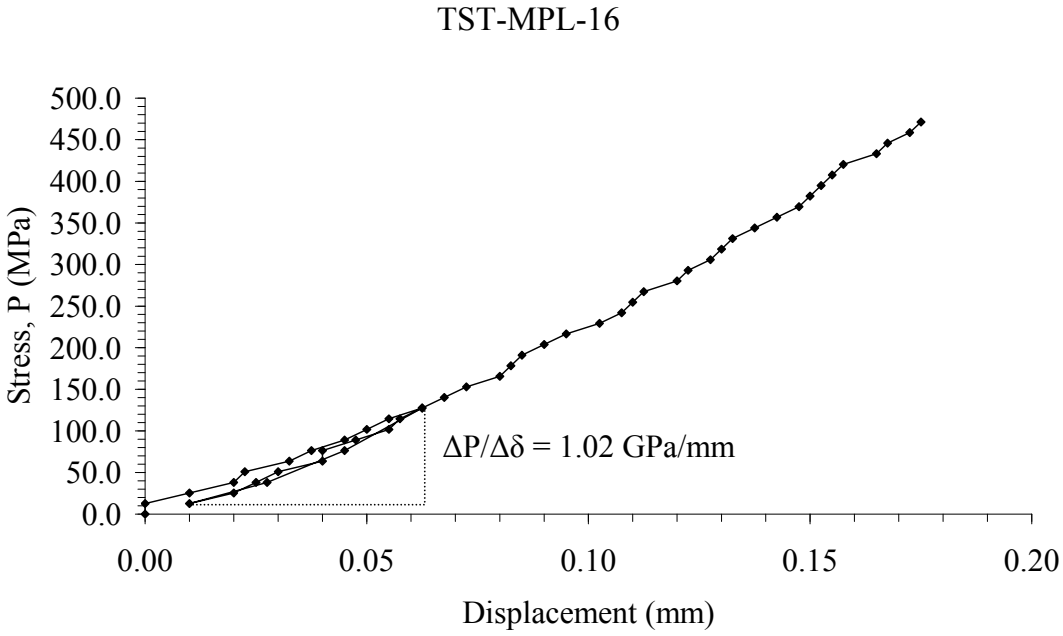

Figure B.116 Applied stress (P) as a function of displacement (δ) for specimen no. TST-MPL-16.

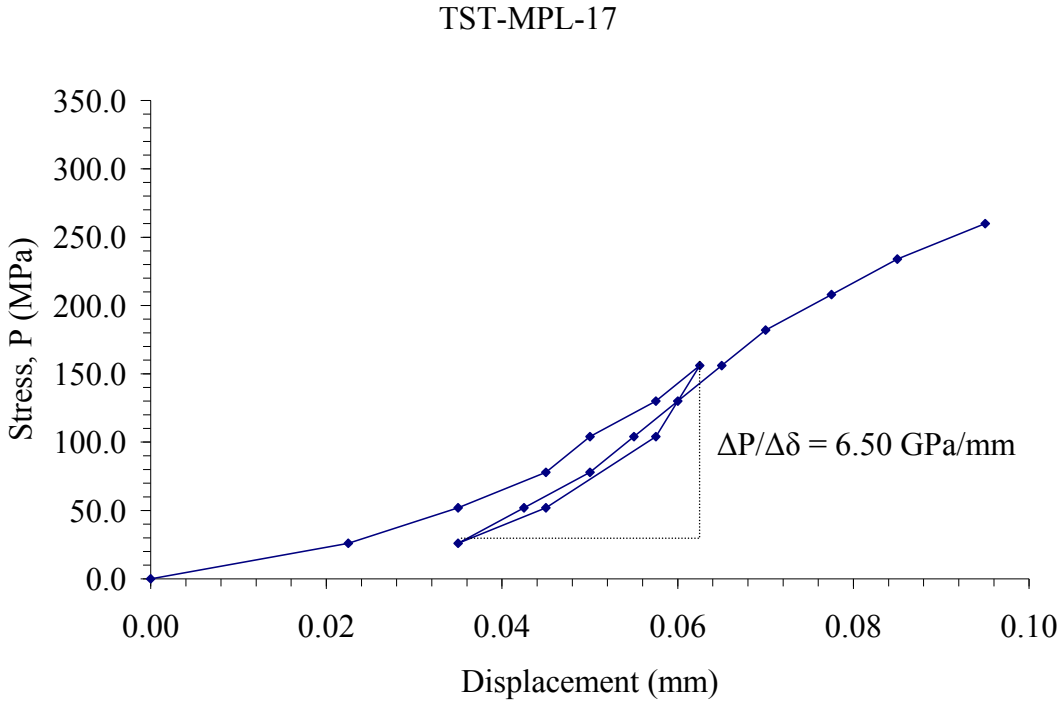

Figure B.117 Applied stress (P) as a function of displacement (δ) for specimen no. TST-MPL-17.

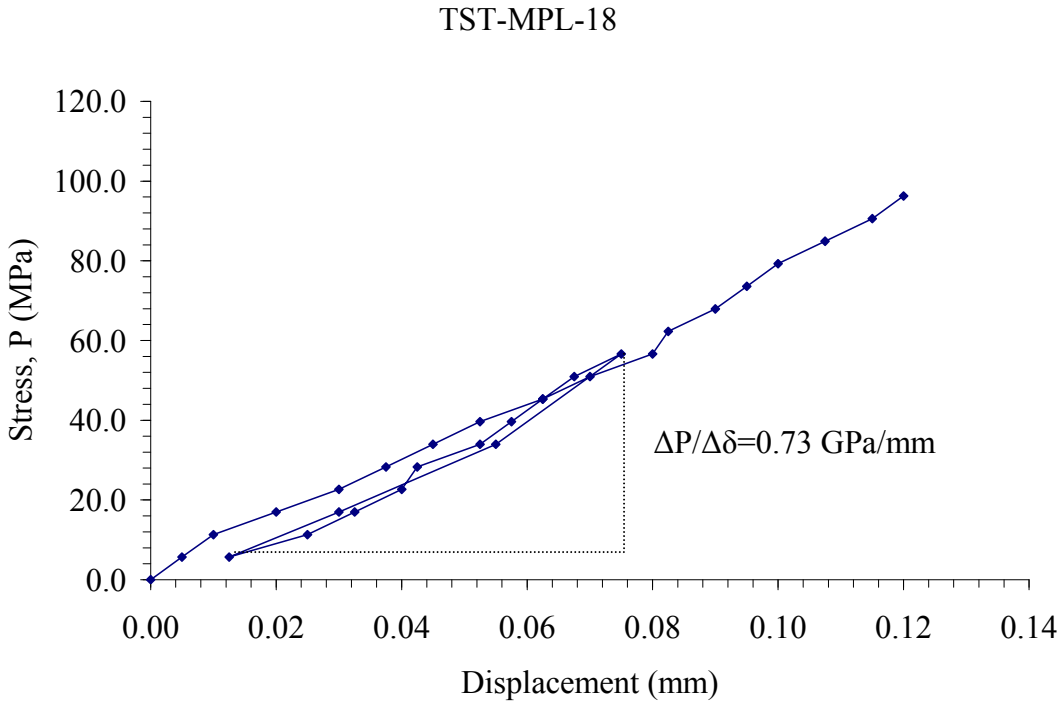

Figure B.118 Applied stress (P) as a function of displacement (δ) for specimen no. TST-MPL-18.

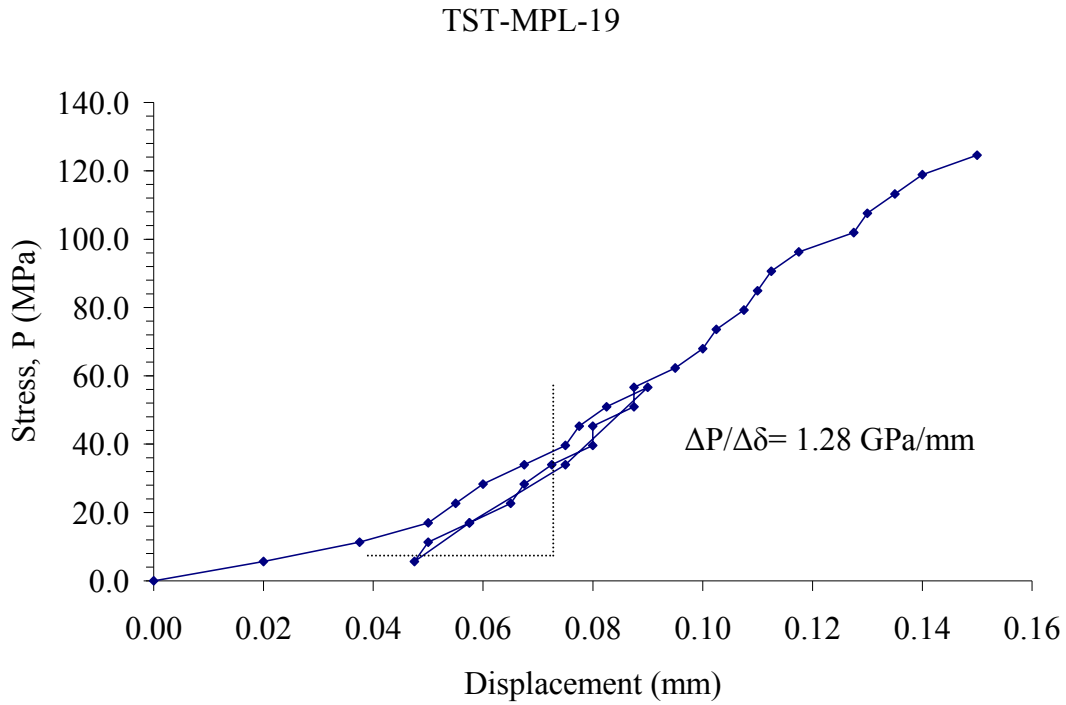

Figure B.119 Applied stress (P) as a function of displacement (δ) for specimen no. TST-MPL-19.

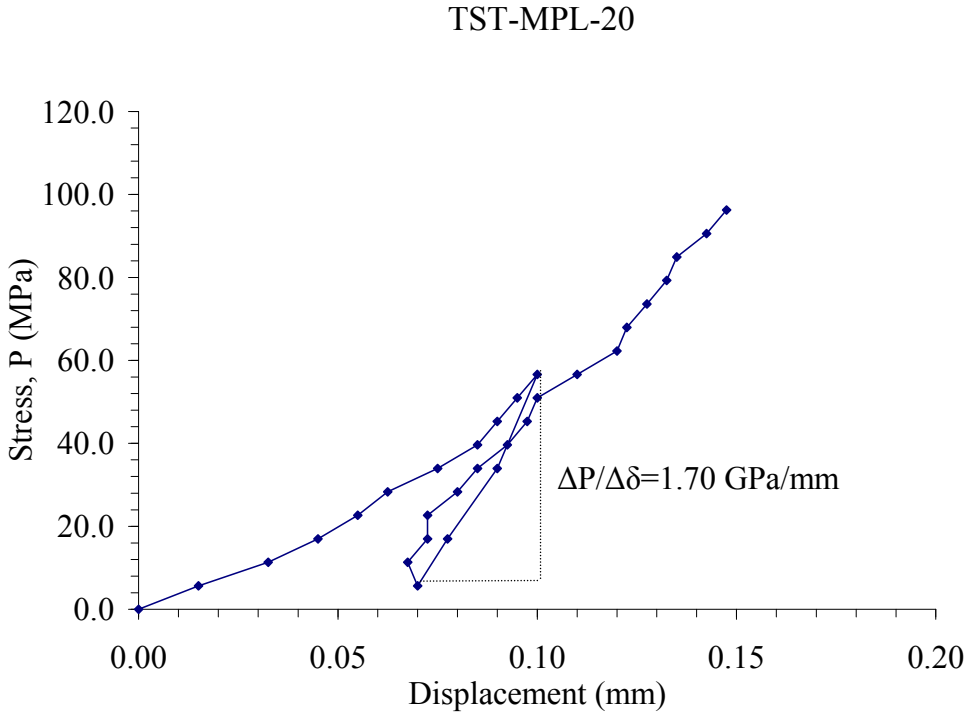

Figure B.120 Applied stress (P) as a function of displacement (δ) for specimen no. TST-MPL-20.

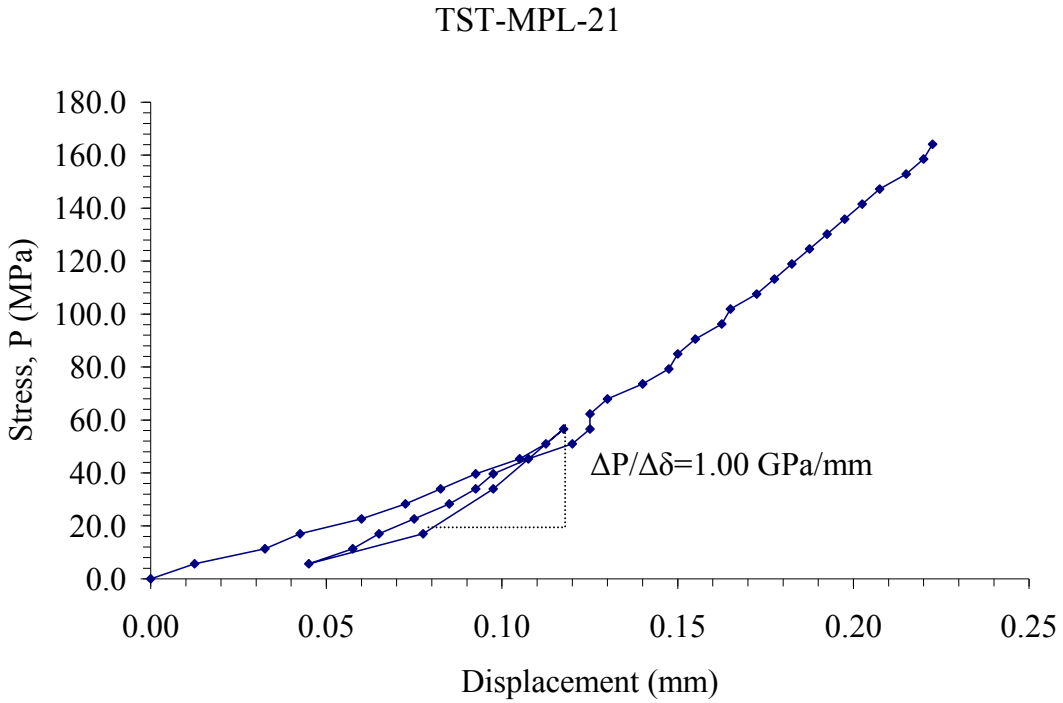

Figure B.121 Applied stress (P) as a function of displacement (δ) for specimen no. TST-MPL-21.

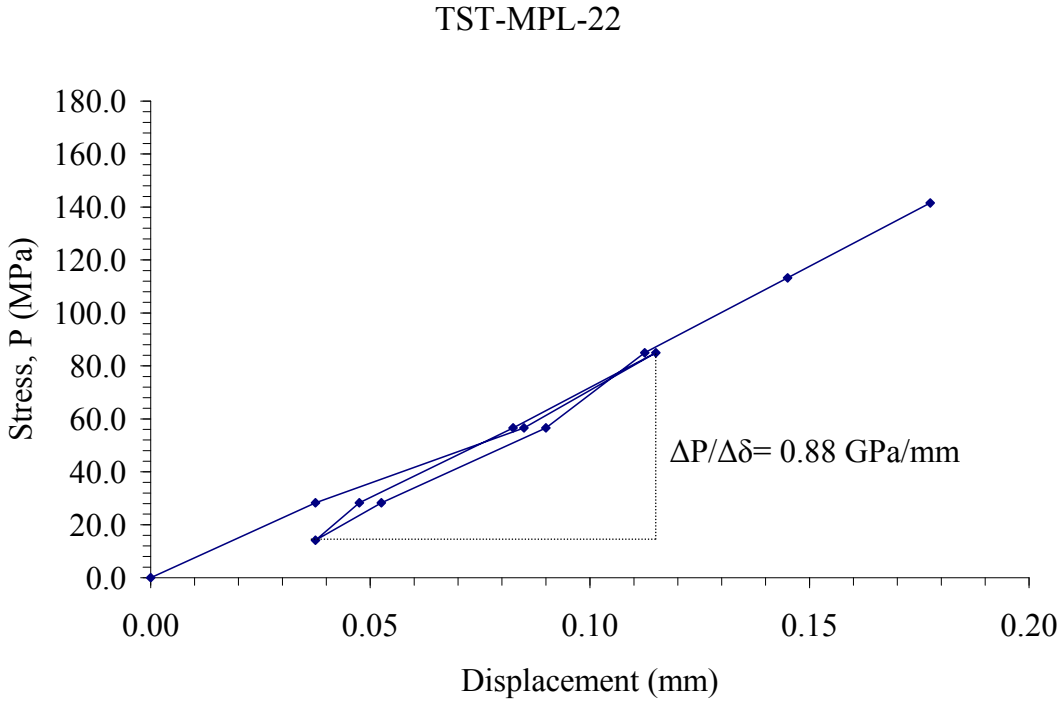

Figure B.122 Applied stress (P) as a function of displacement (δ) for specimen no. TST-MPL-22.

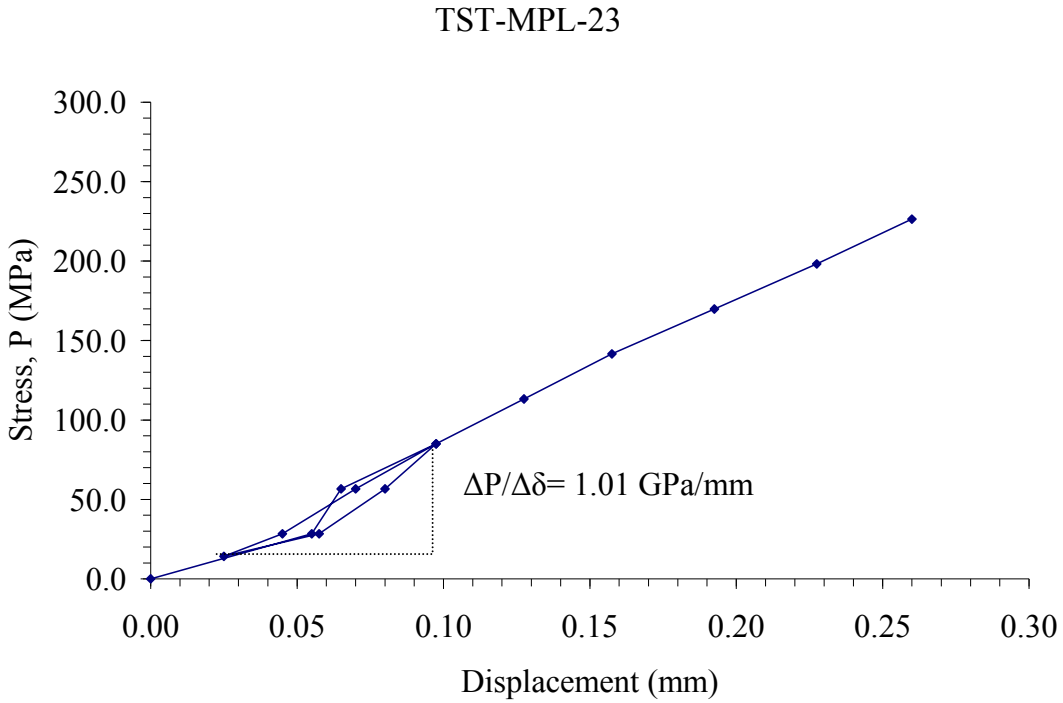

Figure B.123 Applied stress (P) as a function of displacement (δ) for specimen no. TST-MPL-23.

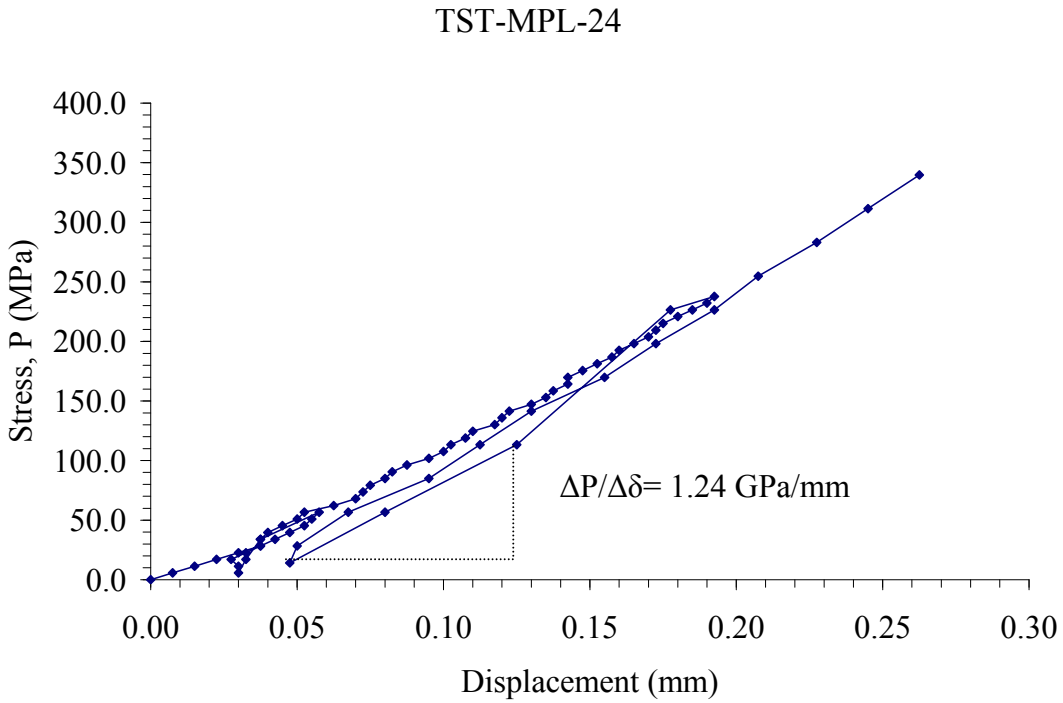

Figure B.124 Applied stress (P) as a function of displacement (δ) for specimen no. TST-MPL-24.

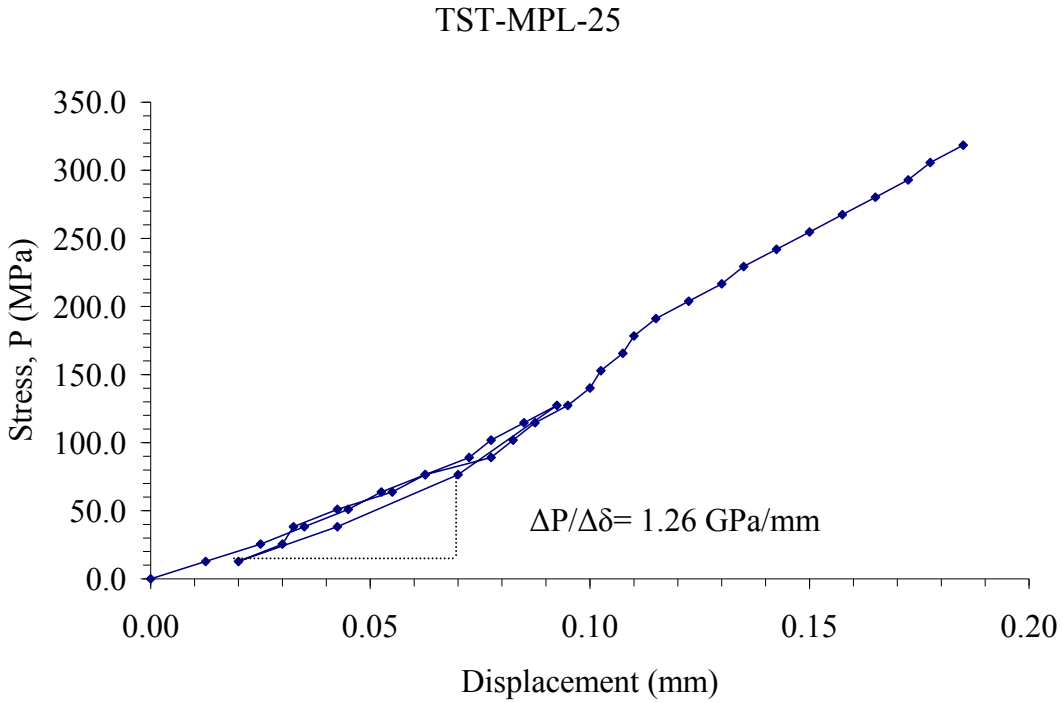

Figure B.125 Applied stress (P) as a function of displacement (δ) for specimen no. TST-MPL-25.

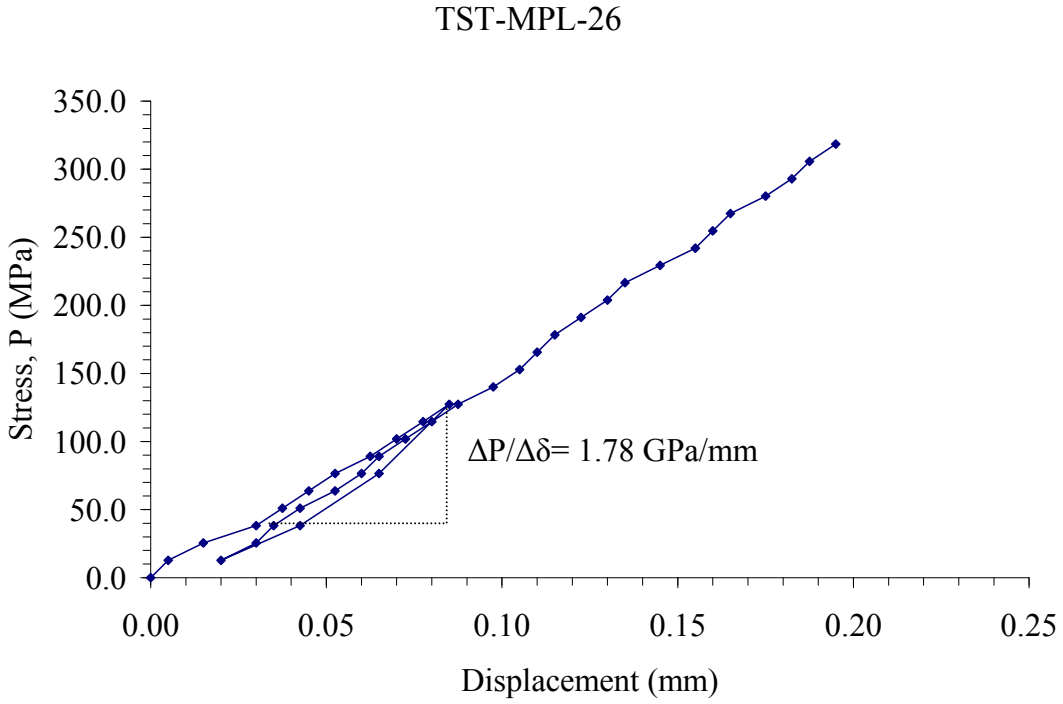

Figure B.126 Applied stress (P) as a function of displacement (δ) for specimen no. TST-MPL-26.

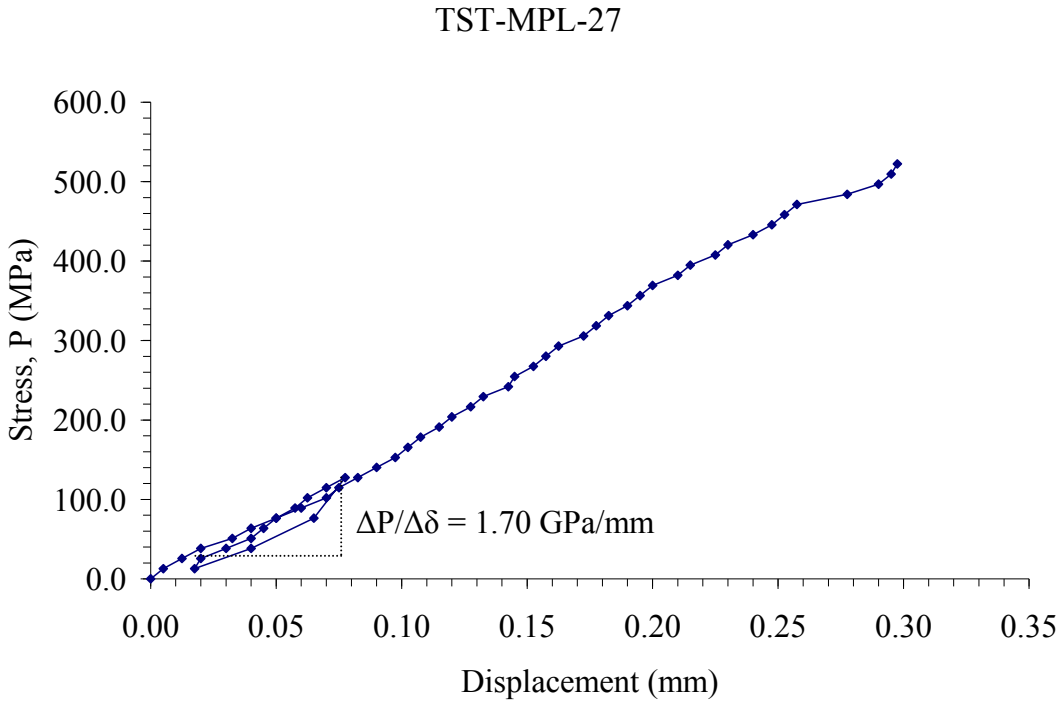

Figure B.127 Applied stress (P) as a function of displacement (δ) for specimen no. TST-MPL-27.

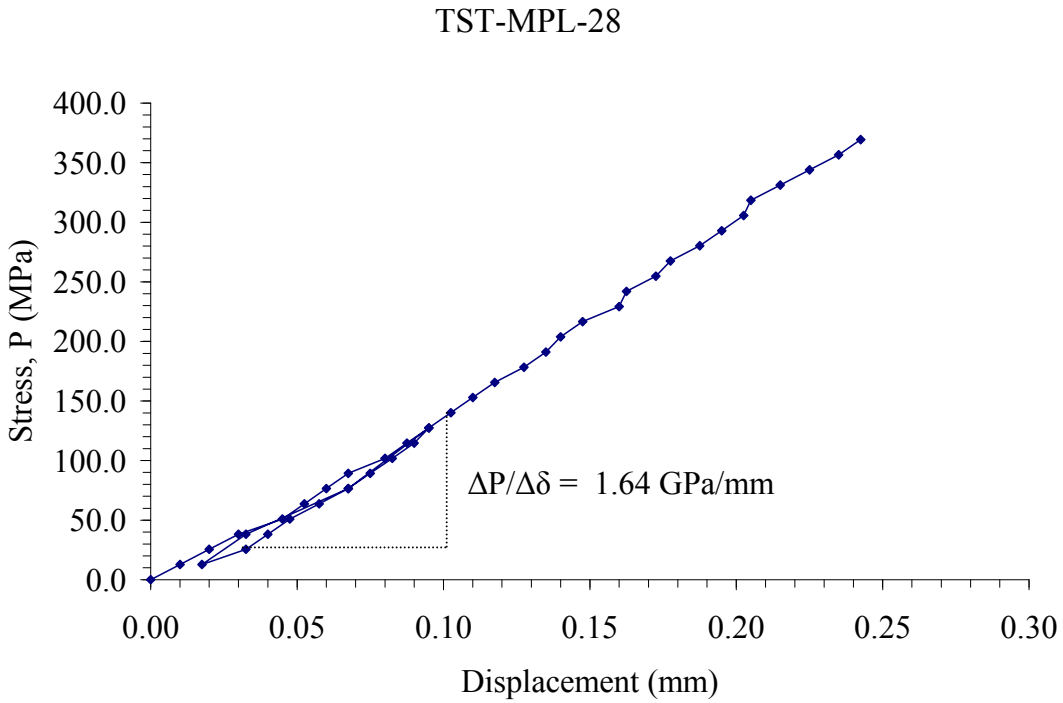

Figure B.128 Applied stress (P) as a function of displacement (δ) for specimen no. TST-MPL-28.

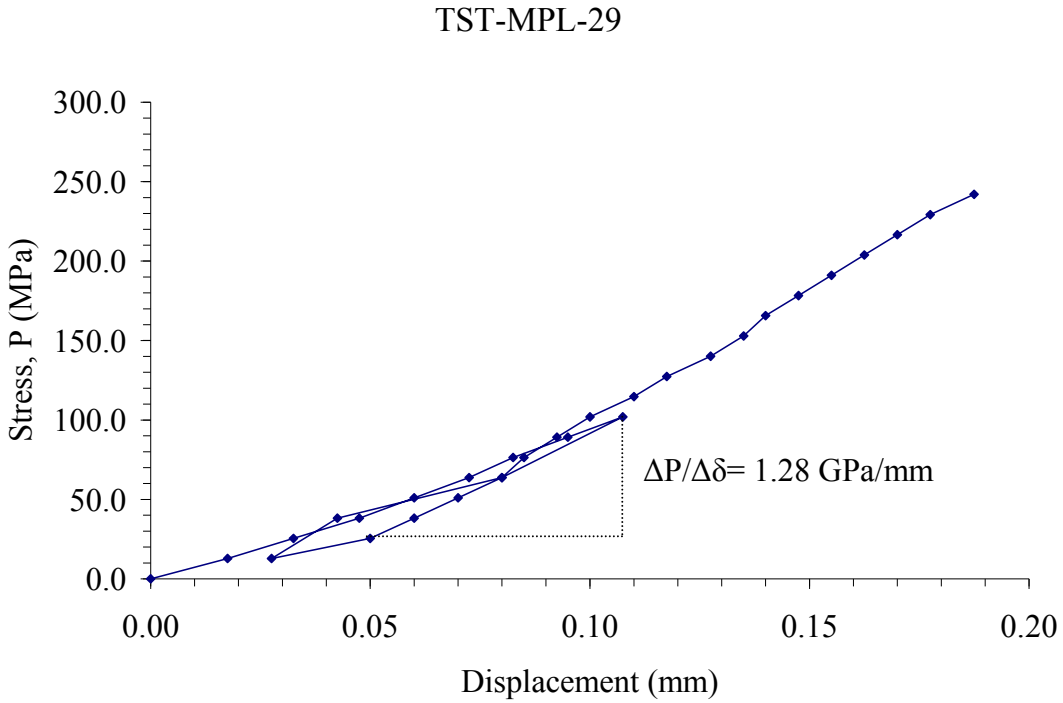

Figure B.129 Applied stress (P) as a function of displacement (δ) for specimen no. TST-MPL-29.

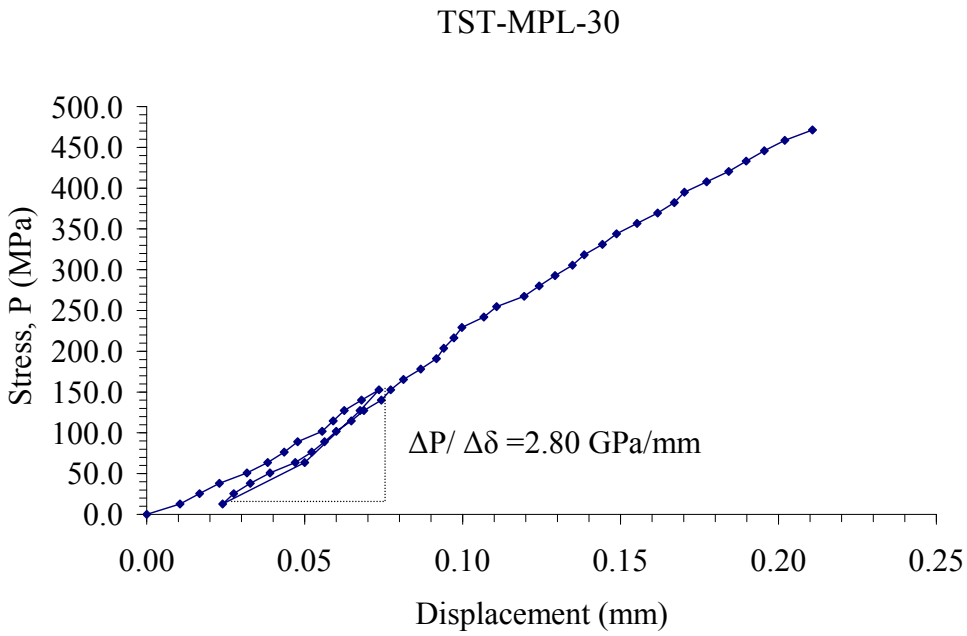

Figure B.130 Applied stress (P) as a function of displacement (δ) for specimen no. TST-MPL-30.

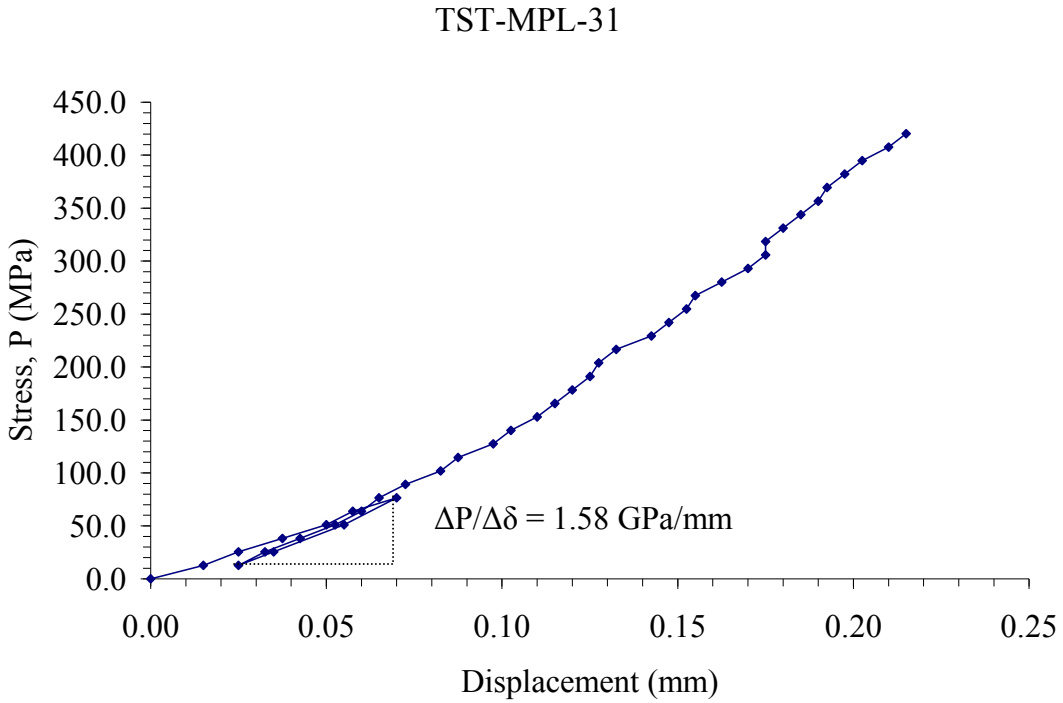

Figure B.131 Applied stress (P) as a function of displacement (δ) for specimen no. TST-MPL-31.

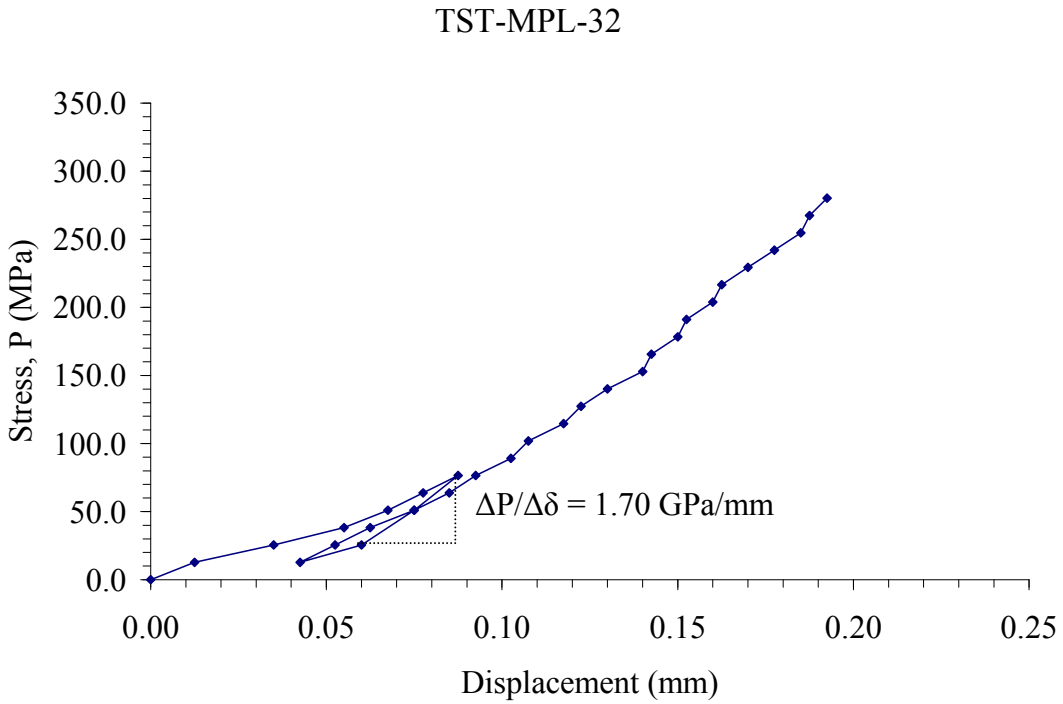

Figure B.132 Applied stress (P) as a function of displacement (δ) for specimen no. TST-MPL-32.

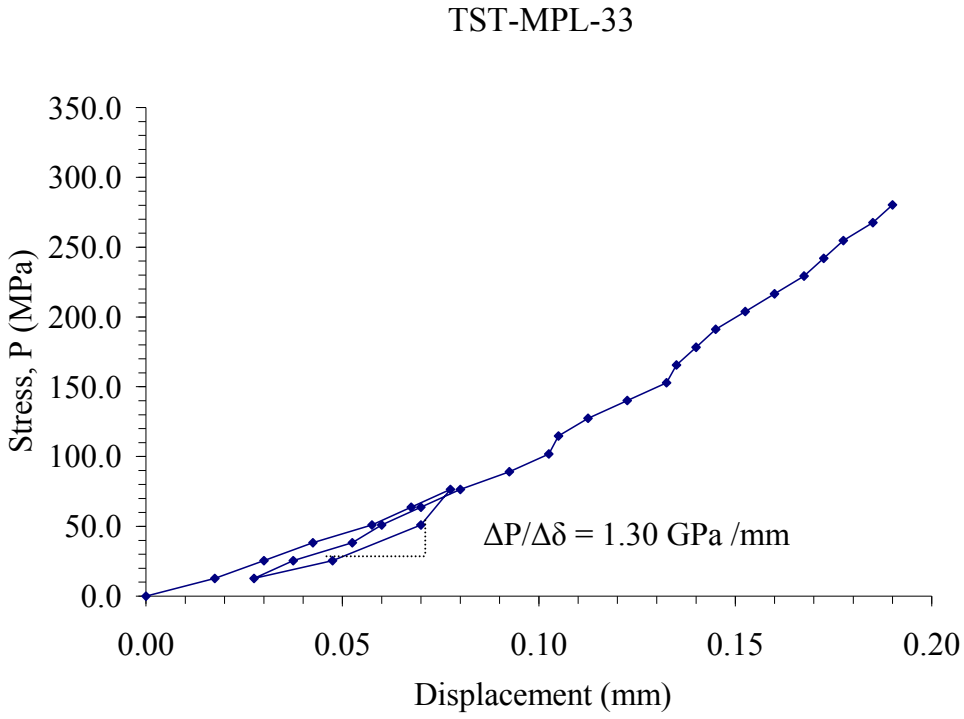

Figure B.133 Applied stress (P) as a function of displacement (δ) for specimen no. TST-MPL-33.

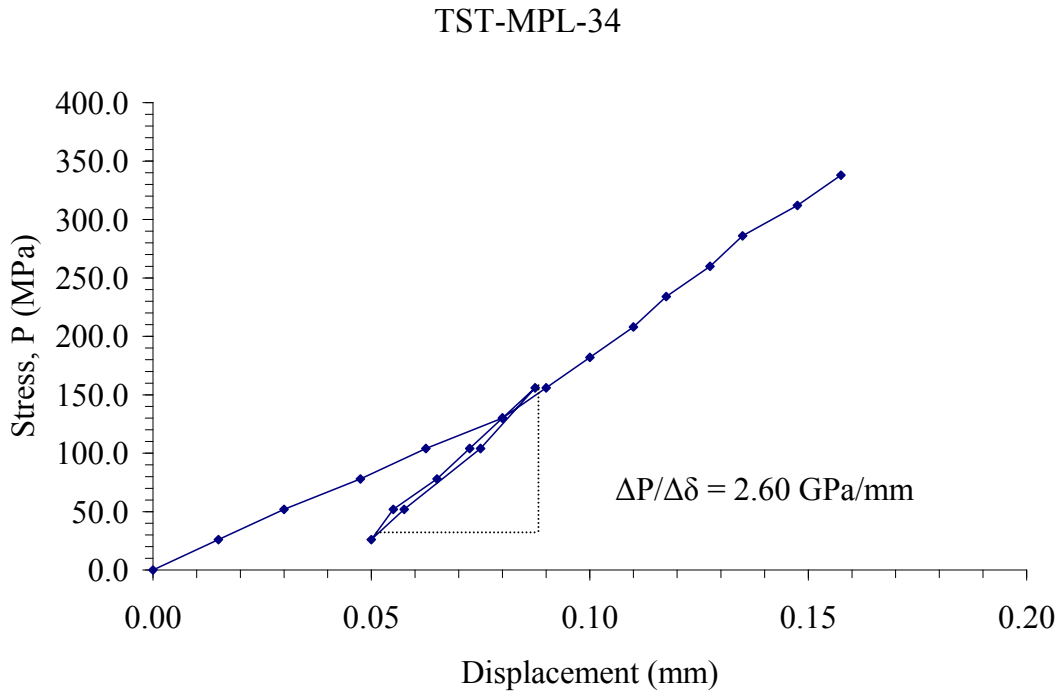

Figure B.134 Applied stress (P) as a function of displacement (δ) for specimen no. TST-MPL-34.

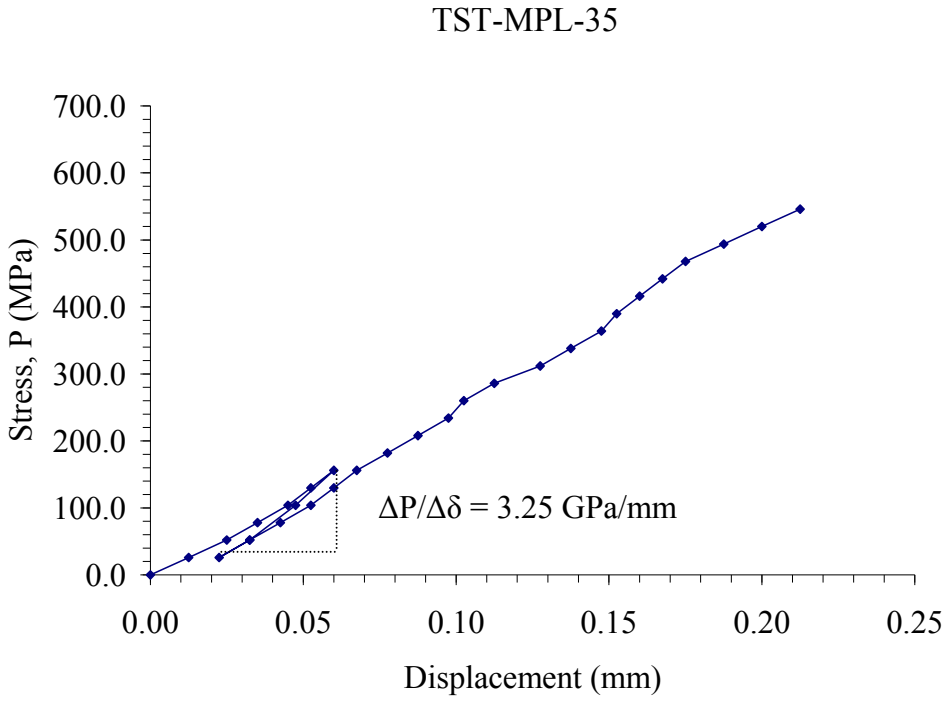

Figure B.135 Applied stress (P) as a function of displacement (δ) for specimen no. TST-MPL-35.

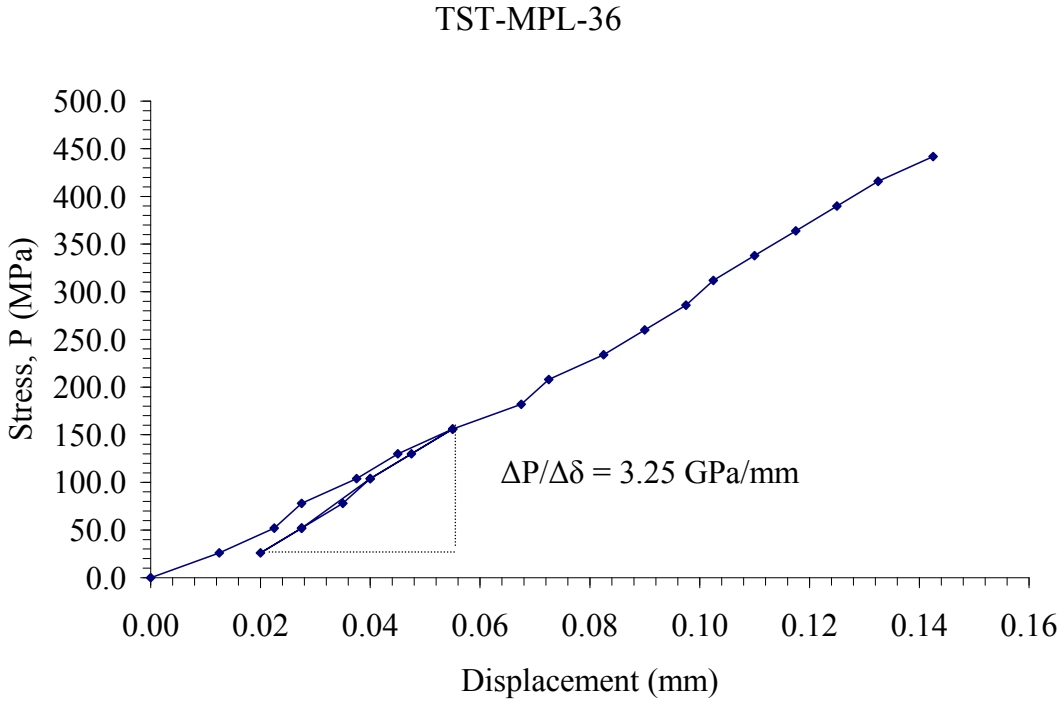

Figure B.136 Applied stress (P) as a function of displacement (δ) for specimen no. TST-MPL-36.

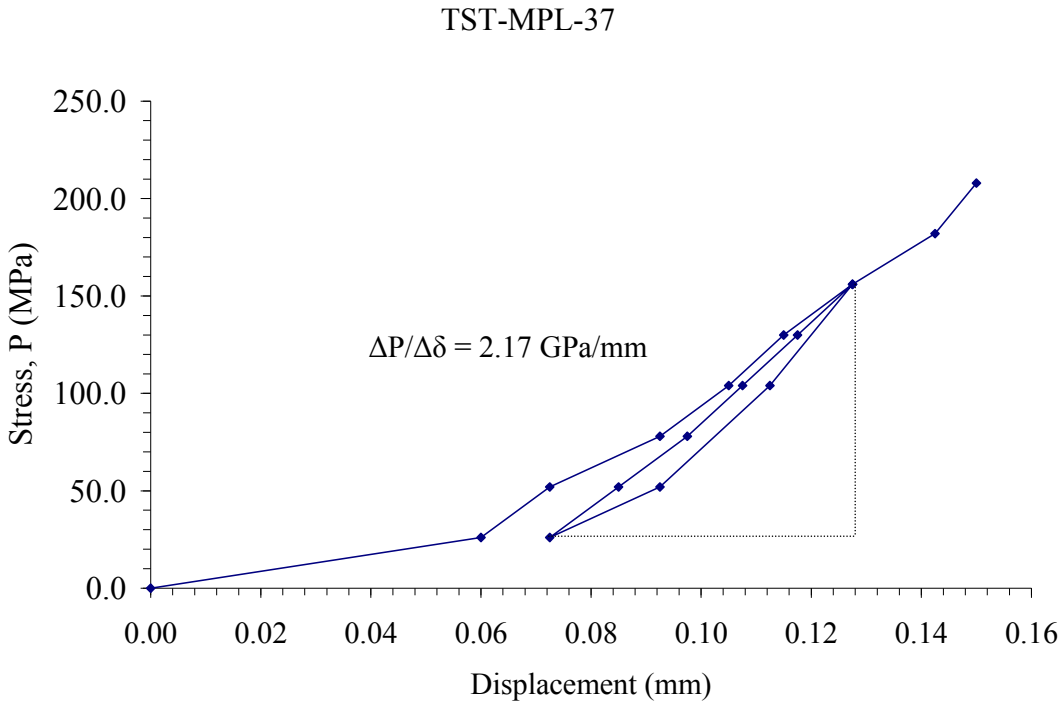

Figure B.137 Applied stress (P) as a function of displacement (δ) for specimen no. TST-MPL-37.

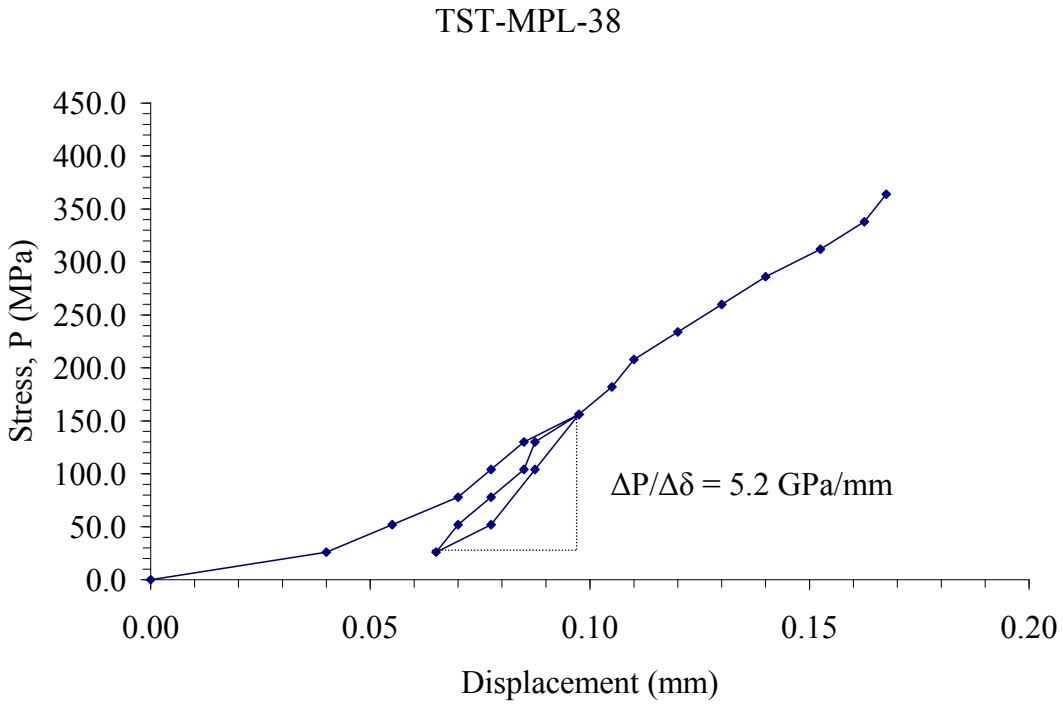

Figure B.138 Applied stress (P) as a function of displacement (δ) for specimen no. TST-MPL-38.

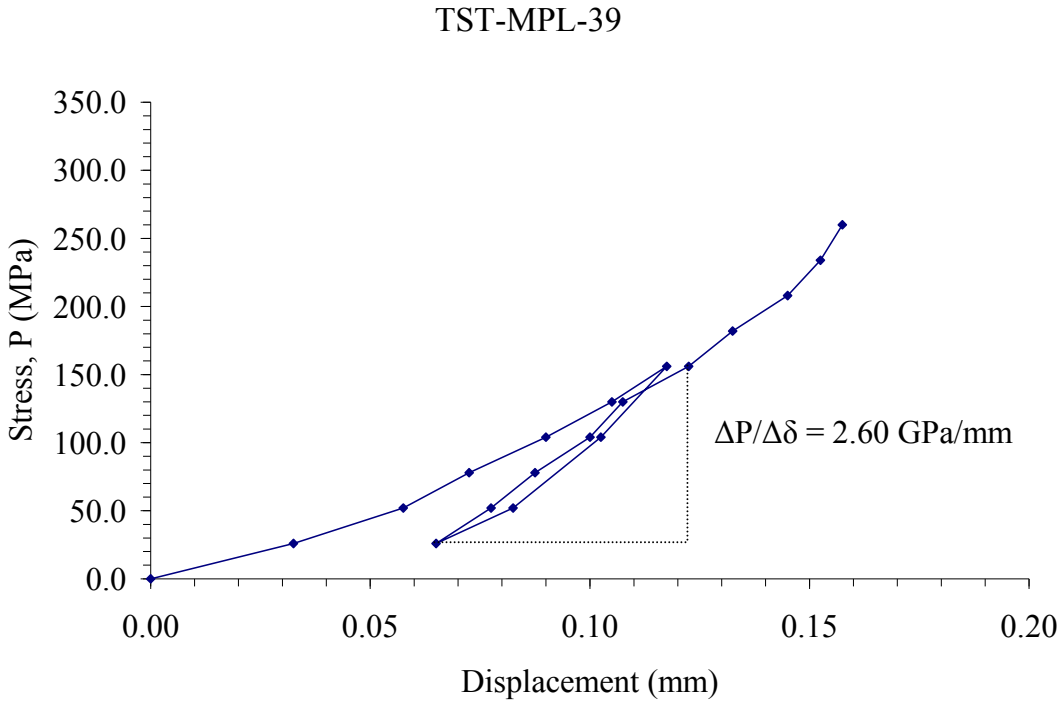

Figure B.139 Applied stress (P) as a function of displacement (δ) for specimen no. TST-MPL-39.

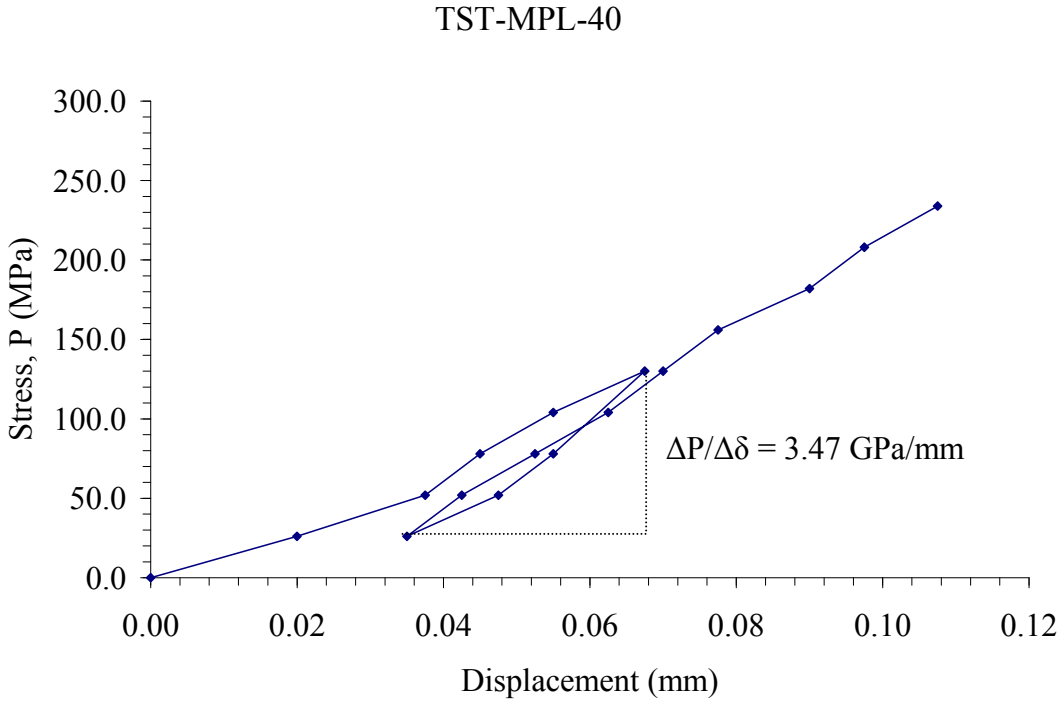

Figure B.140 Applied stress (P) as a function of displacement (δ) for specimen no. TST-MPL-40.

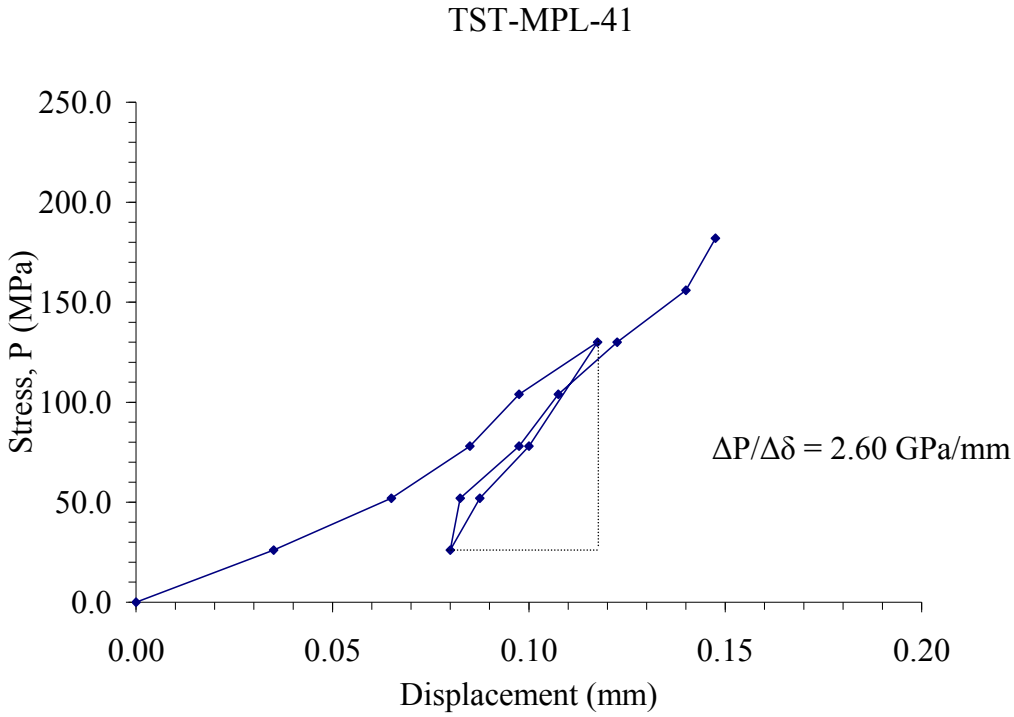

Figure B.141 Applied stress (P) as a function of displacement (δ) for specimen no. TST-MPL-41.

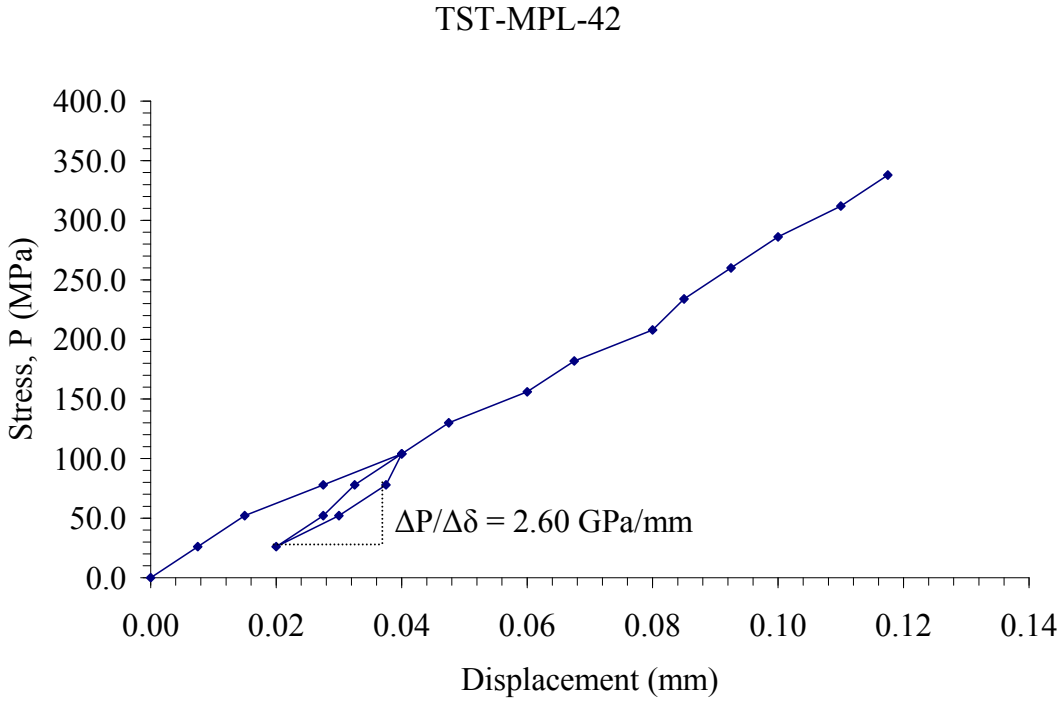

Figure B.142 Applied stress (P) as a function of displacement (δ) for specimen no. TST-MPL-42.

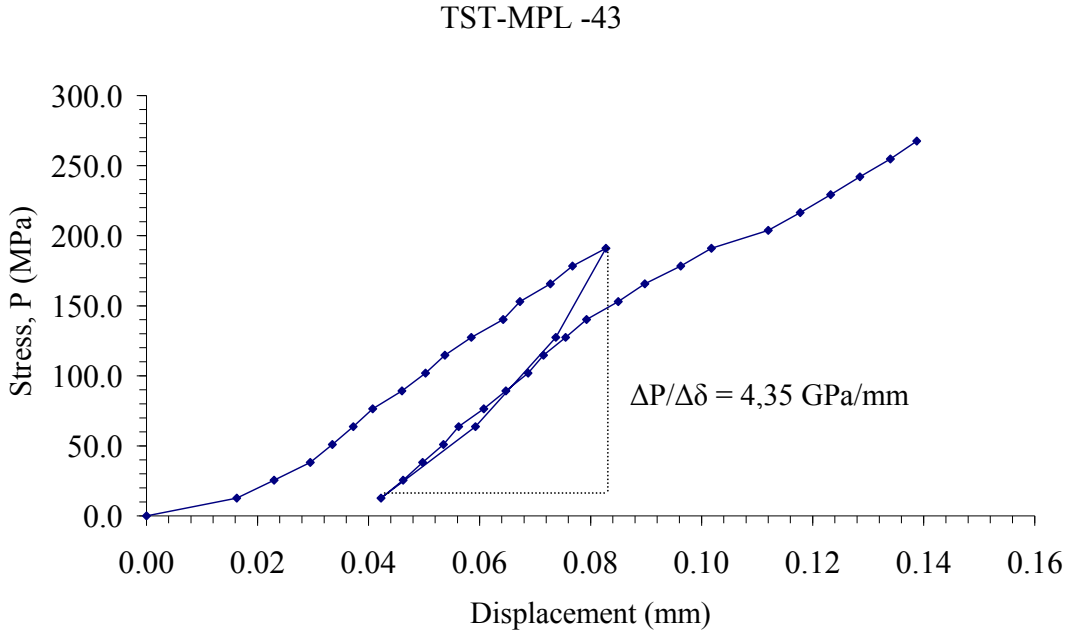

Figure B.143 Applied stress (P) as a function of displacement (δ) for specimen no. TST-MPL-43.

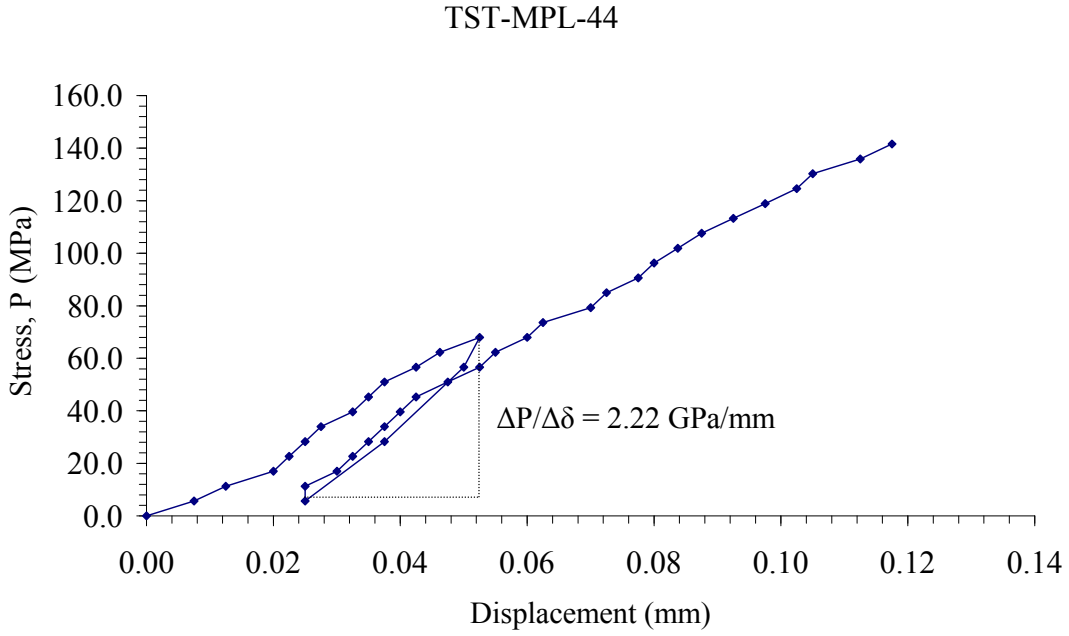

Figure B.144 Applied stress (P) as a function of displacement (δ) for specimen no. TST-MPL-44.

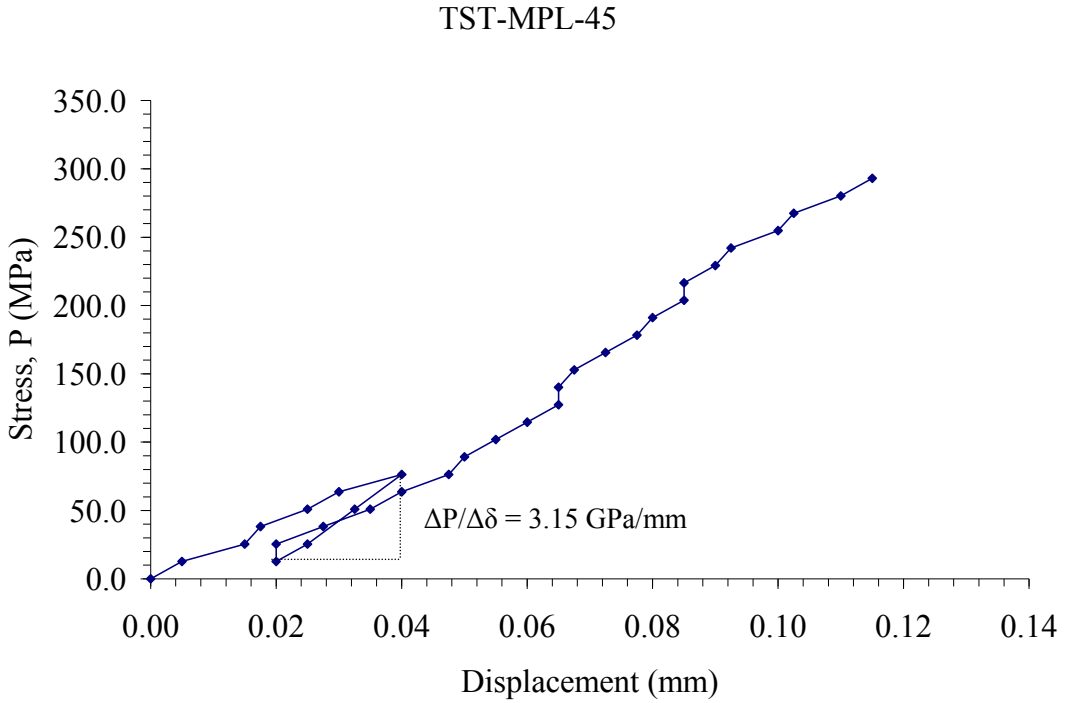

Figure B.145 Applied stress (P) as a function of displacement (δ) for specimen no. TST-MPL-45.

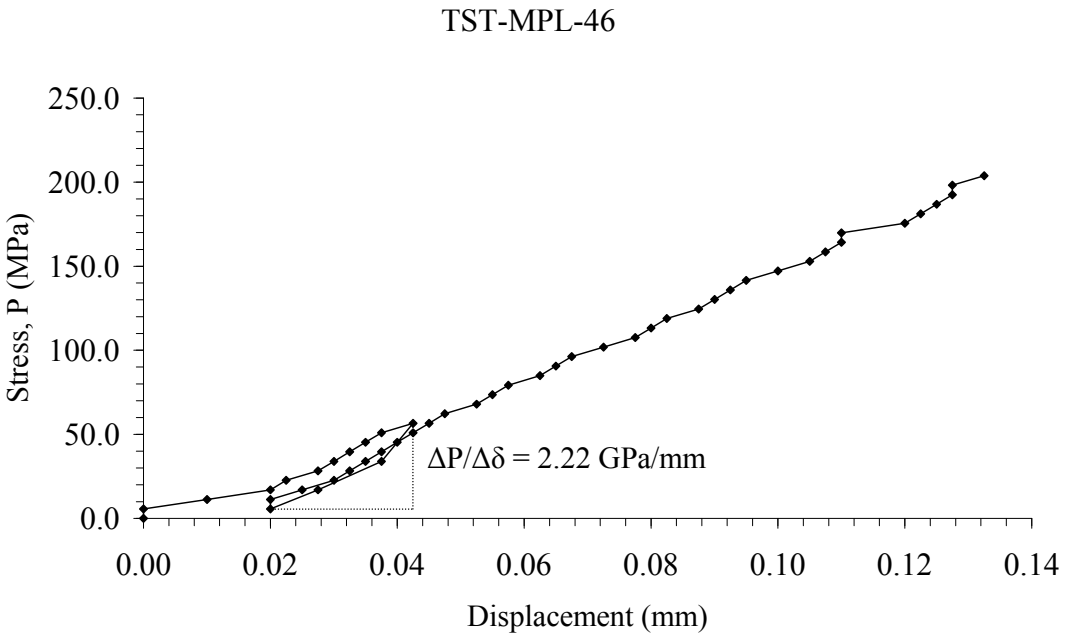

Figure B.146 Applied stress (P) as a function of displacement (δ) for specimen no. TST-MPL-46.

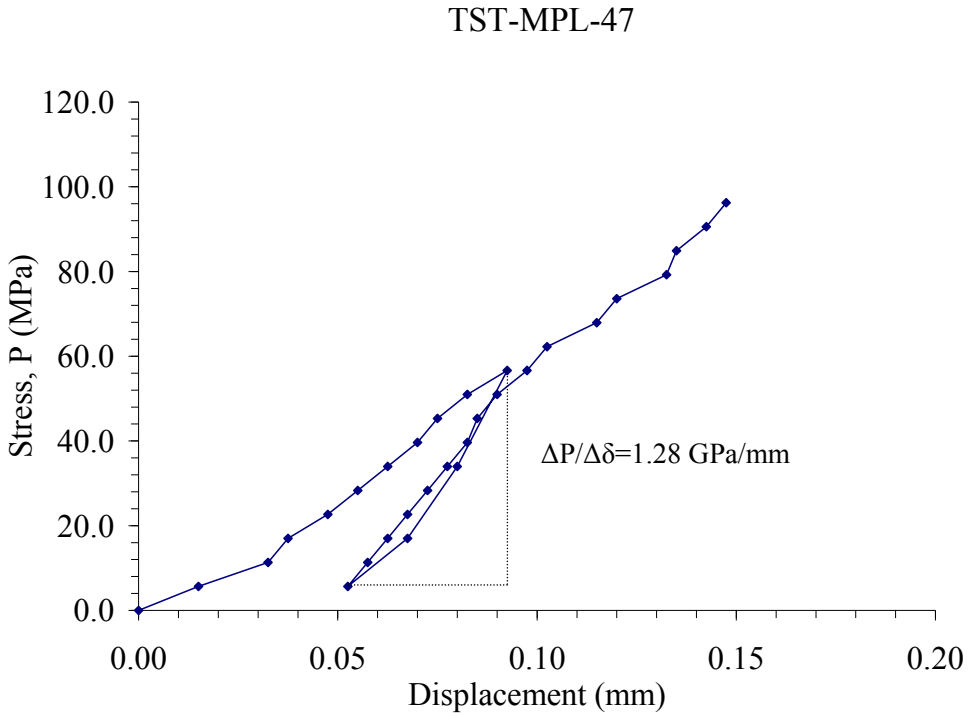

Figure B.147 Applied stress (P) as a function of displacement (δ) for specimen no. TST-MPL-47.

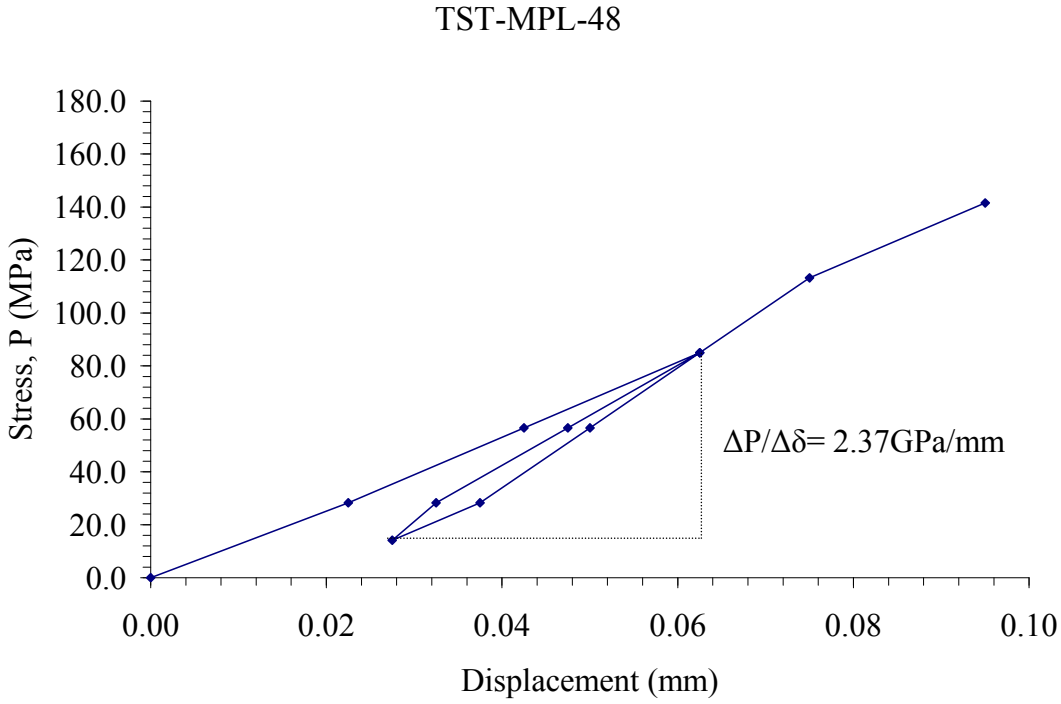

Figure B.148 Applied stress (P) as a function of displacement (δ) for specimen no. TST-MPL-48.

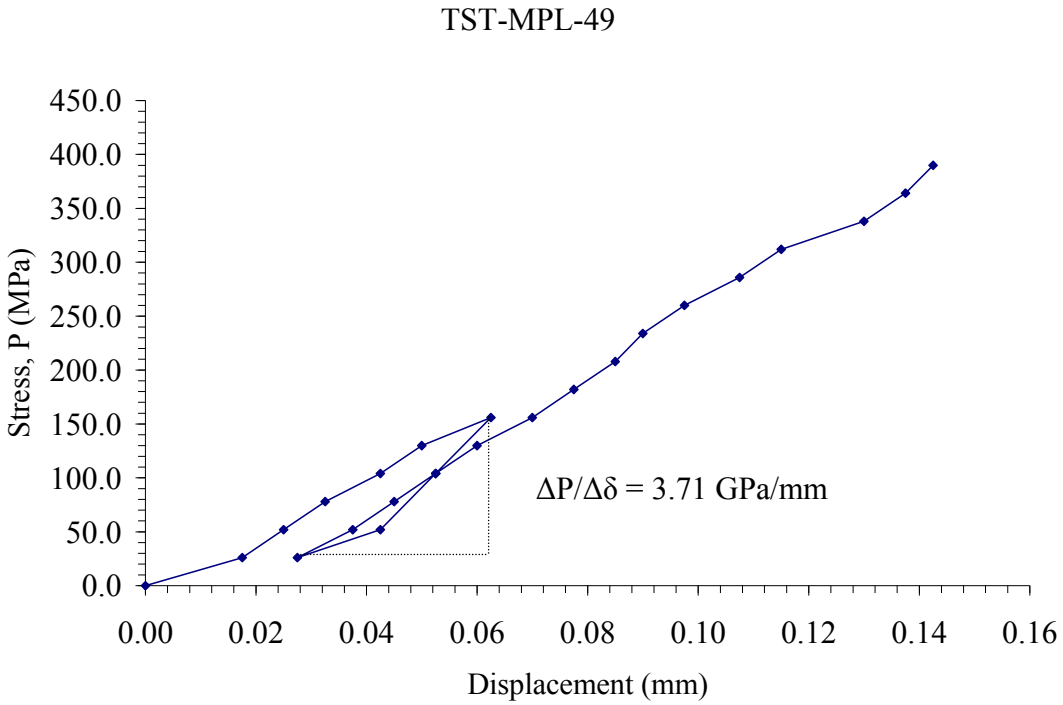

Figure B.149 Applied stress (P) as a function of displacement (δ) for specimen no. TST-MPL-49.

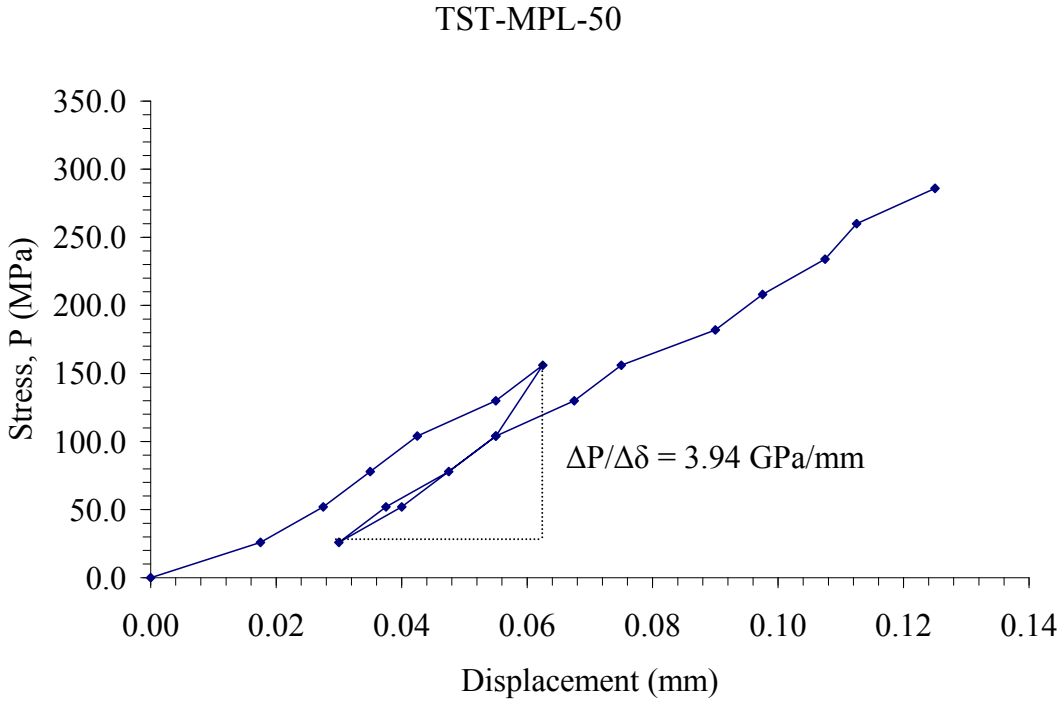

Figure B.150 Applied stress (P) as a function of displacement (δ) for specimen no. TST-MPL-50.

Table 3. Comparison between the elastic modulus conventional method and modified point load tests.

Rock Type	Tangential Elastic Modulus from UCS tests. E_t (GPa)	Elastic Modulus from MPL tests. E_{mpl} (GPa)
Andesite	43±3.4	24.37±6.0
Pebbly Tuffaceous Sandstone	51.3±5.3	18.44±6.3
Silicified Sandstone	63.3±8.0	29.69±10.4

Table 4. Comparison between UCS, CPL Brazilian tensile strength and MPL testing.

Rock Type	Uniaxial Compressive Strength (MPa)			Tensile Strength (MPa)	
	Actual Testing	CPL Prediction	MPL Prediction	Brazilian Testing	MPL Prediction
Andesite	115.0	194.4 ±1.2	100.5	17.0±1.6	13.9±4.3
Pebbly Tuffaceous Sandstone	111.4	244.8±2.0	130.8	13.1±3.3	12.1±7.3
Silicified Sandstone	120.7	259.2±2.2	102.2	19.1±3.2	17.1±12.6

ACKNOWLEDGEMENT

This study is funded by Akara Mining Co. Ltd. Permission to publish this paper is gratefully acknowledged.

REFERENCES

ASTM D 3967-05. Standard Test Method for Splitting Tensile Strength of Intact Rock Core Specimens. *Annual Book of ASTM Standards, 04.08*. West Conshohocken: American Society for Testing and Materials.

ASTM D 5731-07. Standard Test Method for Determination of the Point Load Strength Index of Rock and Application to Rock Strength Classifications. *Annual Book of ASTM Standards, 04.08*. West Conshohocken: American Society for Testing and Materials.

ASTM D 7012-07. Standard Test Method for Compressive Strength and Elastic Moduli of Intact Rock Core Specimens under Varying States of Stress and Temperatures. *Annual Book of ASTM Standards, 04.08*. West Conshohocken: American Society for Testing and Materials.

Brown, E.T. (eds). 1981. *Rock Characterization Testing and Monitoring: ISRM Suggested Methods*. International Society of Rock Mechanics: Pergamon Press.

Fuenkajorn, K. & Daemen, J. J. K., 1992. An empirical strength criterion for heterogeneous tuff. *Int. J. Engineering Geology*. 32: 209-223.

Tepnarong, P. (2001). Theoretical and experimental studies to determine compressive and tensile strengths of rocks, using modified point load testing. M.S. Thesis, Suranaree University of Technology, Thailand

Tepnarong, P. (2006). Theoretical and experimental studies to determine elastic modulus and triaxial compressive strengths of intact rocks by modified point load testing. Ph.D. Thesis, Suranaree University of Technology, Thailand.

Tepnarong, P. & Fuenkajorn, K., 2004. Determination of elasticity and strengths of intact rocks using modified point load test. *Proceedings of the ISRM International Symposium 3rd ASRM*. Vol. 2 (pp 397-392). Millpress: Rotterdam.

BIOGRAPHY

Mr. Chatchai Intaraprasit was born on July 30, 1973 in Khon Kaen province, Thailand. He received his Bachelor's Degree in Science (Geotechnology) from Khon Kaen University in 1996. He worked with the construction company for ten years after graduated the Bachelor's Degree. For his post-graduate, he continued to study with a Master's Degree in the Geological Engineering Program, Institute of Engineering, Suranaree University of Technology. He has published a technical papers related to rock mechanics as; in 2009, "*Modified point load testing of volcanic rocks from Chatree gold mine"* in the proceeding of the second Thailand symposium on rock mechanics, Chonburi, Thailand. For his work, he is working as a geotechnical engineer at Akara mining company limited, Phichit province, Thailand.